

UNCLASSIFIED

AD NUMBER

AD374055

CLASSIFICATION CHANGES

TO: unclassified

FROM: confidential

LIMITATION CHANGES

TO:
Approved for public release, distribution unlimited

FROM:
Distribution authorized to U.S. Gov't. agencies and their contractors; Critical Technology; JUL 1966. Other requests shall be referred to Air Force Rocket Propulsion Laboratory, Edwards AFB, CA.

AUTHORITY

31 Jul 1978, DoDD 5200.10; AFRPL ltr dtd 5 Feb 1986

THIS PAGE IS UNCLASSIFIED

SECURITY

MARKING

The classified or limited status of this report applies to each page, unless otherwise marked.

Separate page printouts ~~MUST~~ be marked accordingly.

THIS DOCUMENT CONTAINS INFORMATION AFFECTING THE NATIONAL DEFENSE OF THE UNITED STATES WITHIN THE MEANING OF THE ESPIONAGE LAWS, TITLE 18, U.S.C., SECTIONS 793 AND 794. THE TRANSMISSION OR THE REVELATION OF ITS CONTENTS IN ANY MANNER TO AN UNAUTHORIZED PERSON IS PROHIBITED BY LAW.

NOTICE: When government or other drawings, specifications or other data are used for any purpose other than in connection with a definitely related government procurement operation, the U. S. Government thereby incurs no responsibility, nor any obligation whatsoever; and the fact that the Government may have formulated, furnished, or in any way supplied the said drawings, specifications, or other data is not to be regarded by implication or otherwise as in any manner licensing the holder or any other person or corporation, or conveying any rights or permission to manufacture, use or sell any patented invention that may in any way be related thereto.

CONFIDENTIAL

AFRPL-TR-66-153

July 1966

30

ADVANCED ROCKET ENGINE--STORABLE (u)
QUARTERLY TECHNICAL REPORT AFRPL-TR-66-153
April through June 1966

374055

Prepared for

AIR FORCE ROCKET PROPULSION LABORATORY
RESEARCH AND TECHNOLOGY DIVISION
AIR FORCE SYSTEMS COMMAND
UNITED STATES AIR FORCE
EDWARDS, CALIFORNIA

D D C
JUL 22 1966
D

In addition to security requirements which must be met, this document is subject to special export controls and each transmittal to foreign governments or foreign nationals may be made only with prior approval of AFRPL (RPPR/STINFO), Edwards, California 93523.

(0947)

AGC Report 10830-Q-4

GROUP 4
DOWNGRADED AT 3 YEAR INTERVALS; DECLASSIFIED AFTER 12 YEARS
THIS DOCUMENT CONTAINS INFORMATION AFFECTING THE NATIONAL DEFENSE OF THE UNITED STATES WITHIN THE MEANING OF THE ESPIONAGE LAWS, TITLE 18, U.S.C. SECTIONS 793 AND 794. ITS TRANSMISSION OR THE REVELATION OF ITS CONTENTS IN ANY MANNER TO AN UNAUTHORIZED PERSON IS PROHIBITED BY LAW.

CONFIDENTIAL

**Best
Available
Copy**

CONFIDENTIAL

15



AEROJET-GENERAL CORPORATION

SACRAMENTO

CALIFORNIA

SACRAMENTO PLANT

9300:0471:JRC:pe

3 August 1966

Subject: Contract AF 04(611)-10830, Quarterly Technical Report No. AFRPL-TR-66-153 entitled, "Advanced Rocket Engine--Storable"(U)

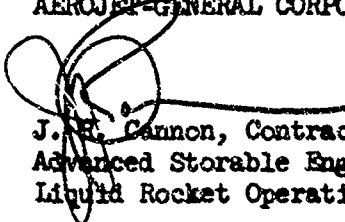
To: Air Force Rocket Propulsion Laboratory
Liquid Rocket Division
Edwards, California 93523

Attention: Clark W. Hawk/RPRZ

Reference: (a) AGC Ltr. 9300:0464, J. R. Cannon to Clark W. Hawk/RPRZ, dated 14 July 1966, Subject: Same

1. Our Quarterly Report submitted via Reference (a) letter contained certain administrative errors in Sections I and IV. The errata sheet provided as Enclosure (1) to this letter cites corrections to be posted to your copy of the subject report.

AEROJET-GENERAL CORPORATION



J. R. Cannon, Contract Manager
Advanced Storable Engine Program
Liquid Rocket Operations

Encl: (1) Errata Sheet to Quarterly Technical Report No. AFRPL-TR-66-153

cc: J. J. Wilt/RNE
AFPRO - AGC

cc: F. W. Brass/R-P&VE-PAC
NASA

C. W. Schnare/RPPP
AFRPL, Edwards AFB

CPIA, Category No. 3

AFRSTD/Maj. Holdener
Headquarters USAF

R. G. Langford/RMKA (ltr only)
AFPRO - AGC

RTTR/Maj. Mott-Smith
Headquarters, RTD

LACMSD (ltr only)

Maj. K. E. Weiss
Ballistic Systems Div.

R. Schuley, 1st Lt./FTMGR-4 (ltr only)
AFFTC, Edwards

V. H. Montell
Aerospace Corporation

IF ENCLOSURE (1) IS WITHDRAWN OR NOT ATTACHED.
THE CLASSIFICATION OF THIS CORRESPONDENCE WILL
BE DOWNGRADED TO DECLASSIFIED.

A SUBSIDIARY OF THE GENERAL TIRE & RUBBER COMPANY

CONFIDENTIAL

AD 374 055

CONFIDENTIAL

ERRATA

REPORT NO: AFRPL Quarterly Technical Report No. AFRPL-TR-66-153
AGC Quarterly Technical Report No. 10830-Q-4

TITLE: Advanced Rocket Engine--Storable (U)

CONTRACT NO: AF 04(611)-10830

RESPONSIBLE RFD ORGANIZATION: Air Force Rocket Propulsion Laboratory
Research & Technology Division
Air Force Systems Command
United States Air Force
Edwards, California

1. Delete the last sentence of Paragraph 6 of Section I, Introduction, Page I-1, and substitute the following two sentences:

"(c) The regeneratively cooled design employs a two-pass system made up of oval tubes. The transpiration cooled system uses a considerable number of thin wafers that are chemically milled to produce the desired pressure-drop pattern required to control the coolant flow."
2. Change the classification of Figures XIV-4 and XIV-5 from Confidential to Unclassified. These figures were classified Confidential in error and should be declassified to conform with DD Form 254, Security Requirements Check List, dated 7 June 1966 to Contract AF 04(611)-10830.

GROUP 4 EXCLUDED FROM AUTOMATIC DOWNGRADING AND DECLASSIFICATION	NO SECURITY CONCERNS PRESENT FOR UNCLASSIFICATION OF THIS INFORMATION DATE 8-24-86 BY 0947
--	--

CONFIDENTIAL

CONFIDENTIAL

AFRPL-TR-66-153

July 1966

ADVANCED ROCKET ENGINE--STORABLE (u)

QUARTERLY TECHNICAL REPORT AFRPL-TR-66-153

April through June 1966

Prepared by

AEROJET-GENERAL CORPORATION
Advanced Storable Engine Program Division
Liquid Rocket Operations
Sacramento, California

Prepared for

AIR FORCE ROCKET PROPULSION LABORATORY
Research and Technology Division
Air Force Systems Command
United States Air Force
Edwards, California

In addition to security requirements which must be met, this document is subject to special export controls and each transmittal to foreign governments or foreign nationals may be made only with prior approval of AFRPL (RPPR/STINFO), Edwards, California 93523.

AGC Report 10830-Q-4

6472T

<p>GROUP 4 DOWNGRADED AT 3 YEAR INTERVALS; DECLASSIFIED AFTER 12 YEARS</p> <p>* THIS DOCUMENT CONTAINS INFORMATION AFFECTING THE NATIONAL DEFENSE OF THE UNITED STATES WITHIN THE MEANING OF THE ESPIONAGE LAWS, TITLE 18, U.S.C. SECTIONS 793 AND 794. ITS TRANSMISSION OR THE REVELATION OF ITS CONTENTS IN ANY MANNER TO AN UNAUTHORIZED PERSON IS PROHIBITED BY LAW *</p>
--

CONFIDENTIAL

CONFIDENTIAL

Report 10830-Q-4

FOREWORD

(u) This is the fourth written progress report submitted under the ARES Program, Contract AF 04(611)-10830. It provides a summary of major accomplishments and discusses the technical aspects of the program. The period covered by this report is 1 April through 30 June 1966. The program structure number is 63409604; the project number is 682A.

(u) This program is under the direction of Mr. R. Beichel, Manager of the Advanced Storable Engine Program Division, Liquid Rocket Operations, Aerojet-General Corporation, Sacramento, California.

(u) The program is sponsored by the Air Force Rocket Propulsion Laboratory, Research and Technology Division, Edwards Air Force Base, California, under the direction of C. W. Hawk/RPRZ.

(u) Publication of this report does not constitute Air Force approval of the report's findings or conclusions. It is published only for the exchange and stimulation of ideas.

Clark W. Hawk
Program Manager

CONFIDENTIAL

UNCLASSIFIED

Report 10830-Q-4

UNCLASSIFIED ABSTRACT

(u) The objective of the ARES (Advanced Rocket Engine, Storable) Program is to demonstrate the engineering practicality and the performance characteristics of an advanced storable propellant modular engine embodying high chamber pressure and the staged-combustion cycle.

(u) This fourth quarterly report describes the technical accomplishments of the reporting period. Generally, the period was characterized as one in which many analyses and designs were completed, fabrication of many components was completed, and testing was accelerated. The most noteworthy accomplishment was the successful hot firing of two different modular injectors using the intensifier test system.

UNCLASSIFIED

Report 10830-Q-4

TABLE OF CONTENTS

	<u>Page</u>
I. Introduction	I-1
II. Summary	II-1
III. Primary Combustor Assembly	III-1
A. General	III-1
B. Primary Combustor Assembly--Design and Fabrication	III-1
C. Development Testing	III-4
IV. Secondary Combustor Assembly	IV-1
A. General	IV-1
B. Secondary Combustor Assembly, Design and Fabrication	IV-1
C. Development Testing	IV-9
V. Advanced TPA (T-Engine)	V-3
A. General	V-1
B. Advanced TPA Design	V-1
C. Pump Design	V-2
D. Turbine	V-3
E. Shaft	V-3
F. Axial Thrust and Bearing Design	V-4
G. Seals	V-4
H. Turbopump Housing	V-4
I. Boost Pump	V-4
VI. Inline (Backup) Turbopump	VI-1
A. General	VI-1
B. TPA Design	VI-1
C. Pump Design	VI-2
D. Turbine Design	VI-3
E. Power Transmission	VI-3
F. Inline Housing Fabrication	VI-5
VII. TPA Housing Development	VII-1
A. General	VII-1
B. Housing A-1 Testing	VII-1
C. Housing A-2 Fabrication	VII-4
D. Housing-B Design	VII-5

UNCLASSIFIED

Report 10830-Q-4

TABLE OF CONTENTS (cont.)

	<u>Page</u>
VIII. Turbopump Bearing Development	VIII-1
A. General	VIII-1
B. Bearing Design	VIII-1
C. Bearing Testing at 40,000 rpm in N ₂ O ₄	VIII-2
D. Bearing Testing at 31,250 rpm in N ₂ O ₄	VIII-3
E. Bearing Testing at 40,000 rpm in AeroZINE 50	VIII-4
F. Bearing Testing at 31,250 rpm in AeroZINE 50	VIII-5
G. Hydrostatic Thrust-Bearing Disc Failure Investigation	VIII-6
IX. Turbopump Wear-Ring Development	IX-1
A. General	IX-1
B. Design	IX-2
C. Fabrication	IX-4
D. Testing	IX-4
X. TPA Seal Development	X-1
A. General	X-1
B. Hydrostatic Combustion Seal	X-2
C. Purge Seal	X-8
XI. Suction Valves	XI-1
A. General	XI-1
B. Design	XI-1
C. Fabrication and Testing	XI-1
XII. Fuel-Control Valves	XII-1
A. General	XII-i
B. Primary Combustor Fuel-Control Valve (PCFCV)	XII-1
C. Secondary Combustor Fuel-Control Valve (SCFCV)	XII-2
XIII. Suction Lines and Auxiliary Systems	XIII-1
A. General	XIII-1
B. Design	XIII-1
C. Fabrication and Testing (Servocontrol System)	XIII-2
XIV. Propulsion System	XIV-1
A. General	XIV-1
B. Summary	XIV-1
C. Module Assembly (Advanced TPA Configuration)	XIV-2

UNCLASSIFIED

Report 10830-Q-4

TABLE OF CONTENTS (cont.)

	<u>Page</u>
XV. Engine Analytical Models	XV-1
A. General	XV-1
B. Start and Shutdown Transients	XV-1
C. Burnoff Seal Tester Transient	XV-2
D. Low-Frequency-Stability Analysis	XV-3
XVI. Nozzle Aerodynamics	XVI-1
A. Summary	XVI-1
B. Cold-Flow Program	XVI-1
C. Warm-Flow Program	XVI-4
XVII. Air-Flow Model Testing	XVII-1
A. General	XVII-1
B. Primary Combustor Studies	XVII-1
C. Fluid Dynamic Testing (TPA)	XVII-3
XVIII. Heat-Transfer Analysis	XVIII-1
A. General	XVIII-1
B. ARES Thrust Chambers	XVIII-1
C. Thermal Barrier Development	XVIII-12
D. Component Design Support	XVIII-14
XIX. Reliability	XIX-1
A. Modes-of-Failure Analysis (MOFA)	XIX-1
B. Design Review	XIX-1
C. Test-Plan Review	XIX-1
D. Test-Data Review	XIX-1
E. Maintainability Analysis	XIX-2
F. Reliability Prediction	XIX-2

UNCLASSIFIED

Report 10830-Q-4

FIGURE LIST

<u>Title</u>	<u>Figure</u>
MRpc and $P_{c,pc}$ vs Throat Area	III-1
MRpc and $P_{c,pc}$ vs Percent Oxidizer Resistance	III-2
MRpc and $P_{c,pc}$ vs Percent Fuel Resistance	III-3
MRpc and $P_{c,pc}$ vs Oxidizer Intensifier Pressure	III-4
MRpc and $P_{c,pc}$ vs Fuel Intensifier Pressure	III-5
Workhorse Primary Combustor Schematic	III-6
Performance Plot, Test 1.2-04-WAG-002	III-7
Combustion Chamber Liner after Test 1.2-04-WAG-003	III-8
Primary Combustor Injector and Turbine Simulator after Test 1.2-04-WAG-003	III-9
Performance Plot, Test 1.2-04-WAG-003	III-10
Performance Plot, Test 1.2-04-WAG-004	III-11
ARES Modular Performance Summary	IV-1
ARES Modular Injector-Chamber Configurations	IV-2
Combustion Loss vs Characteristic Length	IV-3
Mark-125 AE Secondary Injector	IV-4
Mark-125 AE Secondary Injector with Performance Ring	IV-5
Rake Injector with Shroud	IV-6
Injector Erosion after Test 1.2-11-WAM-014	IV-7
Injector Erosion after Test 1.2-11-WAM-015	IV-8
Transpiration-Cooled Distribution System	IV-9
Transpiration-Cooled Engine Schematic (Pump Fed)	IV-10
Transpiration-Cooled Engine Schematic (Intensifier Fed)	IV-11
B Design TPA Layout--Axial Dimensions	V-1
B Design TPA Layout--Radial Dimensions	V-2
B Design TPA Layout--Intensifier-Fed Primary Combustor - TPA Tests	V-3
Pump Diffuser Velocity Ratio	V-4
Mainstage Pump Design Parameters	V-5
Oxidizer Impeller	V-6
Fuel Impeller	V-7

UNCLASSIFIED

Report 10830-Q-4

FIGURE LIST (cont.)

<u>Title</u>	<u>Figure</u>
Shaft	V-8
B Design Turbine Rotor--Steady-State Tangential Stresses (Shallow Slot)	V-9
B Design Turbine Rotor--Steady-State Tangential Stresses (Deep Slot)	V-10
B Design Turbine Rotor--Tangential Stresses at 0.2 sec of Transient	V-11
Oxidizer Boost Pump Axial Thrust	V-12
Boost Pump and Hydraulic Turbine Water Test Fixture Layout	V-13
Inline Turbopump Assembly	VI-1
Engine Performance vs Stage-I Fuel Pump Thrust Balancer Recirculation Flow Rate	VI-2
Engine Performance Stage-II Fuel Pump Thrust Balancer Recirculation Flow Rate	VI-3
Thrust Balancer Flow Rate vs Axial Position, First-Stage Balancer	VI-4
Thrust Balancer Flow Rate vs Axial Position, Second-Stage Balancer	VI-5
Axial Forces as a Function of Thrust Balancer Position	VI-6
Rubbing Contact Seal for Inline TPA	VI-7
Alternative Hydrostatic Seal for Inline TPA	VI-8
Inline TPA Housing	VI-9
Components of Inline TPA Housing before Final Welding	VI-10
Stress Coat Test Housing A-1	VII-1
Stress Coat Test Results Of Housing A-1	VII-2
Housing A-1 Structural Test Setup	VII-3
Housing A-1 Deflection Indicator Locations	VII-4
Housing A-1 Strain Gage Locations	VII-5
Housing A-1 Oxidizer Dome End Deflections	VII-6
Housing A-1 Oxidizer Dome End Weld Repair	VII-7
Housing A-1 Roller Bearing Location Axial Deflections	VII-8
Housing A-1 100% Proof Pressure Deflection Data	VII-9
Housing A-2 Interpassage Leakage Area	VII-10

UNCLASSIFIED

Report 10830-Q-4

FIGURE LIST (cont.)

<u>Title</u>	<u>Figure</u>
Housing A-2 Wall Separation	VII-11
Housing A-2 Modified T-Flange	VII-12
Housing A-2 Oxidizer Dome End Plug Weld Repair	VII-13
Housing A-2 Oxidizer Dome End Plug Flange Weld	VII-14
Housing B Assembly	VII-15
Ball Bearing Cage Design	VIII-1
Roller Bearing Cage Design	VIII-2
Installation of Misaligned Roller Bearing for Test 1.2-03-WAW-006B	VIII-3
Tabulation of Steady-State Data Points of N_2O_4 Bearing Tests	VIII-4
ARES Ball and Roller Test 1.2-03-WAW-005A	VIII-5
ARES Ball and Roller Test 1.2-03-WAW-006B	VIII-6
Tabulation of Ball and Roller Bearing Critical Dimensions	VIII-7
ARES Tandem Ball and Roller Bearings from N_2O_4 Test 1.2-03-WAW-006B	VIII-8
ARES Ball and Roller Bearing Test 1.2-03-WAW-007	VIII-9
ARES Tandem Ball and Roller Bearings from N_2O_4 Test 1.2-03-WAW-007	VIII-10
Tabulation of Steady-State Data Points of AeroZINE 50 Bearing Test	VIII-11
K-5-H Outer Race Wear, Posttest 1.2-03-WAW-008	VIII-12
K-5-H Race and Roller Wear Measurements and Comparison to New K-5-H 4400 Rollers	VIII-13
Ball Bearing Cage Failure, Posttest 1.2-03-WAW-009	VIII-14
ARES Ball and Roller Bearing Test 1.2-03-WAW-010	VIII-15
ARES Tandem Ball and Roller Bearings from AeroZINE 50 Test 1.2-03-WAW-010	VIII-16
Relation Between Notch Burst Strength to Tensile Strength Ratio and Charpy V Notch Impact Energy Absorption at Test Temperature	VIII-17
Dovetail Insert for Impeller Wear Rings	IX-1
Reinforced Dovetail Insert for Impeller Wear Rings	IX-2

UNCLASSIFIED

Report 10830-Q-4

FIGURE LIST (cont.)

<u>Title</u>	<u>Figure</u>
Knurled Insert for Impeller Wear Rings	IX-3
Pressure-Relieved Insert for Impeller Wear Rings	IX-4
Felt-Metal Insert For Impeller Wear Ring	IX-5
Shell-Reinforced Insert for Impeller Wear Ring	IX-6
Hydrostatic Face Seal Stiffness and Clearance vs Impeller Angular Deflections	IX-7
Tabulation of Steady-State Hydrostatic Test Data Points	IX-8
Vespel SP-1 Insert in Flange after Rubbing Hydrostatic Test 4	IX-9
TEC Fluorfil BF ₃ Insert after Rubbing Hydrostatic Test 4	IX-10
Pump Leakage Rates Based upon Preliminary Test Data of Hydrostatic Test 4	IX-11
2D Test Segment	X-1
2D Test Summary	X-2
2D Seal Segments after Testing	X-3
2D Test Data, Test 030	X-4
Imbedded-Thermocouple Temperature versus Run Time and Shield Surface Temperature versus Combustion-Seal Mixture Ratio	X-5
Hydrostatic Combustion-Seal Tester--Cold-Rotating AeroZINE 50 Tests	X-6
Hydrostatic Combustion Seal in Tester--Cold AeroZINE 50 Tests	X-7
Flow Diagram, Rotating Fuel-Calibration Tests, ARES Hydrostatic Combustion-Seal Program	X-8
ARES Seal Test Data Sheet	X-9
Posttest 1.2-04-WAW-008 Seal Faces after Welding during Contact	X-10
Hydrostatic Combustion-Seal Performance, Test 1.2-04-WAW-011	X-11
Hydrostatic Combustion Seal after Test 1.2-04-WAW-011	X-12
Hydrostatic Combustion-Seal Performance, Test 1.2-04-WAW-012	X-13
Hydrostatic Combustion Seal after Test 1.2-04-WAW-012	X-14
Hydrostatic Combustion Seal in Tester (Hot Testing)	X-15
Hydrostatic Combustion-Seal Bellows Redesign	X-16
Seal Clearance and Distortion versus Internal Pressure	X-17
Hydrostatic Combustion-Seal Parameters during Engine Start Transient	X-18

x

UNCLASSIFIED

UNCLASSIFIED

Report 10830-Q-4

FIGURE LIST (cont.)

<u>Title</u>	<u>Figure</u>
ARES Suction Valve	XI-1
Primary Combustor Fuel Control Valve (Module)	XII-1
Secondary Combustor Fuel Control Valve (Module)	XII-2
Secondary Combustor Fuel Control Valve (Test)	XII-3
ARES Module Pressure Schedule, Advanced Turbopump Configuration	XIV-1
ARES Module Flow-Passage Design Requirements	XIV-2
Summary of ARES Module Operating Point	XIV-3
ARES Engine Module, External View	XIV-4
Test Installation Interface	XIV-5
ARES Prototype Model Performance	XVI-1
Performance of Several Nozzles Suitable for ARES Application	XVI-2
Effect of IES Area Ratio Variation	XVI-3
Results of Module-Skirt Merging Study and Effect of Arbitrarily Shortened Nozzle Skirt	XVI-4
Results of Cant Angle Study	XVI-5
Effect of Forced Base Bleed on Forced Deflection Nozzle Performance	XVI-6
Performance with 0, 1, and 2 Modules Out	XVI-7
Thrust Vector Misalignment with 1 and 2 Modules Out	XVI-8
Effect on Vacuum Performance of Engine Throttling by Module Shutdown	XVI-9
Large Radius Primary Combustor Centerbodies	XVII-1
Large Radius Centerbody Potential Flow Dynamic Pressures	XVII-2
Streak Plate Results for Large Radius Centerbodies	XVII-3
Streak Plate Results for Various Turbulator Positions	XVII-4
Streak Plate Results for Selected Configuration	XVII-5
Turbine Inlet Passage Model (L) Installation	XVII-6
Oxidizer Passage Models	XVII-7
Flow Distribution Parameter-Oxidizer Discharge Passage	XVII-8
Advanced Thermal Model	XVIII-1
ARES Prototype Transpiration-Cooled Chamber (Chamber Region) Individual Platelet Film Cooling Effectiveness (Hatch and Papell Model)	XVIII-2

UNCLASSIFIED

Report 10830-Q-4

FIGURE LIST (cont.)

<u>Title</u>	<u>Figure</u>
ARES Prototype Transpiration-Cooled Chamber Wall Temperature versus Length (0.021-in. Platelet)	XVIII-3
ARES Prototype Transpiration-Cooled Chamber Wall Temperature versus Length (Throat Section)	XVIII-4
N ₂ O ₄ Coolant Pressure Drop versus Flow Rate, Compartments 1, 2, 3, 5, and 10	XVIII-5
N ₂ O ₄ Coolant Pressure Drop versus Flow Rate, Compartments 4, 7, 9, and 12	XVIII-6
N ₂ O ₄ Coolant Pressure Drop versus Flow Rate, Compartments 6, 8, and 11	XVIII-7
Trichloroethylene Estimated Flow-Rate Ranges (lb/sec) for Reynolds No. Similarity	XVIII-8
Braze Bonded Laminated Tungsten Cermet Thermal Barrier	XVIII-9
Braze Bonding Microstructure	XVIII-10
Composition of Braze Bond Test Specimens	XVIII-11
Braze Bonding Test Results	XVIII-12
Advanced TPA-B Design Stator, Time = 20 sec	XVIII-13
Advanced TPA-B Design Stator, Steady State	XVIII-14
Advanced TPA-B Design Stator Boundary Conditions	XVIII-15
Mass Flow Distribution around Primary Fuel Injector	XVIII-16

CONFIDENTIAL

Report 10830-Q-4

I.

INTRODUCTION

(u) The principal objective of the ARES (Advanced Rocket Engine-Storable) Program is to demonstrate the engineering practicality and performance characteristics of a high-chamber-pressure staged-combustion engine module.

(u) The modular engine is a highly integrated assembly in which the turbopump assembly housing combines the fuel and oxidizer pumps, the turbine, the engine controls, and the primary combustor chamber into a single assembly. Turbine exhaust is ducted directly into the secondary combustion chamber, where additional fuel is added. The resultant combustion products are exhausted through a cooled 20:1 area-ratio nozzle. Thrust from the rocket nozzle is transmitted through the turbopump assembly housing to the vehicle frame.

(c) The engine is designed to produce 100,000 lb of thrust at sea level and operates at a secondary combustion chamber pressure of 2800 psia using N_2O_4 and AeroZINE 50 as propellants. The engine module is designed for ready use either as a single unit, in parallel-axis clusters, or in forced-deflection or plug-nozzle propulsion systems.

(c) The modular engine uses a staged-combustion cycle in which all the oxidizer and 19% of the fuel are injected into the primary combustor at 4775 psia to produce a turbine working fluid at approximately $1240^\circ F$. This fluid passes through the turbine, which operates at a pressure ratio of about 1.5, at a mixture ratio of 11.5, and passes through the secondary combustor injector where additional fuel is added to produce a mixture ratio of 2.1 in the thrust chamber. The resultant combustor products exhaust through the nozzle producing thrust.

(u) Engine control is achieved through the use of eyelid valves (located at pump suction) wherein the segment of a ball is rotated out of the flow stream and admits propellant to the engine. For the development engine, auxiliary fuel control valves are installed to govern fuel admittance to the primary and secondary combustion chambers during transient and steady-state operation. All valves are powered independently to achieve the flexibility desired during the program.

(c) The secondary combustor uses a flameholder injector consisting of a series of radial vanes from which fuel is injected into the oxidizer-rich turbine exhaust stream. The resulting mixture burns in the thrust chamber and is exhausted through the nozzle. Two cooling systems are under consideration for the modular engine. These employ regenerative and transpiration cooling. The regeneratively cooled system uses a considerable number of thin wafers that are chemically milled to produce the desired pressure-drop pattern required to control the coolant flow.

(u) Phase I of the two-phase program is devoted principally to the development of individual components such as cooled combustion chambers, injectors, turbopump housings, bearings and seals, suction valves, and engine fuel controls.

CONFIDENTIAL

Report 10830-Q-4

I, Introduction (cont.)

The Phase II program is devoted to performance improvement of the thrust-chamber components, development of the turbopump system, and the integration of turbopump, thrust chamber, and controls into an engine module.

(u) This report, covering activity during the fourth quarter of the program, is organized into four groups of sections. The first group, Sections III and IV, covers the combustion system development effort. Sections V through X cover the turbopump design and development tasks. Controls are reported in Sections XI through XIII. The remaining sections, XIV through XIX, cover the activity associated with the propulsion system as well as a series of related analytical activities.

Page I-2

(This page is Unclassified)

CONFIDENTIAL

CONFIDENTIAL

Report 10830-Q-4

II.

SUMMARY

(u) Major mileposts in the thrust chamber, turbopump, and controls areas were met during the fourth quarter of the ARES program. The primary combustor was completed and testing initiated, a secondary combustor injector was selected, a number of requirements for propellant-lubricated tests were met successfully, suction valves and fuel-control valves were successfully tested, and the aerodynamics test program at Fluidyne Corporation was completed. Considerable effort was devoted to accelerating the completion of critical components required to support the test program.

(u) A major primary-combustor milepost was met with the conversion of Test Stand H-3, the installation of the workhorse primary combustor, and the completion of the first six tests, four of which are reported in Section III. During Test 3, the primary combustor liner was damaged, and oscillations of 600 cps were observed throughout the combustion and hydraulic circuits during Tests 2, 3, and 4. The cause of the anomalies was identified correctly, as verified by the elimination of these oscillations in Tests 5 and 6, in which the oxidizer injector ΔP was increased and straightening vanes were added in the combustion zone.

(c) The Mark-125 injector has been selected for use throughout the remainder of Phase-I testing because of its demonstrated superior performance over that of the Rake injector. With a demonstrated performance of 93.5% of theoretical specific impulse, the Mark-125 injector should be adequate for demonstrating Phase-I performance goals.

(u) Eleven secondary combustor tests were conducted. Fifteen tests, including five tests conducted in the last week of March, are summarized in Section IV. Mark-125 injectors experienced erosion damage due to fuel leakage on three unrelated occasions.

(u) The transpiration-cooled combustion chamber was completed and will be tested in July. Three regeneratively cooled combustion chambers are being assembled, the first of which is scheduled for completion in mid-July.

(u) The advanced-TPA housing was pressure-tested and exceeded 100% of proof pressure for a short time in one of the tests. A revised pressurization system is being obtained to allow testing over durations specified by the Work Statement.

(u) Fabrication of the inline TPA housing was completed, and the housing will be tested in the near future.

(u) Excellent results were obtained in the bearing test program. Ball and roller bearings were demonstrated successfully (1) at 31,250 rpm in N_2O_4 and AeroZINE 50 and (2) at 40,000 rpm in N_2O_4 . Cage problems caused failures during the fuel-lubricated 40,000-rpm tests, and new cages were therefore ordered. Testing will resume late in July.

CONFIDENTIAL

Report 10830-Q-4

II, Summary (cont.)

(u) Turbopump wear-ring development testing was delayed because of utilization of the test heads for bearing and seal testing in preference to wear-ring testing. A new turbopump housing was received, and six tests were conducted with water as a working fluid. Of the three tests reported, one was nonrotating with stepped labyrinths and two were rotating tests using straight labyrinths. The flow before and after rubbing on one of the tests was essentially the same, and no damage to the hardware occurred.

(u) Twelve tests of the hydrostatic combustion seal are reported. The test series culminated with two successful cold-rotating tests of 84- and 78-sec duration, respectively.

(u) Eleven segment tests were conducted on the two-dimensional tester to evaluate a 0.001-in.-wide slot. This narrow slot closed because of thermal expansion during preburner operation, calling attention to the possibility of difficulties during the hot rotating testing of the hydrostatic combustion seal.

(u) The design of the hydrostatic combustion seal was modified to incorporate a two-ply bellows of revised configuration. This revised design strengthens the resistance to external pressure by a factor of eight.

(u) Testing of the experimental suction valves has been conducted satisfactorily. Design of a prototype version was completed and fabrication has been initiated. A satisfactory technique for electron-beam-welding of the storage seal has been developed.

(u) Testing of the primary and secondary fuel-control valves was completed. Modular configurations of these valves have been designed and are being fabricated. The primary combustor fuel-control valve will begin testing in July; the secondary valve is being tested, and results will be reported after conclusion of this effort.

(u) All analytical and testing efforts to date continue to validate the feasibility of the ARES advanced engine concept.

UNCLASSIFIED

Report 10830-Q-4

III.

PRIMARY COMBUSTOR ASSEMBLY

A. GENERAL

(u) A major milestone in the primary combustor assembly program was met this quarter: fabrication of the workhorse primary combustor housing was completed and the primary combustor test program was initiated. Four tests have been made to date.

(u) Detailed discussions of the design and fabrication effort for the primary combustor assembly are given in Section III,B, below, and a detailed discussion of the test program is presented in Section III,C.

B. PRIMARY COMBUSTOR ASSEMBLY--DESIGN AND FABRICATION

1. Summary

(u) The design and fabrication activities on the primary combustor program were continued. Principal design activities involved (1) redesign of the primary injector orifices to increase pressure drop, (2) redesign of the liner for increased stiffness and incorporation of gas-flow-distribution vanes, (3) completion of detailed turbulator designs for the primary combustor, and (4) completion of the injector layout for the Mod-B turbopump assembly (three-walled housing). Principal fabrication activity included completion and build-up of the first primary combustor workhorse housing assembly, hydrotesting the assembly to proof conditions, flow-testing the housing both with and without injectors, and delivery of the completed assembly to the test area. In addition, the primary combustor turbulators were completed, liner stiffeners and distribution vanes were completed, and substantial fabrication progress was made toward completion of the second primary combustor housing.

(u) Primary combustor testing was initiated, and four successive tests have been performed. The description and results of these tests are presented in Section III,C.

2. Injectors

(u) Flow tests were performed on each of the three primary combustor injectors. Two of the three injectors, the full-flow and the quadlet, yielded flow resistances in the oxidizer circuit considerably different from calculated design values, but the pentad injector offered flow resistances (for both the fuel and the oxidizer) in reasonable agreement with the calculated design values.

(u) Investigations of the pressure-drop discrepancies detected for the full-flow and the quadlet injectors revealed that the outside supplier had furnished Aerojet-General with face material (Rigimesh) of wrong porosity for the full-flow injector, which resulted in an extremely high pressure-drop. In the quadlet design, the pressure drop was found to have been caused by an orifice sizing error in combination with the selection of a discharge coefficient that was too low.

UNCLASSIFIED

Report 10830-Q-4

III, B, Primary Combustor Assembly--Design and Fabrication (cont.)

(u) The following paragraphs present additional information on each of the injector designs.

(u) Proof, leak, flow, and pattern check tests were performed on the pentad injector. Pressure drops of 230 psi in the oxidizer circuit and of 408 psi in the fuel circuit were measured; the nominal design pressure-drop values for all injectors are 300 and 400 psi, respectively, for the two circuits. No modifications of this injector are currently planned because the measured pressure drops agree reasonably well with the planned values.

(u) The first flow test of the full-flow injector showed that the pressure drop of the oxidizer circuit exceeded the design calculations by 2230 psi. It was found that the porous face material was 75% denser than called for by the design. In an attempt to increase the effective flow area, an acid mixture of water, hydrochloric acid, nitric acid, and ferritic chloride was flowed through the porous injector face to chemically etch-out some of the obstructing material. This operation reduced the pressure drop to 1161 psi. Based on subscale experiments and on the etching attempt on this injector, it was determined that the etching operation was not sufficiently predictable. It was therefore decided to remove the injector face and to replace the porous material with material of proper porosity. A sample of the new porous material has been received, and flow-testing confirmed that the material has the proper porosity. Installation of the new porous material will be completed early in July 1966. The flow test of the fuel circuit on the full-flow injector showed a measured pressure drop of 444 psi, which is considered satisfactory.

(u) The first flow test of the quadlet injector yielded the following pressure-drop data: 602 and 63 psi for the fuel and oxidizer circuits, respectively. An error in tube sizing combined with the selection of an assumed discharge-coefficient value which was too low caused the very low pressure-drop in the oxidizer circuit. However, the pressure drop in the fuel circuit, although high, is considered satisfactory.

(u) A flow test was performed on samples of the porous face material from which the quadlet injector is made to determine the flow rate through the actual porous face material under steady-state conditions. The measured flow rate was 80% of the calculated design value, which is considered satisfactory.

(u) After the initial hot-firing tests were completed, the quadlet injector was returned to the shop for rework. Tubes of 0.180-in. ID were welded inside of the existing 0.242-in. ID oxidizer tubes. The revised configuration showed a measured pressure drop of 264 psi, which is satisfactory.

(u) A layout was completed of a new injector designed to fit the Mod-B three-walled TPA housing. This injector can be made from the Mod-A injector by machining metal from the turbine stator interface and from the backside of the injector fuel manifold. Matching grooves, machined into the housing and injector body, provide a positive locking method for the injector by the use of a retaining

CONFIDENTIAL

Report 10830-Q-4

III, B, Primary Combustor Assembly--Design and Fabrication (cont.)

ring. In addition to its restraining function, the retaining ring also acts as a seal because it replaces the second expanding N_2O_4 -sealing ring used in the Mod-A design.

3. Workhorse Primary Combustor Housing (WPCH)

(u) As reported in the previous quarterly report, the first WPCH (SN-1) cracked severely and had to be scrapped. This caused considerable delay and corrective action was therefore immediately instituted for Housing SN-2 to prevent a recurrence. Accelerated schedules were implemented to regain the lost time as fast as possible. The fabrication and assembly of WPCH SN-2 was subsequently completed successfully. The assembly was proof-, leak-, and flow-tested and the finished unit was delivered to the test area, installed on the test stand, and successfully test-fired in four successive tests. A discussion of these tests is presented in Section III,C.

(u) Inspection of the test records and of the test hardware showed evidence of high-amplitude pressure oscillations. Following the initial test series, the housing was therefore disassembled and returned to the machine shop for various machining operations including the installation of high-frequency (Photocon) instrumentation ports. These ports will provide means for accurately recording the pressure oscillations in the primary combustor during the next test series.

(u) The WPCH was then used for hydrotesting the reworked injectors. At the end of this reporting period, the reworked quadlet injector was assembled into the reworked housing and the entire assembly was returned to Test Stand H-3 for installation.

(u) WPCH SN-3 is being fabricated using the same heat treatments and welding procedures as for WPCH SN-2. Joining of the insert to the outer housing, final-machining, and hydrotesting are scheduled to be completed by mid-July.

4. Other Primary Combustor Components

(u) The chamber liner of WPCH SN-2 was slightly damaged during the initial test series. To prevent a recurrence, a reinforcing band of 0.063-in.-thick by 1.60-in.-wide sheet metal was TIG tack-welded around the OD of the liner. This band should prevent further cracking of the slotted elements. Five vanes were also welded inside the liner. These vanes are designed to prevent tangential pressure oscillations.

CONFIDENTIAL

Report 10830-Q-4

III, Primary Combustor Assembly (cont.)

C. DEVELOPMENT TESTING

1. Summary

(u) The development program for the primary combustor was initiated, and four tests were conducted. Prior to testing, detailed steady-state and transient analyses were performed to determine both the proper engine sequences and the operating balance point. The transient analysis indicated that oxidizer-manifold fill time is critical for obtaining the correct start transient; it was therefore decided to perform a cold-flow test of the oxidizer circuit only, before initiating the hot firing tests. Furthermore, the first hot-firing test series was designed to verify start-transient operation only, by ending each successive test later during the start transient, at times indicated as significant by the transient computer program. This step-wise approach also provided maximum protection for the limited and expensive hardware prior to committing the combustor to full-duration testing.

(c) In accordance with the test plan, the first test was an oxidizer flow test only; the three other tests were start-transient hot firings. Maximum chamber pressure attained was 3450 psia, and minimum mixture ratio during the start transient was about 22. Nominal steady-state conditions for this series of tests would be a pressure of 4775 psia and a mixture ratio of 14.0.

(u) Examination of test records revealed persistent feed-system-coupled oscillations of about 600 to 700 cps. A detailed investigation to determine the exact nature of the oscillations, their cause, and the required modifications to prevent a recurrence, is being performed. Since this test series was performed during the closing week of this quarter, no conclusions have yet been drawn.

(u) The analytical effort performed in preparation for primary combustor testing is described in Paragraph III,C,2, below. A description of the engine test system is given in Paragraph III,C,3, whereas a detailed discussion of each test is presented in Paragraph III,C,4.

2. Analysis

a. Steady-State Analysis

(u) A series of steady-state computer runs were made to determine the effect of parameter variations on the balance point of the modular primary combustor. The parameters varied were: throat area, oxidizer system resistance, fuel system resistance, oxidizer intensifier pressure, and fuel intensifier pressure.

(u) In operation, nominal balance is obtained first, and then the parameters are varied one at a time in series. The combustor readjusts itself to the new operating conditions by varying its chamber pressure and mixture ratio. The nominal value for any parameter is restored at the time a new parameter variation is begun.

UNCLASSIFIED

Report 10830-Q-4

III, C, Development Testing (cont.)

(u) The mixture ratio for the first steady-state duration test was to be 14.0 and the pressure 4775 psig. Figure III-1 shows a mixture-ratio shift from 14.07 to 13.57 with a 10% increase in throat area, and a chamber-pressure decrease from 4775 to 4664 psig with the same throat growth. There is little change in chamber pressure with throat growth due to the ability of the intensifiers to maintain their pressure at the required increase in propellant flow rate.

(u) A change in oxidizer system resistance from +20 to -20% results in a minimum mixture ratio of 12.6, as a maximum pressure of 4823 psia, and at opposite ends of the range, as noted in Figure III-2. Since the design mixture ratio is 11.5 and the proof pressure is 7200 psig, both of the above extremes are considered safe.

(u) A similar change in fuel-system resistance results in a mixture-ratio range of 15 to 12.85 and in a pressure range of 4708 to 4852 psia. From Figure III-3 it is noted that the extremes of mixture ratio and pressure occur simultaneously at -20% fuel resistance. The hardware should be capable of withstanding this extreme without difficulty.

(u) A 400-psi decrease in oxidizer intensifier pressure would result in a mixture ratio of about 11.0. However, Figure III-4 indicates this would occur at less than 4775 psig and is unlikely to happen since all intensifier data indicate an overshoot rather than an undershoot of set pressure. The cool gas at a mixture ratio of 17, which is attendant to an oxidizer overpressure of 400 psig, reduces the possibility of damage at the overpressure of 4847 psia.

(u) Figure III-5 demonstrates that a 400-psig overpressure of the fuel intensifier would simultaneously decrease the mixture ratio and increase the pressure to levels below and above those desired, respectively. Experience with the fuel intensifier has demonstrated close control of fuel pressure. In addition, the period of maximum overpressure of fuel occurs simultaneously with a like excursion of oxidizer intensifier pressure on start. The result would be a higher pressure, but at a higher mixture ratio and at a lower temperature than the nominal conditions.

b. Transient Analysis

(u) The method of analyzing the system transients of Test Stand H-3 was similar to that used on the sector engine of Test Stand H-2. An analytical model of the system was constructed. The same analytical theories and techniques that were used successfully on Test Stand H-2 were used on the modular primary analysis. The waterhammer wave equations describing the system were solved continuously by the method of characteristics on a digital computer.

(u) The design of the primary combustor and its installation on the test stand were studied in detail to determine problem areas affecting the

UNCLASSIFIED

Report 10830-Q-4

III, C, Development Testing (cont.)

start and shutdown transients. Special attention was directed toward propellant phasing and purging during these two phases. The overall goal of this program was mixture-ratio control during transient operations. On the basis of this study, it was concluded that a cold-flow test of the oxidizer circuit should be performed to ascertain the fill characteristics of the complex manifolding.

(u) The analytical model was used to determine valve sequencing, the preset pressures for the propellant intensifier, the time of ramp initiation, and the feed-pressure ramp-rise rate for the start and the valve sequence on shutdown. Because of the complexity of the oxidizer manifold, the oxidizer cold-flow Test 1.2-04-WAG-001 was used to verify the time required to fill the manifold. The model predicted a time of 0.290 sec, whereas test data showed a time of 0.255 sec. Therefore, confidence in the predicted propellant phasing was established.

(u) The analytical model predicted a high chamber-pressure spike at ignition (i.e., about 1800 psia) and chamber-pressure oscillations of 250 millisecc caused by chamber combustion coupled with the waterhammer in the feed system. The model predicted these chamber-pressure oscillations would dampen out by FS-1 + 1.0 sec. To verify these predictions, it was decided to conduct two short-duration tests: one of a 0.90-sec duration to check out the ignition characteristics of the primary, and one of 1.1-sec duration to determine if the feed-system oscillations would dampen out.

3. Engine Description

(u) The modular primary combustor, as installed on Test Stand H-3, consists of the workhorse primary housing, the quadlet injector, the reverse-flow combustion chamber, the turbine-simulator nozzle assembly, the secondary combustor diffuser section, and the burnoff stack assembly. A schematic drawing of the test setup is presented in Figure III-6. The burnoff stack assembly is used to burn off oxidizer-rich gases produced by the primary combustor.

(u) The propellant-distribution system receives high-pressure propellant from the intensifiers on the second level to Test Stand H-3 through 3- and 4-in.-dia SCH-XX pipe. The oxidizer flows through a flowmeter and a 2-1/2-in.-dia ball valve into the hardware, whereas the fuel flows through a flowmeter and a 1-in.-dia ball valve into the hardware. There is a blanked-off 3-in. tap for future use to supply secondary combustor fuel.

(u) Tests 1.2-04-WAG-001 through -003 were performed with the combustion-chamber liner in place. Test 1.2-04-WAG-004 was performed without this liner to determine if the liner had any effect on chamber-pressure oscillations.

(u) The feed line pressures were monitored with both static and dynamic transducers. Combustion-chamber performance was measured with three Taber transducers and five high-response thermocouples. Exhaust gases were monitored with one Taber pressure transducer and three high-response thermocouples.

CONFIDENTIAL

Report 10830-Q-4

III, C, Development Testing (cont.)

(u) Flush-mounted photocon pressure transducers will be used for the next primary combustor tests.

4. Tests

a. Test 1.2-04-WAG-001

(1) Purpose

(u) This test was a cold oxidizer-flow test for the purpose of obtaining information required to verify or modify the analytical transient model and the firing sequence of hot testing. The questions to be answered by this test were: (a) When does the oxidizer manifold fill with liquid? (b) Does the combustion chamber fill with liquid oxidizer? (c) What is the fuel manifold pressure during fuel fill? (d) Do the intensifiers provide the desired pressure rise rates? (e) What electrical-mechanical sequence delays are present? and (f) Does the burn-off stack ignite and eliminate excess oxidizer?

(2) Attempted

(c) A full engine firing sequence was attempted, with the fuel-valve discharge and the fuel-injector manifold blanked-off. Excessive pressure drop across the injector face was eliminated by limiting the upper pressure setting for the oxidizer intensifier to 2500 psi. The dead-headed condition of the fuel intensifier was considered to be equivalent to flow conditions since the piston displacement due to compressibility was very nearly equal to the test condition.

(3) Obtained

(u) A duration of 1.7 sec with oxidizer flow only.

(4) Discussion

(a) Test Hardware

(u) All hardware was undamaged.

(b) Test

(u) The oxidizer manifold filled 35 millisecc earlier than estimated; 200 millisecc later the combustion chamber filled with liquid oxidizer producing a fuel manifold pressure of 30 psia. A nitrogen purge in the fuel manifold will be used during hot firing to prevent entry of oxidizer during fuel fill. All electromechanical sequence delays were close to estimates. The burnoff stack worked well, although stack ignition was later than desired due to the long filling time of the RP-1 circuit. Subsequent testing would initiate filling 0.5 sec earlier.

CONFIDENTIAL

Report 10830-Q-4

III, C, Development Testing (cont.)

(c) The oxidizer intensifier created the required rise rate up to a pressure of 2500 psia. The fuel intensifier pressure did not rise until 0.100 sec after the expected ramp initiation and then rose at a rate limited by the flow capacity of the 2-in.-dia valve. The ramp rise was clearly out of control since the fuel-system GN_2 -flow-control valve was fully open until steady state.

(u) Several tests were subsequently made in which fuel-intensifier control-valve operation, ullages, and amplifier gains were varied to obtain a satisfactory fuel-pressure rise rate prior to the first hot firing.

b. Test 1.2-04-WAG-002

(1) Purpose

(u) This short-duration test was performed to determine the fuel-manifold and ignition characteristics of the quadlet injector.

(2) Attempted

(u) A 0.9-sec-duration test with full primary combustor firing sequence.

(3) Obtained

(c) The test, of 0.917-sec duration, was performed on 8 June 1966 to a maximum chamber pressure of 2053 psia and a mixture ratio of about 30.

(4) Discussion

(a) Test Hardware

(u) The test hardware showed some minor chamber-liner heat marks, but was otherwise capable of refiring.

(b) Test

(u) At FS-1, both valves were signaled open. The oxidizer valve and the fuel valve opened in 0.4 and 0.9 sec, respectively. The oxidizer intensifier pressure began its ramp at 0.69 sec and continued upward until 1.00 sec when its rise rate began to decrease. Pressure appeared to be following its programmed rise rate.

(u) The fuel intensifier began its pressure rise ramp at 0.70 sec and continued to rise virtually linearly until 1.0 sec when its rise rate began to decrease.

CONFIDENTIAL

Report 10830-Q-4

III, C, Development Testing (cont.)

(u) Ignition began at 0.777 sec; chamber pressure rose in accordance with the high initial fuel flow rate, then rapidly decreased as fuel flow decreased in response to the resistance offered by chamber pressure. Both pressure and flows then increased with the intensifier ramps until 1.071 sec when closing of the fuel valve began to reduce fuel weight flow. Shutdown was normal.

(u) The oscillograph traces indicated a 600-cps cycle oscillation on all chamber- and feed-system pressure traces. This was attributed to waterhammer in the feed system caused by the ignition spike and by the off-design operating conditions. Preparations were therefore made to increase the duration of Test 1.2-04-WAG-003 to 1.1 sec.

(u) A performance plot for this test is presented in Figure III-7.

c. Test 1.2-04-WAG-003

(1) Purpose

(u) The purpose of this test was to provide sufficient duration to determine if the feed-system induced chamber-pressure oscillations, predicted by the transient computer program, would dampen out.

(2) Attempted

(u) The test was performed on 9 June 1966 with an intended duration of 1.1 sec and an intended chamber pressure of 2500 psia.

(3) Obtained

(u) Test duration was 1.115 sec, with the intensifiers providing excellent pressure ramps.

(4) Discussion

(a) Test Hardware

(u) The combustion-chamber liner was damaged, as shown in Figure III-8, but the remainder of the hardware was in good condition, as illustrated in Figure III-9:

(b) Test

(u) The oscillograph traces exhibited the same 600-cps oscillations as in the previous test, with no sign of any decrease in amplitude or change in frequency. Two microsystem transducers installed on the propellant feed lines yielded the following data:

CONFIDENTIAL

Report 10830-Q-4

III, C, Development Testing (cont.)

(c)

<u>Transducer</u>	<u>Time, sec</u>	<u>Frequency, cps</u>	<u>Peak-to-Peak Amplitude, psi</u>
PFD-F(M)	0.973	580	60
	1.115	640	130
	1.125	640	160
	1.178	640	195
FOD-F(M)	0.973	600	55
	1.115	620	110
	1.125	660	150
	1.178	680	305

(c) Maximum chamber pressure was 3380 psia, and the minimum mixture ratio was about 23.

(u) Performance plots for this test are presented in Figure III-10.

d. Test 1.2-04-WAG-004

(1) Purpose

(u) This test was made to obtain additional firing data at higher pressure and temperature for determining if the 600-cps oscillations would continue without the chamber liner and at a lower mixture ratio.

(2) Attempted

(u) This test was to be a 1.2-sec-duration test of the quadlet injector and workhorse primary combustor, without the chamber liner.

(3) Obtained

(u) The test, conducted on 14 June 1966, had a duration of 1.211 sec. Intensifier operation and sequencing were as programmed.

(4) Discussion

(a) Test Hardware

(u) The test hardware was undamaged and capable of refiring.

CONFIDENTIAL

Report 10830-Q-4

III, C, Development Testing (cont.)

(b) Test

(u) The oscillograph traces again exhibited oscillations with the same frequency on all chamber and feed-system parameters. Toward the end of this extended-duration test, a trend toward a higher frequency was noted, which is attributed to the higher gas temperature caused by the lower mixture ratio attained.

(u) High-frequency tape data were analyzed to determine the exact frequencies and their amplitudes. These data are summarized in the following tabulation:

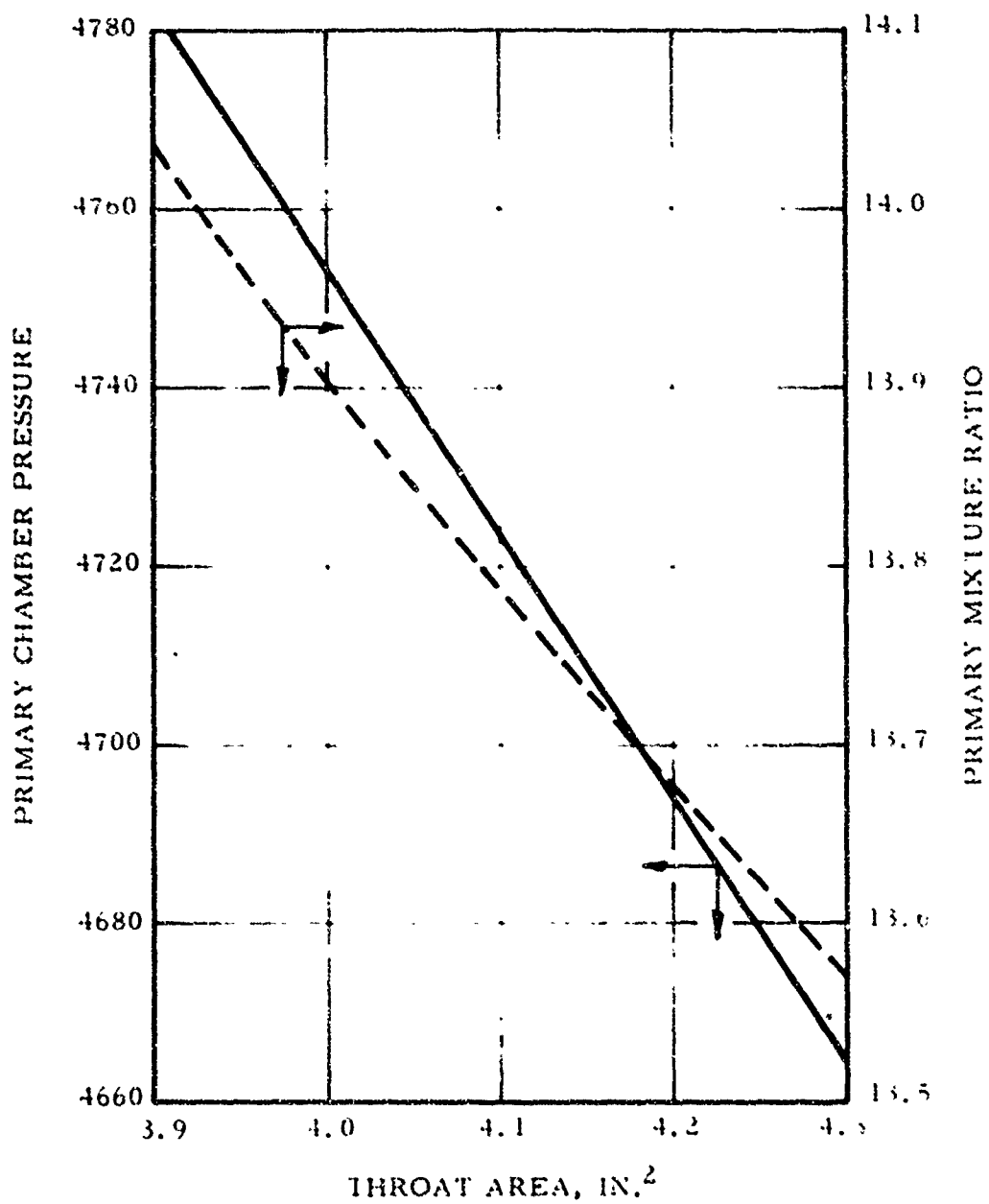
<u>Transducer</u>	<u>Time, sec</u>	<u>Frequency, cps</u>	<u>Peak-to-Peak Amplitude, psi</u>
PFD-F(N)	0.618	450	75
	0.973	0	---
	1.115	630	250
	1.211	680	215
	1.261	1480	120
PoD-F(N)	0.618	350	80
	0.973	0	---
	1.115	630	320
	1.211	680	400
	1.261	740	160

(c) Maximum chamber pressure was 3450 psia and minimum mixture ratio was about 22.

(u) A performance plot for this test is shown in Figure III-11.

UNCLASSIFIED

Report 10830-Q-4



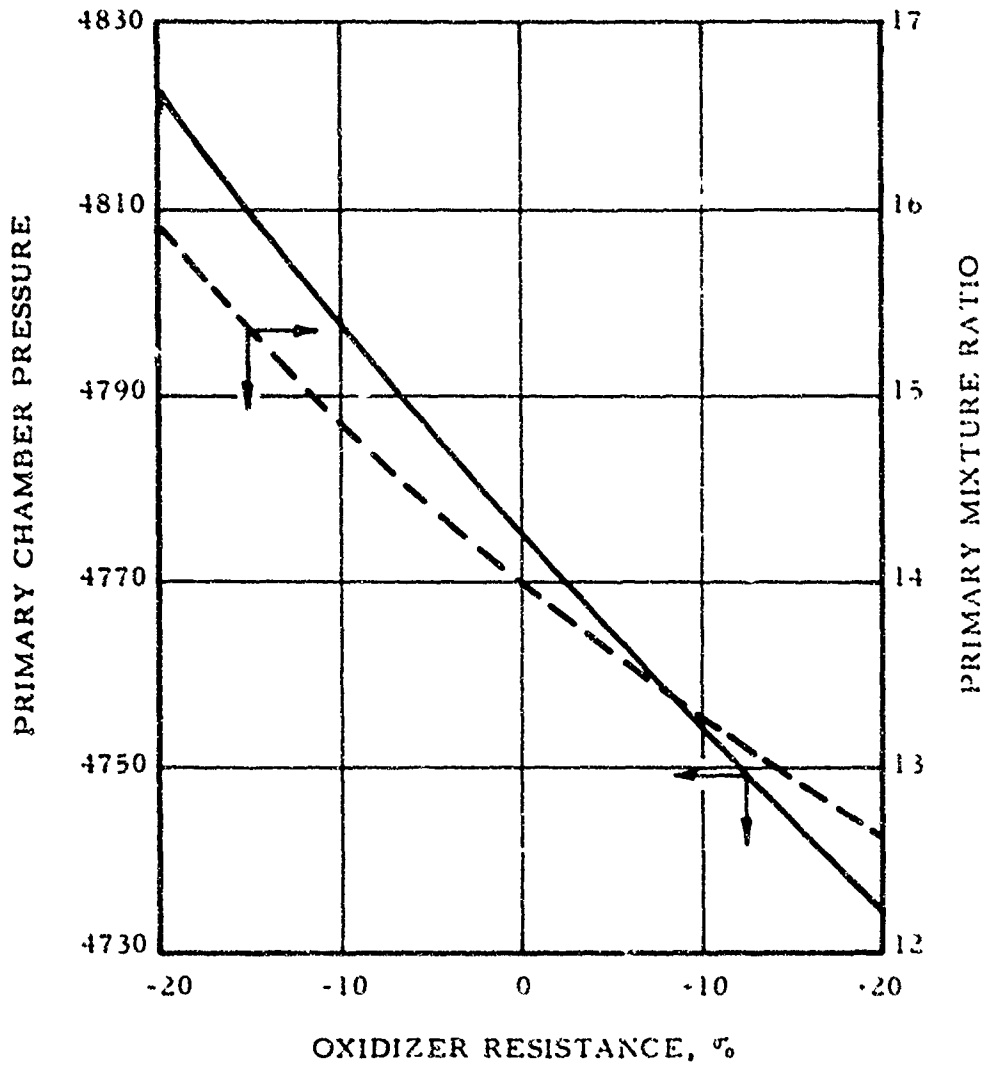
MR_{pc} and P_{c pc} vs Throat Area

Figure III-1

UNCLASSIFIED

UNCLASSIFIED

Report 10830-Q-4



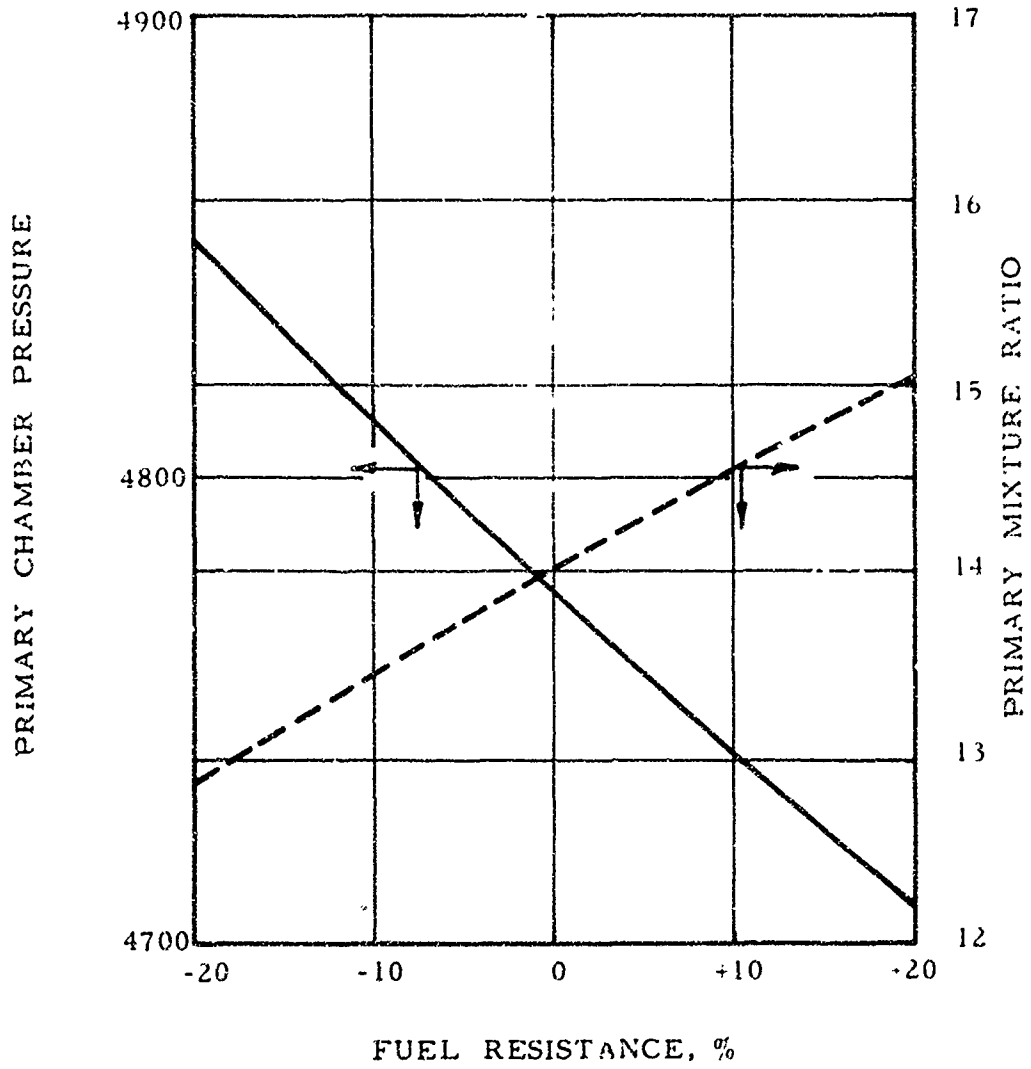
MR_{pc} and P_{pc} vs % Oxidizer Resistance

Figure III-2

UNCLASSIFIED

UNCLASSIFIED

Report 10830-Q-4



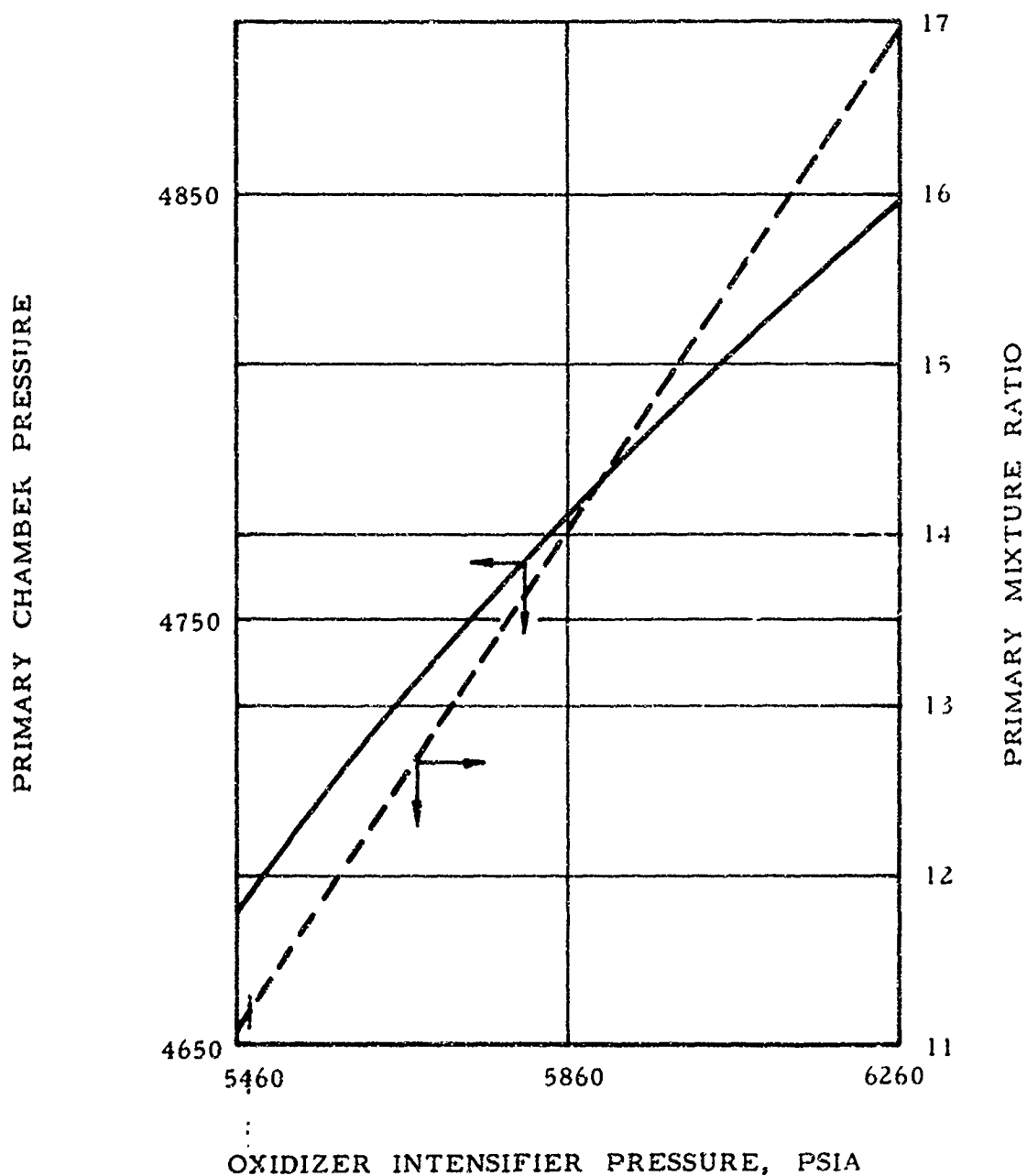
MR_{pc} and P_{c pc} vs % Fuel Resistance

Figure III-3

UNCLASSIFIED

UNCLASSIFIED

Report 10830-Q-4



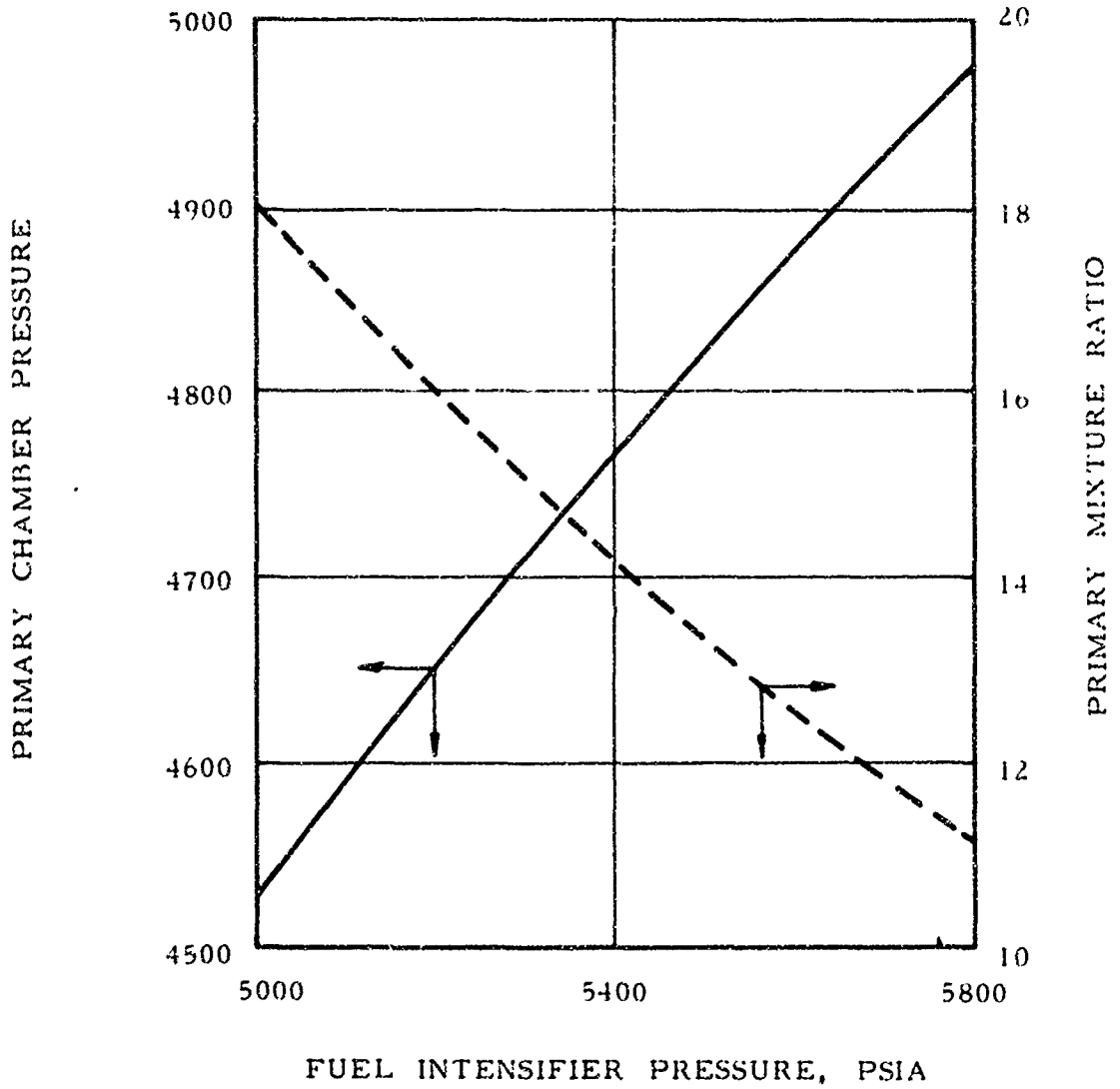
MR_{pc} and P_{cpc} vs Oxidizer Intensifier Pressure

Figure III-4

UNCLASSIFIED

UNCLASSIFIED

Report 10830-Q-4



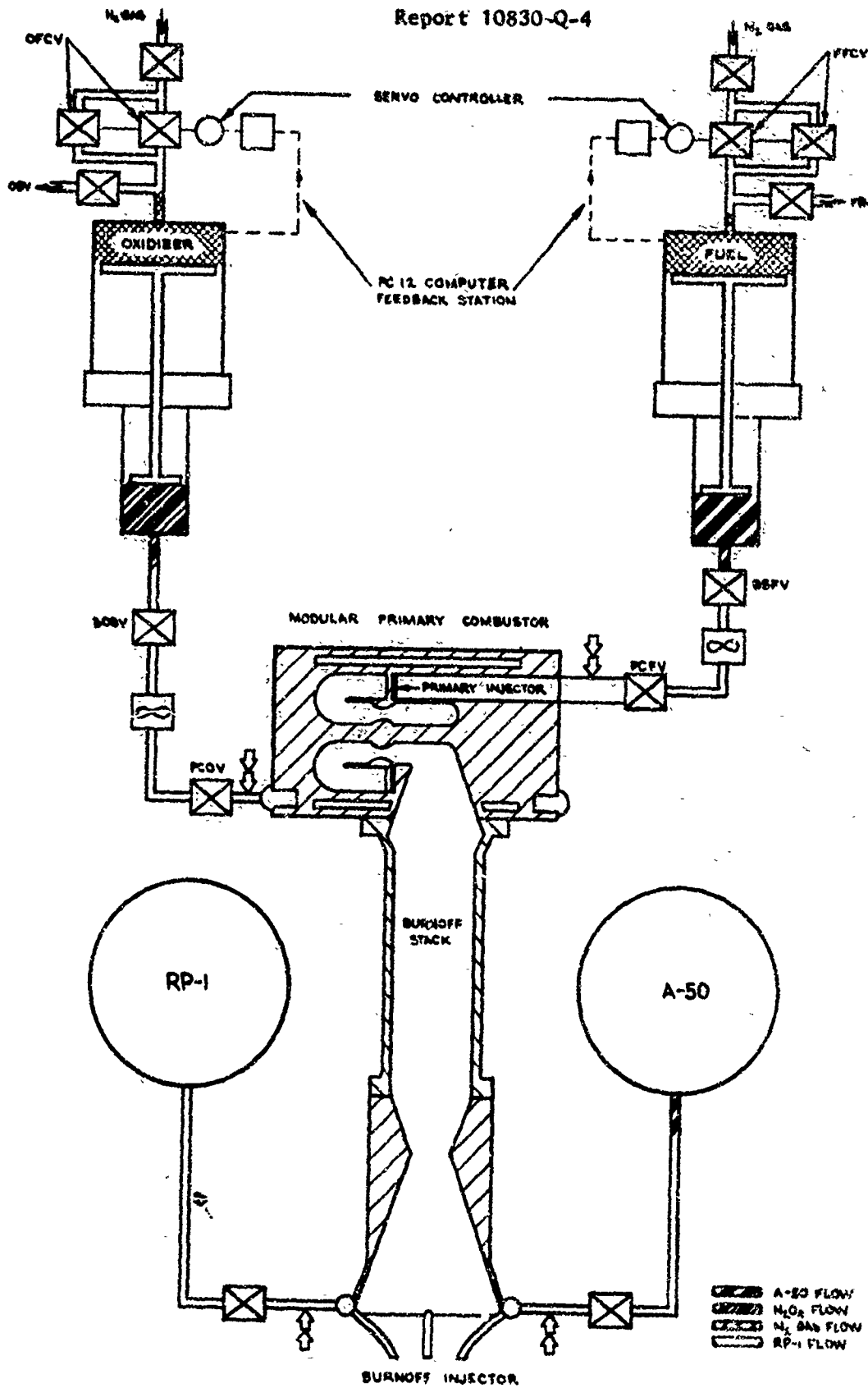
MR_{pc} and P_{cpc} vs Fuel Intensifier Pressure

Figure III-5

UNCLASSIFIED

UNCLASSIFIED

Report 10830-Q-4



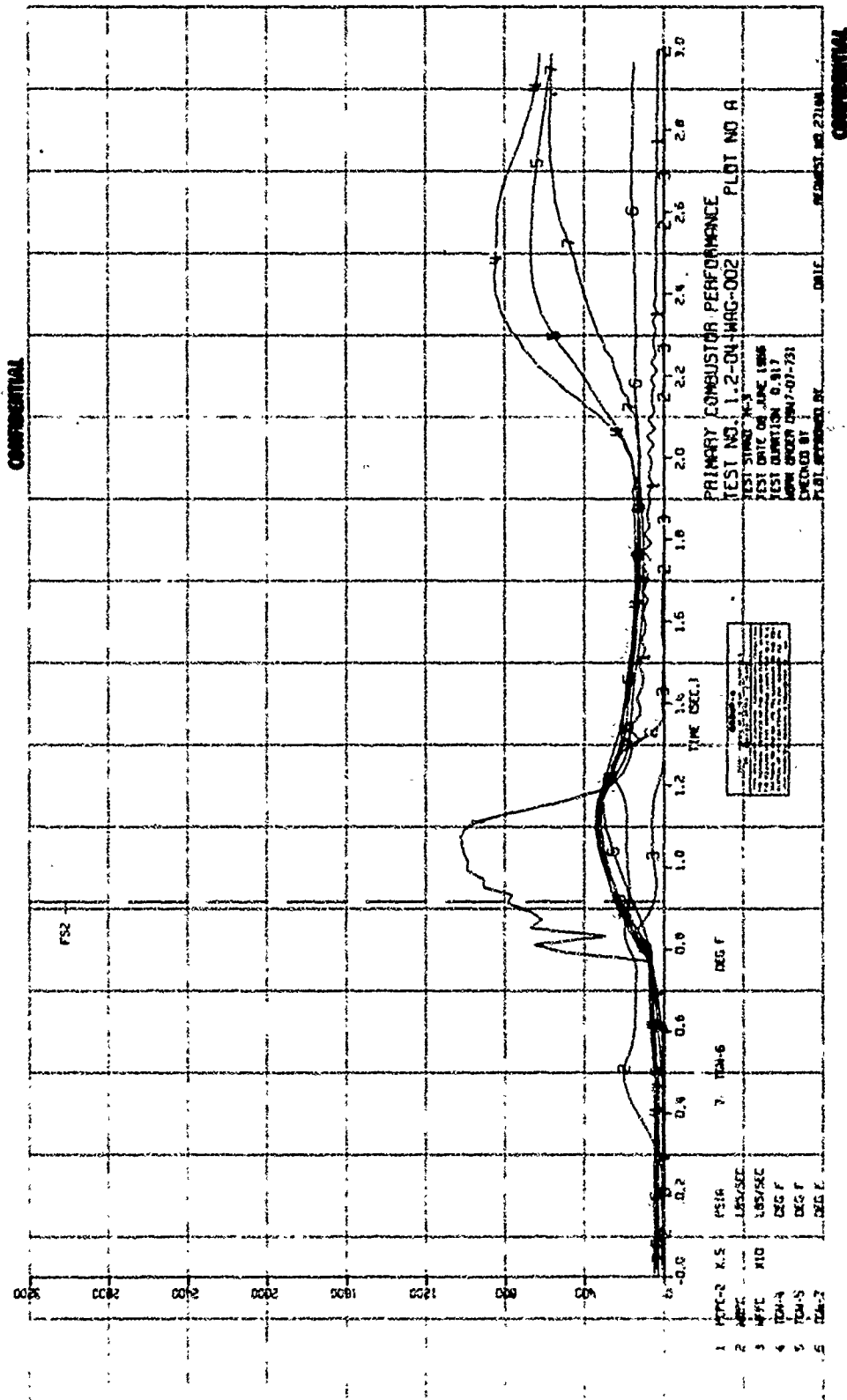
Workhorse Primary Combustor Schematic

Figure III-6

UNCLASSIFIED

CONFIDENTIAL

Report 10830-Q-4



Performance Plot, Test 1.2-04-MAG-002 (u)

Figure III-7

CONFIDENTIAL

CONFIDENTIAL

Report 10830-Q-4



Combustion-Chamber Liner after Test 1.2-04-WAG-003

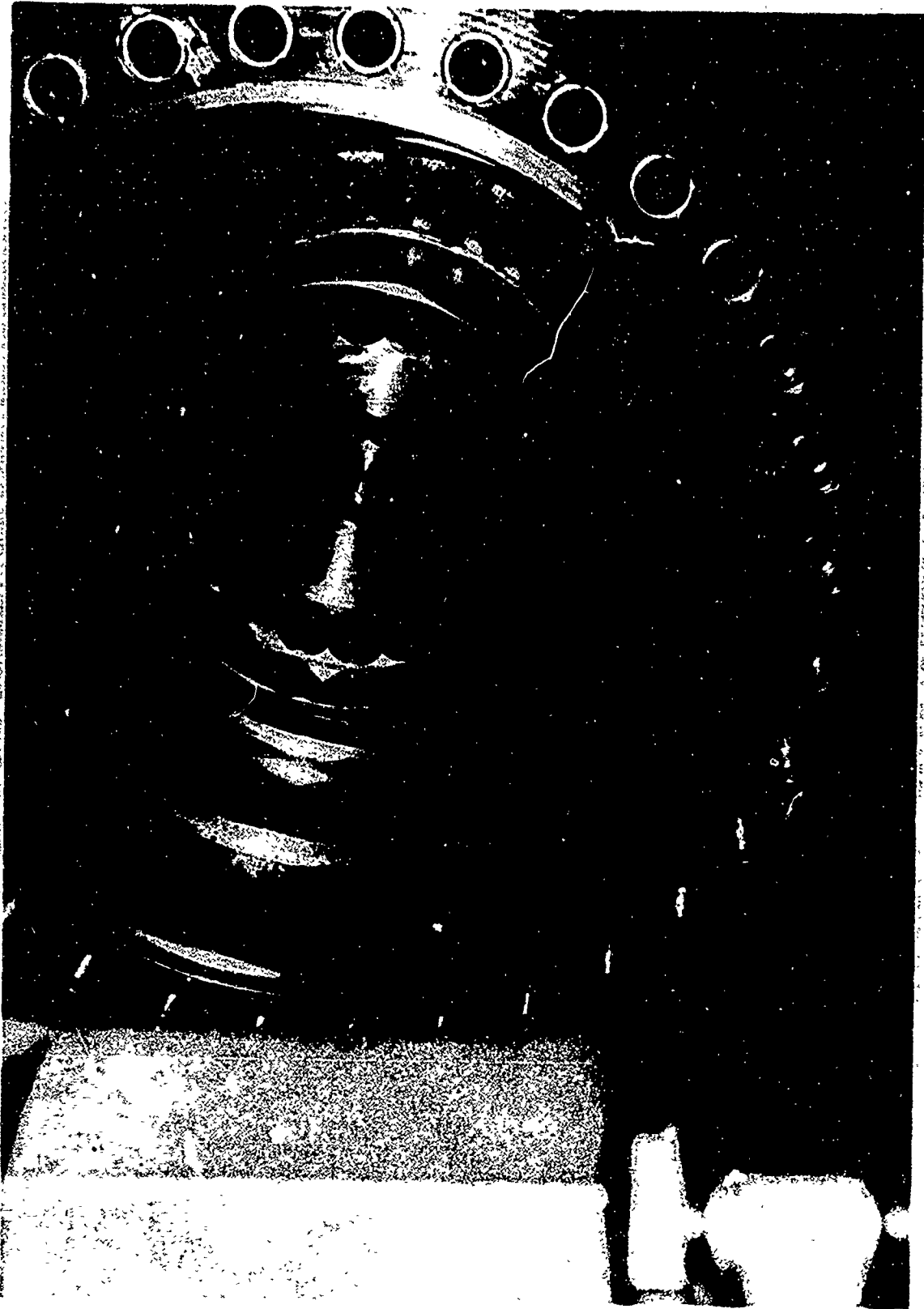
Figure III-8

(This page is Unclassified)

CONFIDENTIAL

CONFIDENTIAL

Report 10830-Q-4



Primary Combustor Injector and Turbine Simulator after Test 1.2-04-WAG-003

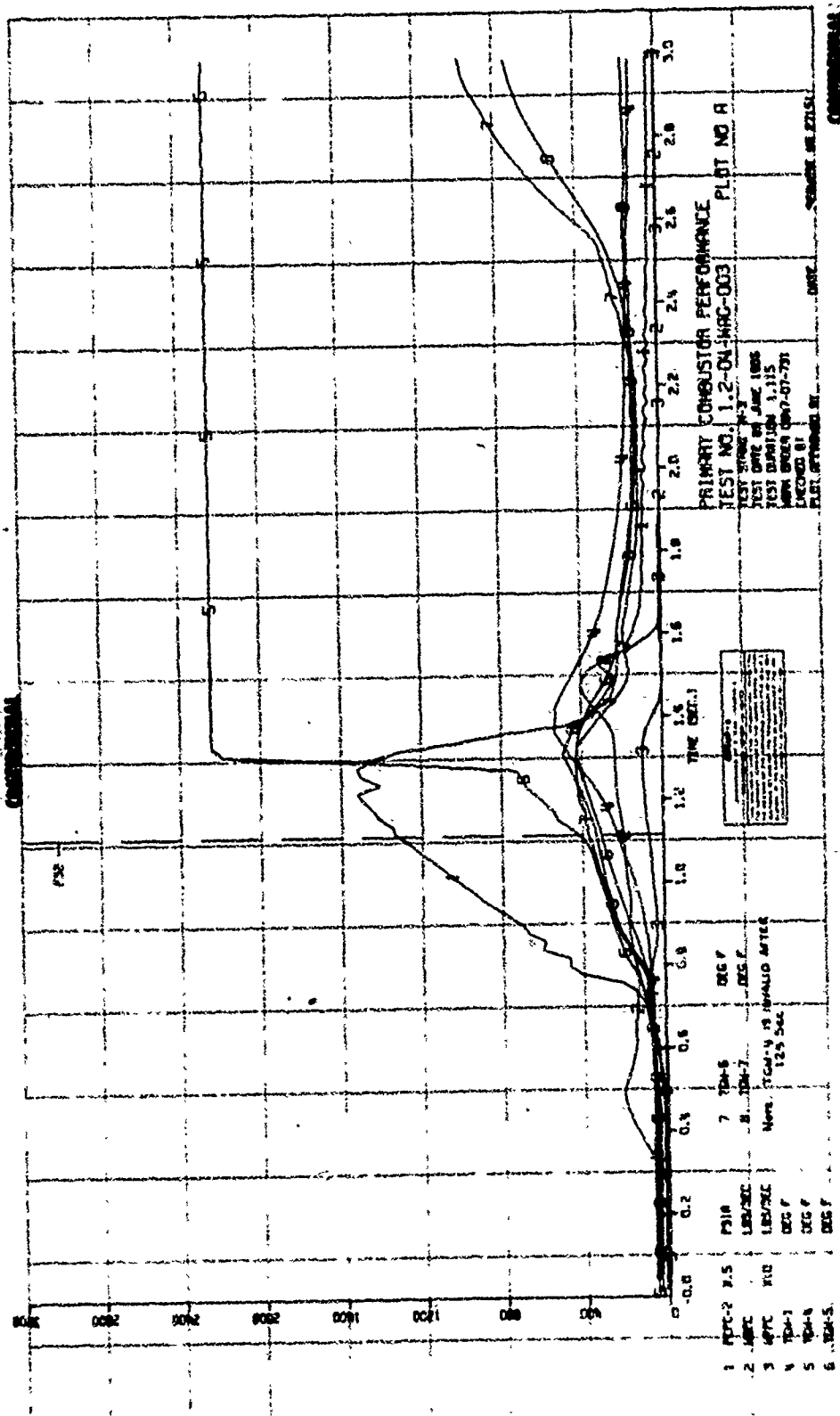
Figure 111-0

(This page is Unclassified)

CONFIDENTIAL

CONFIDENTIAL

Report 10830-Q-4



Performance Plot, Test 1.2-04-WAG-003 (u)

Figure III-10

CONFIDENTIAL

CONFIDENTIAL
Report 10830-Q-4

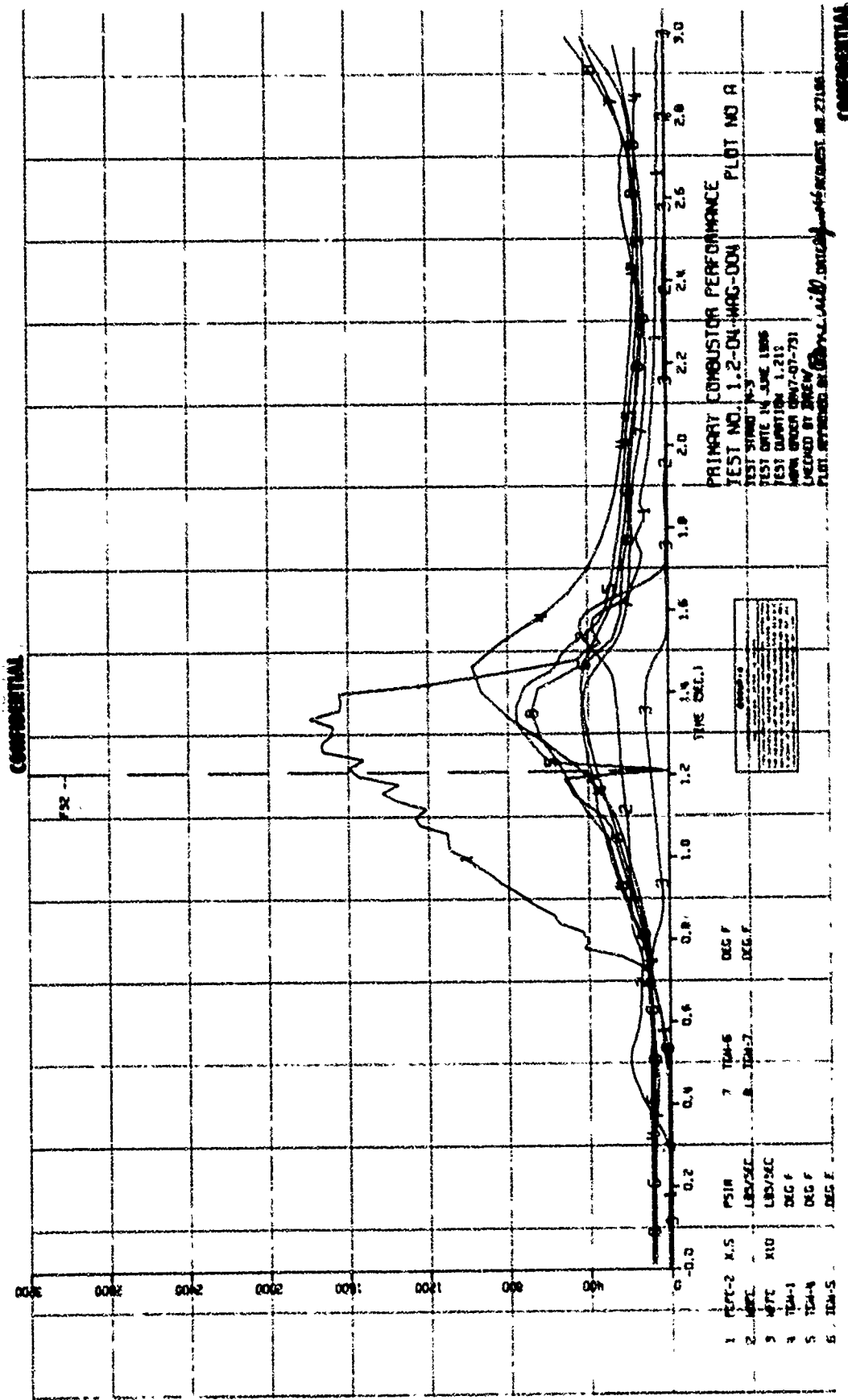


Figure III-11

CONFIDENTIAL

Performance Plot, Test 1.2-04-MAG-004 (u)

CONFIDENTIAL

Report 10830-Q-4

IV.

SECONDARY COMBUSTOR ASSEMBLY

A. GENERAL

(u) The secondary combustor program was continued, with emphasis on injector development testing, fabrication of cooled thrust chambers, and design support for the fabrication and test programs.

(c) Fifteen secondary injector evaluation tests were performed, in which the Mark 125 and the Rake injectors were evaluated. Results of this testing led to the selection of the Mark 125 injector for the ARES engine. The performance level demonstrated with this injector was 93.5% theoretical of specific impulse which, when coupled with a cooled chamber, is sufficiently high to meet the Phase-I performance requirement. The Rake injector, also successful but somewhat lower in performance, has been relegated to back-up status.

(u) Fabrication of the cooled thrust chambers continued. The first of two transpiration-cooled chambers was completed and now awaits testing early in July. Three regeneratively cooled chambers are being assembled, the first of which is scheduled for completion of 15 July 1966.

(u) All design and fabrication activity of secondary combustor components is discussed in detail in Section IV,B, below. A detailed discussion of the test program is given in Section IV,C.

B. SECONDARY COMBUSTOR ASSEMBLY, DESIGN AND FABRICATION

1. Summary

(u) The secondary injectors have been redesigned and reworked slightly as a result of experience gained in hot firing tests. A special stress analysis is currently in progress to define the effects of temperature and vibration on the Mark 125 injector vanes because thermal and vibration-induced stresses may contribute to fuel leakage from the vanes. A formal stress analysis was completed and a final report published for both injector configurations. Ablative liners have been replaced in the uncooled chambers after test firings if required. Fabrication is currently in progress for the two-dimensional nozzle chamber.

(u) Fabrication of cooled chambers was continued on a maximum level of effort. A major fabrication event occurred in the closing weeks of this reporting period when the first transpiration-cooled chamber was completed. Work is currently continuing on transpiration-cooled Chamber SN-2.

CONFIDENTIAL

Report 10030-Q-4

IV, B, Secondary Combustor Assembly, Design and Fabrication (cont.)

(u) Progress on regeneratively cooled chambers has been substantial. Three regeneratively cooled chambers are currently in fabrication at Aerojet-General. The first chamber, SN-1, should be available by 15 July 1966. Outside vendors are presently at work on tube sets for Chambers SN-4 through SN-10. The required metal parts for these additional chambers are presently being fabricated at Aerojet-General, Sacramento.

2. Uncooled Combustion Chamber Components

a. Injectors

(1) Mark-125 Injector

(u) Fabrication and testing of the Mark-125 injector continued. A description of testing and a discussion of test results are presented in Section IV,C.

(u) Leakage has occurred in numerous tube-to-vane braze joints and in several vane-to-manifold weld joints of the Mark-125 injectors SN-1 and SN-2. The thermal and vibration loads are being calculated and injector-fabrication procedures examined to locate the possible cause of the leakage.

(u) The vanes in Injectors SN-1 and SN-2 that had been eroded by fuel leakage were replaced by using part of the vane set intended for Injector SN-3. A fourth set of vanes is 70% complete; fabrication of a fifth set will begin in July. Including the fifth set of vanes, there are now enough vanes for a total of four Mark-125 injector assemblies plus 20 spare vanes.

(u) Injector SN-1 is now available for testing. Injector SN-2 is currently scheduled for completion early in July, whereas Injectors SN-3 and SN-4 are scheduled for completion late in July and mid-August, respectively.

(2) Fuel-Swirl Rake Injector

(u) Performance of the Fuel-Swirl Rake injector has been found to be less than that of the Mark-125 injector in identical chambers under identical test conditions (see Section IV,C,2,b). Therefore, the Rake injector has been relegated to back-up status and will not be tested again unless difficulties arise during continued testing of the Mark-125 configuration.

(u) The injection elements of Rake Injector SN-1 were destroyed in a recent test firing when the mixture ratio in the primary combustor shifted to an off-design value. A new set of fuel elements has been received and could be installed into Injector SN-1 if so desired. However, such an installation is not planned at this time, and the body of this injector will be used, rather, for assembly of a Mark-125 injector. Rake Injector SN-2 is available and is in storage.

UNCLASSIFIED

Report 10830-0-4

IV, B, Secondary Combustor Assembly, Design and Fabrication (cont.)

(u) A design effort is currently in progress to incorporate performance-improvement features in the Rake injectors. The design, when completed, will not be fabricated unless a decision is made to re-activate this injector concept.

(3) Injector Stress Analysis

(u) A final report presenting the stress analysis of the secondary injector was completed and issued. The report concludes that (a) the primary stresses are low and give relatively high margins of safety, (b) the stresses induced by thermal gradients are peak stresses, (c) the combined primary and peak stresses will withstand at least 55 cycles of operation and will not fail by a brittle-type failure because of the large elongation that Type 347 stainless steel can withstand, and (d) either design will maintain its structural integrity during 55 cycles of normal operation.

b. Ablative-Lined Combustion Chamber

(u) The characteristic lengths (L^*) of ablatively lined combustion chambers are now designated nominally 20-, 35-, and 50-in.- L^* . These values more closely correspond to the actual L^* s than the originally designated 30-, 40-, and 50-in.- L^* values.

(u) Fabrication of ablatively lined liners during this reporting period consisted of replacing the liners as required after test firings.

c. Two-Dimensional Nozzle

(u) Five quotations from suppliers for the fabrication of the two-dimensional nozzle were received. Four were "no bid," and the fifth was considered too high. It was therefore decided to fabricate the metal parts at Aerojet-General, Sacramento, and to purchase the liners. The half-angle of the contoured divergent nozzle was changed to $23^\circ 22'$. This change, which will reduce fabrication cost, has a negligible effect on aerodynamic and heat-transfer characteristics.

(u) A purchase order for the divergent-nozzle liner has been placed, and delivery is expected early in July 1966. Machining of the throat contour using templates has begun and fabrication of the metal parts is in progress.

3. Cooled Combustion Chambers

a. ARES Regeneratively Cooled Combustion Chambers

(u) The engineering, procurement, and fabrication efforts on regeneratively cooled combustion chambers were continued. Combustion chambers SN-1, -2, and -3 are being fabricated at Sacramento, with chamber SN-1 nearing completion. The current status of each of the three chambers is reported in the following paragraphs.

UNCLASSIFIED

Report 10830-Q-4

IV, B, Secondary Combustor Assembly, Design and Fabrication (cont.)

(1) Regeneratively Cooled Combustion Chamber SN-1

(u) Fabrication of combustion chamber SN-1 is progressing satisfactorily. Major mileposts accomplished during this reporting period included: receipt of first tube set at Aerojet-General; successful lay-up and brazing of the chamber; attachment of all metal parts to the forward end of the chamber; explosive welding of the tubes to the flange; and initiation of final machining on the forward flange assembly. The following work remains to be done: completion of leak checks (initiated during this quarter); application of the glass wrap; high-pressure proof, leak, and flow testing; final-machining of the forward flange; and application of a thermal-barrier coating. This chamber should be available for hot firing on 15 July 1966.

(2) Regeneratively Cooled Combustion Chamber SN-2

(u) Three furnace-braze cycles were performed on regeneratively cooled combustion chamber SN-2. Some leakage was noted to occur after the third braze cycle and after chamber aging at the tube-to-tube braze joints in the aft section of the chamber. These leaks are currently being repaired by manual brazing. A leak check will be performed to ensure that all leaks have been eliminated. The remaining work on the chamber includes: attachment of the forward flange and remaining metal parts; explosive welding; interim machining; leak checking; application of the glass wrap; proof-, leak-, and flow-testing; final flange machining; and application of the thermal-barrier coating. The chamber should be completed during the first week in August 1966.

(3) Regeneratively Cooled Combustion Chamber SN-3

(u) Lay-up of this chamber began in the closing weeks of this reporting period. Preparations are being made for the first chamber-brazing cycle. This chamber, a capillary tube design, differs from chambers SN-1 and SN-2 by having two film-coolant injection stations instead of one. An additional braze cycle will be required to secure the capillary tubes in the valleys between adjacent regeneratively cooled chamber tubes. The planned completion date for this chamber is 1 September 1966.

(4) Regeneratively Cooled Combustion Chamber SN-4 through SN-10

(u) At the end of May 1966, a large quantity of Inconel-718 tubing was delivered from the mill to the tube-forming vendor. This tubing will be used for chambers SN-4 through SN-10. Processing of the tubing was promptly initiated at the vendor's plant. Fabrication of the small-diameter tubes (nominal OD, 0.480 in.; nominal wall thicknesses, 0.015 in.) is being accomplished in a multiple-stage tapering operation with in-process annealing. Initial tube sets from this lot will be completed early in August 1966.

UNCLASSIFIED

Report 10830-Q-4

IV, B, Secondary Combustor Assembly, Design and Fabrication (cont.)

(u) Tapering of the 0.778-in.-OD (nominal) tubing presented no problems. Tapering was accomplished in a single operation.

(u) The tube turn-around manifold was revised during this reporting period in the original design utilized on chambers SN-1, -2, and -3; the right-hand and the left-hand tube subassemblies were joined by TIG-welding, followed by fitting and electron-beam-welding an end cap (turn-around assembly) to the tube assembly. Difficulty has been experienced in making this joint leak-tight (TIG welds have cracks); and the strength of this joint becomes marginal when subjected to chamber operating pressures. To alleviate this condition, the original end cap was replaced by machined fittings that are brazed into the tube subassemblies and then brazed together to form the completed tube assembly. Structural analysis of this joint indicates a good margin of safety is present even when the design is subjected to the proof pressures for the modular engine. Chamber SN-4 will be the first chamber to incorporate this design change. Completion dates for the machined fittings are compatible with the tube delivery schedule for this chamber.

(5) Other Items Related to the Regeneratively Cooled Chamber

(u) Fabrication of all chamber-layup and machining tooling was completed. Two complete mandrel assemblies are now available for chamber buildup. Tooling designed during the previous reporting period for proof-, leak-, and flow-testing the chambers was fabricated. One complete set of proof-, leak-, and flow-test tooling is available for use. All tooling required for application of the thermal-barrier coating to the chamber was completed. Modifications to the coating machine have been made and checked out. The coating facility is currently awaiting receipt of the first chamber assembly.

(u) An internal final report on the stress analysis of the regeneratively cooled chamber was issued. This report summarizes, and discusses in detail, all structural-analysis efforts undertaken on the ARES regeneratively cooled chamber.

(u) Fabrication of chamber metal parts is continuing at Aerojet-General, Sacramento, and will be completed well in advance of the chamber tube sets. Metal parts are currently on order for all chambers through chamber SN-6.

b. Transpiration-Cooled Combustion Chamber

(u) Fabrication of the transpiration-cooled chambers remained on a Task-Force basis, culminating in completion of the first chamber at the end of this reporting period.

(u) Laboratory tests, performed during the previous reporting period, determined that the best method of joining the flow-control washer to the flow-diffusion washer was by spot-welding and that joining these washers into unitized compartments could be best achieved by TIG-welding the outer periphery with the washer stack compressed between two copper plates.

UNCLASSIFIED

Report 10830-Q-4

IV, B, Secondary Combustor Assembly, Design and Fabrication (cont.)

(u) The most difficult remaining task; i.e., that of obtaining a satisfactory compartment contour, had yet to be demonstrated. Therefore, an experimental prototype compartment composed of rejected washers was fabricated to demonstrate the unitizing and machining operations to be performed on each compartment. To determine the effect of machining the contour, the compartment was water-flow tested before and after machining the inside diameter. Hydraulic Laboratory data revealed that pressure-drop-versus-flow-rate values were not affected by machining.

(u) By the end of April, all 0.001- and 0.010-in.-thick washers had arrived from the vendors. Six compartments composed of these washers were completed up to the point of machining the inside contour. Contour-machining of these compartments was initiated during the first week of May.

(u) Concurrently, several sample instrumentation washers were machined. The object was to obtain a satisfactory 0.012-in.-wide by 0.014-in.-deep radial groove in a 0.020-in.-thick flow-diffusion washer into which a thermocouple would be brazed. The best thermocouple grooves were obtained by electric-discharge machining. A purchase order for the fabrication of six grooves in each of 12 washers was let during the middle of May. Upon completion of these grooves, the washers were shipped to a brazing vendor where the first washer was used to determine the proper amount of braze required per thermocouple. Upon receipt of the completed instrumentation washers, it was noted that five of the eleven washers were slightly warped. Although this warpage is undesirable, it did not appear to have affected the assembly or the cold-flow data.

(u) Delivery of the 0.020-in.-thick flow-diffusion washers continued to be a problem. The die used in punching-out the washers produced unacceptable, eccentric parts. Extensive coordination with the vendor resolved the problem, and all washers were available by the end of May.

(u) By the end of May, the first compartments became available for flow evaluation. As discussed in the previous quarterly report, the best fluid for flow-evaluating the compartments is trichloroethylene, a degreasing fluid which is readily available. At 77°F, the fluid has a specific gravity of 1.46 and a viscosity of 0.55 (as compared to 1.43 and 0.393, respectively, for N_2O_4). Thus, the Components Evaluation Laboratory in Test-Area A prepared a facility for flowing the compartments with trichloroethylene. Compartment 8 was the first available for test evaluation. The compartment was flowed at inlet pressures of 500 to 3000 psi at 500-psi increments. Initial data appeared questionable because an increase in back pressure would increase the flow rate for a given pressure drop. It was determined that the flow fixture separates from the washer stack as much as 0.001 in. at a back pressure of 600 psi. Data at 100-psi back pressure appeared to correlate well. All remaining compartments were flowed as they became available, at a back pressure of 100 psi. Several retainers were remachined as a result of these flow tests to ensure proper seating of the washer stack. Flow data were very close to predicted values, in most instances being slightly higher but never less than the value predicted.

UNCLASSIFIED

Report 10830-Q-4

IV, B, Secondary Combustor Assembly, Design and Fabrication (cont.)

(u) All compartments were completed and individually flow-tested by mid-June. Final assembly of the chamber was accomplished during one shift. Assembly was accomplished by placing the aft flange on the assembly fixture first. Compartment 12 was then carefully lowered into the flange recess. The retainer for Compartment 11, to which the instrumentation washer had been spot-welded, was next placed on the aft flange. Washer Compartment 11 was then carefully lowered into its retainer. This procedure was continued until all compartments and retainers had been assembled.

(u) The chamber compartments were compressed in the assembly fixture, until all parts bottomed out, by means of a 5-in.-dia solid shaft, which is secured at the forward end by 16 bolts and runs up the center of the chamber.

(u) Twelve circumferential seal welds were then made to join the outer retainers and the forward and aft flanges into one unitized chamber. Although care was exercised in making the 1/8-in. circumferential TIG welds, it appeared that the epoxy used in sealing the thermocouple wires into the steel retainer had been scorched.

(u) Proof-testing of the chamber with trichloroethylene verified this conclusion. Some seepage was obtained which, although minor, was considered a safety hazard. Before attempting to seal the thermocouple exit ports, it was decided to reflow the chamber compartments in the assembled condition to confirm the flow parameters established during the individual compartment tests.

(u) The resultant flow data were exceptionally satisfactory. Whereas some compartments flowed somewhat higher than predicted in individual compartment flow tests, the flow data for the assembled compartments were somewhat lower, more closely approximating the predicted values. Compartment 1 is the only compartment whose flow characteristics were less (about 5%) than predicted.

(u) Various methods of sealing the thermocouple leaks were considered. TIG-welding closed the leaks, but this most expedient and positive method was considered unsatisfactory because it would destroy the thermocouple. The most promising method appeared to be to apply a thinned epoxy compound to the leaking thermocouple port while a vacuum was produced inside of the chambers. This method proved to be successful.

(u) All compartment retainers, forward and aft flanges, studs, nuts, and seals are currently available for the second chamber. About 1900 washers have already been received, and the remainder is expected to be available during the first half of July.

(u) Several modifications on the second chamber are being considered as a result of experience gained in fabricating the first chamber. The most important modification will be a redesign of the retainer-instrumentation ports to eliminate any chance of leakage.

UNCLASSIFIED

Report 10830-Q-4

IV, B, Secondary Combustor Assembly, Design and Fabrication (cont.)

(u) The ID contour of the first two compartments is being modified to increase the performance potential of the secondary injector. This modification eliminates the need of a separate outer periphery shroud, currently being evaluated. A change order for the washers of the first two compartments has been issued.

(u) Additional brazing experiments will be conducted on sample washers to eliminate a recurrence of warping.

(u) Although the washers must still be handled and fabricated with care, almost all problems in fabricating the first chamber have been resolved. The chamber is scheduled for completion early in August.

CONFIDENTIAL

Report 10830-Q-4

IV, Secondary Combustor Assembly

C. DEVELOPMENT TESTING

1. Summary

(u) This phase of the sector-engine test program was conducted to obtain performance data for the two prospective injector concepts. Both the Rake and the Mark-125 injector were tested in a secondary combustor configuration identical to that of the ARES modular hardware. The data indicated that the performance of the Mark-125 injector is 1.4% higher than that of the Rake injector, and the Mark-125 injector will therefore be used on all subsequent testing.

(u) Fifteen tests were conducted, of which eleven were successful. The Rake and the Mark-125 injectors were tested four and seven times, respectively, in chambers with L^* ranging from 19.7 to 46.8 in. A cumulative summary of all testing is shown in Figure IV-1.

(c) The single most significant accomplishment was the attainment of 93.5% engine I_g with the Mark-125 injector. This performance, when adjusted for predicted film-coolant losses, will meet Phase-I contract commitments. Other significant accomplishments included:

- a. The demonstration of 91.1% I_g with the Rake injector.
- b. Evaluation of variations in L^* on engine performance.
- c. Evaluation of mixture-ratio distribution effects on engine performances
- d. Evaluation of ablative-nozzle friction effects.
- e. Evaluation of combustion losses with both the Rake and the secondary injector.

(u) Testing during this quarter revealed a performance degradation, which is directly attributable to the physical configuration of the modular injector and of the chamber. The analyses and hardware modifications required for a successful solution of this problem are discussed in detail in Section IV,C,2,b, below. The modifications are now being designed for incorporation in the ARES modular engine.

(u) Another problem, resolved in this quarter, was that of inconsistent flow data. The uncertainties as to the reliability of flow data were eliminated by a series of intensifier water-flow tests in a precisely controlled environment. The resulting data established a flow-rate accuracy of $\pm 0.6\%$. This testing is discussed in Section IV,C,2,e.

CONFIDENTIAL

Report 10830-Q-4

IV, C, Development Testing (cont.)

(u) Preparations for testing the transpiration cooled chamber are 75% completed. This series will constitute the next phase of hot testing. Testing of film-cooled, ablatively-lined, instrumented hardware will follow, immediately followed by testing of regeneratively cooled chambers.

(u) Detailed discussions of each test are presented in Section IV,C,3. The analysis performed in support of engine testing, together with the interpretation of performance data, is presented in Section IV,C,2.

2. Analysis

a. Summary

(u) Four areas were analyzed in detail: (1) injector performance, (2) test support using the transient engine model, (3) test support using the steady-state engine model, and (4) the engine flow-measurement systems.

(u) The performance analysis centered on three topics: mixture-ratio-distribution (MRD) losses, combustion losses, and nozzle friction effects. Testing revealed that MRD losses exceeding 18 sec in I_s were being generated by both the Rake and the Mark 125 injectors. Detailed examination of injector and chamber configurations revealed that primary oxidizer gas was escaping through an annulus and remained unreacted. The MRD loss was eliminated by installing a steel ring about the injector, forcing the primary gas to mix and burn with the secondary fuel. Continued testing further defined the performance loss incurred by the relatively rough ablatively nozzle. Combustion-loss analysis indicated that the performance of the Mark 125 injector is 1.4% higher than that of the Rake injector in a comparable configuration.

(u) Steady-state and transient engine analyses were used to support engine testing. In addition, parametric studies are being conducted to define engine system requirements for the forthcoming cooled testing.

(u) A detailed investigation of the engine flow-measurement systems resolved the problem of inconsistent flow data. The investigations established that the tape system is best, with the rotor-meter system being nearly as accurate. The potentiometric and orifice systems appear to be relatively inaccurate and, at this time, will be used for back-up data only (see Section IV,C,2,e).

b. Performance Analysis

(u) The first 15 ARES modular-configuration tests were conducted between 25 March and 30 June 1966. Two secondary injector configurations were tested: the Mark 125 and the Rake injectors. Performance analyses of the 11 valid modular-configuration tests are summarized in Figure IV-1.

(u) The design of the ARES Mark-125 secondary injector was based upon results of the Mark-125 ICP injector. The importance of uniformly distributing the injected secondary fuel was recognized from ICP test results.

UNCLASSIFIED

Report 10830-Q-4

IV, C, Development Testing (cont.)

Initial test results with both the ARES Mark-125 and the Rake secondary injectors yielded lower performance values than had been anticipated on the basis of projected ICP performance data. Tests 1.2-11-WAM-002 through -005 were made with Configurations A and D of Figure IV-2. Closer examination of the secondary injector-chamber interface configuration indicated the possibility that oxidizer-rich gases from the primary combustor were being diverted into the annulus provided by the diverging chamber and not combusting with the secondary fuel, thus resulting in a mixture-ratio-distribution (MRD) loss. This was confirmed by installing a steel ring in the chamber gap during Tests 1.2-11-WAM-007, -008, and -010, as shown in Configuration B of Figure IV-2. Although performance was increased by the ring, it was not increased by as much as had been expected. Further inspection indicated a 0.1-in. tolerance gap between the secondary injector vanes and the chamber through which oxidizer-rich gases from the primary combustor were flowing. When a steel shroud was installed to fill the gap, as shown in Configurations C, E, and F of Figure IV-2, performance was improved further. For purposes of comparative analysis, zero mixture-ratio-distribution loss was assumed for the secondary injectors when tested in the last three configurations. With this assumption, there is a MRD loss of 10.3 and of 18.9 sec, respectively, if the Mark-125 injector is tested with only the chamber ring or tested with neither the ring nor the shroud. The Rake injector has a MRD loss of only 7.5 sec when tested without the ring and the shroud. The MRD loss with the Rake injector is believed to be lower because the swirl-fuel injector of this design permitted some fuel to burn with the oxidizer-rich gases in the outer chamber annulus and thus to reduce the MRD loss. In this analysis, the MRD losses for the injector configurations tested with a shroud were taken to be zero, based on the assumption of an even oxidizer-rich gas distribution at the secondary injector.

(u) Combustion-loss analyses of these tests indicate that the performance of the Mark-125 secondary injector is about 1.4% higher than that of the Rake injector in a comparable L^* ARES chamber. Further, it appears that the performance of the modular Mark-125 injector (9.5 in. dia) is almost 1% lower than that of the ICP configuration (8.5 in. dia). Combustion loss data vs L^* are shown in Figure IV-3 for the three secondary injector configurations. The test data were corrected to represent the combustion loss at a nozzle area ratio of 20, i.e., that of the ARES modular configuration.

(u) When repeat firings are made with a given ablative nozzle, the nozzle wall becomes progressively rougher, which causes a corresponding increase in nozzle friction loss. The performance data in Figure IV-1 reflect the adjustment made in nozzle friction loss to account for the varying degrees of nozzle surface roughness.

c. Steady-State Analysis

(u) The steady-state computer program was used to study the effect on the balance condition of a series of variations in film-coolant manifold

UNCLASSIFIED

Report 10830-Q-4

IV, C, Development Testing (cont.)

resistance for both ablative and regeneratively cooled chambers. These studies included pump-fed and intensifier-fed systems. Pending the receipt of water-flow resistance data, these studies will be completed and discussed in the next report.

(u) The steady-state program was also used for reducing the test data and for predicting engine-balance conditions during tests on the sector engine.

d. Transient Analysis

(u) The verified analytical model of the ARES TCA H-2 test system was used to determine the controls requirements for testing during this quarter. Some valve times were changed to optimize the transients. The opening time on the SCFV was shortened to decrease the time delay between ignition of the primary and the secondary combustors, whereas the closing time of the PCOV was shortened to decrease the amount of oxidizer lag on shutdown. The ramp-pressure rise rates were increased over a series of five tests to provide faster start transients.

(u) A problem was encountered during the start transient between primary and secondary ignition: The oxidizer-rich primary gas was pressurizing the secondary chamber sufficiently to force the gas into the secondary fuel manifold prior to its filling. A pressure spike on the fuel-injector pressure indicated some burning in the fuel manifold. This problem was solved by isolating the fuel from the oxidizer gas with a N₂ gas purge, which is automatically terminated by a check valve at 450 psig.

(u) The control sequence for the film-cooled test series was developed. Except for the film-coolant valve, the sequence is the same as that for the uncooled tests.

e. Flow-Rate Calibration

(u) Engine testing during this and the preceding quarter revealed large uncertainties in flow measurement. The intensifier-configured engine has four means of flow measurement: rotor meters and delta orifices in the engine lines, a linear tape system, and a potentiometer system measuring intensifier piston travel. The discrepancies between these measurement systems were found to be as high as 4%. Because these discrepancies affect performance evaluation, tests were made with precisely calibrated flow to resolve the uncertainties.

(u) The calibration objectives were two-fold: (1) to verify the dimensional accuracy of the intensifiers, and (2) to determine how well the position of the piston is measured by the potentiometric and tape systems. Calibrations were made at 1000 and 5000 psig using water as the working fluid. Flow was measured with two standard meters in series, whereas intensifier piston position was measured with a highly accurate break-wire system.

CONFIDENTIAL

Report 10830-Q-4

IV, C, Development Testing (cont.)

(u) The intensifier volumes calculated by the break-wire system were compared to those found by flow measurement. Differences of only +0.01 and -0.047% were found for the oxidizer and fuel intensifiers, respectively. This excellent correlation confirmed the intensifier dimensions, and the intensifiers can therefore be considered as secondary standards when used with the break-wire system.

(u) Initial analysis of the tape system revealed some data loss caused by electrical noise of the system. This condition was also apparent in hot testing. The noise problem was eliminated by increasing system voltage. Sufficient tape data were salvaged for comparison with the break-wire reference system and indicated little difference between oxidizer and fuel intensifier operation. Both intensifier tape systems were compared, yielding an output 0.17% lower than the break-wire indications, with a 1 σ -deviation of +0.22% about the mean. Therefore, the measured flow should be increased 0.17% to obtain valid flow rates. The flow uncertainty, at increased flow, would be +0.66%.

(u) In contrast to the tape system, the potentiometer system is biased by set-up prior to testing. Review of the data indicated a +0.457% oxidizer bias and a -0.187% fuel intensifier bias. The 1 σ repeatability about the bias point was +0.166 and +0.082% for the oxidizer and fuel intensifiers, respectively. It must be emphasized that the bias error is not consistent and is dependent only on pretest setup. If a means of eliminating or ensuring a constant bias is used, the potentiometric system becomes highly accurate. The error as a function of piston travel, without bias or with constant bias, is listed below:

<u>Distance, in.</u>	<u>3σ Error, %</u>
18	0.696
36	0.492
54	0.402
72	0.348

(u) With the information generated by the calibration tests, the hot-test flow data were re-analyzed using the flow tape as a standard. The engine flowmeters were found to be accurate within +1.0%. Flow through the orifices appeared to be 3% high on the fuel side and +2% on the oxidizer side.

(u) Future performance calculations will be based on tape flows as a first source and on meter flows as a second source. Orifice and potentiometric data will be used as back-up data only. Currently, work is being directed toward eliminating the random potentiometer bias and, when completed, this measurement system will offer another excellent means of obtaining flow information.

CONFIDENTIAL

Report 10830-Q-4

IV, C, Development Testing (cont.)

3. Modular Secondary Injector Evaluation

a. Summary

(u) Fifteen tests were conducted, 11 of which produced valid performance data. Two injector concepts, the Rake and the Mark-125 injector, were tested. The Rake injector was fired four times in chambers with characteristic lengths (L^*) ranging from 19.7 to 46.5 in. The Mark-125 injector was fired successfully seven times in chambers with L^* ranging from 20.0 to 46.8 in. The four invalid tests included two tests which were terminated due to start malfunctions; one test was terminated due to an intensifier malfunction, and the data from the other test were considered compromised because the exit liner had been ejected.

(u) Engine system operation, in general, was smooth and stable, with no temperature excursions. The intensifiers continued to perform reliably and well (except in one test). Control difficulties in earlier testing were completely eliminated, and startup and shutdown transients were as predicted.

(c) Significant accomplishments in this quarter included:

(1) Demonstration of over 91% I_S with both the Rake and the Mark-125 injectors (see Figure IV-1 for a complete tabulation of performance).

(2) Evaluation of L^* effects on engine performance.

(3) Evaluation of injector-chamber MRD effects on engine performance.

(4) Continued evaluation of the ablative-nozzle friction characteristics.

(5) Evaluation of inherent injector combustion losses, from which it was established that the performance of the Mark-125 injector was higher than that of the Rake injector.

(c) Testing revealed that lower-than-expected performance could be attributed to an adverse mixture-ratio distribution. The adverse distribution was caused by a gap between the injector and the chamber through which primary oxidizer gas could escape. The resulting distribution produced a fuel-rich core surrounded by oxidizer-rich gas (see Section V,C,2,e for a complete discussion). This condition was rectified by plugging the gap with a shroud and a ring. The various shroud-ring modifications are shown in Figure IV-2. This solution successfully increased Mark-125 injector performance from 85.6 to 93.5% of theoretical I_S .

(c) The attainment of 93.5% I_S is noteworthy because this engine would meet the Phase-I commitment when fired in the cooled configuration,

CONFIDENTIAL

Report 10830-Q-4

IV, C, Development Testing (cont.)

with coolant losses as predicted by ICP testing. The Rake injector, although demonstrating 91.1% I_s , produced 2.4% I_s less than the Mark-125 injector in a comparable chamber configuration. The test program will therefore be continued with the Mark-125 secondary injector.

b. Engine Description

(u) The ARES-configuration sector engine remained essentially unchanged. A complete description of the engine system was given in the third quarterly report.

c. Tests

(1) Test 1.2-11-WAM-001

(a) Purpose

(u) The major objective of this test was to evaluate the performance of an ARES modular secondary injector in a chamber-injector configuration identical to that of the regeneratively film-cooled engine (see Figure IV-2, Configuration A). Engine mixture ratio was to be 2.5 to permit a comparison with previously generated Integrated Components Program (ICP) data. In addition, the testing was to demonstrate the mechanical integrity of the engine system.

(b) Attempted

(c) The Mod-II primary injector, the Mark-125 secondary injector (see Figure IV-4), an ablative 46.8-in. L^* cylindrical secondary chamber, an ablative expansion nozzle with an area ratio of 13, and a modular secondary-to-primary adapter section were used in this test. High-pressure propellants were provided by intensifiers. Scheduled duration was 2 sec at a chamber pressure of 2800 psia.

(c) Obtained

(u) Testing was prematurely terminated at FS-1 +0.903 sec by an erroneous flow signal.

(d) Discussion

1 Hardware

(u) No hardware damage was sustained; all components were suitable for retesting.

CONFIDENTIAL

Report 10830-Q-4

IV, C, Development Testing (cont.)

2 Test

(u) Examination of test records disclosed that a secondary fuel-flow-sensing device was operating erratically. This signal indicated a higher-than-safe fuel flow, which resulted in premature engine shutdown. This device was subsequently removed from the malfunction circuit.

(2) Test 1.2-11-WAM-002

(a) Purpose

Test 1.2-11-WAM-001. (u) The objectives were identical to those of

(b) Attempted

(u) The repeat test on 26 March 1966 was to be performed with the hardware and at the engine conditions of Test 1.2-11-WAM-001.

(c) Obtained

(c) The engine performed successfully for 1.909 sec. In the 46.8-in.-L* chamber, the engine delivered a specific impulse of 270.2 lbf-sec/lbm at a chamber pressure of 2848 psia for a steady-state duration of 0.30 sec.

(d) Discussion

1 Hardware

(u) No damage was sustained, and all components were suitable for retesting.

2 Test

(u) Engine operation was completely satisfactory; startup and shutdown were smooth and stable; no temperature excursions were noted, and steady-state engine operation was as predicted.

(3) Test 1.2-11-WAM-003

(a) Purpose

(u) The objectives of this test were to evaluate the performance and mechanical integrity of the Mark-125 secondary injector at the ARES design point.

CONFIDENTIAL

Report 10830-Q-4

IV, C, Development Testing (cont.)

(b) Attempted

(c) The test was to be performed with the hardware used in Test 1.2-11-WAM-001. The intended chamber pressure and the secondary mixture ratio were 2800 psia and 2.20, respectively.

(c) Obtained

(c) Satisfactory operation was again obtained on 29 March 1966 for the prescribed duration of 2.313 sec. Specific impulse in the 46.8-in.-L* chamber was 273.1 lbf-sec/lbm at a chamber pressure of 2811 psia for a steady-state duration of 0.66 sec.

(d) Discussion

1 Test Hardware

(u) No damage was sustained, and all components were suitable for retesting.

2 Test

(u) Analysis of the test records indicated excellent engine operation. The control system operated as predicted. Injector performance was lower than indicated by previous ICP experience. The lower performance was attributed to an adverse mixture-ratio distribution across the injector face due to a gap about the periphery of the fuel elements (see Figure IV-2, Configuration A).

(4) Test 1.2-11-WAM-004

(a) Purpose

(u) The objective of this test was to evaluate the performance of the Rake injector in a nominal 45-in.-L* ARES cooled TCA configuration.

(b) Attempted

(u) The Rake secondary injector (Figure IV-2, Configuration D) was used. Engine balance was at the ARES design point. The remaining hardware was unchanged.

CONFIDENTIAL

Report 10830-Q-4

IV, C, Development Testing (cont.)

(c) Obtained

(c) The test was conducted satisfactorily on 30 March 1966 for a total duration of 2.026 sec. Specific impulse in the 46.6-in.-L* chamber was 285.0 lbf-sec/lbm at a chamber pressure of 2850 psia for a steady-state duration of 0.37 sec.

(d) Discussion

1 Test Hardware

(u) No major damage was noted. Only the tips of the fuel elements on the Rake injector exhibited minor random erosion; however, the hardware was suitable for retesting.

2 Test

(u) Engine operation was as predicted; shut-down, steady-state, and control functions operated normally. Performance, although higher than in previous Mark-125 tests, was still below that required by regeneratively film-cooled operation. Low-frequency, high-amplitude oscillations occurring during the low levels of the start transient, attenuated at half the chamber pressure and also appeared at steady state.

(5) Test 1.2-11-WAM-005

(a) Purpose

(u) The objectives of this test were identical to those of Test 1.2-11-WAM-001; in addition the test was made to establish a second performance-data point at a longer duration for the Rake injector.

(b) Attempted

(u) Again, the balance point and the hardware configuration remain unchanged. Steady-state duration was scheduled to be 0.5 sec.

(c) Obtained

(c) The test was completed on 30 March 1966; total engine running time was 2.309 sec. Again, engine operation was normal; specific impulse in the 46.1-in.-L* chamber was 285.0 lbf-sec/lbm at a chamber pressure of 2820 psia. Steady-state duration was 0.66 sec.

UNCLASSIFIED

Report 10830-Q-4

IV, C, Development Testing (cont.)

(d) Discussion

1 Test Hardware

(u) No major damage was noted. Again, the tips of the fuel elements eroded slightly, but the remaining hardware was suitable for refiring.

2 Test

(u) All engine functions were as predicted. Low-frequency, high-amplitude oscillations were again present and attenuated upon approaching steady-state operation. Performance was nearly identical to that in Test-004--still lower than required.

(u) Performance analysis indicated a loss in specific impulse as high as 18 lbf-sec/lbm, caused by an adverse MRD attributed to a gap between the injector and the chamber which allowed primary gas to escape radially from the injector. This phenomenon and the analysis are explained in Section IV,C,2. The effects of the gas were eliminated by installing a ring about the injector (see Figure IV-2, Configuration B).

(u) Disassembly of the engine revealed large distortions in the injector-adapter seal. This condition was corrected by replacing the Parker V-seal with an omni-seal.

(6) Test 1.2-11-WAM-006

(a) Purpose

(u) The test objective was to evaluate the performance of the Bake injector with the injector-chamber gap removed.

(b) Attempted

(u) The test was conducted at the same balance point as in Test-005. The only hardware change was the addition of the performance ring to fill the 0.5-in.-wide gap between the chamber and the injector.

(c) Obtained

(u) The test was conducted on 1 April 1966, with a total engine running time of 1.728 sec. The test was terminated when a malfunction sensing device indicated that the fuel-intensifier pressure was greater than the oxidizer pressure.

UNCLASSIFIED

Report 10830-Q-4

IV, C, Development Testing (cont.)

(d) Discussion

1 Hardware

(u) Posttest inspection revealed severe erosion of the primary combustor chamber, turbulator section, Rake injector, and performance ring.

2 Test

(u) Data analysis revealed that the shutdown was caused by the premature failure of a 4-in.-dia burst diaphragm located in the oxidizer-intensifier gas-supply system. The diaphragm is a safety device that protects the intensifier from large overpressures.

(u) Venting the oxidizer intensifier rapidly reduced both oxidizer flow and pressure, decreasing chamber pressure and increasing primary fuel flow, which shifted primary-combustor mixture ratio from oxidizer-rich, through stoichiometric, to fuel-rich. The shift resulted in very hot gases, which ultimately attacked and destroyed the hardware.

(u) Future failures of this type will be prevented by installing seven 1-1/2-in.-dia diaphragms in parallel, thus allowing a more gradual mixture-ratio shift in the event of a random diaphragm failure. The diaphragms were sized to permit a compensation for flow reductions, caused by failure of one diaphragm, by action of the 2- or 4-in. flow-control valves without subjecting the engine to mixture-ratio excursions.

(7) Test 1.2-11-WAM-007

(a) Purpose

(u) The test objectives were to evaluate the performance of the Mark-125 secondary injector with the performance ring installed.

(b) Attempted

(u) Test conditions were identical to those of Test-006 except that the Mark-125 secondary injector and the performance ring were used.

CONFIDENTIAL

Report 10830-Q-4

IV, C, Development Testing (cont.)

(c) Obtained

(c) Testing in a 43.2-in.-L* chamber was completed on 19 April 1966. Total engine running time was 2.010 sec. Operation was as predicted. The engine generated a specific impulse of 282.4 lbf-sec/lbm at a chamber pressure of 2854 psia for a steady-state duration of 0.48 sec.

(d) Discussion

1 Test Hardware

(u) No damage was noted. The hardware was suitable for retesting.

2 Test

(u) All engine functions were as predicted. A specific impulse efficiency gain of 4% was recorded and was attributed to the addition of the performance ring. This performance increase was not yet high enough for the operation of a regeneratively film-cooled chamber.

(8) Test 1.2-11-WAM-008

(a) Purpose

(u) The major objective was to evaluate the Mark-125 injector-performance ring (see Figure IV-5) in a chamber of reduced L*. A second objective was to establish the friction loss of an ablative nozzle with a steel exit section.

(b) Attempted

(u) The engine balance point remained unchanged. Substitution of the steel exit section and a 35.0-in.-L* chamber constituted the only hardware changes.

(c) Obtained

(c) Testing was completed on 20 April 1966. Total engine running time was 2.011 sec. Again, the engine operated successfully, generating a specific impulse of 286 lbf-sec/lbm at a chamber pressure of 2891 psia over a steady-state duration of 0.37 sec.

CONFIDENTIAL

Report 10830-Q-4

IV, C, Development Testing (cont.)

(d) Discussion

1 Hardware

(u) No damage was noted. The engine was suitable for retesting. The ablative expansion nozzle exhibited slight roughening just downstream of the throat.

2 Test

(u) All engine functions were as predicted. Performance was improved 0.90%. Sufficient data were obtained to establish the friction loss of the ablative nozzle.

(9) Test 1.2-11-WAM-009

(a) Purpose

(u) This test was a continuation of the Mark-125 injector-evaluation test in a chamber of reduced L*.

(b) Attempted

(u) The test was conducted at the ARES-engine balance point. The secondary chamber had a characteristic length of 20 in. and was equipped with an ablative nozzle.

(c) Obtained

(u) Testing was terminated at FS-1 +0.41 sec due to an "open" condition of the first-motion oxidizer-valve microswitch.

(d) Discussion

1 Hardware

(u) No damage resulted from the premature shutdown.

2 Test

(u) Posttest examination revealed satisfactory microswitch operation. The "open" condition was the result of a broken electrical connector. The connection was repaired and the engine set up for a repeat firing.

CONFIDENTIAL

Report 10830-Q-4

IV, C, Development Testing (cont.)

(10) Test 1.2-11-WAM-010

(a) Purpose

(u) The test was a repeat of Test-009.

(b) Attempted

(u) The engine balance point and the hardware were identical to those of Test-009.

(c) Obtained

(c) Testing was completed on 20 April 1966 with the engine operating satisfactorily. The engine ran 2.009 sec, generating a specific impulse of 278.8 lbf-sec/lbm at a chamber pressure of 2841 psia. Steady-state duration was 0.44 sec.

(d) Discussion

1 Test Hardware

(u) No damage was noted. The engine was suitable for retesting. Nozzle roughening was minimal.

2 Test

(u) Engine operation was as predicted. The specific impulse attained in the 20.0-in.-L* chamber was 7.3 lbf-sec/lbm lower than the 35-in.-L* chamber, indicating the characteristic relationship between combustion loss and stay time.

(u) At this point, testing was suspended to permit a careful analysis of all performance data. It was noted that agreement between the four flow-measurement systems was poor. A flow-calibration investigation, described in Section IV,C,2, was therefore conducted to define and correct this condition. The information gained made a precise determination of performance possible. The detailed performance analysis (see Section IV,C,2) indicated that performance could be increased another 3 lbf-sec/lbm by removing a tolerance gap between the injector and the performance ring.

(u) Although the performance ring completely filled the 1/2-in.-wide chamber step, primary gas still bypassed the secondary injector, resulting in a mixture-ratio-distribution loss. The gas escaped through a 0.102-in.-wide gap between the injector blades and the ring (see Figure IV-2, Configuration-B). The gap was plugged by welding a cylindrical shroud to the injector blades; the shroud extended 1 in. below the injector face, retaining the primary gas within the fuel elements (Figure IV-2, Configuration-C).

CONFIDENTIAL

Report 10830-Q-4

IV, C, Development Testing (cont.)

(11) Test 1.2-11-WAM-011

(a) Purpose

(u) The objective was to ascertain the effect of the performance ring-shroud combination on injector performance.

(b) Attempted

(u) The Mark-125 injector and the performance ring-shroud combination were fired in the 35-in.-L* chamber at ARES-engine balance conditions. This configuration is shown as Configuration-C in Figure IV-2. A steel nozzle-exit section was used in this test.

(c) Obtained

(u) Testing was completed on 2 May 1966, with the engine running successfully for 2.003 sec. The engine generated a specific impulse of 295.5 lbf-sec/lbm at a chamber pressure of 2828 psia for a steady-state duration of 0.52 sec.

(d) Discussion

1 Test Hardware

(u) The injector exhibited erosion on two of the fuel vanes at the manifold attachment point. The erosion is attributed to fuel leakage at the weld causing high-temperature combustion. The performance ring was eroded back to the meeting point of ring and shroud.

2 Test

(u) Engine operation was as predicted. Performance was significantly improved, confirming that performance loss was due to adverse MR distribution. Based on predicted film-coolant losses, this engine would meet the Phase-I contract commitment when fired in the cooled configuration, assuming that coolant losses are commensurate with those developed during the ICP residual-hardware test series.

(12) Test 1.2-11-WAM-012

(a) Purpose

(u) Test objectives were to evaluate the performance of the Rake injector and of the performance ring-shroud combination in a short L* chamber.

CONFIDENTIAL

Report 10830-Q-4

IV, C, Development Testing (cont.)

(b) Attempted

(u) The Rake injector was tested at ARES-engine balance conditions in a 19.7-in.-L* ablative chamber with a steel nozzle. This assembly is shown as Configuration-E in Figures IV-2 and IV-6.

(c) Obtained

(c) Testing was completed on 3 May 1966, with the engine running successfully for 2.002 sec. The engine generated a specific impulse of 281.9 lbf-sec/lbm at a chamber pressure of 2820 psia for a steady-state duration of 0.49 sec.

(d) Discussion

1 Test Hardware

(u) Again, slight erosion was present on the tips of the fuel elements, but the injector was suitable for retesting. The performance ring showed slight erosion on the trailing edge.

2 Test

(u) Engine operation was as predicted. The combination of Rake injector and short L* chamber produced a specific impulse efficiency 4.5 less than the Mark-125 injector in a similar chamber.

(13) Test 1.2-11-WAM-013

(a) Purpose

(u) The test objective was to determine the performance of the Rake injector in a 42.1-in.-L* chamber.

(b) Attempted

(u) The engine balance point was identical to that of the previous test; all other conditions were identical except that a 42.1-in.-L* chamber was used.

(c) Obtained

(c) The engine was fired successfully on 3 May 1966 and operated for 2.006 sec. This hardware combination generated a specific impulse of 286.1 lbf-sec/lbm at a chamber pressure of 2771 psia for a steady-state duration of 0.60 sec.

CONFIDENTIAL

Report 10830-Q-4

IV, C, Development Testing (cont.)

(d) Discussion

1 Hardware

(u) No damage was noted.

2 Test

(u) The specific impulse efficiency attained with the Rake injector was 2.4% lower than that attained with the Mark-125 in a comparable configuration (Test 1.2-11-WAM-011). This test therefore established the superiority of the Mark-125 injector.

(14) Test 1.2-11-WAM-014

(a) Purpose

(u) The objective was to fire the Mark-125 injector in a 40-in.-L* chamber.

(b) Attempted

(u) The engine balance point remained unchanged; the only hardware change was the use of a shorter chamber.

(c) Obtained

(u) The engine was fired on 11 May 1966 and ran for 2.010 sec. Performance data were compromised because the liner of the steel exit cone was ejected late in the start transient.

(d) Discussion

1 Test Hardware

(u) The liner-supporting structure was completely destroyed, but the liner sustained only minor damage and was subsequently repaired. Seven vanes of the Mark-125 injector were damaged by fuel-lube leakage and subsequent combustion (see Figure IV-7).

2 Test

(u) Separation of the liner from the nozzle shell was precipitated by a weak silicon-based adhesive bonding agent (RTV 60). The poor bond enabled hot exhaust gas to leak behind the liner, to further weaken the bond, and to create a large unbalanced pressure which ultimately expelled the liner. Future assemblies will be welded circumferentially to preclude similar failures.

CONFIDENTIAL

Report 10830-Q-4

IV, C, Development Testing (cont.)

(u) The fuel-tube leakage was corrected by modifying the injector-assembly procedures.

(15) Test 1.2-11-WAM-015

(a) Purpose

(u) The objective of the test was to evaluate the Mark-125 injector with a modified shroud in a 42.0-in.-L* chamber.

(b) Attempted

(u) The test was conducted, at ARES engine design conditions, with the 42.0-in.-L* chamber and an ablative exit-cone section. The injector shroud configuration was as shown in Figure IV-2.

(c) Obtained

(u) Testing was completed on 13 June 1966, with the engine operating for 2.00 sec. The engine generated a specific impulse of 291.1 lbf-sec/lba at a chamber pressure of 2660 psia. Steady-state duration was 0.77 sec.

(d) Discussion

1 Hardware

(u) Three Mark-125 injector blades were eroded. The shroud at the location of the damaged blades was burned back to the injector face (Figure IV-8). Burning was attributed to local ignition on the face of the shroud, which subsequently burned back to, and damaged, the injector blades.

2 Test

(u) All engine functions were as predicted. Specific impulse efficiency, although high, was 0.90% lower than in Test 13, which was made with a comparable chamber configuration. The lower performance is tentatively ascribed to the damaged injector and shroud and to the resulting interaction with the gas stream. In addition, both chamber and exit section were very rough, which also degraded engine performance.

4. Transpiration-Cooling Evaluation

a. Summary

(u) Preparations for testing of transpiration-cooled hardware are about 75% completed, with major emphasis being placed on test-system configuration design, transient operation, and test philosophy. A conservative approach is followed in processing both the test-system plan and the operating sequence to yield a maximum of heat-transfer and performance data. The activities leading to the completion of these objectives are summarized in the following paragraphs.

CONFIDENTIAL

Report 10830-Q-4

IV, C, Development Testing (cont.)

(u) During the initial test phase, the high-pressure intensifier systems will supply both the oxidizer (N_2O_4) and the fuel (AeroZINE 50) to the primary and secondary combustors. The first test series will be of short duration and will be designed to display chamber integrity and system (engine and chamber) balance, and to demonstrate the transpiration-cooled concept. Test 1 will be conducted at a secondary injector mixture ratio of about 2.5 while flowing a maximum amount of film coolant through the chamber. Test 2 will be made at the design mixture ratio for the secondary injector with maximum film-coolant flow for the same test duration as in Test 1. Test 3 will be identical to Test 2, except that its duration will be extended. The remainder of the series will be devoted to optimizing the chamber-coolant flow rate. Thermal equilibrium of the transpiration-cooled chamber is not expected to be achieved during this first series of tests.

(u) Following the initial short-duration chamber checkout and balance tests, the ICP breadboard pumping system (Contract AF 04(611)-8548) will be installed to replace the intensifier propellant-feed system. The second test series, designed to demonstrate the performance of the transpiration-cooled chamber, will be for durations exceeding 5 sec.

b. Engine Description

(u) The intensifiers and the pumping system supply propellants to the engine in an almost identical manner. The oxidizer is routed from either the pump discharge or the intensifier discharge through a system-balance orifice into the secondary injector adapter, through a control valve, and into the primary combustor injector where it is burned with about 20% of the total fuel flow. The oxidizer-rich gas is then fed into the secondary combustor injector where it combines with the remaining fuel. Coolant flow for the cooled chamber is directed from upstream of the control orifice in the main oxidizer feed system through a rotary flowmeter and through a flow-control valve into a distribution manifold which, in turn, feeds the individual segments of the chamber. The flow of the oxidizer film coolant to the cooled chamber is controlled by orifices located in the distribution-manifold discharge lines (see Figures IV-9, -10 and -11).

c. Test Preparation

(u) A pretest analysis of testing the transpiration-cooled thrust chamber is presently being conducted. The analysis will investigate three areas: startup and shutdown transients, steady-state operation, and test philosophy.

(u) The startup and shutdown transients are being designed to ensure that (1) the film coolant (N_2O_4) does not react with the main stream, (2) sufficient film coolant is present prior to ignition, and (3) injector mixture-ratio excursion does not occur during the transients. Particular emphasis is being placed on the type and on the sequencing of the purges for exhausting the propellant manifolds during shutdown.

UNCLASSIFIED

Report 10830-Q-4

IV, C, Development Testing (cont.)

(u) All hydraulic characteristics of the thrust chamber have been determined by laboratory tests to ensure close coolant flow control during steady-state operation. Individual flow factors have been obtained for each manifold arm, and the flow versus pressure-drop values have been plotted for the individual sections of laminar-flow platelets. The sizes required for the first test-balance orifices in each chamber section are presently being determined. After the first tests, the actual chamber-pressure profile will be defined to permit the fabrication of orifices for any required section flow rate. Rapid turn-around during testing and coolant flow control within 0.5 lb/sec will then be ensured for flows ranging from 25 to 40 lb/sec.

UNCLASSIFIED

CONFIDENTIAL

Test No.	Date	Duration FS ₁ to FS ₂ sec.	Secondary Injector	A ₁ in. ²	Area Ratio	L [*] in.	PGSC psia	MRSC	MRPC	F _v lbf	F _g lbf/sec	F _{PC} lbf/sec	c [*] ft/egg	
1.2-11-4AN-001	3-25-66	0.903	125AE	Malfunction									0	
002	3-26-66	1.909	125AE	21.12	11.92	46.8	2848	2.57	14.9	99,847	369.5	0	5250	
003	3-29-66	2.313	125AE	21.02	11.96	46.8	2811	2.03	11.6	97,532	357.1	0	5320	
004	3-30-66	2.026	Make	21.02	11.92	46.5	2350	2.22	11.6	99,627	350.2	0	5500	
005	3-30-66	2.309	Make	21.16	11.87	46.1	2820	2.21	11.5	99,370	349.6	0	5500	
006	4-1-66	1.728	Make	Malfunction									0	
007	4-19-66	2.010	125AE	22.34	11.32	43.2	2854	2.27	11.9	102,288	362.2	0	5650	
008	4-20-66	2.011	125AE	21.24	11.70	35.0	2891	2.27	11.6	103,421	361.5	0	5,470	
009	4-20-66	0.41	125AE	Malfunction									0	
010	4-20-66	2.009	125AE	21.90	11.53	20.0	2541	2.26	11.5	100,309	350.8	0	5570	
011	5-2-66	2.003	125AE	22.61	10.96	32.9	2828	2.18	11.3	105,515	357.1	0	5760	
012	5-3-66	2.002	Make	21.18	11.35	19.7	2321	2.19	11.4	101,307	359.4	0	5349	
013	5-3-66	2.006	Make	22.91	11.02	42.1	2771	2.27	11.7	103,527	361.8	0	5644	
014	5-11-66	2.010	125AE	Malfunction									0	
015	6-13-66	2.00	125AE	23.32	10.78	42.0	2660	2.34	12.15	104,850	360.2	0	5541	

(1) Combustion loss includes mixture ratio distribution loss

CONFIDENTIAL

CONFIDENTIAL
Report 10830-Q-4

CONFIDENTIAL

Case	V _{FC} lbm/sec	c*	I _{SV} lbm	LMRD	LNC	LNF	LC	LPC	I _{SVT} lbm	MI _{SV} Percent	Remarks
				Chamber Total lbm-sec	Chamber Total lbm-sec	Chamber Total lbm-sec	Chamber Total lbm-sec	Chamber Total lbm-sec			
0											Malfunction due to erratic fuel-flow signal. No hardware damage.
0	5250	270.2	13.4 18.9	0 4.7	0 5.0	5.1 9.2			307.0	94.0 88.0	Satisfactory 125AK performance test. No hardware damage.
0	5320	273.1	18.3 27.5	0 4.7	0 4.2	5.4 9.6			319.1	92.6 85.8	Satisfactory 125AK performance test. No hardware damage.
0	5500	285.0	---	0 4.9	0 4.2	13.0 23.2 (1)			317.3	95.9 89.8	Satisfactory Bake performance test. No hardware damage.
0	5500	285.0	---	0 4.9	0 4.2	12.8 22.9 (1)			317.0	95.0 89.9	Satisfactory Bake performance test. No hardware damage.
0											Malfunction due to venting of ex. intensifier resulting in destruction of secondary injector.
0	5650	282.4	6.4 10.5	0 4.9	0 7.3	5.7 10.0			315.1	96.2 89.8	Satisfactory 125AK performance test. No hardware damage.
0	5470	286.1	6.3 10.3	0 4.9	0 3.0	6.6 11.7			316.0	95.9 90.3	Satisfactory 125AK performance test. No hardware damage.
0											Engine malfunction due to broken electrical connection. No hardware damage.
0	5570	278.8	6.3 8.9	0 4.8	0 4.2	10.2 18.1			315.6	94.8 88.4	Satisfactory 125AK performance test. No hardware damage.
0	5760	295.3	0	0 5.4	0 4.9	7.3 12.3			316.1	92.8 89.5	Satisfactory 125AK performance test. No hardware damage.
0	3349	281.9	0	0 4.9	0 7.3	12.8 18.7			316.8	95.8 89.0	Satisfactory Bake-injector performance test. No hardware damage.
0	5644	286.1	0	0 3.0	0 7.3	8.9 15.8			314.2	92.1 91.1	Satisfactory Bake-injector performance test. No hardware damage.
0											Performance data compromised by exit liner expulsion.
0	5541	291.1	0	0 3.0	0 7.9	6.9 10.3			314.5	94.4 82.8	Satisfactory 125AK performance test. Slight injector and shroud erosion.

CONFIDENTIAL

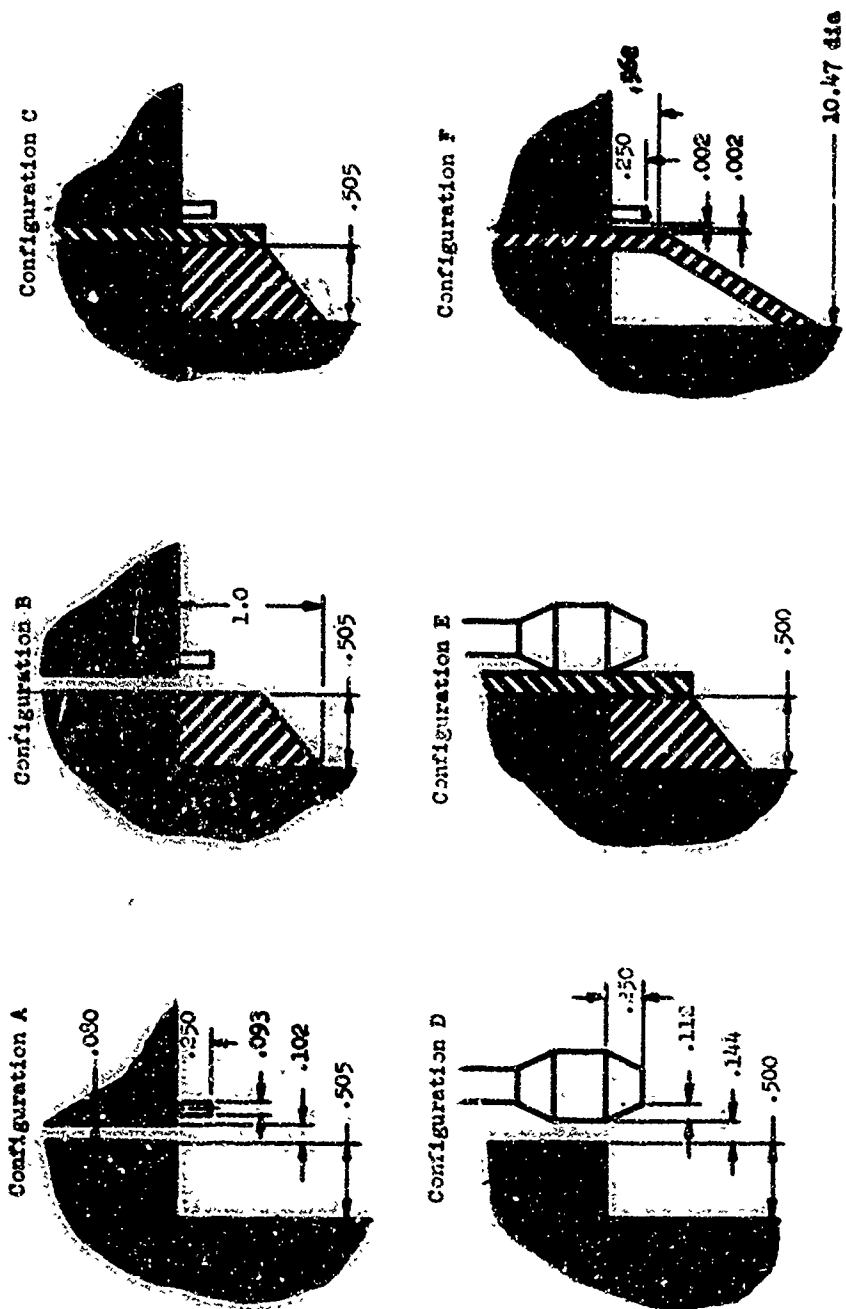
ARES Modular Performance Summary (u)

Figure IV-1

CONFIDENTIAL

2

CONFIDENTIAL
Report 10830-Q-4



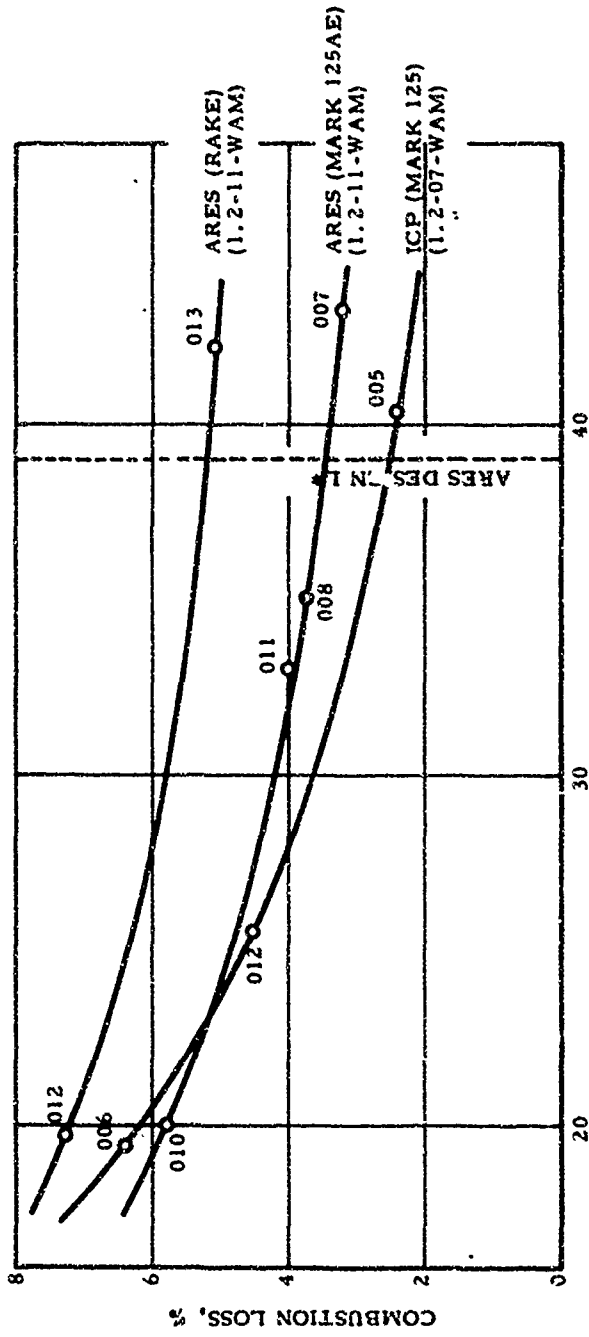
ARBS Modular Injector-Chamber Configurations

Figure IV-2
(This page is Unclassified)

CONFIDENTIAL

EFFECT OF CHARACTERISTIC LENGTH ON
COMBUSTION LOSS OF THREE SECONDARY
INJECTOR CONFIGURATIONS

$N_2O_4/A-50$
CORRECTED TO $A_c/A_t = 20:1$



CHARACTERISTIC LENGTH (L*), IN.

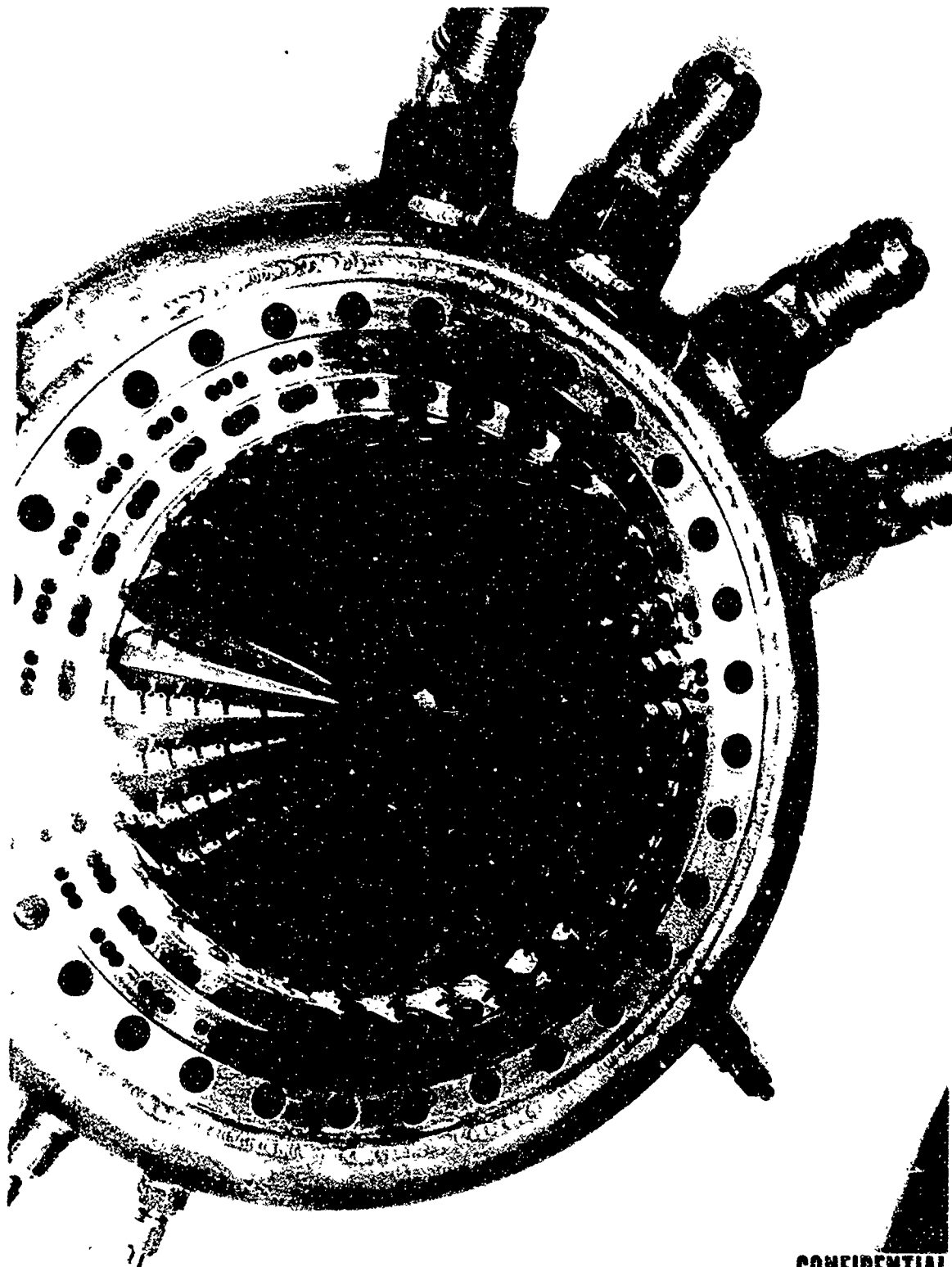
CONFIDENTIAL

Combustion loss vs Characteristic Length (u)

Figure IV-3

CONFIDENTIAL

Report 10830-Q-4



CONFIDENTIAL

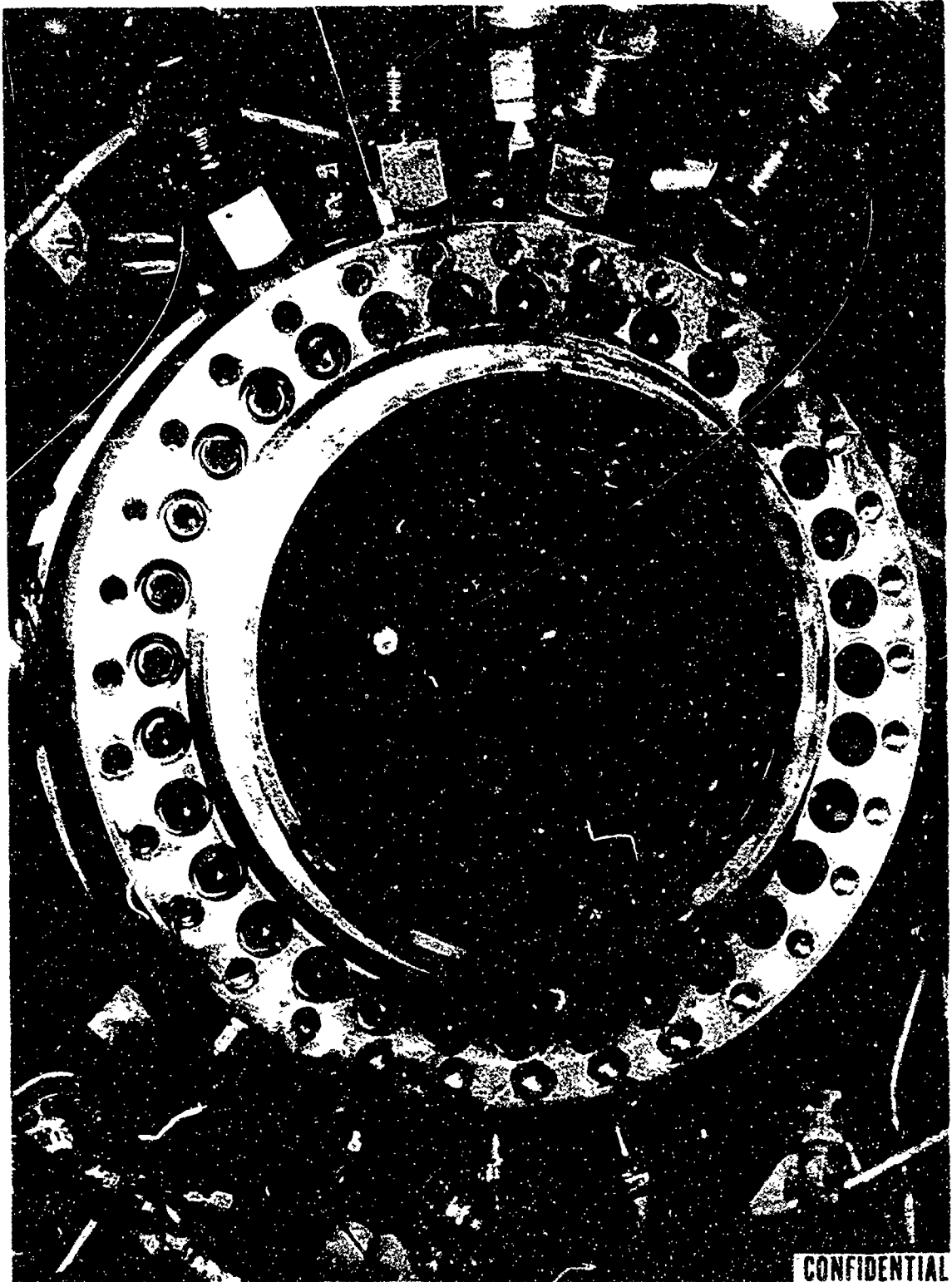
Mark-125 AE Secondary Injector (u)

Figure IV-4

CONFIDENTIAL

CONFIDENTIAL

Report 10830-Q-4



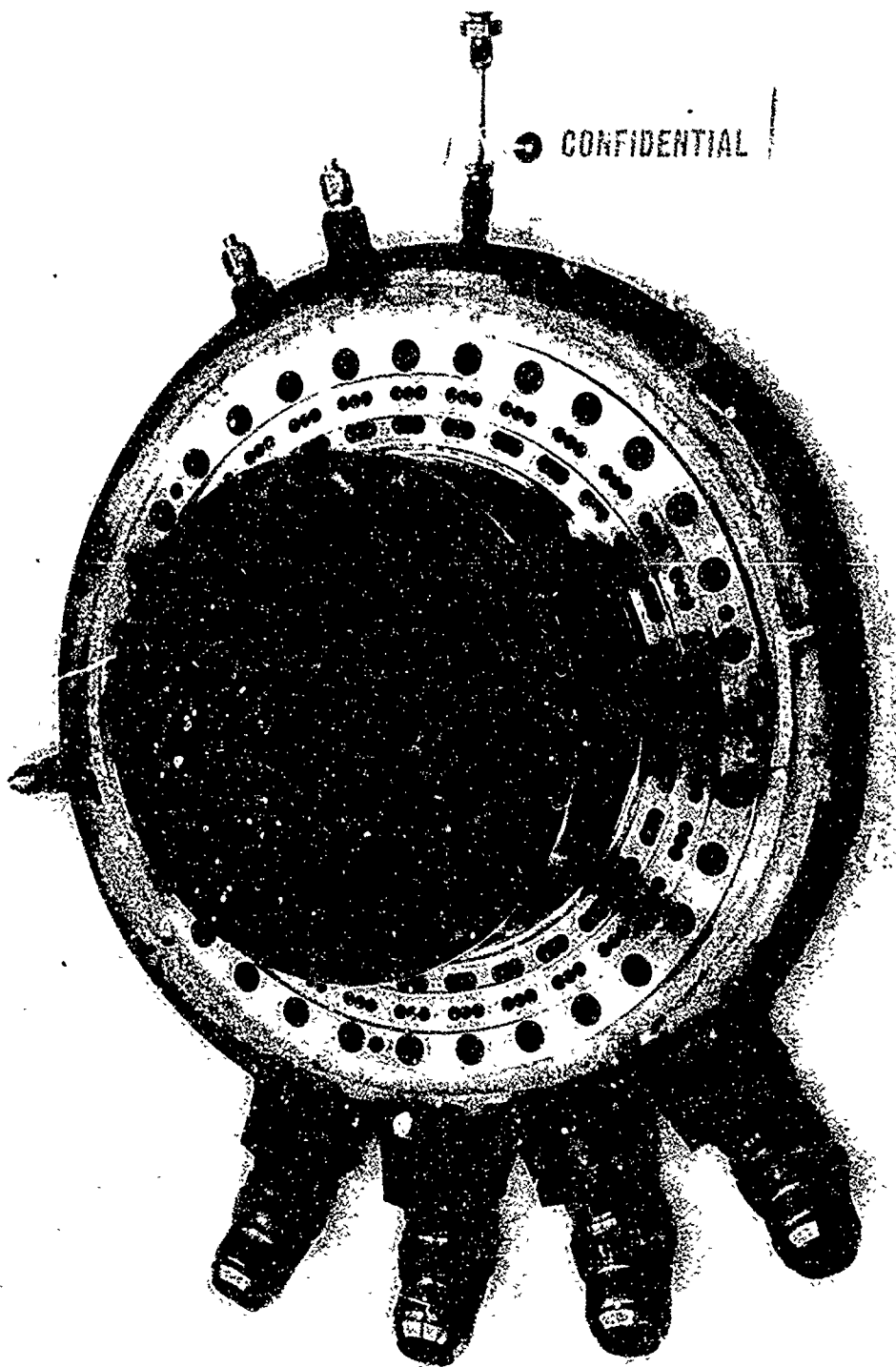
Mark-125 AE Secondary Injector with Performance Ring (u)

Figure IV-5

CONFIDENTIAL

CONFIDENTIAL

Report 10830-Q-4



CONFIDENTIAL

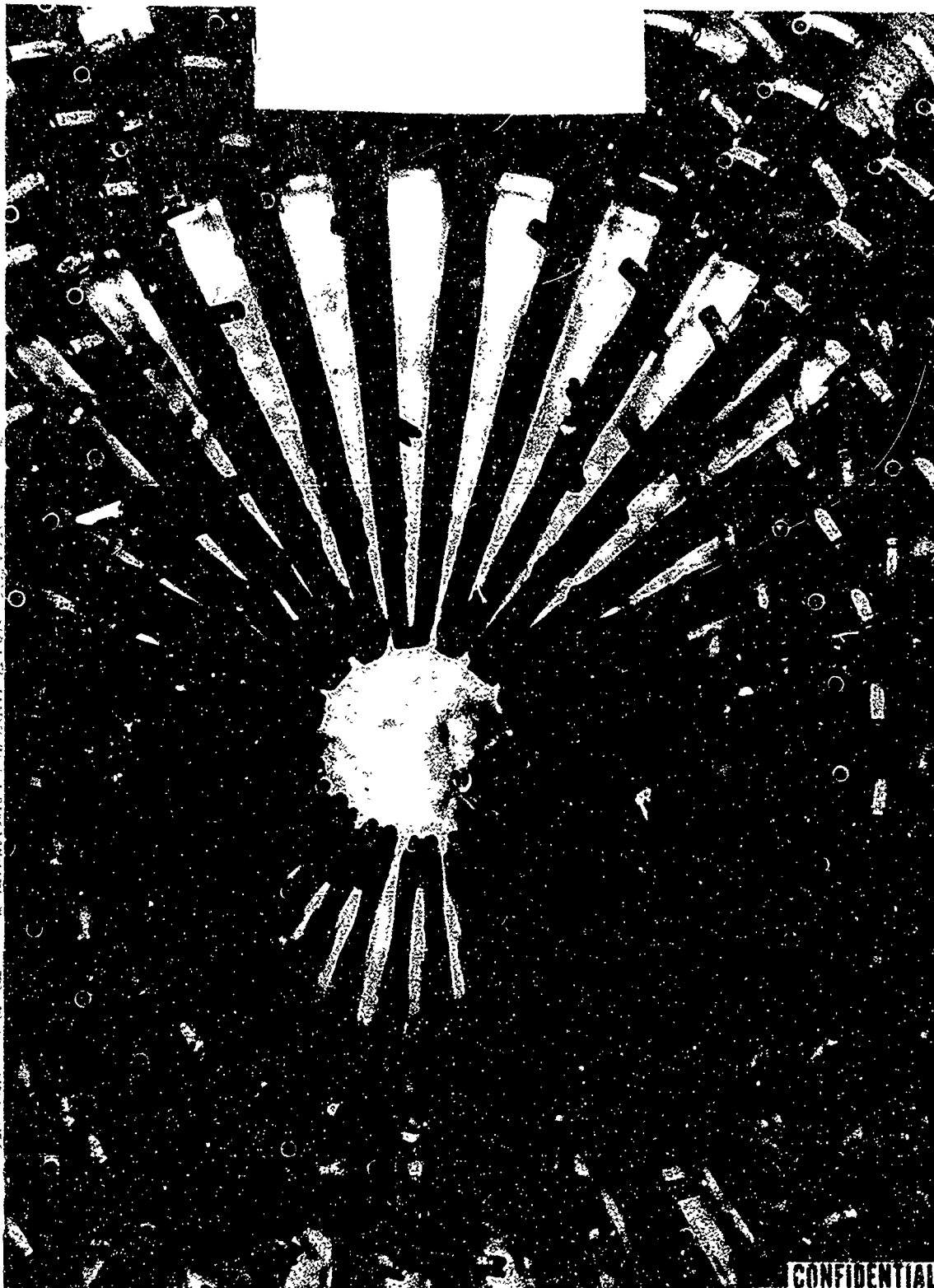
Rake Injector with Shroud (u)

Figure IV-6

CONFIDENTIAL

CONFIDENTIAL

Report 10830-Q-4



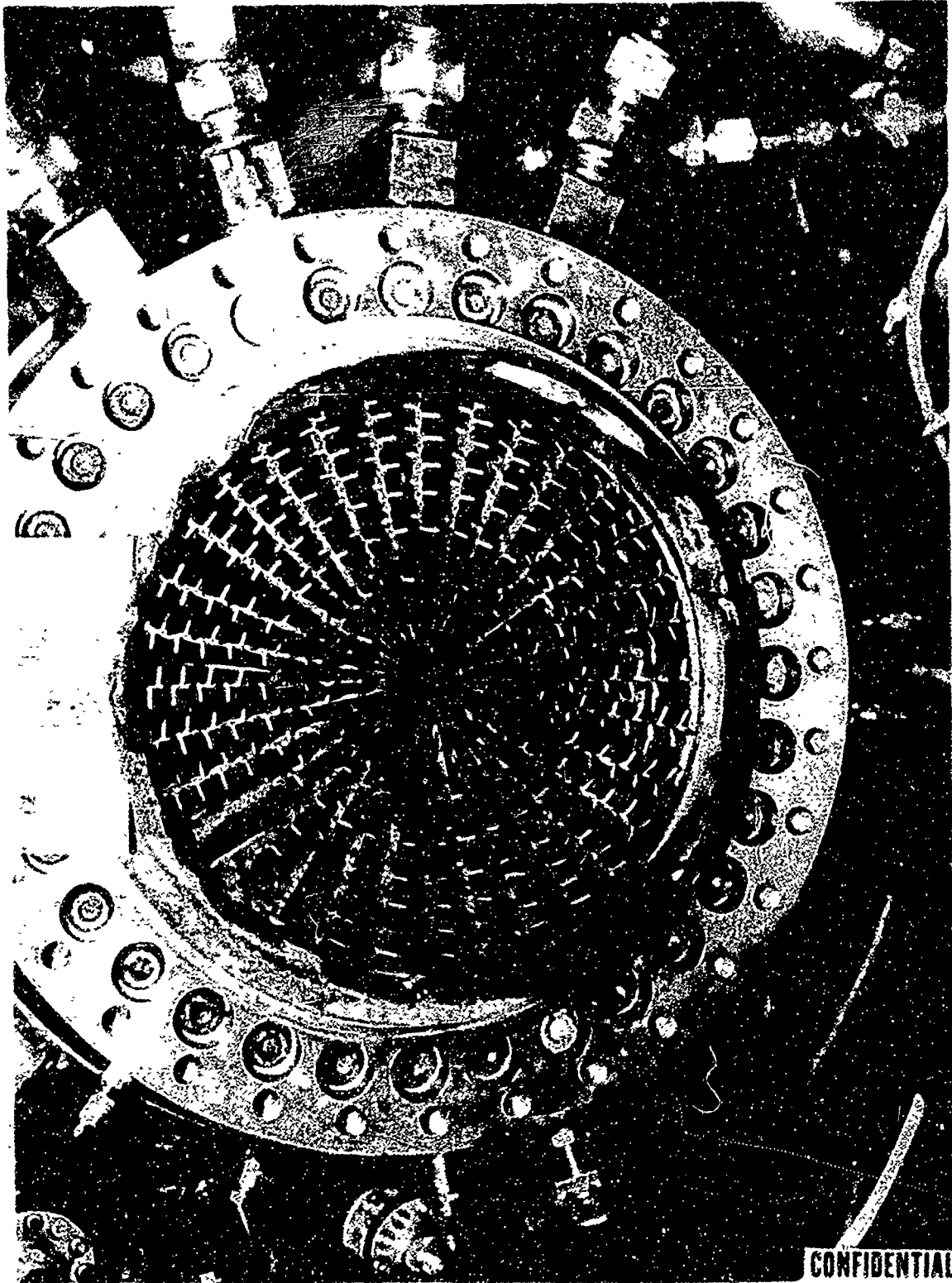
Injector Erosion after Test 1.2-11-WAN-014 (u)

Figure IV-7

CONFIDENTIAL

CONFIDENTIAL

Report 10830-Q-4



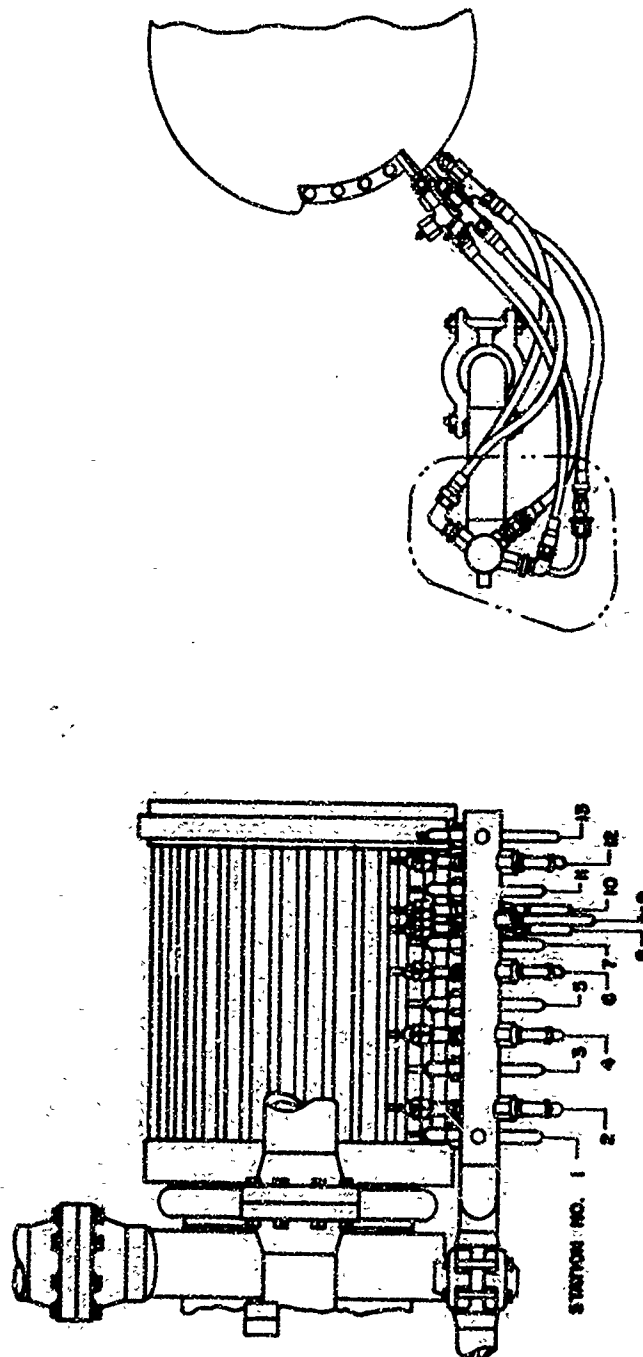
Injector Erosion after Test 1.2-11-WAM-015 (u)

Figure IV-8

CONFIDENTIAL

UNCLASSIFIED

Report 10830-Q-4



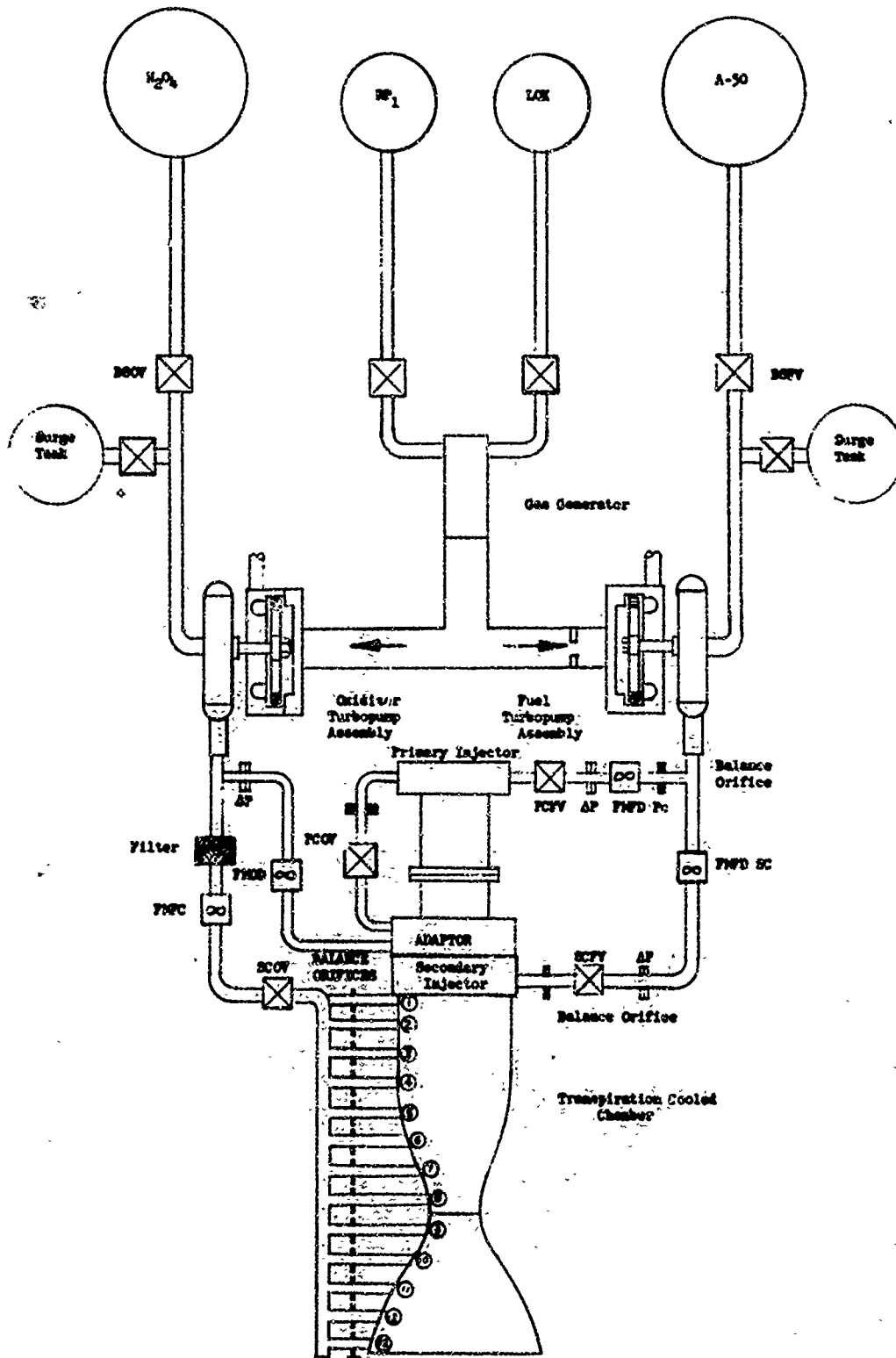
Transpiration-Cooled Distribution System

Figure IV-9

UNCLASSIFIED

UNCLASSIFIED

Report 10830-Q-4



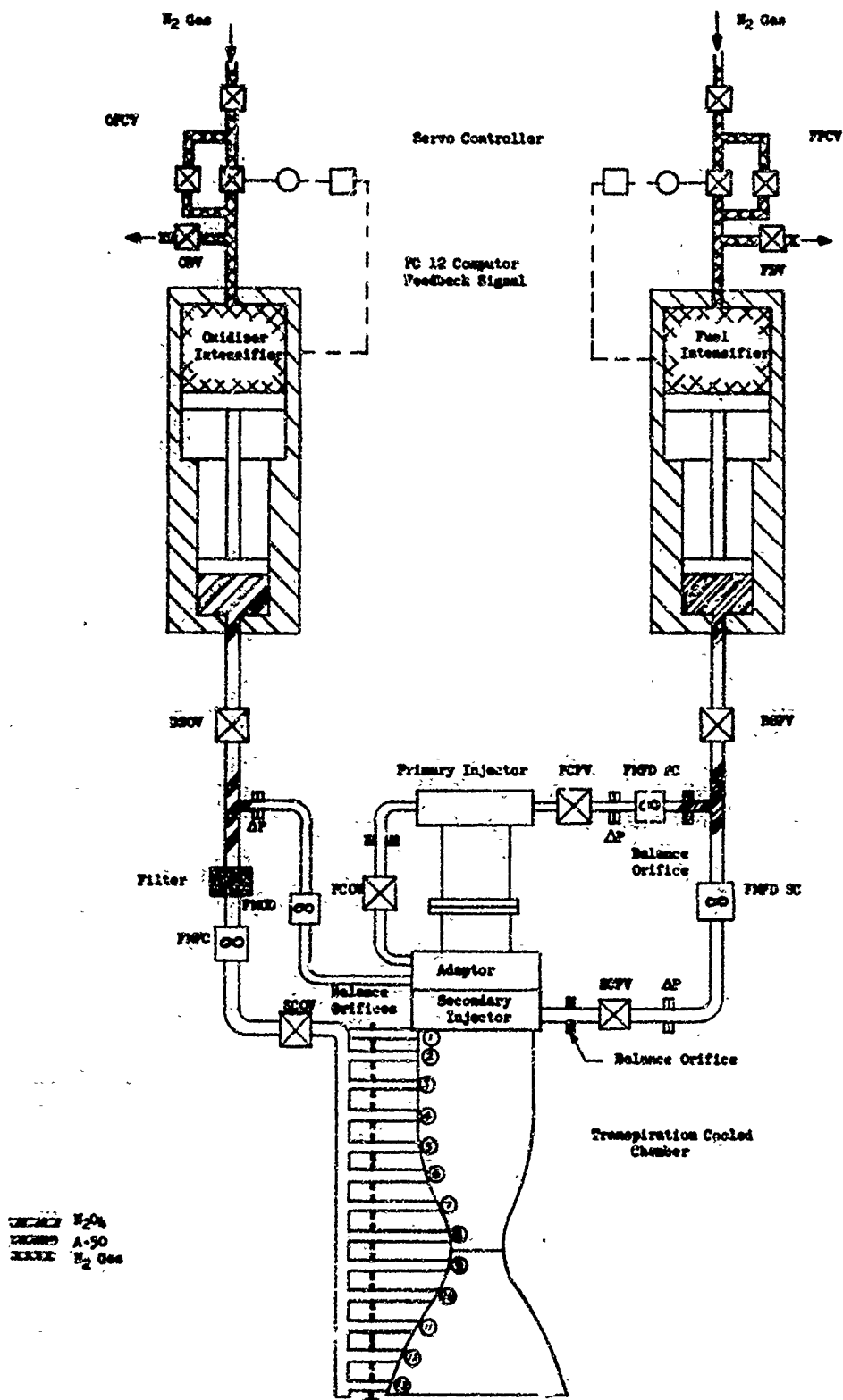
Transpiration-Cooled Engine Schematic (Pump-Fed)

Figure IV-10

UNCLASSIFIED

UNCLASSIFIED

Report 10830-Q-4



Transpiration-Cooled Engine Schematic (Intensifier-Fed)

Figure IV-1'

UNCLASSIFIED

UNCLASSIFIED

Report 10830-Q-4

V.

ADVANCED TPA (T-ENGINE)

A. GENERAL

(u) The three-walled B-design TPA was finalized, and detail drawings of the fuel and oxidizer housings were completed. Quotations received for the B-design fuel and oxidizer housing indicated that costs were too high for Phase-II production. Therefore, various changes will be incorporated into a revised C-design. Detail drawings of long-lead-time items for the pumps and the turbine (e.g., inducers, impellers, turbine rotor shaft, and turbine stator) are being prepared to obtain advanced quotations and delivery dates for Phase-II test planning. Additional heat-transfer and stress analyses pertaining to the fuel housing and turbine rotor shaft were completed.

(u) Test results on the A-housing are very promising, and axial bearing-housing displacements agree well with predicted values. Test results on the oxidizer-lubricated bearings were completely satisfactory, but those for the fuel-lubricated bearings indicated that further refinements of the bearing-cage design are necessary. Wear-ring tests to date in water were satisfactory; wear-ring attachments of various designs performed successfully at pressure differences of 2400 psi across the labyrinth. Successful cold-flow rotating seal tests were also conducted after test-facility problems had been resolved.

B. ADVANCED TPA DESIGN

(u) Final stress and displacement studies for the B-housing configuration at maximum engine operating pressure and temperature were completed. Under these conditions, high thermal stresses exist at the wall of the fuel-pump housing that is exposed to the turbine exhaust gases. These high thermal stresses cause unacceptable axial displacements of the housing balance-piston lands. The radial face of the fuel-pump housing wall will therefore be cooled regeneratively with oxidizer that is presently used to cool the conical bearing-housing portion of the fuel pump. All other axial and radial displacements of the oxidizer and fuel housing are satisfactory. TPA buildup dimensions and critical clearances for the impeller wear-rings, the turbine stator piston rings, the turbine rotor tip, the primary combustor piston rings, and the balance-piston gaps are presented in Figures V-1 and V-2.

(u) Normalized axial-thrust forces for off-design TPA operation are currently being calculated for each major turbopump component (e.g., fuel pump, oxidizer pump, and turbine). These normalized thrust forces will be incorporated into the engine steady-state and transient computer model to establish allowable TPA axial-thrust off-design operating capabilities for Phase-II development testing.

UNCLASSIFIED

Report 10830-Q-4

V, B, Advanced TPA Design (cont.)

(u) Small sample filters (of 2, 5, 10, and 17 average micron filtering size) for the bearing coolant were ordered and will be flow-tested in water to determine pressure drop versus flow rate and filtering size.

(u) Test of the intensifier-fed primary combustor will be conducted after water tests of components have been completed in Phase-II and will evaluate the performance and mechanical integrity of the turbopump. Initially, the tests will be made at reduced speed and subsequently at design speed. A layout of the TPA test fixture is shown in Figure V-3.

C. PUMP DESIGN

(u) The hydraulic design of the advanced TPA pumps was reviewed on 27 April 1966 by an Aerojet-General consultant, Professor A. J. Acosta, California Institute of Technology. Dr. Acosta agreed with the overall hydraulic design and felt that the predicted performance of the pumps should be obtained readily.

(u) The ARES pumps (for both the T-engine and the inline engine) are designed for supercavitation at a suction specific speed of about 30,000. This value was selected because of inducer-vane stress limitations. The boost pumps will supply NPSH values that will allow normal operation at suction specific speeds of 15,000 to 18,000. This design margin was provided to eliminate possible operational difficulties such as pressure oscillations, head-bias shifts, and cavitation damage. The boost pumps will also permit the engine to be used without redesign, in many different applications including those with very low NPSH values.

(u) Missile-application studies have shown that NPSH values of 60 to 195 ft would be available for typical missions. For normal operating conditions, at suction specific speed of about 17,000, the T-engine pumps require a NPSH of 381 ft for the oxidizer and of 355 ft for the fuel, whereas the inline turbopump requires 329 ft for the oxidizer and 260 ft for the fuel. These requirements are well above the 195-ft maximum available unless tank pressures are increased at the expense of air-frame weight. These studies therefore clearly indicate that boost pumps are required for almost all applications.

(u) The main-stage impeller discharge coefficients of 0.15 for the oxidizer and of 0.12 for the fuel are typical design values for commercial pumps and also agree with those for the Aerojet-General high-efficiency Titan-II pumps. The diffuser designs are also based on past performance data for Aerojet-General pumps and follow commercial design practice. Since the throat area of

UNCLASSIFIED

Report 10830-Q-4

V, C, Pump Design (cont.)

the diffuser controls the shape of the head-flow curve for a given impeller-discharge angle and flow coefficient, the area was sized in accordance with the empirical curve shown in Figure V-4, which also indicates design values for other Aerojet-General diffuser-type pumps. In the oxidizer pump, additional diffusion occurs in the discharge-turning vanes downstream of the diffusers, and the fluid enters the cylindrical section of the oxidizer housing with no whirl. The volute sections of the first- and second-stage fuel pumps are constant-velocity designs and were selected over constant-area designs to minimize pump radial loads. Finalized pump design parameters and dimensions are presented in Figure V-5.

(u) Detailed drawings of the pump inducers and impellers are nearing completion. These long-lead-time items will be submitted to vendors for advanced quotation early in July. The designs of the inducers are straightforward, and these components will be machined from forgings. However, the impellers are considerably more complex (Figures V-6 and -7), and several methods of fabrication will therefore be investigated (e.g., electrochemical milling, investment-casting, and three-dimensional machining plus brazing or welding on the shrouds).

D. TURBINE

(u) Tooling for the highly twisted turbine rotor blade and matching stator was completed, and fabrication of the air-test model is scheduled for completion on 15 July 1966.

(u) Detail drawings of the long-lead-time turbine rotor and stator are almost complete. Several fabrication methods (e.g., three-dimensional machining of the blades plus electron-beam welding of the rotor-shaft assembly, and investment casting of the entire rotor-shaft assembly, Figure V-8) are being considered in order to evaluate cost and to estimate delivery dates.

E. SHAFT

(u) A stress analysis of the integral turbine-rotor shaft, which considered both a shallow and a deep slot between the turbine rotor and the rotating ring of the hydrostatic seal, was completed. Figures V-9 and V-10 show the tangential stress distribution for the two configurations during steady-state operation. Figure V-11 shows the stresses for the short-slot design, 0.2 sec after the turbine is exposed to maximum gas temperatures. The low stress of 50,000 psi for both slots indicates that slot depth is not critical and that stress concentrations are low. The highest stress occurs at the rim of the rotor disc after 0.2 sec of operation and is about equal to the stress conditions presented earlier in Report 10830-Q-3.

UNCLASSIFIED

Report 10830-Q-4

V, E, Shaft (cont.)

(u) The rotational distortion of 0.00465 rad on the rotating face of the hydrostatic combustion seal during steady state operation (Figures V-9 and V-10) exceeds the acceptable limit of about 0.0005 rad. Methods of reducing this seal-face distortion, caused by thermal gradients in the turbine-rotor, are being investigated.

F. AXIAL THRUST AND BEARING DESIGN

1. Axial-Thrust Balance

(u) Several methods were investigated to predict TPA axial thrust on the engine computer model at off-design operating conditions and also account for hardware and/or performance tolerances. The following method, considered to be the most flexible, was selected: The normalized thrust at design and off-design operating conditions will be determined separately for the pumps, the turbine, and the balance piston and these values will be fed into the engine computer model in a manner similar to that used for the pump normalized head-versus-flow characteristics.

2. Bearing Design and Development

(u) The testing of N₂O₄-lubricated bearings that met advanced-TPA requirements was completed. Satisfactory operation of both aligned and misaligned roller bearings was achieved. Detailed discussions and results of these tests are presented in Section VIII.

G. SEALS

(u) A complete discussion of the seal development effort is given in Section X.

H. TURBOPUMP HOUSING

(u) A complete discussion of the housing analysis and development effort is given in Section VII.

I. BOOST PUMP

(u) The hydraulic design of the boost pumps was also reviewed by Dr. Acosta who agreed that the selected mixed-flow design is preferred over the axial-flow concept for the specific speeds of the pumps.

UNCLASSIFIED

Report 10830-Q-4

V, I, Boost Pump (cont.)

(u) The mixed-flow design is essentially the same as that described in Report 10830-Q-3 except that the speed of the fuel pump was increased to its original value of 8000 rpm. This change was made because the available fuel-turbine inlet pressure was reduced by about 150 psi due to higher line losses and as a result, the optimum efficiency of both the oxidizer and the fuel turbines occurs when both operate at 8000 rpm.

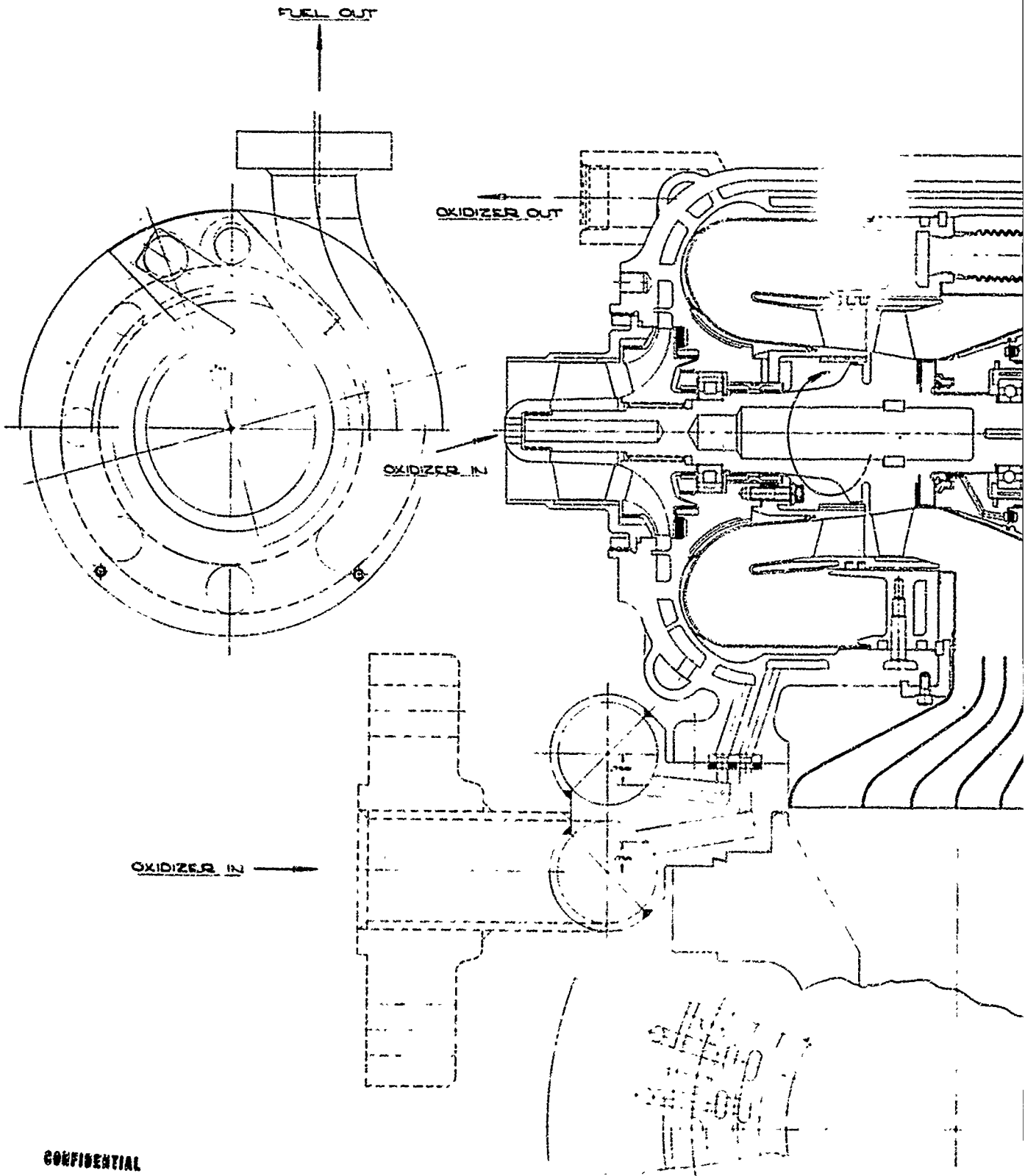
(u) The impeller vane configurations have been finalized, and vane coordinates are being generated on a computer program. The combined stress at the root of the impeller blade is 25,200 and 15,600 psi for the oxidizer impeller and the fuel impeller, respectively, at the 110% overspeed condition. The allowable stress for forged Al-7075 is 38,000 psi, which is sufficient.

(u) The free-body pressure distributions for the oxidizer impeller and the turbine rotor are shown in Figure V-12; the resulting axial thrust is 600 lb in the direction of pump suction. However, since the impeller backvane and turbine-disc pressure gradients are not precisely known, the maximum axial thrust assumed for bearing design purposes is 1000 lb.

(u) The hydraulic design of the boost-pump turbines was completed; preliminary calculations show that the stress of the shrouded rotor blade is 42,000 psi. The allowable design stress for AM-355 steel under shock loading caused by the partial-admission nozzle appears to be adequate, but blade stresses of existing Aerojet-General partial-admission turbines and other references will be reviewed to confirm that these stress limits under shock loading are safe.

(u) The critical-speed investigation for two bearing configurations was completed. The critical speed for the duplex-mounted ball bearing, described in Report 10830-Q-3, is 20,000 rpm--well above the operating speed. The ball bearing nearest the turbine must carry a radial load of 1000 lb, in addition to sharing an equal thrust load. Since the radial load can exceed the thrust load (a condition which is not recommended), the duplex-mounted ball bearing was replaced with a roller bearing and a ball bearing. The ball bearing for this design is located on the shaft side where a radial load of 285 lb occurs, whereas the roller bearing is located on the shaft side exposed to a radial load of 1000 lb. The critical speed for this design is 40,000 rpm; the predicted life at this value and at 110% of critical speed for the roller and for the thrust bearing with propellant lubrication is conservatively estimated at 150 and 28 hr, respectively.

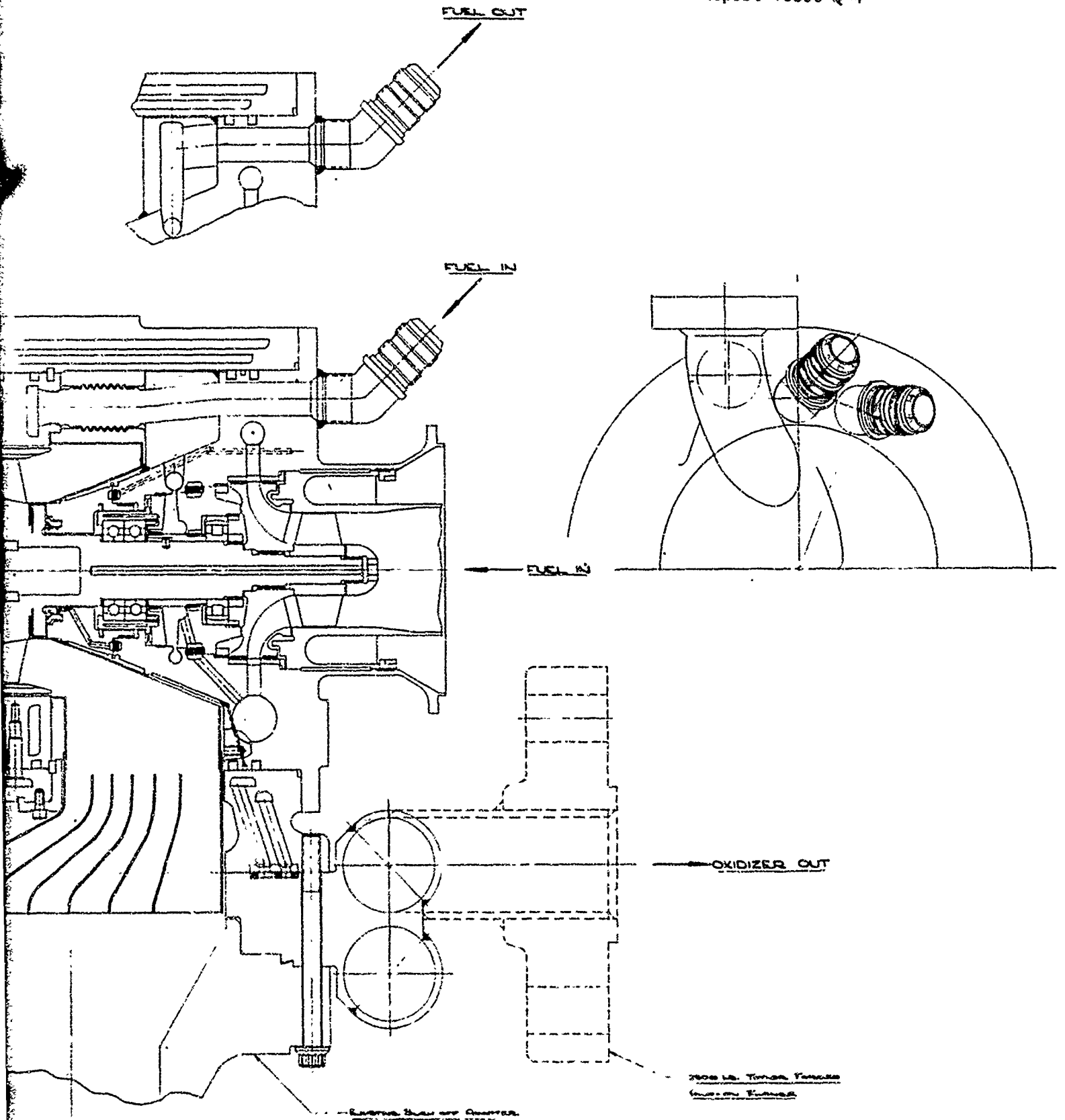
(u) Test-fixture layouts for water tests of the boost pump and of the hydraulic turbine are shown in Figure V-13. Initially, the boost-pump impeller and the hydraulic turbine will be tested separately, but subsequent tests with a bootstrap-fed system will evaluate boost-pump performance as a unit.



CONFIDENTIAL

CONFIDENTIAL

Report 10830-Q-4



B Design TPA Layout--Intensifier-Fed Primary Combustor-TPA Tests (u)

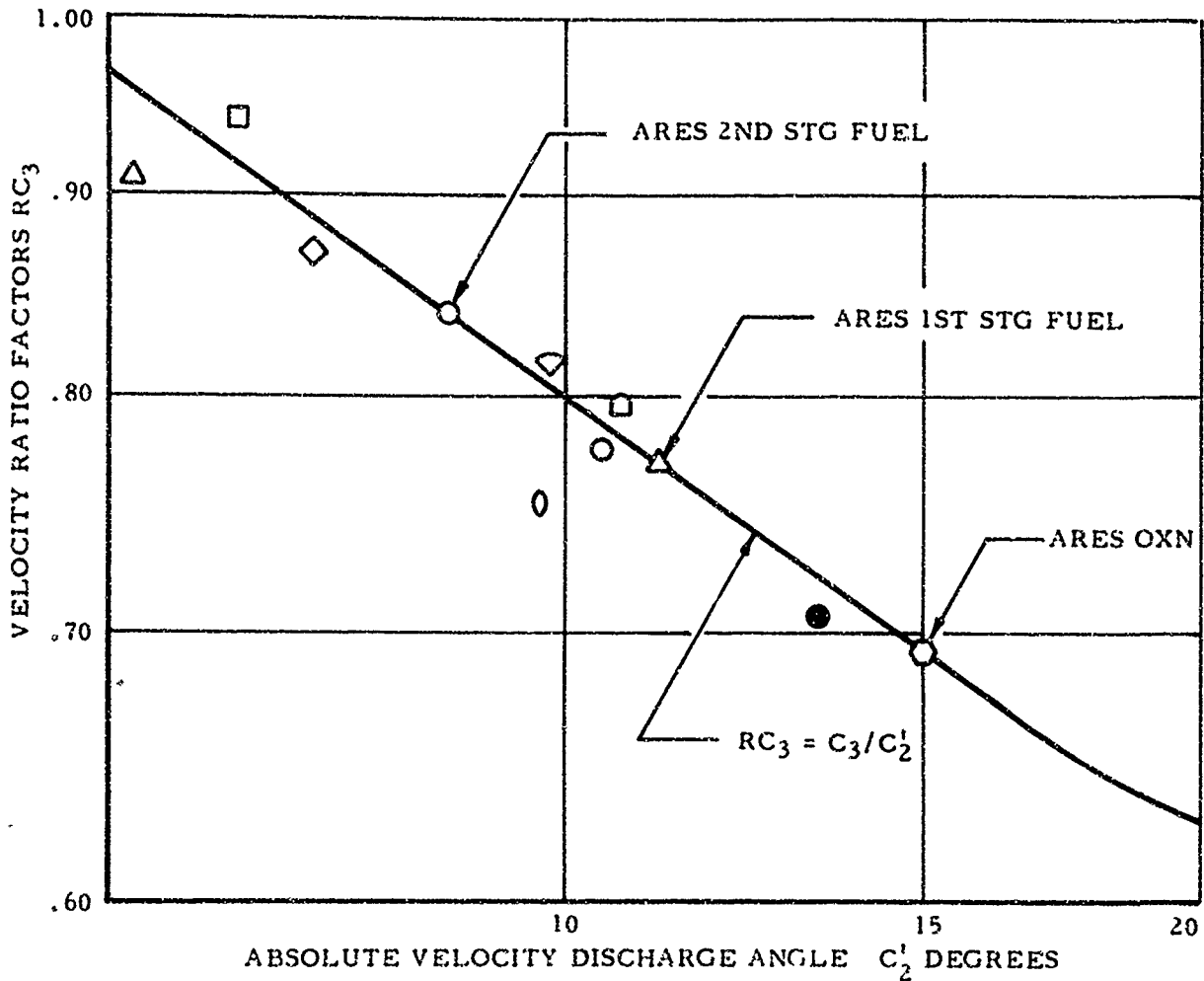
Figure V-3

CONFIDENTIAL

CONFIDENTIAL

Report 10830-Q-4

VELOCITY RATIO FACTOR



- C_3 = DIFFUSER THROAT VELOCITY OR VOLUTE VELOCITY FOR VANELESS DIFFUSER DESIGNS
- C_2' = ABSOLUTE FLUID VELOCITY IMPELLER DISCHARGE
- NERVA 48 VANE $B_2 = 90^\circ$
- ◇ NERVA 24 VANE $B_2 = 90^\circ$
- NERVA 48 VANE $B_2 = 90^\circ$
- ◊ NERVA 18 VANE $B_2 = 90^\circ$
- BB FUEL $B_2 = 90^\circ$
- ◇ BB OXID $B_2 = 90^\circ$
- △ H_1P_c $B_2 = 90^\circ$
- GRAND COULEE MODEL PUMP $B_2 = 24^\circ$

Pump Diffuser Velocity Ratio

Figure V-4

(This page is Unclassified)

CONFIDENTIAL

CONFIDENTIAL

Report 10830-Q-4

	<u>Oxidizer</u>	<u>1st Fuel</u>	<u>2nd Fuel</u>
Speed - RPM	40,000	40,000	40,000
Flow - GPM, Impeller (Diffuser)	1579 (1420)	1170 (960)	177 (168)
Head Rise - ft	9650	9280	6040
Impeller - Discharge Vane Angle - Degrees	28	28	22.5
Impeller Vane Height - in.	.324	.344	.091
No. of Impeller Vanes	9	9	7
No. of Diffuser Vanes	8	8	-
Imp. Base Circle Ratio	1.08	1.06	1.05
Impeller Discharge Flow Coefficient	.15	.12	.09
Diff. Inlet Angle (high pressure side) - Deg.	14.55	5.6	-
Diff. Throat Area - in ²	.173	.098	-
Diff. Inlet Port Width - in.	.360	.315	.120
Diff. Exit Port Width - in.	.360	.315	.120
Impeller Discharge Diameter - in.	4.79	4.48	3.61
Impeller Discharge Absolute Fluid Angle - Deg.	15.2	11.1	8.4
Impeller Discharge Relative Fluid Angle - Deg.	18.6	17.1	13.0
Absolute Fluid Angle at Base Circle - Deg.	9.34	6.75	4.99
Incidence to Diffuser Vane Angle Ratio	.36	-.21	-
Diffuser Velocity Ratio, $\frac{\text{Inlet}}{\text{Outlet}}$	2.46	1.96	-
Volute Velocity - ft/sec	-	200	362
Discharge Velocity - ft/sec	50	134	145
Head Coefficient	.44	.49	.49
Efficiency	74	66	57

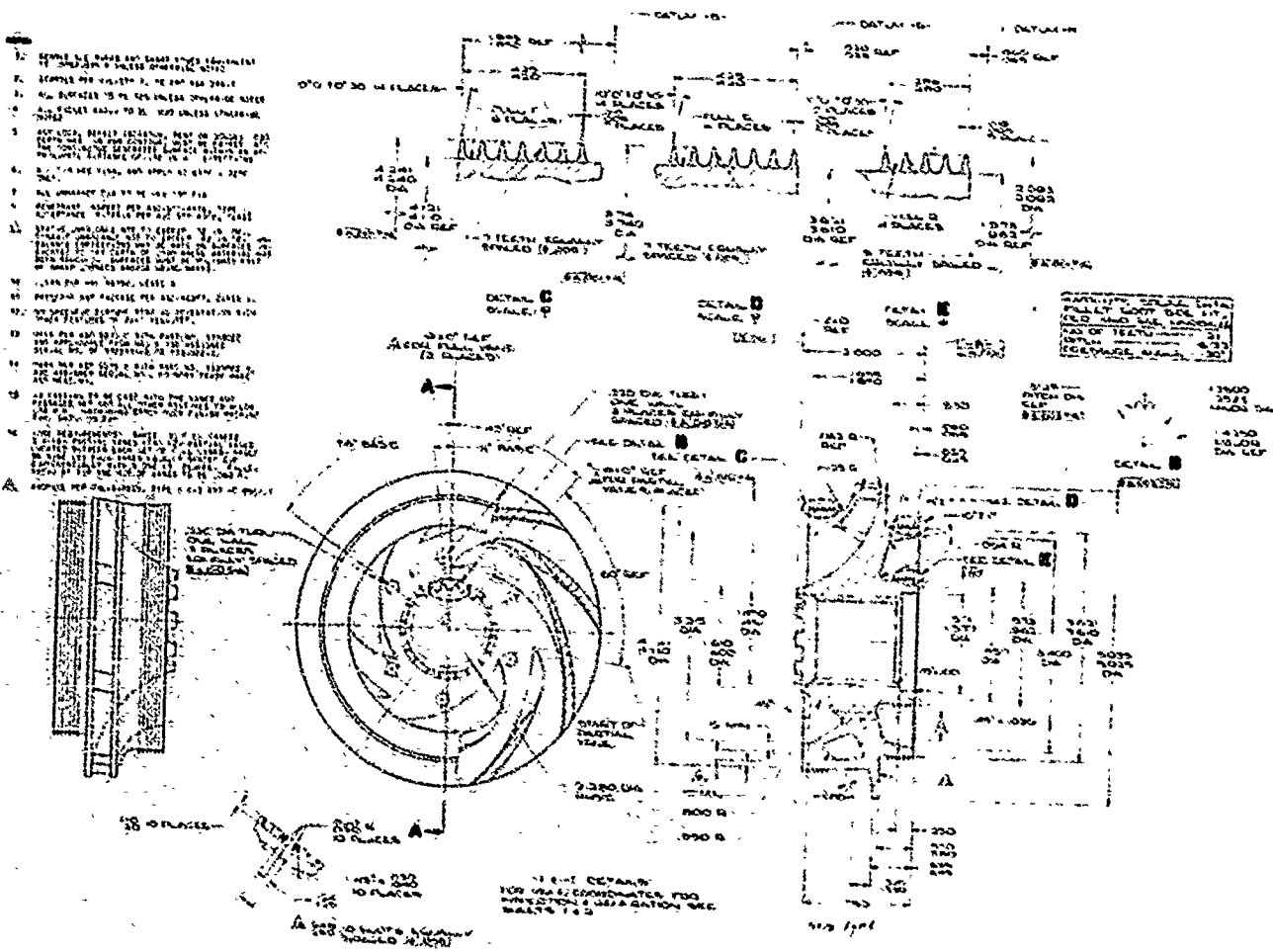
Mainstage Pump Design Parameters (u)

Figure V-5

CONFIDENTIAL

CONFIDENTIAL

Report 10830-Q-4



Oxidizer Impeller

Figure V-6

(This page is Unclassified)

CONFIDENTIAL

UNCLASSIFIED

Report 10830-Q-4

OPER. CONDITION

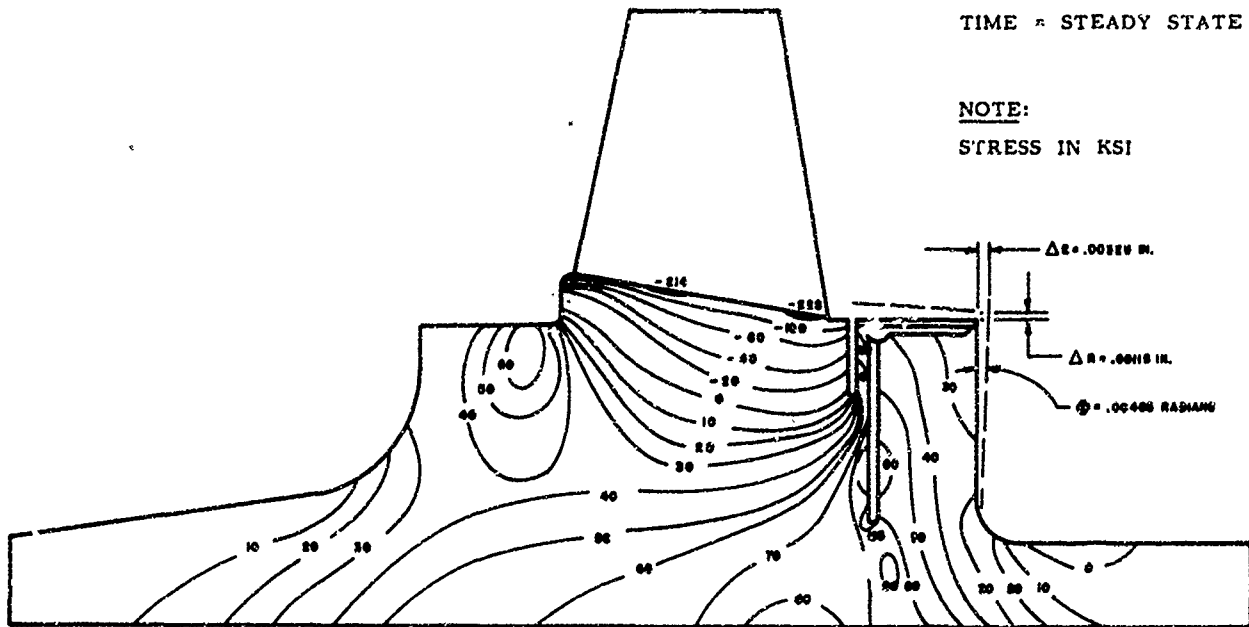
GAS TEMP = 1500°F

SPEED = 40,000 RPM

TIME = STEADY STATE

NOTE:

STRESS IN KSI



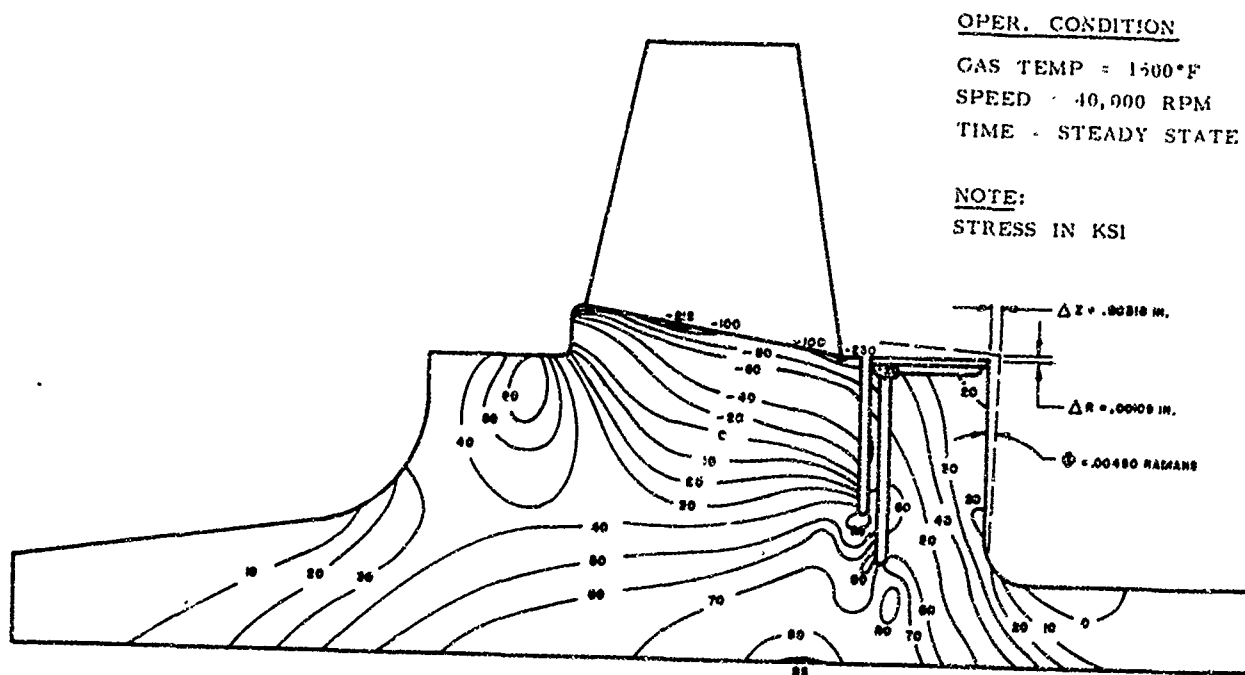
B-Design Turbine Rotor--Steady-State Tangential Stresses (Shallow Slot)

Figure V-9

UNCLASSIFIED

UNCLASSIFIED

Report 10830-Q-4



B-Design Turbine Rotor--Steady-State Tangential Stresses (Deep Slot)

Figure V-10

UNCLASSIFIED

UNCLASSIFIED

Report 10830-Q-4

OPER. CONDITION

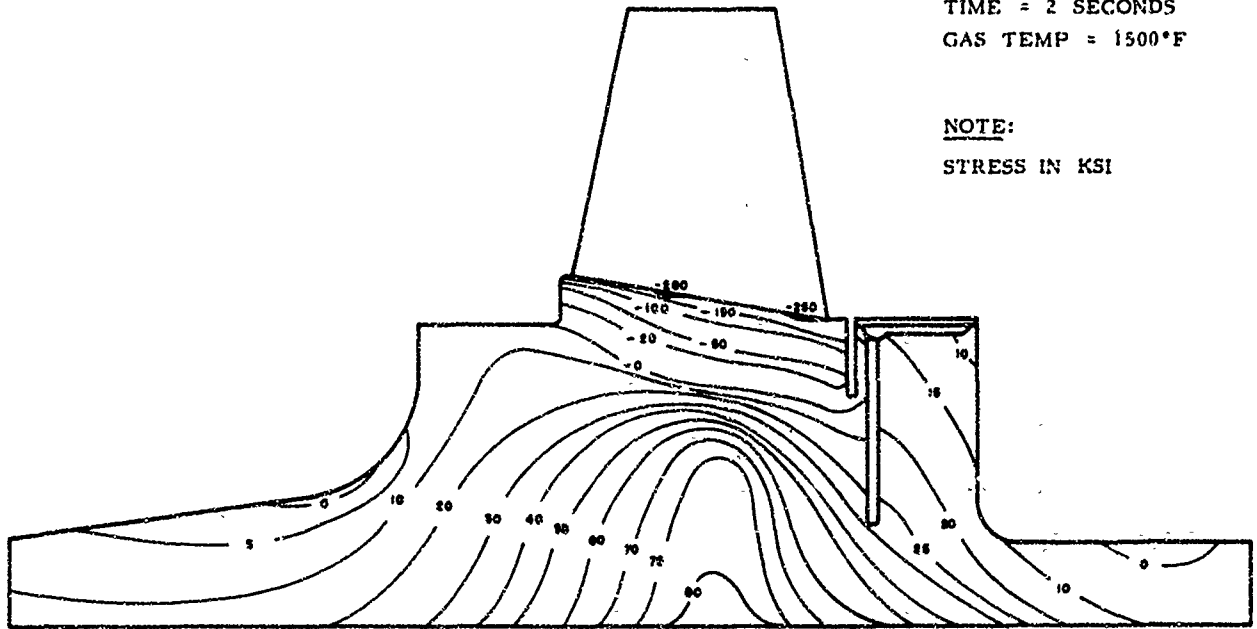
SPEED = 40,000 RPM

TIME = 2 SECONDS

GAS TEMP = 1500°F

NOTE:

STRESS IN KSI



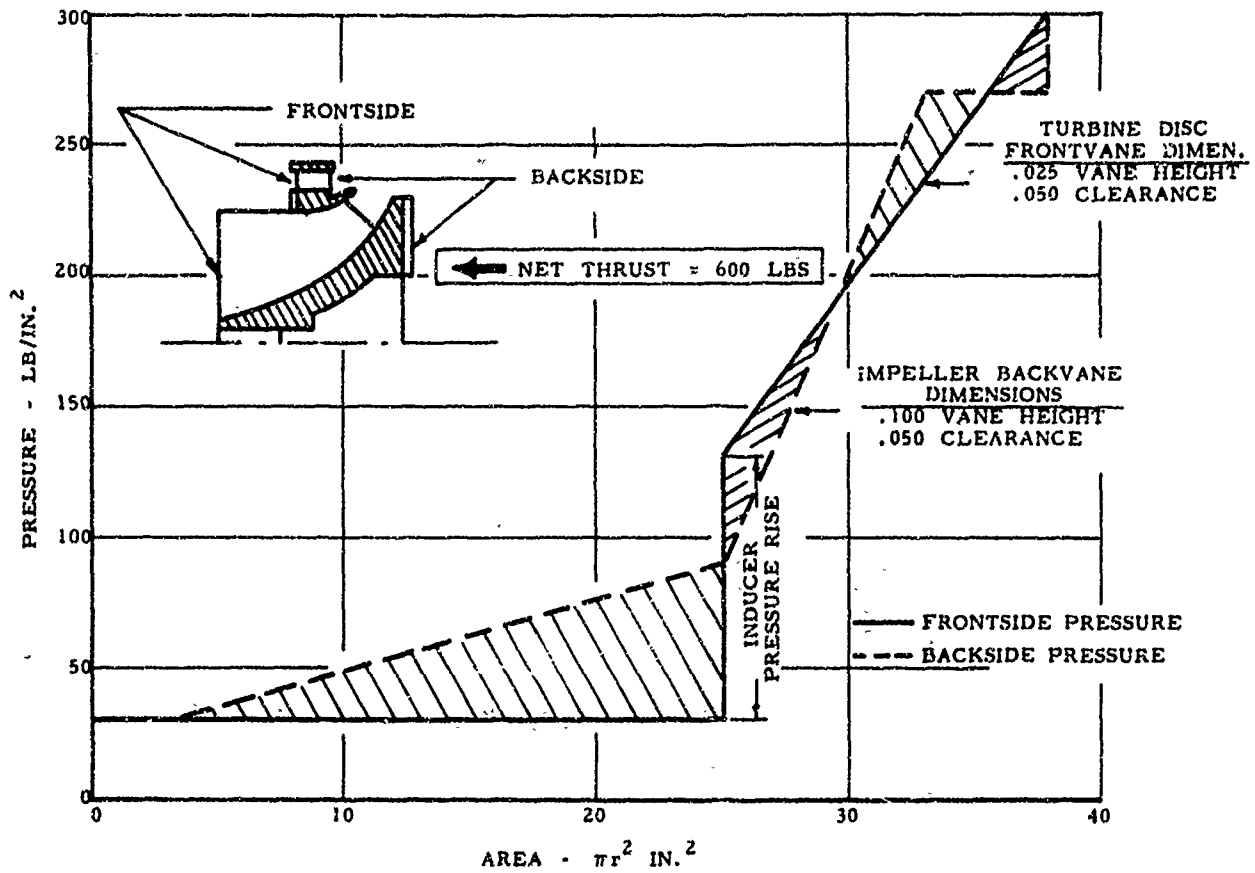
B-Design Turbine Rotor--Tangential Stresses at 0.2 sec of Transient

Figure V-11

UNCLASSIFIED

UNCLASSIFIED

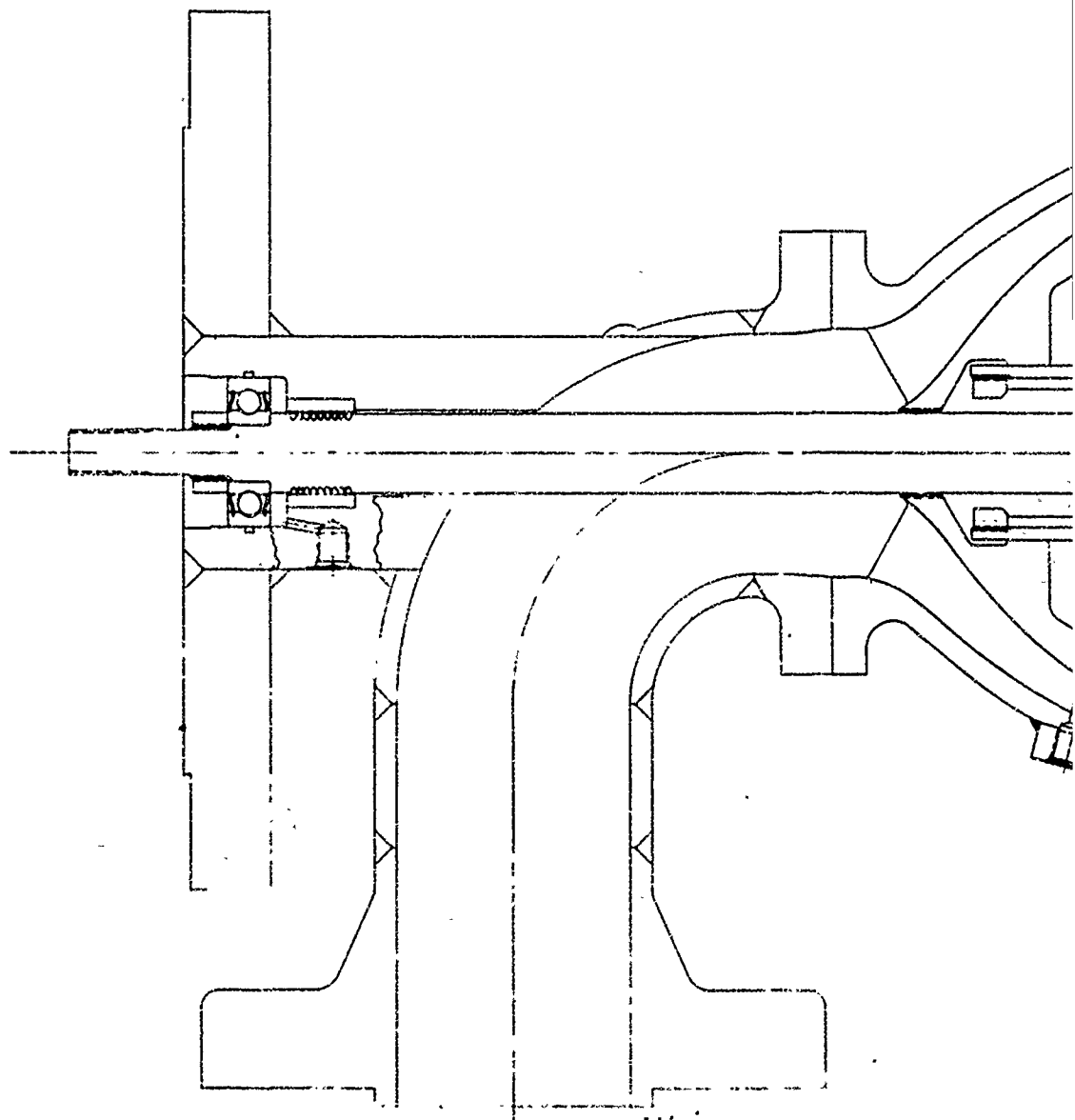
Report 10830-Q-4



Oxidizer Boost Pump Axial Thrust

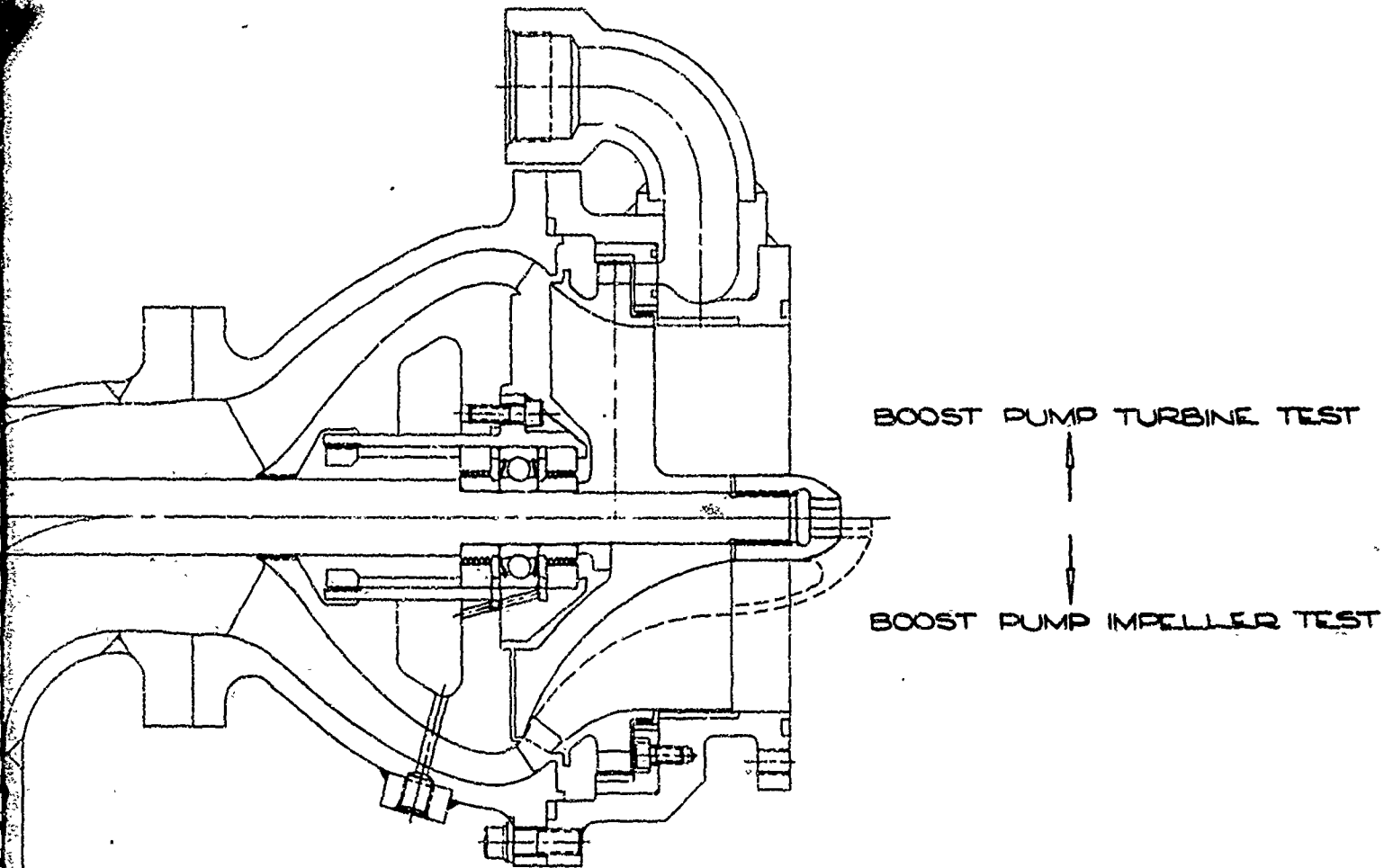
Figure V-12

UNCLASSIFIED



UNCLASSIFIED

Report 10830-Q-4



Boost Pump and Hydraulic Turbine Water Test Fixture Layout

Figure V-13

UNCLASSIFIED

Report 10830-Q-4

VI.

INLINE (BACKUP) TURBOPUMP

A. GENERAL

(u) The inline, or backup, turbopump of conventional configuration is being designed for the ARES program and will be used if critical aspects of the advanced turbopump are not adequately proven. The basic objective of design conservatism in the backup turbopump, together with other considerations discussed in detail in the first quarterly report, resulted in the selection of a configuration with the shaft parallel to the line of thrust. This turbopump, consequently designated the "inline design," has a nominal operating speed of 30,000 rpm. Design features include moderate bearing DN values; self-acting axial-thrust balance; low-pressure, ambient-temperature, purged dynamic shaft seals; conventional housings; hydraulically balanced twin-discharge volutes; and an end-mounted axial-flow turbine which confines the high-temperature elements to the thrust-chamber end of the TPA. All work on this TPA configuration to date indicates acceptable accomplishment of technical and cost objectives.

(u) Fabrication of the structural test housing was completed, the hydrotest fixture has been received, and structural testing will be initiated early in the next reporting period. A final stress analysis of the housing was completed. Analytical results indicate that all stresses and deflections are low, suggesting the possibility of future weight reduction.

(u) The feasibility of the bearing designs selected for the inline TPA has been demonstrated by appropriate tests in N_2O_4 and AeroZINE 50 at high speed (31,250 rpm) and at higher loads than anticipated. These tests, which satisfy the work statement objectives, were accomplished without incident.

(u) The analytical design of the pumps, the turbine, the bearings, the seals, and the axial-thrust-balance system is nearing completion, including final revisions to this system. Results from an analysis of the axial-thrust balance system indicate higher flow recirculation than formerly anticipated. This, together with results of a refined hydraulic-loss analysis of the housing, made it desirable to revise the profile geometries of the pump impellers. This effort is under way. The basic design work on the inline TPA will be completed as soon as this work is accomplished.

B. TPA DESIGN

1. Configuration Refinements

(u) Continued analysis of the various axial-thrust-balance system concepts resulted in the selection of a configuration which uses the first-stage fuel impeller as the primary thrust-balancing element. This choice required minor changes in fuel housing geometry, revised impeller contours in all pumps as discussed in paragraph VI,C below, and a modified mounting of the fuel-end roller bearing. These revisions have been incorporated on a completed master dimensional layout of the overall turbopump assembly and are shown in Figure VI-1.

UNCLASSIFIED

Report 10830-Q-4

VI, B, TPA Design (cont.)

2. Performance Refinements

(u) Results of a computer analysis to determine the effects of varying flow recirculation during thrust-balance-system operation show that a significant effect on engine operation occurs when the second-stage fuel pump is used to balance thrust. Figures VI-2 and VI-3 illustrate the effects on various cycle parameters of first- and second-stage balancing, respectively. The analysis led to the selection of the first-stage fuel pump as a thrust balancer.

(u) The overall changes of the revised design will be correlated and a final computer run of the ARES engine cycle, using the inline TPA, will be made to establish the engine specifications with this turbopump.

C. PUMP DESIGN

1. Oxidizer Pump

(u) The oxidizer-pump discharge housing has an annular channel, which discharges into 52 drilled holes matching the 52 down-flow tubes of the thrust chamber. Analysis showed that the fluid would enter the drilled holes at a very sharp angle with attendant high hydraulic losses unless additional turning of the flow to the meridional direction is provided. Accordingly, a second set of diffusing guide vanes was designed to provide the extra turning and to reduce the velocity of the fluid before it enters the drilled passages. These vanes can be machined on the dome of the housing closure, which is a separate part, thus minimizing fabrication complexity.

(u) The selected thrust-balance system requires that the oxidizer impeller be inherently and hydraulically balanced. Therefore, it was decided to replace the backvanes with a labyrinth. This eliminates backvane losses but increases recirculated flow. As a result of the higher throughflow, the exit port had to be widened slightly and a maximum impeller diameter (6 in.) had to be used to maintain the desired head rise. Analysis of the revised impeller is under way.

2. First-Stage Fuel Pump

(u) As with the oxidizer impeller, recirculated flow in the first-stage fuel impeller is increased by the new thrust-balance configuration. Shroud profiles and vane geometry are being modified in a similar manner to meet the revised requirements. No change in diffuser or volute geometry is anticipated.

3. Second-Stage Fuel Pump

(u) The recirculated flow of the second-stage fuel impeller is reduced by the new thrust-balance system. To maintain a reasonably high flow coefficient, appropriate for a H-Q curve with a steep slope, the width of the

UNCLASSIFIED

Report 10830-Q-4

VI, C, Pump Design (cont.)

exit port on this impeller must be reduced. In addition, the impeller will be open-faced and will use backvanes to minimize its effect on shaft axial thrust. Revised design work has been initiated.

D. TURBINE DESIGN

(u) The turbine design is essentially complete. Tasks remaining include review of the design analysis, operating-life predictions at elevated temperature, and preparation of the design report.

E. POWER TRANSMISSION

1. Critical Speed

(u) A further critical-speed analysis on the inline TPA has been completed in which revised impeller weights and bearing stiffnesses were used. The new values correspond to those of the chosen axial-thrust-balance system. Results indicate that critical speed was slightly increased by the changes: the first critical speed is predicted to fall in the range of 40,000 to 42,000 rpm. Since this exceeds operational speed by more than 30%, the result is acceptable.

2. Bearings

(u) The work statement stipulates that 40mm roller bearings and tandem thrust bearings be tested in N_2O_4 and AeroZINE 50 at 31,250 rpm or at a DN value of 1,250,000. Both objectives were achieved during the first tests attempted. No anomalies were encountered. Results are described in detail in Section VIII.

(u) The N_2O_4 -cooled roller bearing at the turbine end of the inline TPA would have a diameter of 45mm or a DN value of 1,350,000 at a TPA speed of 30,000 rpm. This larger shaft diameter is required to carry the full shaft torque. Since 40mm bearings have also been demonstrated at shaft speeds of 40,000 rpm or a DN value of 1,600,000 (see Section VIII), the feasibility of the 45mm bearing is adequately demonstrated. Thus, no difficulty is anticipated with the larger bearing, the design of which has been completed.

(u) The feasibility of the AeroZINE 50-cooled 40mm roller bearing and tandem thrust-ball bearings was demonstrated on the first test without difficulty at 32,000 rpm or a DN value of 1,280,000, as described in Section VIII. The final inline TPA design would utilize 35mm AeroZINE 50-cooled bearings. With the thrust balancer and with symmetrical pump discharge, the loads would be lower than the demonstrated values.

UNCLASSIFIED

Report 10830-Q-4

VI, E, Power Transmission (cont.)

3. Axial Thrust Balance

(u) The axial thrust-balance system has been revised, and its related effects on various components have been discussed in preceding sections. The arrangement of the revised system is shown in Figure VI-1 and should be compared to Figure VII-1 of the third quarterly report, AFRPL-TR-66-82.

(u) In the revised design, each rotor element is essentially balanced hydraulically, producing very little, if any, axial force. However, the first-stage fuel impeller is responsive to axial position, as desired, and produces a righting force if shifted from its neutral position. Maximum restoring force is on the order of 30,000 lb.

(u) A predominant factor in selecting the first-stage fuel impeller instead of the second-stage impeller for thrust balancing was the relative effect of the two methods on engine cycle parameters caused by the variation in flow recirculation relative to rotor position. Figures VI-4 and VI-5 show first- and second-stage balance-system recirculation flow rates as a function of axial position. Because the second-stage impeller, feeding the primary combustor, has a H-Q curve with a steep slope, the recirculation variation shown in Figure VI-5 caused a substantial shift in primary combustor mixture ratio and, hence, large variations in other parameters shown in Figure VI-3.

(u) Use of the first-stage impeller substantially reduced the H-Q shift caused by recirculation. Also, since the first stage feeds the secondary injector, discharge-pressure variations have less pronounced effects on engine parameters. Although there will be some variation in inlet pressure to the second-stage fuel impeller, these variations will be small in comparison to the total primary combustor inlet pressure and, as shown in Figure VI-4, overall effects will be minor.

(u) Stability of the selected thrust balancer is expected to be acceptable because of the relatively high stiffness of the system, illustrated in Figure VI-6, and because of the dash-pot damping inherent in the design.

4. Dynamic Shaft Seal

(u) The basic approach followed in the design of the dynamic shaft seal for the inline turbopump has been to adopt a conventional rubbing-contact, face-riding pair of seals with an inert-fluid purge between the seals. However, an envelope of adequate size was provided to allow other types of seals (e.g., the hydrostatic design) to be used if improved reliability is demonstrated by such concepts. To determine their reliability, both concepts should be tested in Phase II.

UNCLASSIFIED

Report 10830-Q-4

VI, E, Power Transmission (cont.)

(u) The selected design is an off-the-shelf seal illustrated in Figure VI-7. This configuration will provide a seal even if ΔP is reversed, thus minimizing the hazards associated with loss or depletion of the inert fluid. A small slinger is machined integral with the oxidizer running ring to reduce the oxidizer pressure at the seal face to approximately the pressure of the fuel. Thus, both seals will operate at the same ΔP (purge pressure minus propellant pressure). In addition, the slinger permits the use of oxidizer as the purge-system pressurant at inlet pressure which simplifies the system.

(u) The alternative hydrostatic seal, illustrated in Figure VI-8, has an operating flow rate of 0.05 lb/sec for each seal. This higher seal flow rate requires more purge fluid and a larger purge tank than the basic rubbing-contact seal. The weight for this system, assuming 3-min engine operation, would be 20 lb higher than that of the basic seal system.

(u) As indicated in Figure VII-11 of the third quarterly report, it is planned to use an integrated purge-and-suction valve. The design of this valve has been discussed with a potential vendor, who recommended that an integrated hydraulic actuation system be used which will permit positive, controllable sequencing of the purge fluid and of the main propellant valves. Since such a system would obviously increase engine startup and shutdown reliability, its use is planned for the inline TPA. The main propellant valves selected for the inline TPA are of the shearable butterfly type. The purge valve can be readily integrated; the basic design has already been flight-qualified. Opening and closing sequences of the main propellant valves will conform to the existing curves established for the ARES engine. Purge flow will lead propellant flow by an experimentally established time, and will lag main-propellant cutoff sufficiently to permit the system to be emptied of propellant residuals.

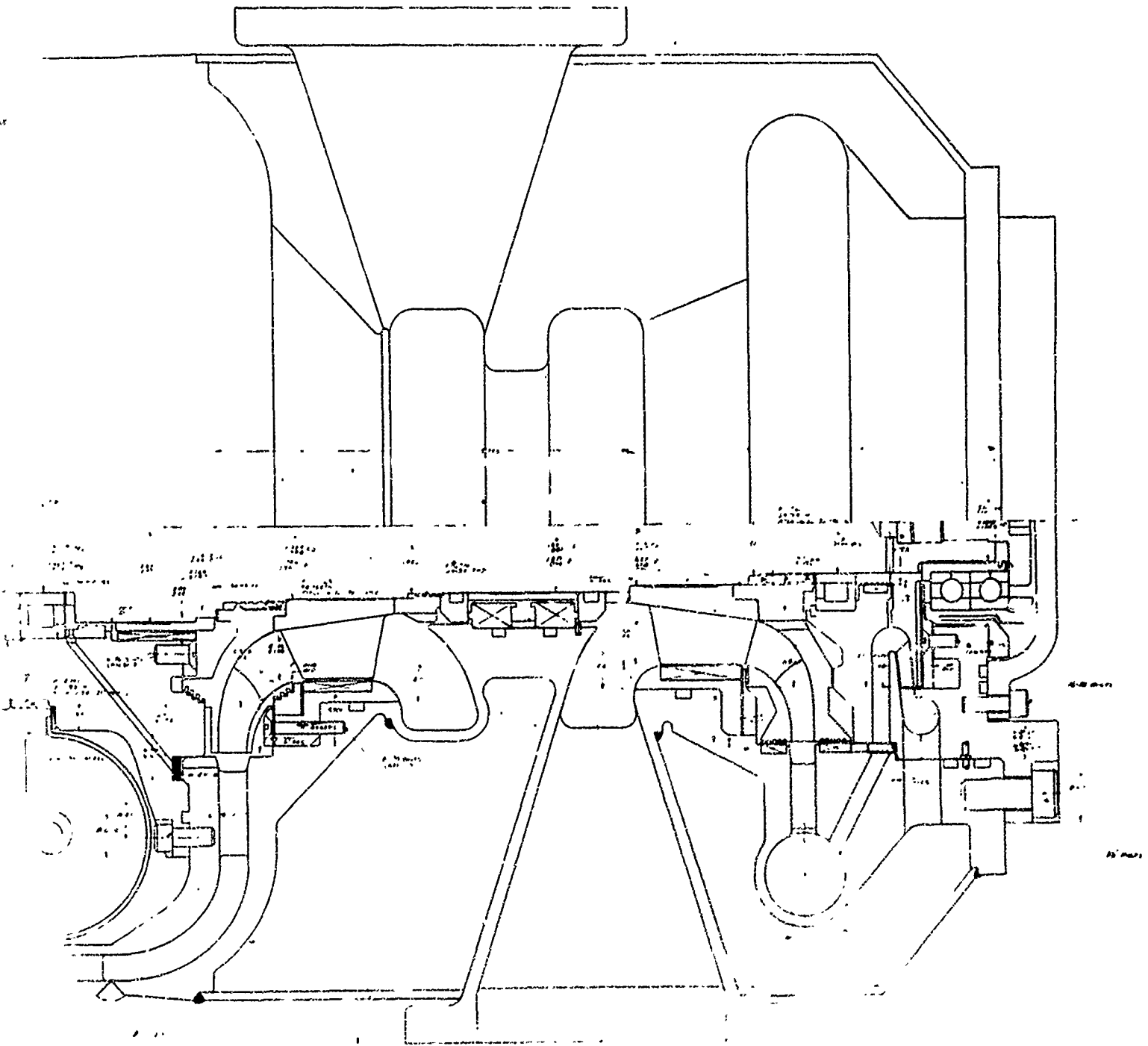
F. INLINE HOUSING FABRICATION

(u) The inline housing, Figure VI-9, was received on 22 June 1966. Some fabrication problems were encountered: The electron-discharge machining of the diffuser vanes in the oxidizer and fuel housings was performed in series instead of in parallel as originally planned. This caused a delay of about two weeks. Also, welding of the 347 stainless-steel sheet-metal stampings to the forged Inconel 718 internal ring caused excessive distortion of the sheet-metal stampings. The stampings were therefore removed and replaced, using improved welding techniques. During final welding of the three main sections (Figure VI-10), the distortion due to welding was difficult to control. Improved tooling would be desirable in future fabrication.

(u) The inline housing has been shipped to the Structural Test Laboratory for instrumentation and testing. The weight of the structural test housing as fabricated was 17 $\frac{1}{2}$ lb.

CONFIDENTIAL

Report 10830-Q-4



CONFIDENTIAL

Inline Turbopump Assembly '(u)'

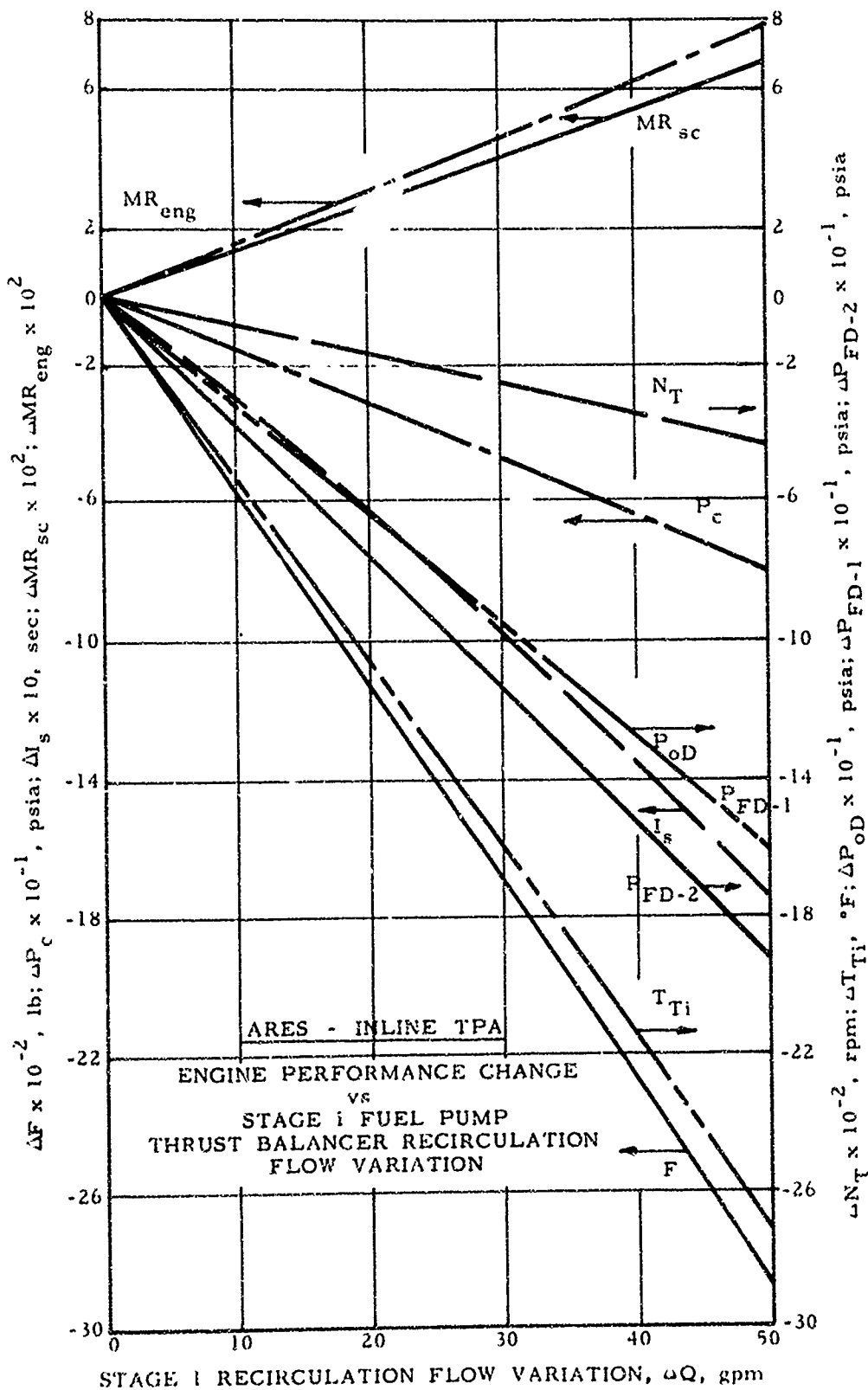
Figure VI-1

CONFIDENTIAL

2

CONFIDENTIAL

Report 10830-Q-4



Engine Performance vs Stage 1 Fuel Pump Thrust Balancer Recirculation Flow Rate

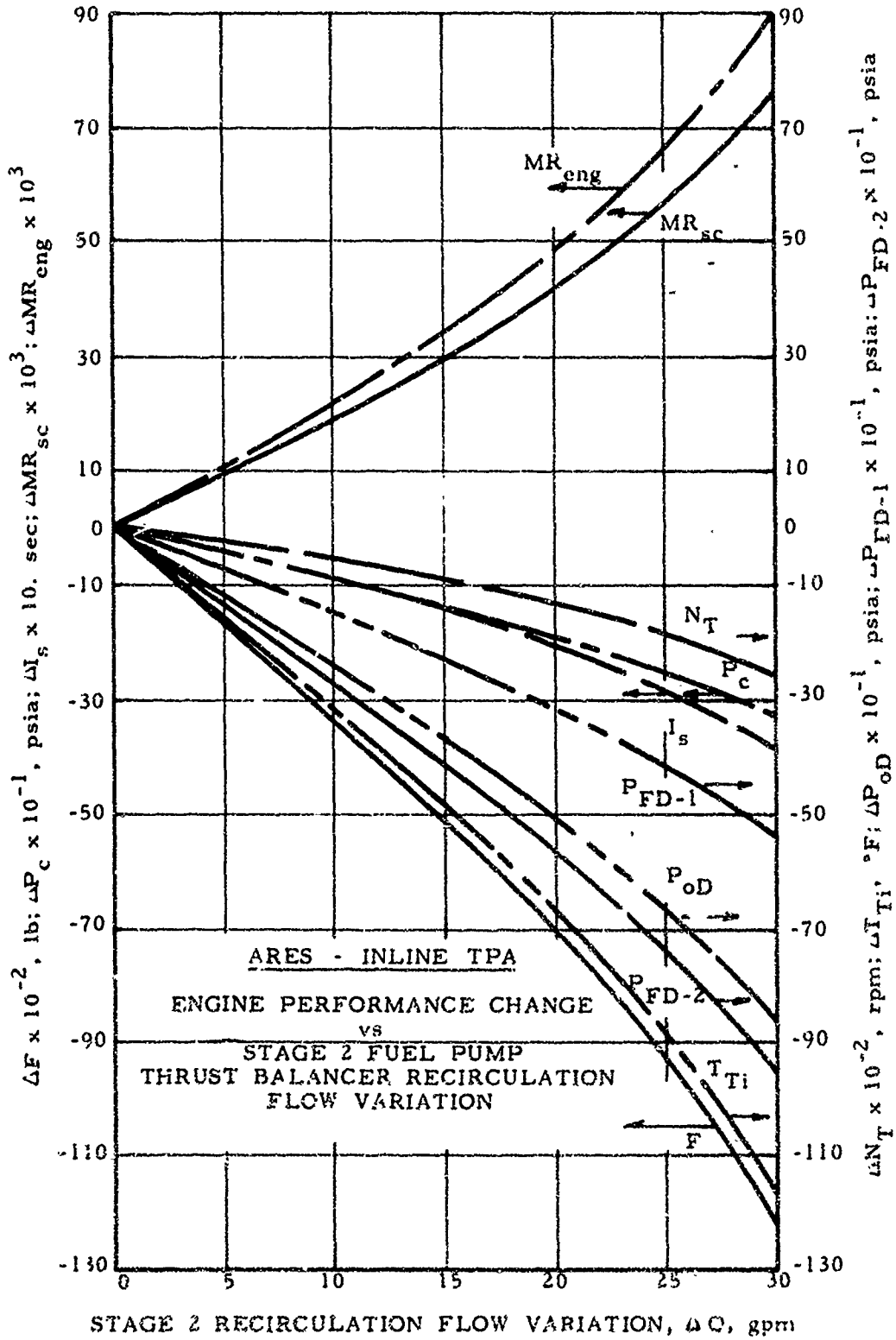
Figure VI-2

(This page is Unclassified)

CONFIDENTIAL

UNCLASSIFIED

Report 10830-Q-4



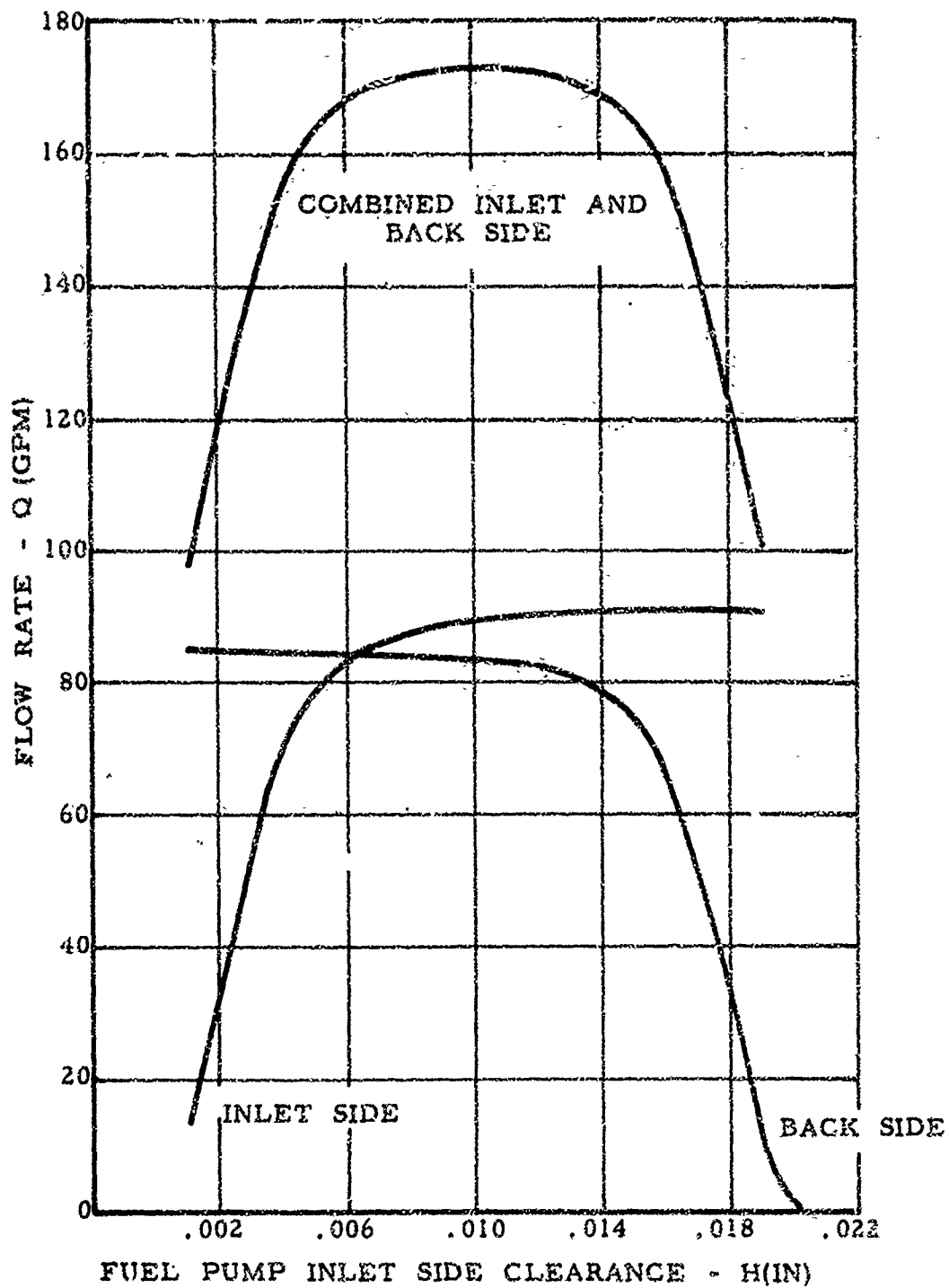
Engine Performance vs Stage II Fuel Pump Thrust Balancer Recirculation Flow Rate

Figure VI-3

UNCLASSIFIED

UNCLASSIFIED

Report 10830-Q-4



NOTES:

1. SPEED 30,000 RPM
2. THRUST BALANCER LABYRINTH CLEARANCE .007 IN.
3. AXIAL TRAVEL = 0 to 0.020 IN.

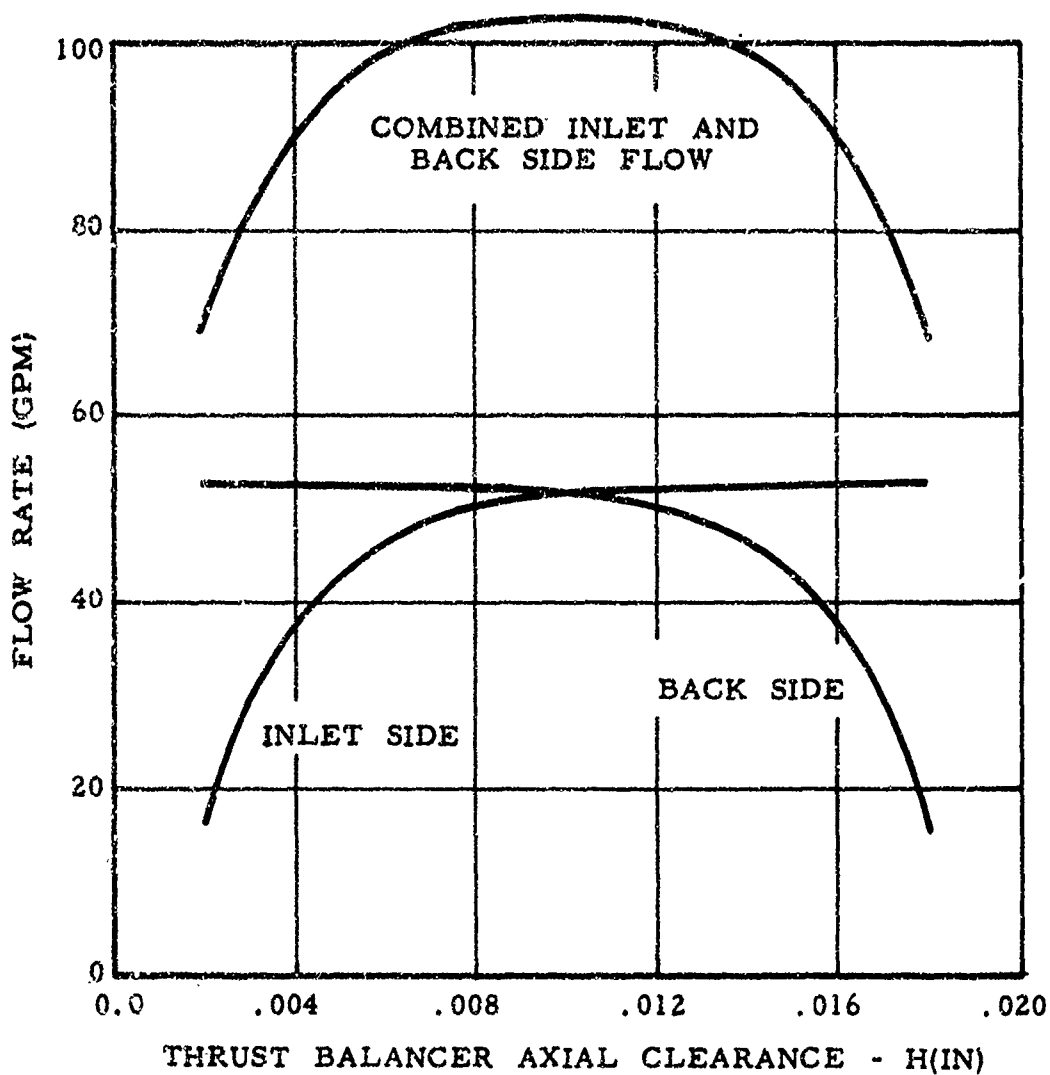
Thrust Balancer Flow Rate vs Axial Position, First-Stage Balancer

Figure VI-4

UNCLASSIFIED

UNCLASSIFIED

Report 10830-Q-4



NOTES:

1. SPEED 30,000 RPM
2. AXIAL CLEARANCE INLET AND BACKSIDE .010 IN.
3. LABYRINTH RADIAL CLEARANCE .007 IN.
4. AXIAL TRAVEL = 0 TO 0.020 IN.

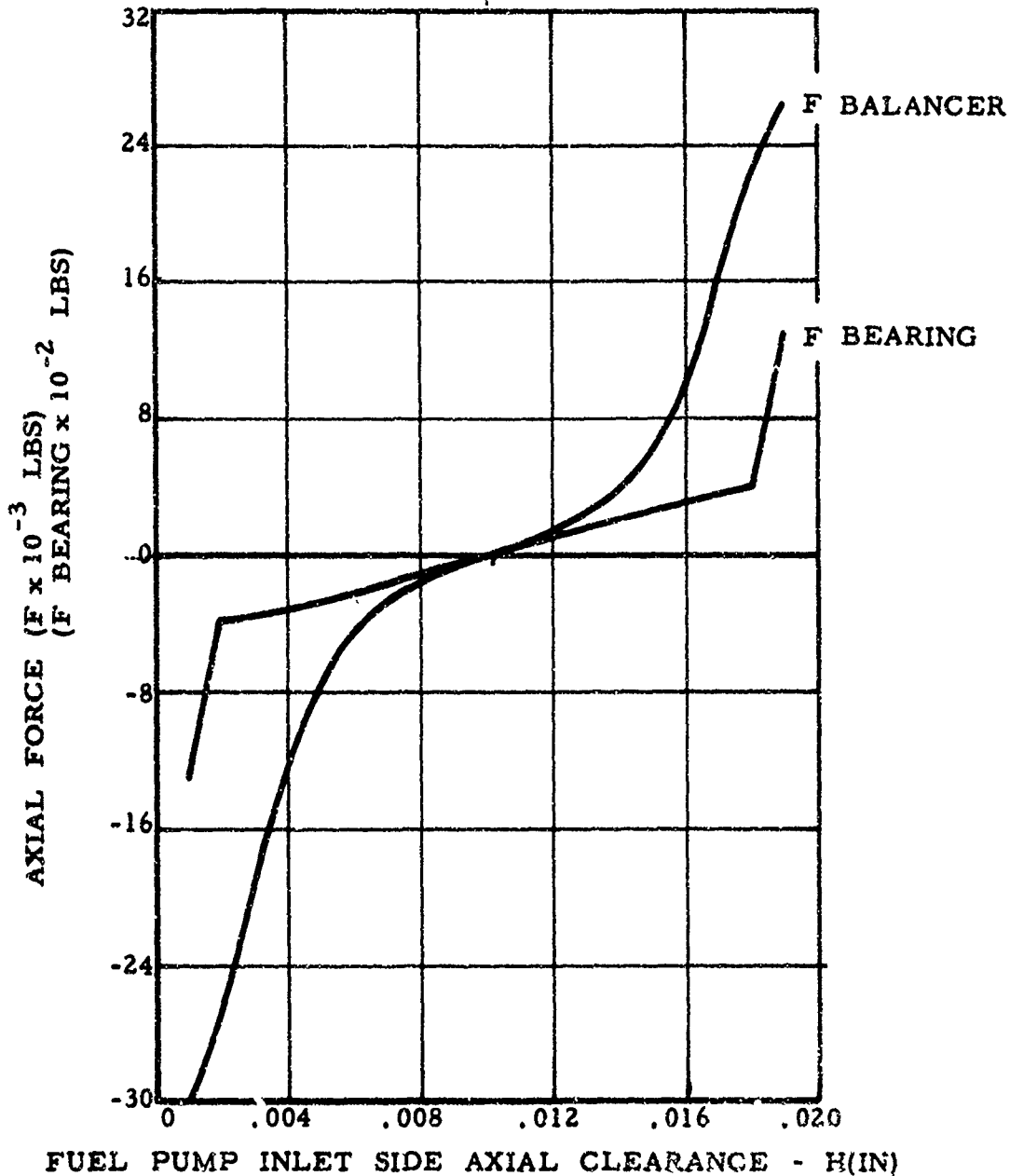
Thrust Balancer Flow Rate vs Axial Position, Second-Stage Balancer

Figure VI-5

UNCLASSIFIED

UNCLASSIFIED

Report 10830-Q-4



NOTES:

1. SPEED 30,000 RPM
2. THRUST BALANCER LABYRINTH CLEARANCE .007 IN.
3. POSITIVE FORCE TOWARDS TURBINE
4. BALL BEARING CARRIER AXIAL STOPS SET AT 0.002 IN. AND 0.018 IN.

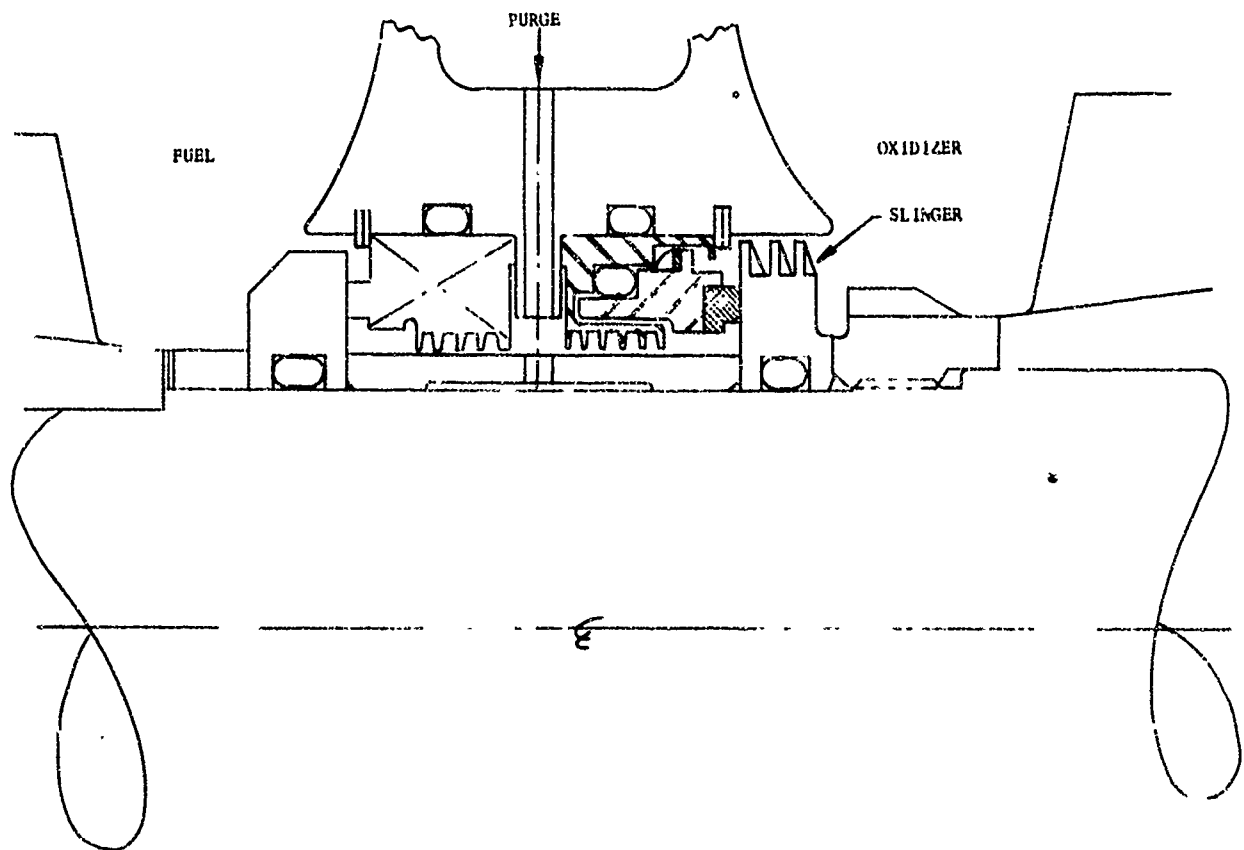
Axial Forces as a Function of Thrust Balancer Position

Figure VI-6

UNCLASSIFIED

UNCLASSIFIED

Report 10830-Q-4



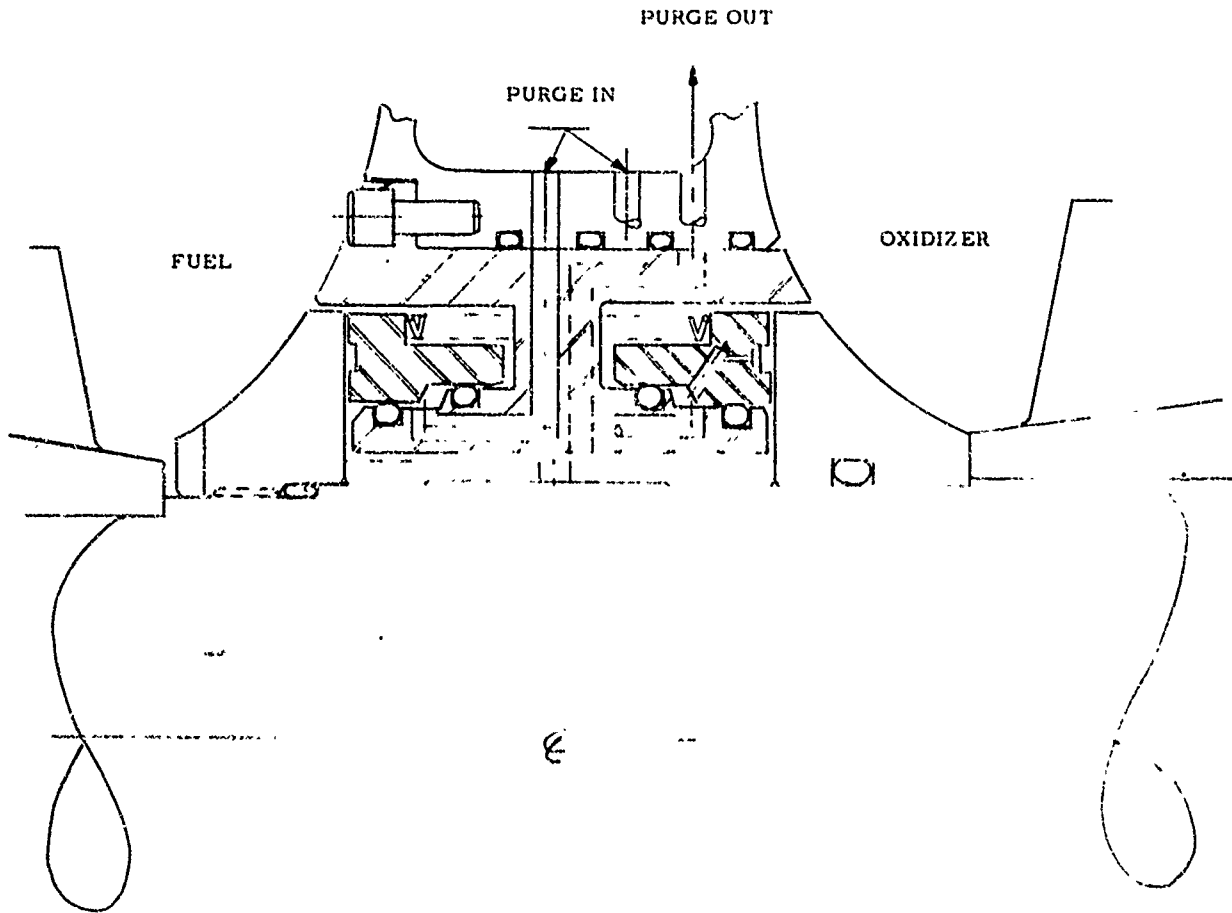
Rubbing Contact Seal for Inline TPA

Figure VI-7

UNCLASSIFIED

UNCLASSIFIED

Report 10830-Q-4



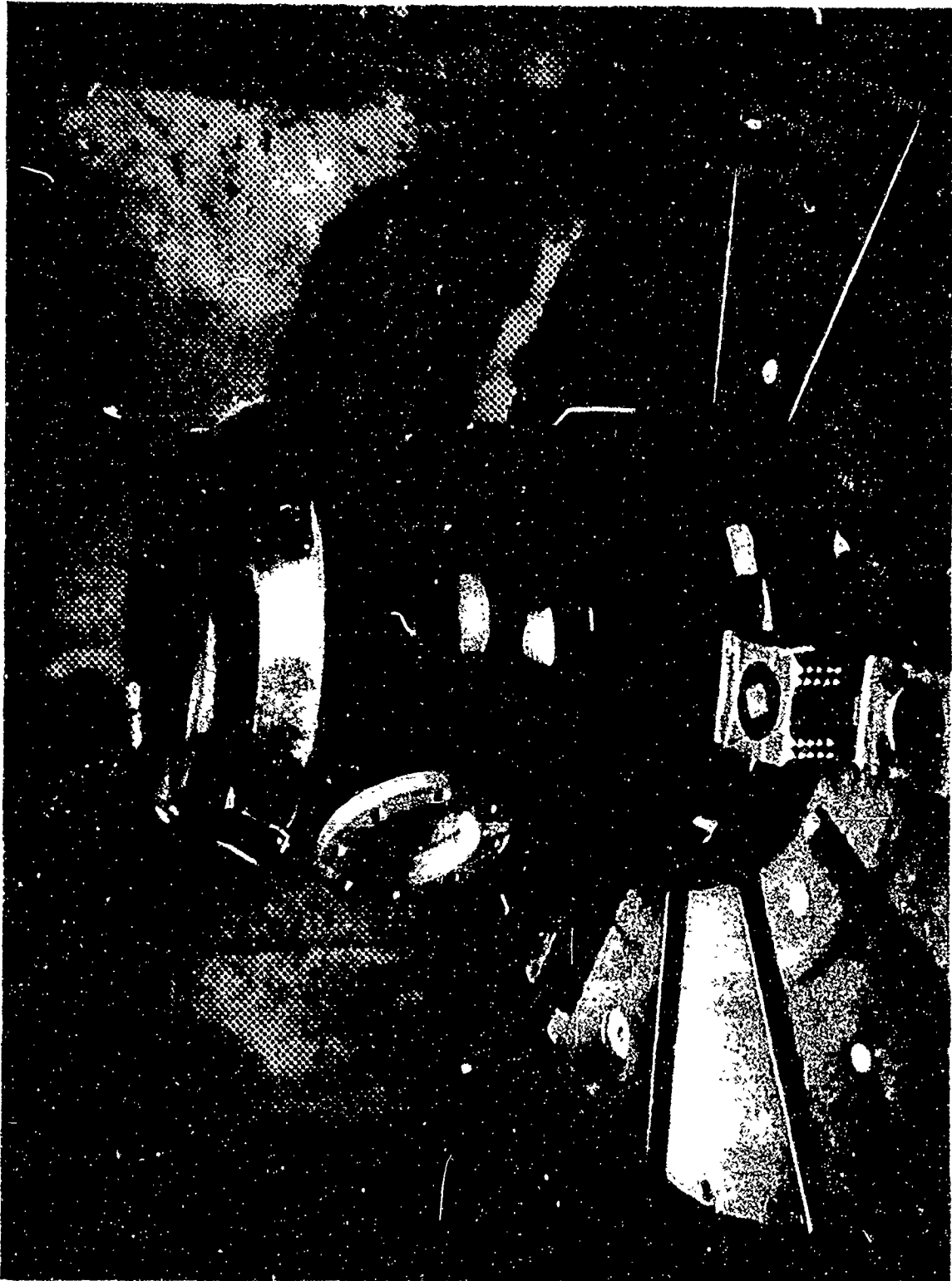
Alternative Hydrostatic Seal for Inline TPA

Figure VI-8

UNCLASSIFIED

UNCLASSIFIED

Report 10830-Q-4



Inline TPA Housing

Figure VI-9

UNCLASSIFIED

UNCLASSIFIED

Report 10830-Q-4



OXIDIZER END



PUMP INLETS



FUEL END

Components of Inline TPA Housing before Final Welding

Figure VI-10

UNCLASSIFIED

UNCLASSIFIED

Report 10830-Q-4

VII.

TPA HOUSING DEVELOPMENT

A. GENERAL

(u) The objective of this effort is the development of housings that will withstand the required fluid and gas pressures, transmit the fluids and gases from station to station with minimum pressure drops, provide a stable base for the rotating components, and transmit the thrust load developed by the thrust chamber to the missile's frame.

(u) The testing of Housing A-1 (plug-welded rib-to-shell joints) is nearly completed. The stress-coat test, the test to design pressure without thrust load, and the test to 50% of design thrust without internal pressure were completed with excellent results. Preliminary results from proof testing to 1.41 times the design pressure and thrust appear to be satisfactory. However, some test-system modifications are required to provide more stable pressures at proof conditions.

(u) The design of Housing-B was completed and quotations have been received. Some revisions will be required to reduce the cost of these housings.

B. HOUSING A-1 TESTING

(u) Housing A-1 was received on 31 March 1956 and immediately shipped to the Structural Test Laboratory for instrumentation and testing.

(u) Leak-testing of the instrumented housing (with internal strain gages in place) revealed a leakage area of 0.007 sq in. between the oxidizer-pump discharge passage and the oxidizer return passage. Leakage apparently occurred at an internal joint around the circumference of the thrust-chamber flange connection where a shrink fit was relied upon to seal the joint. The leakage area would allow 15 gal/min of oxidizer flow to bypass the thrust-chamber coolant tubes, which would be entirely acceptable for an operational turbopump. However, the flow capacity of the structural-test system permits a leakage rate of only 0.01 gal/min, which made it impossible to maintain the required pressure differential between the two pressure zones. Therefore, various means of sealing the leakage were investigated.

(u) The outside of the housing was stress-coated and the housing tested to ascertain the severity of the setup problems and to determine the need for additional external strain gages. The oxidizer discharge passage was pressurized to the same value as the return passage. The results were highly satisfactory, with stresses at predicted levels within $\pm 10\%$ when tested to 36% of proof conditions. The internal strain gages were functioning properly and showed a linear rise in strain. The test results for the stress-coated housing are shown in Figure VII-1 and are summarized in Figure VII-2.

(u) After the stress-coat test, the unit was cleaned and a coating of soft rubber-like material (RTV-11) applied to the surface of the oxidizer-pump discharge passage. This material sealed the leak, and the unit was again set-up for test. However, since the internal strain gages had been lost during cleaning,

UNCLASSIFIED

Report 10830-Q-4

VII, B, Housing A-1 Testing (cont.)

it was decided to perform the pressure-only and the thrust-only tests without internal strain gages in an attempt to determine if any setup or structural irregularities existed. The housing was set-up as shown in Figure VII-3, instrumented with deflection indicators (Figure VII-4) and strain gages (Figure VII-5), and tested to 70% of proof pressure. On completion of the pressure test, the thrust-load test was made without internal pressurization. The test data showed that the stresses and deflections at a thrust load of 50,000 lb were satisfactory. During testing to 70% of proof pressure, the oxidizer bearing housing moved 0.0207 in. toward the fuel housing (predicted deflection, 0.0078 in. outward) and the fuel housing deflected outward 0.0347 in. (predicted: 0.0098 in.). An examination of the test data indicated that the pressure in the oxidizer discharge passage (Zone 1) and in the oxidizer return passage (Zone 2) had equalized above 40% of proof pressure at Zone-1 pressure. This higher pressure in Zone 2 increased the differential pressure across the primary combustor, which increased the load transmitted through the connecting support shells to the fuel housing and, consequently, produced excessive deflections.

(u) To check the data, a second test to 40% of proof pressure was made with an additional deflection transducer on the oxidizer flange and visual indicators on deflection-transducer rod (Rod 48, Figure VII-4) for the fuel end and deflection transducer (Rod 44, Figure VII-4) for the oxidizer end. This test indicated that the oxidizer-dome end-flange was expanding outward 0.007 in. and that the oxidizer bearing housing was expanding toward the fuel housing 0.0115 in. A third test to 60% of proof pressure was performed at rapid pressurization to determine if pressure equalization was due to the rate of pressurization. Equalization occurred again at about 40% of proof pressure. Since pressure equalization occurred at about the same bearing deflection in each test, it was suspected that the seal between the oxidizer bearing-housing flange and the oxidizer housing had failed because of flange rotation.

(u) A 1000-psi leak check was performed between Zones 1 and 2. No leakage occurred in the aforementioned coating, but test results indicated that the bearing-housing seal was leaking. The unit was therefore disassembled (except for the bearing housing) and examined, but no damage was detected.

(u) A spare bearing housing was subsequently assembled in a loading fixture and tested twice at an axial mechanical load of 50,000 lb, with bolts torqued to design value and twice the design value, respectively. The deflection pattern remained relatively unchanged.

(u) An axial mechanical load was applied to the oxidizer-bearing housing before the bearing housing was removed from the oxidizer housing. The deflections, measured on the outside flange, on the inner shell flange, and on the oxidizer-bearing housing (Figure VII-6) showed that the outer wall and the internal ribs were separating 0.0085 in.

(u) Housing A-1 was returned for repair. Further investigation revealed that the ribs between shells on the oxidizer-dome end under the oxidizer-end flange were not properly attached. Originally, the weld joint between the outer wall and the internal ribs had been made by electron-beam welding. However,

UNCLASSIFIED

Report 10830-Q-4

VII, B, Housing A-1 Testing (cont.)

a special X-ray examination revealed that, during pressurization, the outer wall separated from the internal ribs. The procedure followed during repair of the housing is shown in Figure VII-7. After the plug-welded slots were machined in the outer shell over the ribs, an examination of the rib surface revealed very poor penetration of the electron-beam weld. This weld was subsequently repaired by TIG welding and by peening after each pass to stress-relieve the weld area. During this operation, the housing was immersed in water to within 2 in. of the weld area to prevent weld distortion. The weld was built-up 0.125 in. above the surface to equalize the bending moment of inertia caused by yield-strength differences between the aged parent material and the as-welded material. The housing was not re-aged because of the rubber material in the outer passage and because of possible effects on final-machined dimensions.

(u) Repair was completed on 2 June 1966 and the housing was returned to the structural test facility. The unit was set-up and tested at 1000 psi in Zone 1 to ensure that the rubber coating in Zone 1 had not been damaged during repair operations. No leakage occurred in 10 min.

(u) The housing was now reinstrumented and set-up for further testing. The first of these tests on 17 June 1966 was a repeat of the test to 70% of proof pressure, followed by a retest at 50% of design thrust load with no internal pressure. The proof-pressure data indicated average deflections of 0.0018 in. for the oxidizer-end bearing, of 0.0077 in. for the oxidizer-dome flange, and of 0.0242 in. for the fuel-end bearing. The pressure in Zones 1 and 2 had again equalized.

(u) Visual pressure gages were installed for the four internal pressure zones, and a leak rate was determined by pressurizing to 30 and 40% of proof pressure in all zones and then increasing Zone-1 pressure to 1000 psi over Zone 2 pressure. Zone 2 was bled to keep the pressure uniform, and the oil discharge was measured over a 5-min interval. The leakage rate varied from 0.46 to 0.68 cu in./min. Since these leakage rates were small in comparison to the 40-cu-in. capacity of the pressurizing cylinder, the test to 70% of proof pressure was completed using the bleed system to maintain the proper pressure in Zone 2. The results of this test were excellent. The oxidizer dome end moved 0.005 in. Bearing-span deflections are shown in Figure VII-8. The maximum stress occurred at the point predicted by photoelastic testing (Location 27, Figure VII-5) and was 84,500 psi versus 70,500 psi predicted at 70% of proof pressure.

(u) The next phase of testing was to apply 100% of proof pressure (1.41 times design pressure) combined with 1.4 times the design thrust. This test proceeded very well until the pressures reached 103.5% in Zone 1, 97.5% in Zone 2, 103.5% in Zone 3, 96.5% in Zone 4, and 102.5% in Zone 5. However, during an attempt to adjust the pressure levels the Zone-2 pressure became difficult to control and overshot the 100% proof pressure by 4% in Zone 1, by 5% in Zone 2, by 6.5% in Zone 3, and by 5% in Zone 5. The pressure in Zone 4 was 4.2% low. The unit was immediately depressurized. The fuel-end deflection readings remained at 0.017 in. after depressurization.

UNCLASSIFIED

Report 10830-2-4

VII, B, Housing A-1 Testing (cont.)

(u) This phenomenon may have been due to two causes, transducer slip-page or fuel-housing yielding. The simulated shaft in the housing is highly stressed at 100% proof pressure. The extensometer rods pass through the end of the shaft to the fuel roller-bearing locations. The extensometer rods are spring-loaded to maintain contact and to counteract the internal pressure load on the rod ends. At 100% of proof pressure, the spring-load differential is reduced, and a torquing movement of one degree in the shaft-end due to stress would lift the rods from their sockets. This would change the zero point of the extensometers. Three 0.050-in.-deep holes were therefore drilled in the fuel housing to hold the extensometer rods in place to prevent the rods from moving out of the sockets. Examination of the data further indicated that some local yielding may have occurred in the fuel housing after exceeding 100% of proof pressure.

(u) The deflection data are shown in Figure VII-9. The Zone-1 and Zone-4 pressurizing cylinders bottomed out during the test. To alleviate this problem two boosters were attached to Zone-1, and the Zone-4 pressure was supplied directly from the pump supply. The difficulty in pressure control was attributed to the fact that the pressurizing cylinders bottomed out.

(u) The unit was then pressurized to 70% of proof pressure and proof thrust. However, at 70% of proof pressure, the pressures in Zones-1 and 2 became uncontrollable and the unit was therefore depressurized. Examination revealed that the O-rings used at the thrust-chamber flange had failed. These O-rings are being replaced with omiseals used in TCA testing, and testing will continue after further modification to the pressurizing system.

C. HOUSING A-2 FABRICATION

(u) Fabrication of Housing A-2 was in the final stages when the inter-channel leakage in Housing A-1 was discovered. A leak check of Housing A-2 revealed leakage between the oxidizer discharge passage and the oxidizer return passage at the T-juncture. A series of tests were made to locate and identify the leakage areas. The tests indicated that the leakage was confined to two areas at the T-juncture. An electron-beam weld was attempted over a 30° arc in each of these areas but was unsuccessful. The unit was then taken to a 2,000,000 ev betatron in a Los Angeles hospital for X-ray examination. An Aerojet-General team of welding and NDT personnel directed the examination and interpreted the findings. The X-rays revealed a 0.030-in.-wide separation between the outer shell and the middle shell at the T-juncture.

(u) The T-section of the housing was machined off and a 0.375-in.-deep groove was milled out between the passage holes to the middle shell as shown in Figure VII-10. The surface of the middle shell was acid-etched which revealed very poor penetration of the weld. The separation of walls (Figure VII-11) varied from 0.003 to 0.015 in. The subvendor's techniques, welding schedule, and processing sequences were closely examined, which revealed that the subvendor had ignored the advice of Aerojet-General's welding personnel, had kept very poor records, had applied dubious techniques, and had performed poorly despite previously demonstrated high-quality workmanship.

UNCLASSIFIED

Report 10830-Q-4

VII, C, Housing A-2 Fabrication (cont.)

(u) The groove between the holes was subsequently TIG-welded to ensure positive separation of the passages. In addition, fifteen 0.375-in.-dia plug welds were made on the pad surface, inside of the inner hole circle, to ensure that the outer shell and the middle shell were joined. Prior to welding on the T-flange, a leak check was made on the cylindrical portion of the housing and no leakage between passages could be found.

(u) Since material was readily available the T-flange was changed as shown in Figure VII-12. The partial-flange ring was electron-beam-welded to the inner shell and the inner shell was welded to the cylindrical portion. The outside of the inner shell and the inside of the outer shell were machined to match. The outside shell was welded in place and the remaining portion of the thrust-chamber flange was electron-beam-welded to the outer shell and to the inner portion of the flange. Electron-beam welds were then made circumferentially around the T-section, 1 in. apart, to join the two cylinders. The 32-1/4-in.-dia passage holes in each shell were then drilled to meet the passage holes in the cylinder.

(u) In addition, the oxidizer end flange was plug-welded to the internal ribs in a manner similar to the repair procedure for Housing A-1. Since Housing A-2 had not been final-machined, a portion of the oxidizer flange was removed to reduce the depth of the plug welds, as shown in Figure VII-13. After this preparation for plug welding, the top of the ribs revealed insufficient penetration of the electron-beam weld. The plug welds were made by TIG-welding and were peened after each pass. After welding and machining, a new ring was attached by electron-beam-welding, as shown in Figure VII-14. The final welding operation was completed satisfactorily, and the housing has been sent to the heat-treatment vendor for solution-annealing prior to final rough machining. Delivery of the housing is expected in July.

D. HOUSING-B DESIGN

(u) The oxidizer housing for the Housing-B turbopump was completed and detailed drawings were released in mid-May. The three-walled welded-rib design includes all the instrumentation holes, refined oxidizer diffuser vanes, refined oxidizer flow passages, and has fine-machined surfaces required for an operational turbopump. The oxidizer-bearing housing is an integral part of the unit, and the T-section is a solid forging welded to the main cylindrical portion and has drilled oxidizer passages. The oxidizer boost-pump-turbine supply manifold is an integral part of the oxidizer dome end.

(u) The fuel housing for the Housing-B turbopump was also completed, and detailed drawings were released late in May. The housing is fabricated from Inconel-718 forgings and is electron-beam welded at the major joints. The housing includes fuel-diffuser vanes, valve interfaces, instrumentation holes, fuel feed lines, and has fine-machined surfaces required for an operational turbopump. It also includes an attachment for the combustion seal and provisions for cooling the internal face of the housing from hot turbine exhaust gas.

UNCLASSIFIED

Report 10830-Q-4

VII, D, Housing-B Design (cont.)

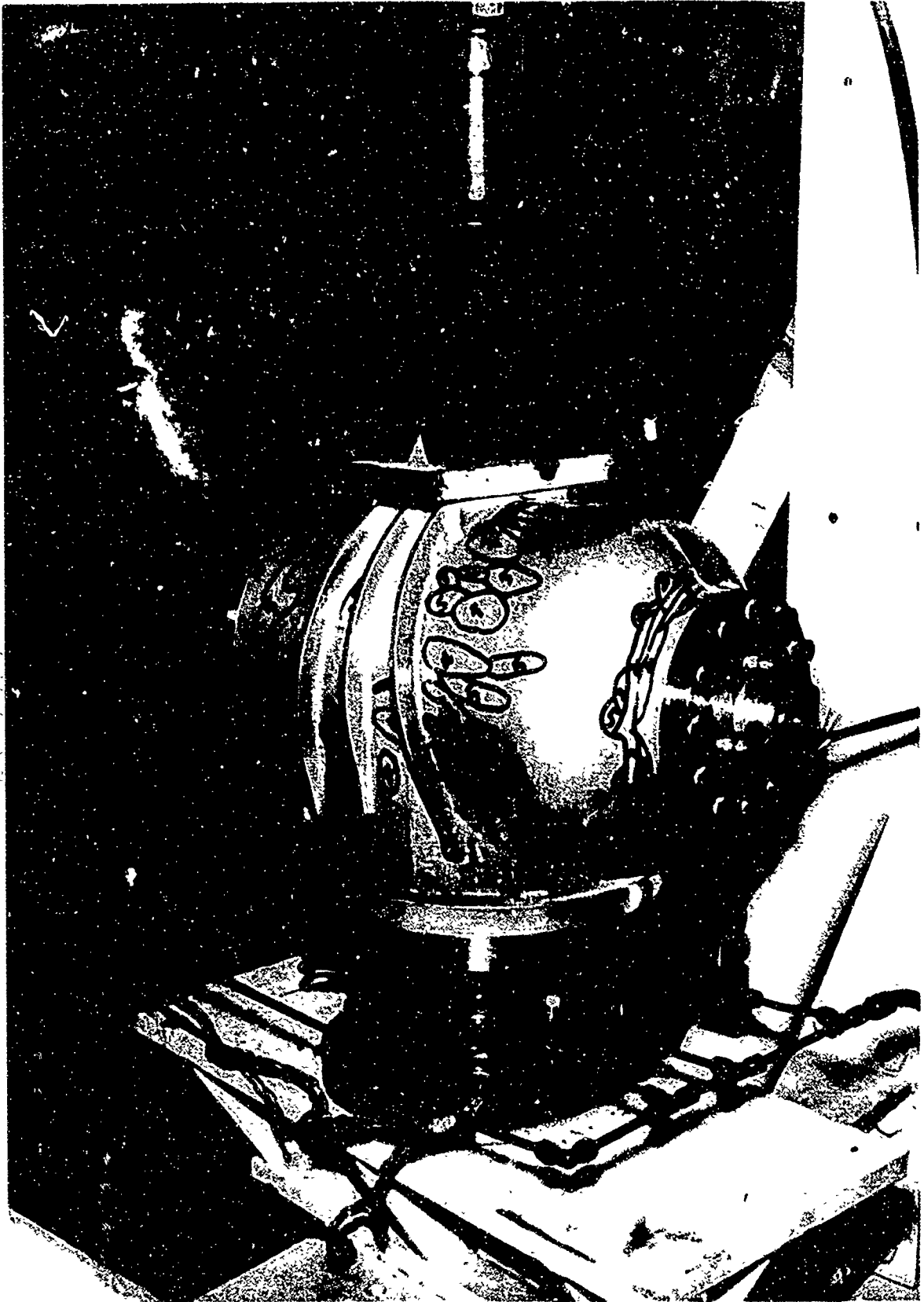
(u) The Housing-B assembly is shown in Figure VII-15. The thrust force acting on the primary combustor, caused by the differential pressure between the discharge areas of the primary combustor and the turbine, is retained with a shear-lock ring. The expansion joint between the primary combustor and the fuel housing is a multiconvolution multiply Inconel bellows.

(u) Forgings for oxidizer-housing of the Housing-B turbopump were made late in May, and some of them have been shipped. The forgings had been due late in April, but were delayed because the forging vendor experienced some difficulty in procuring material.

(u) Quotations for the oxidizer and fuel housing were received. Prices are extremely high because of the special fabrication techniques required for short-lead-time production, because only one unit is required, and because of the high risk involved. Fabrication of the fuel and oxidizer housings for the B-design turbopump was deferred pending results of Housing A-1 testing. If Housing A-1 does not meet Work Statement requirements, fabrication orders will be placed immediately for a simplified version of Housing-B. Housing-C design is being prepared for Phase-II production to reduce cost and to incorporate modifications to the oxidizer-flow passages as indicated by model testing. This design will consider casting, die-forging, explosive-forming, and other fabrication techniques to reduce housing costs. Costs are expected to be reduced significantly because more fabrication lead time is available, because more tooling can be justified for a larger number of housings, and because the design can be simplified on the basis of information available from flow tests and from structural tests.

UNCLASSIFIED

Report 10830-Q-1



Stress Coat Test-Housing A-1

Figure VII-1

UNCLASSIFIED

UNCLASSIFIED

Report 10830-Q-4

POSITION OF NEW CRACKS IN STRESS COAT	PRESSURE % OF PROOF	STRESS TO CRACK TO CRACK STRESS COAT	STRESS AT CRACK LOCATIONS EXTRAPOLATED TO DESIGN COND. (70% OF PROOF PRESS.)	STRAIN GAUGE DATA EXTRAPOLATED TO DESIGN COND.	ORIGINAL DESIGN CALC. STRESS	HIGHEST EXTERNAL STRESSES ARE AT OXIDIZER END AS PREDICTED, MAGNITUDE OF STRESS CONFIRMED.
1	15	18,000	84,000	87,000	80,000	HIGHEST EXTERNAL STRESSES ARE AT OXIDIZER END AS PREDICTED, MAGNITUDE OF STRESS CONFIRMED.
2	20	19,500	68,000			
3	25	21,000	59,000			
4	30	20,000	47,000	46,500	53,000	SECOND HIGHEST EXTERNAL STRESSES ARE DUE TO LOCAL BENDING BETWEEN RIBS AS PREDICTED.
5	36	20,500	40,000	42,000		

CONCLUSION: ALL RESULTS SHOW THAT THE MAGNITUDE AND LOCATION OF HIGH STRESSES IS AS PREDICTED. HOUSING IS READY FOR HIGHER PRESSURES.

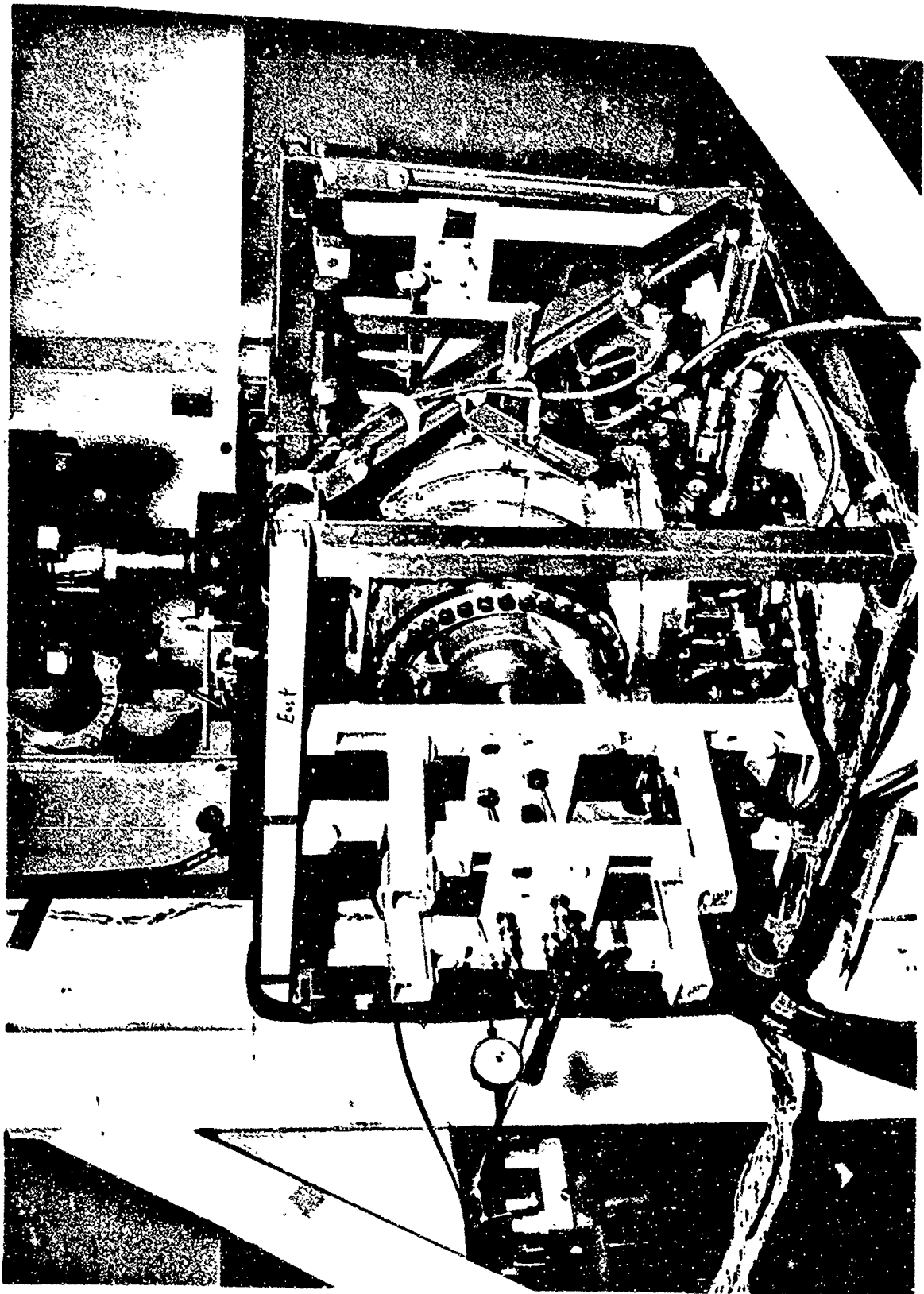
Stress Coat Test-Results of Housing A-1

Figure VII-2

UNCLASSIFIED

UNCLASSIFIED

Report 105 31-Q-4



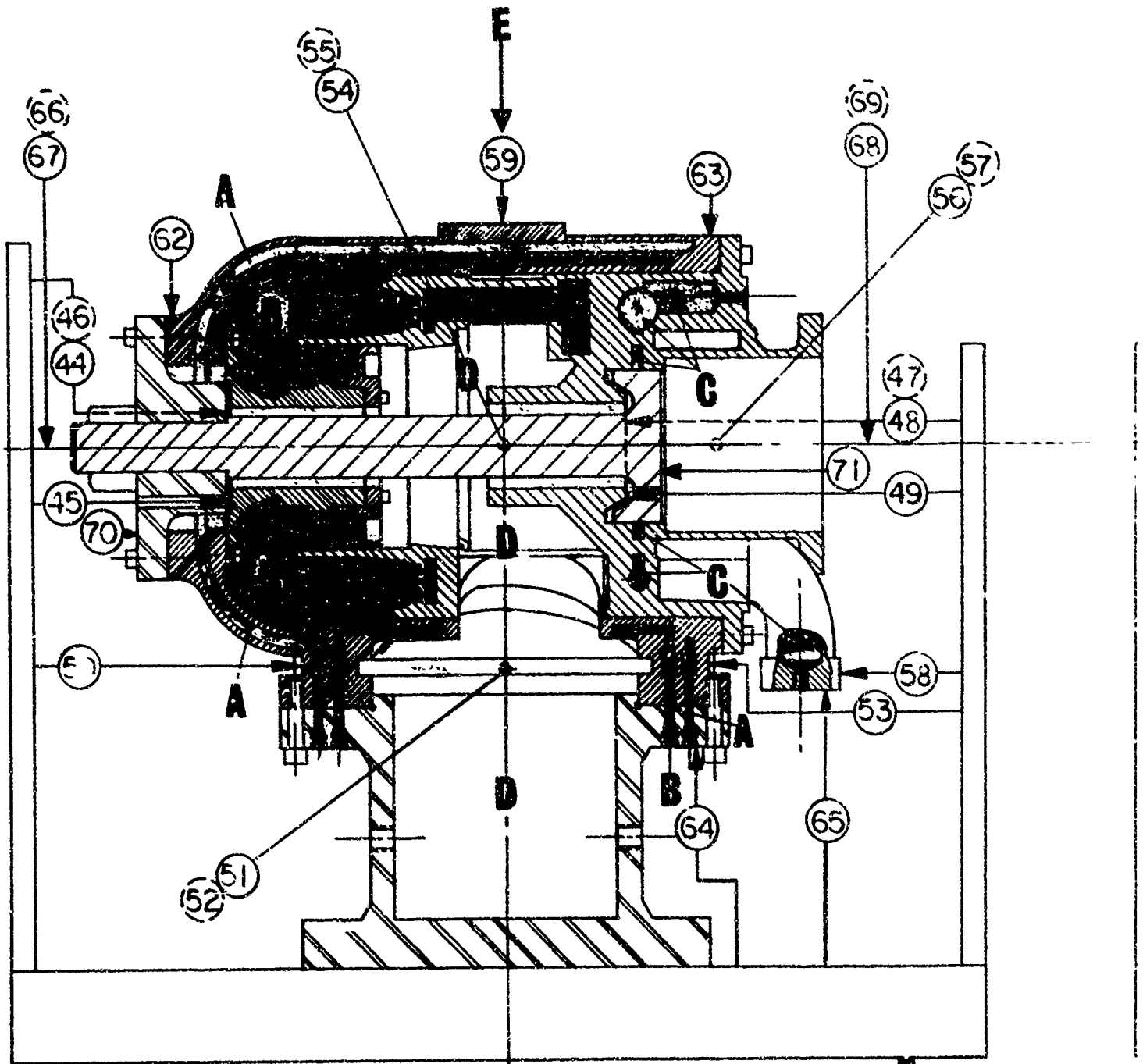
Housing A-1 Structural Test Setup

Figure VII-3

UNCLASSIFIED

UNCLASSIFIED

Report 10830-Q-4



LEGEND

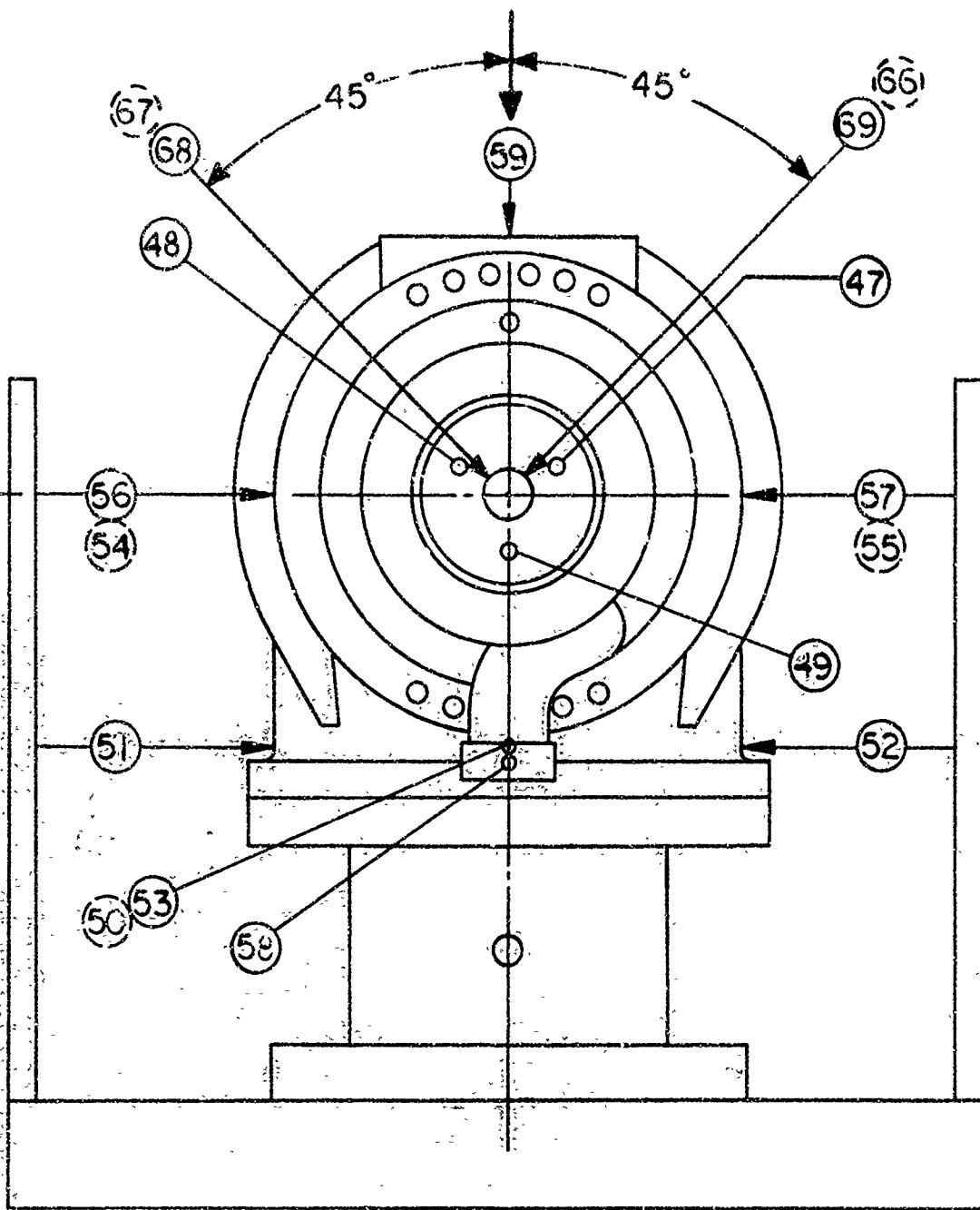
- A** ——— DENOTES PRESSURE ZONE NO.1
- B** ——— DENOTES PRESSURE ZONE NO.2
- C** ——— DENOTES PRESSURE ZONE NO.3
- D** ——— DENOTES PRESSURE ZONE NO.4

E ↓ DENOTES FORCE

Housing A-1 Deflection Indicator Locations

Figure VII-4

UNCLASSIFIED

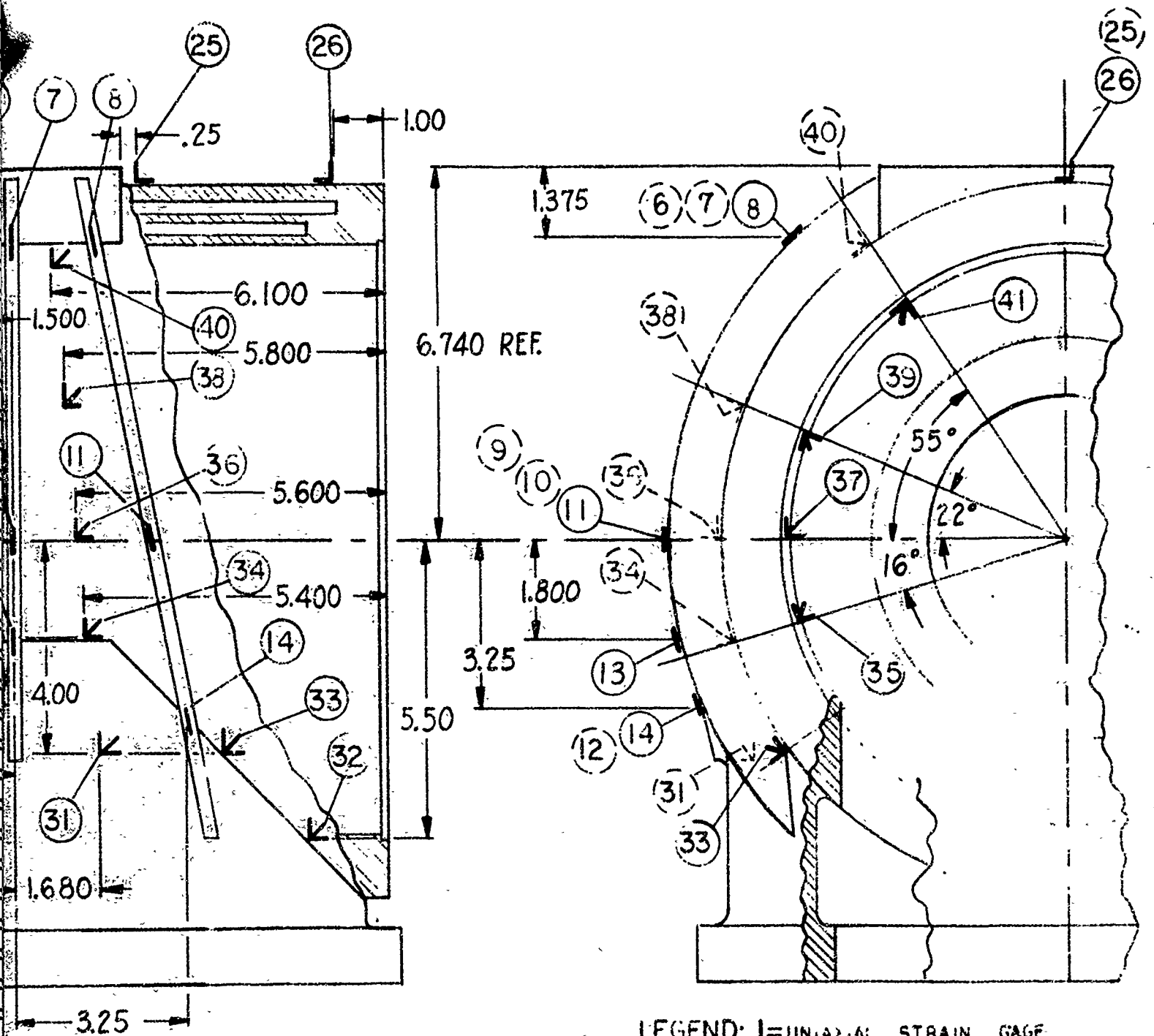


OTES PRESSURE ZONE NO. 5

2 1/2 - 4

UNCLASSIFIED

Report 10830-Q-4



LEGEND; I=UNIAXIAL STRAIN GAGE
L=BIAXIAL STRAIN GAGE
V=ROSETTE STRAIN GAGE

Housing A-1 Strain Gage Locations

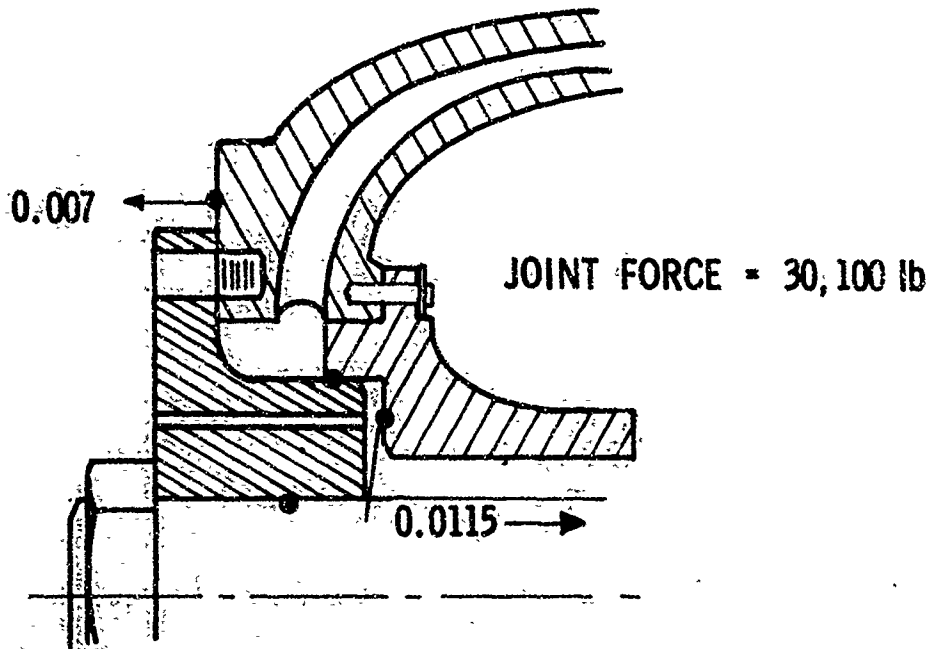
Figure VII-5

UNCLASSIFIED

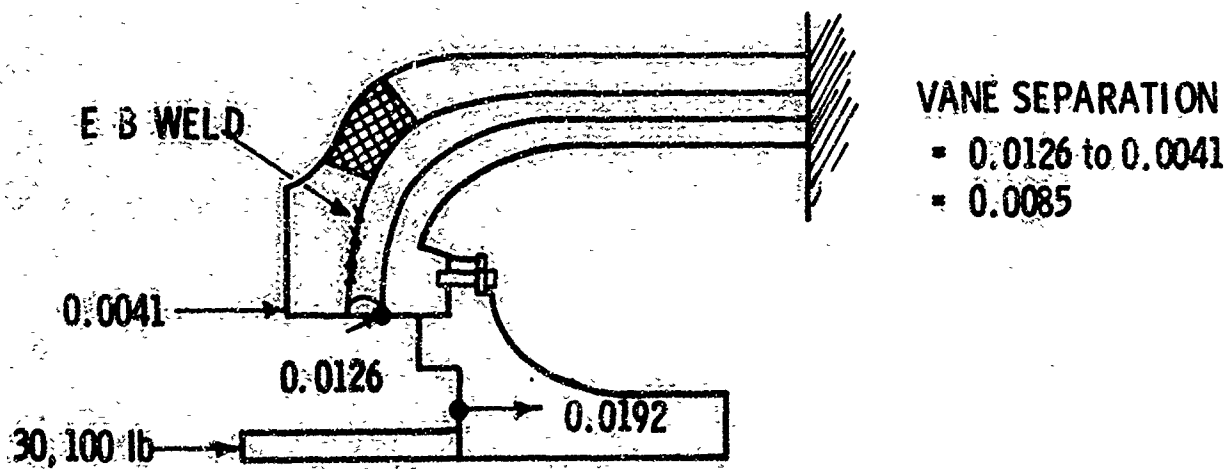
Report 10830-Q-4

HYDROTEST CONDITION

40% PROOF



MECHANICAL LOAD



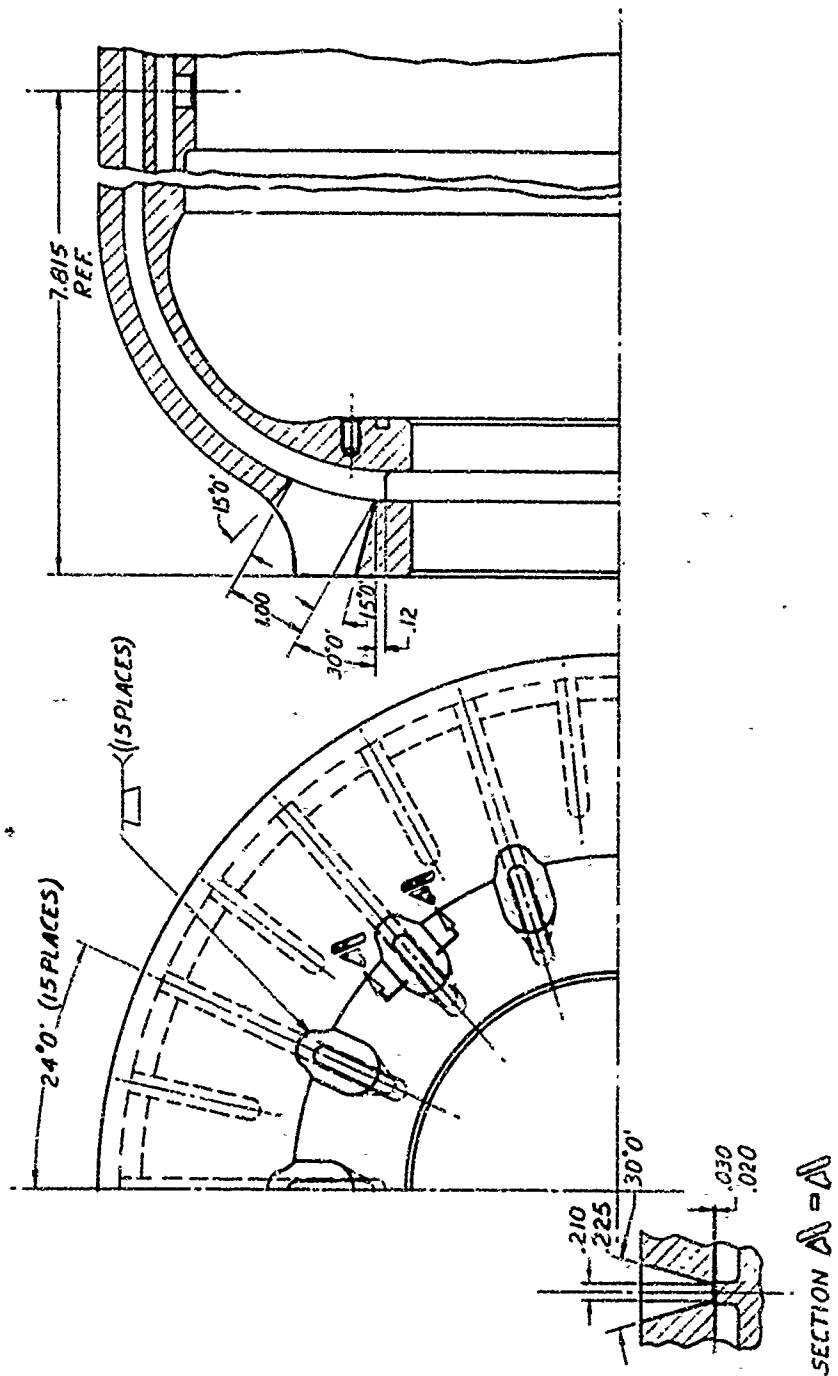
Housing A-1 Oxidizer Dome End Deflections

Figure VII-6

UNCLASSIFIED

UNCLASSIFIED

Report 10830-Q-4



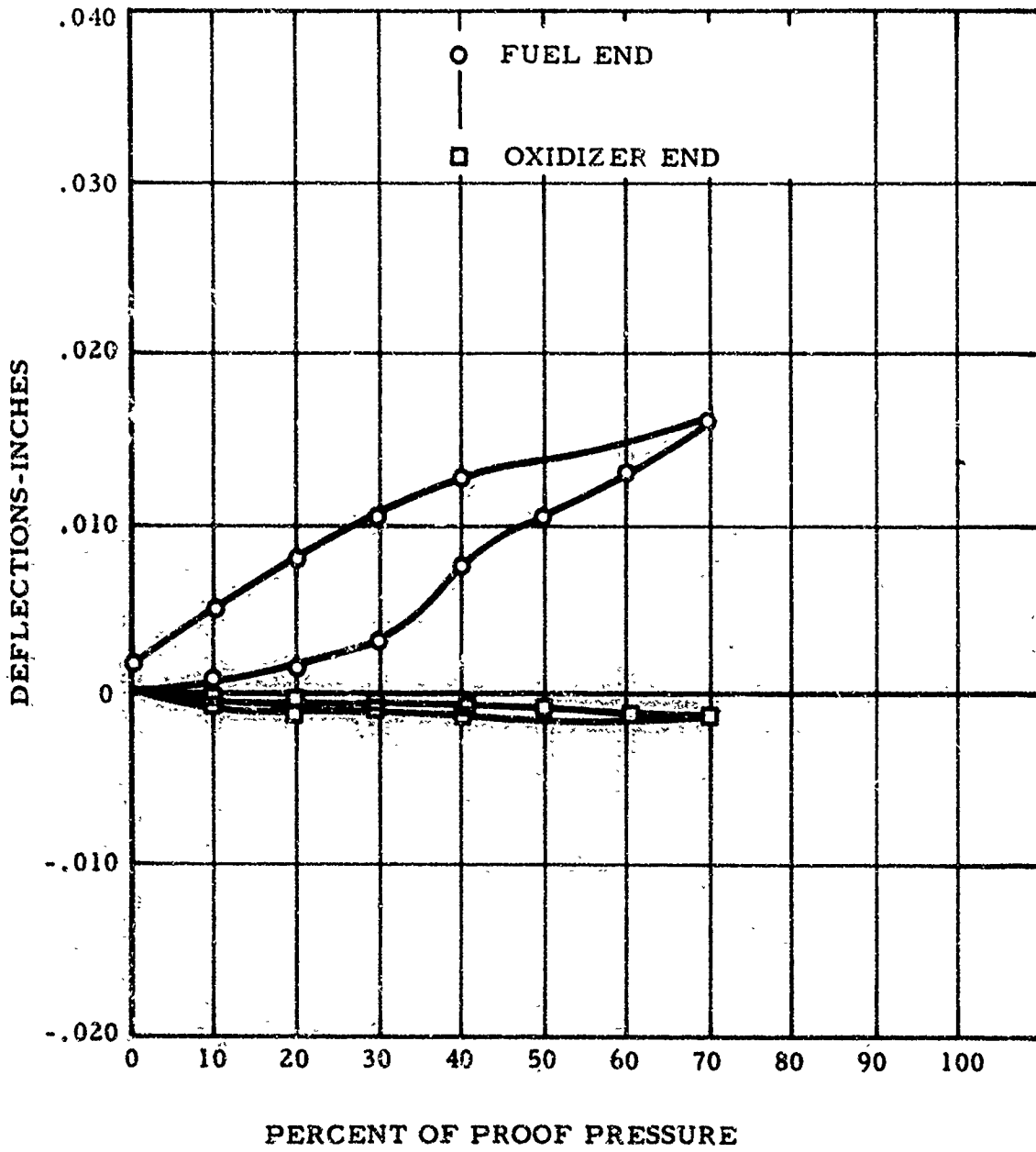
Housing A-1 Oxidizer Dome End Weld Repair

Figure VII-7

UNCLASSIFIED

UNCLASSIFIED

Report 10830-Q-4



Housing A-1 Roller Bearing Location Axial Deflections

Figure VII-8

UNCLASSIFIED

CONFIDENTIAL

Report 10830-Q-4

CONFIDENTIAL

CASE # LOAD	PRESSURE										DEFLECTIONS IN.																												
	1	2	3	4	5	6	7	8	9	10	44	45	46	47	48	49	50	51	52	53																			
0	0	0	0	0	0	0	0	0	0	0	0	0	0	0	0	0	0	0	0	0	0	0	0	0	0	0	0	0	0	0	0	0	0	0	0	0	0	0	0
10	900	700	500	400	200																.0007	-.0010	0	0	0	0	0	0	0	0	0	0	0	0	0	0	0	0	
20	1820	1400	1100	800	600																.0013	-.0005	0	0	0	0	0	0	0	0	0	0	0	0	0	0	0	0	
30	2700	2100	1600	1100	800																.0020	-.0005	0	0	0	0	0	0	0	0	0	0	0	0	0	0	0	0	
40	3740	2940	2170	1610	1200																.0024	0	0	0	0	0	0	0	0	0	0	0	0	0	0	0	0	0	
50	4440	3600	2770	2220	1600																.0024	0	0	0	0	0	0	0	0	0	0	0	0	0	0	0	0	0	
60	5320	4210	3300	2600	1800																.0034	0	0	0	0	0	0	0	0	0	0	0	0	0	0	0	0	0	
70	6480	5000	3800	3000	2100																.0034	0	0	0	0	0	0	0	0	0	0	0	0	0	0	0	0	0	
80	7240	5700	4610	3400	2400																.0025	0	0	0	0	0	0	0	0	0	0	0	0	0	0	0	0	0	
90	8220	6640	5000	3840	2600																.0025	0	0	0	0	0	0	0	0	0	0	0	0	0	0	0	0	0	
100	8700	6700	5000	4120	3000																.0025	0	0	0	0	0	0	0	0	0	0	0	0	0	0	0	0	0	
MAX	9830	7240	5640	3940	3100																.0022	0	0	0	0	0	0	0	0	0	0	0	0	0	0	0	0	0	
0 RETURN	0	0	0	0	0																.0022	.002	0	0	0	0	0	0	0	0	0	0	0	0	0	0	0	0	

CONFIDENTIAL

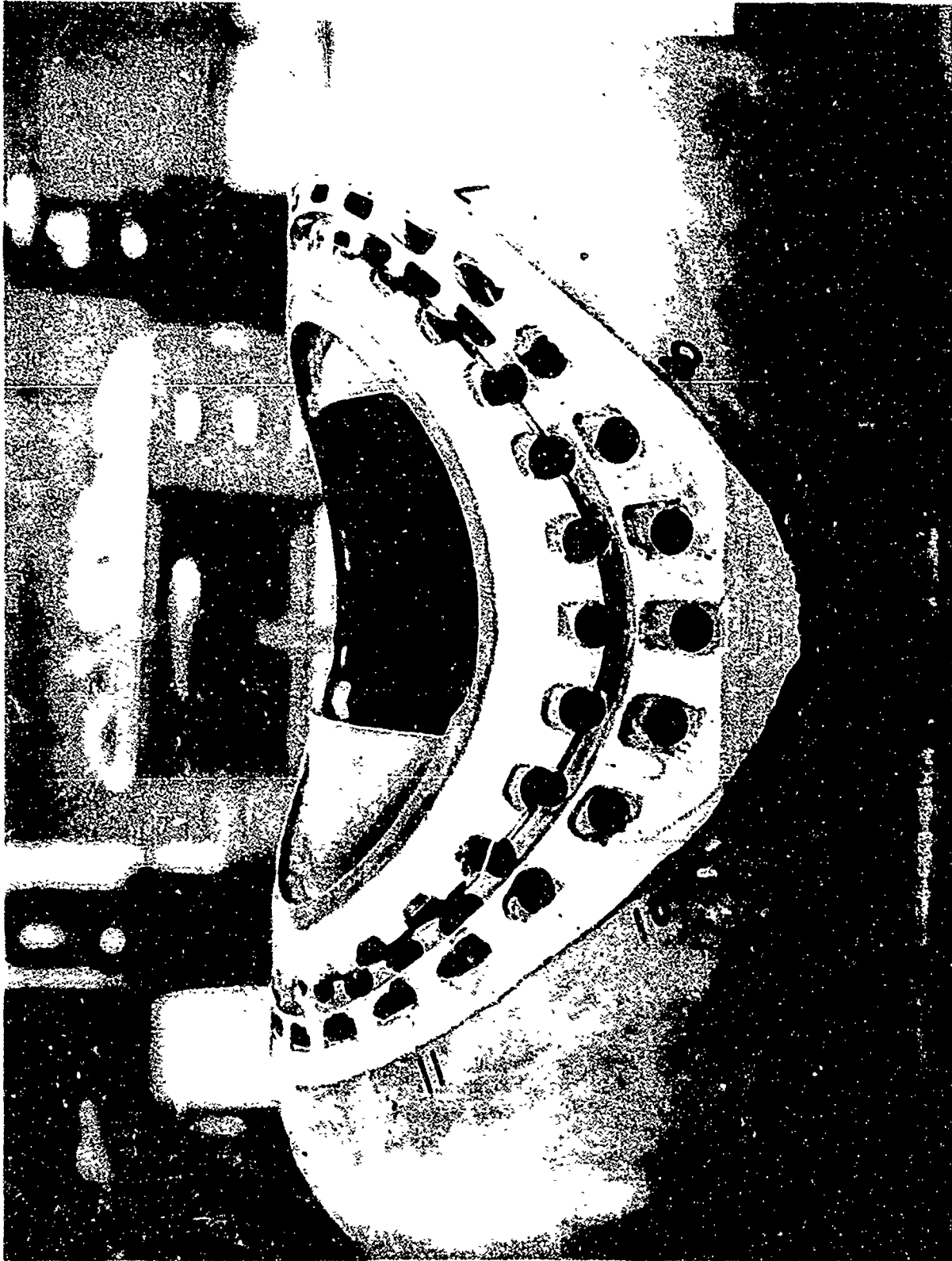
Housing A-1 100% Proof Pressure Deflection Data (u)

Figure VII-9

CONFIDENTIAL

CONFIDENTIAL

Report 10830-Q-4



Housing A-2 Interpassage Leakage Area

Figure VII-10

(This page is Unclassified)

CONFIDENTIAL

UNCLASSIFIED

Report 10830-Q-4



Housing A-2 Wall Separation

Figure VII-11

UNCLASSIFIED

UNCLASSIFIED

Report 10830-Q-4

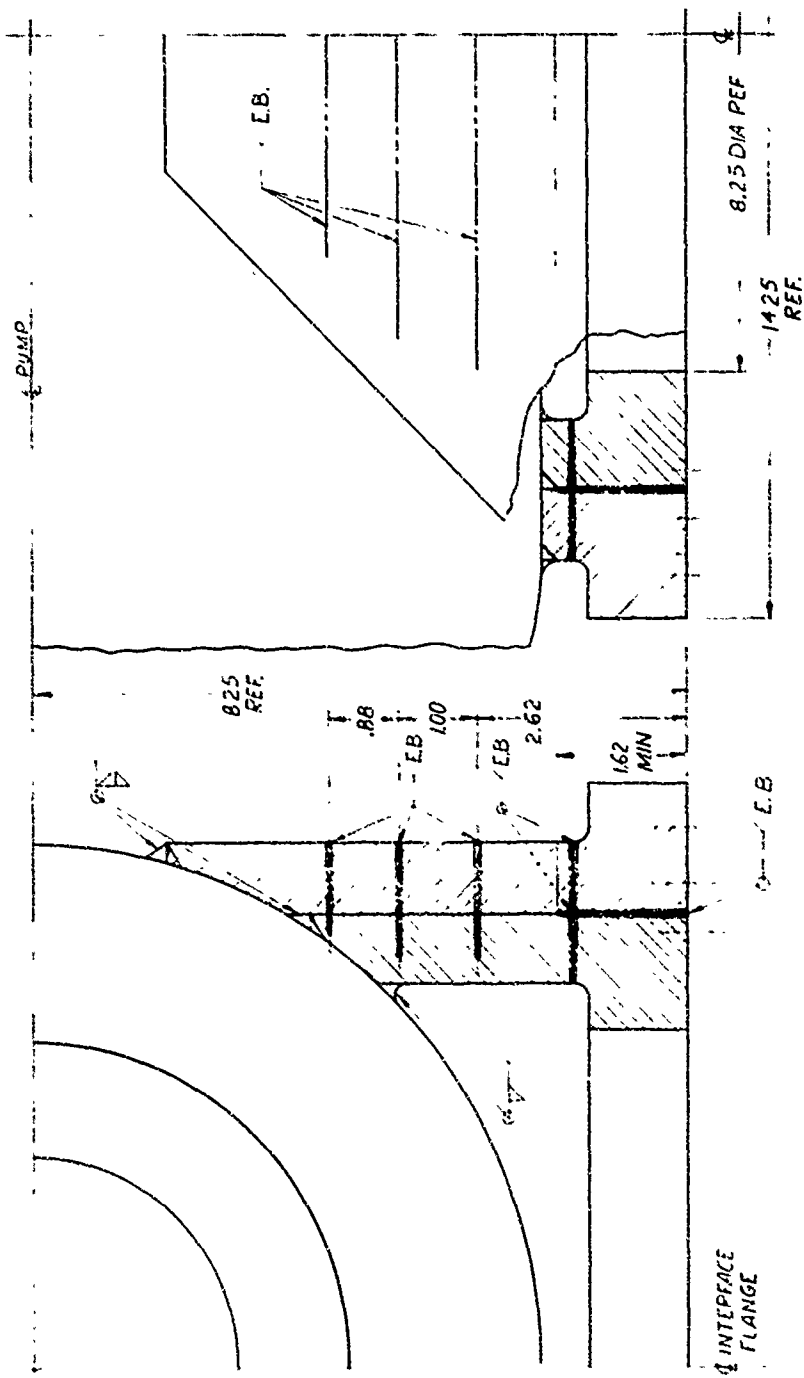


Figure VII-12

UNCLASSIFIED

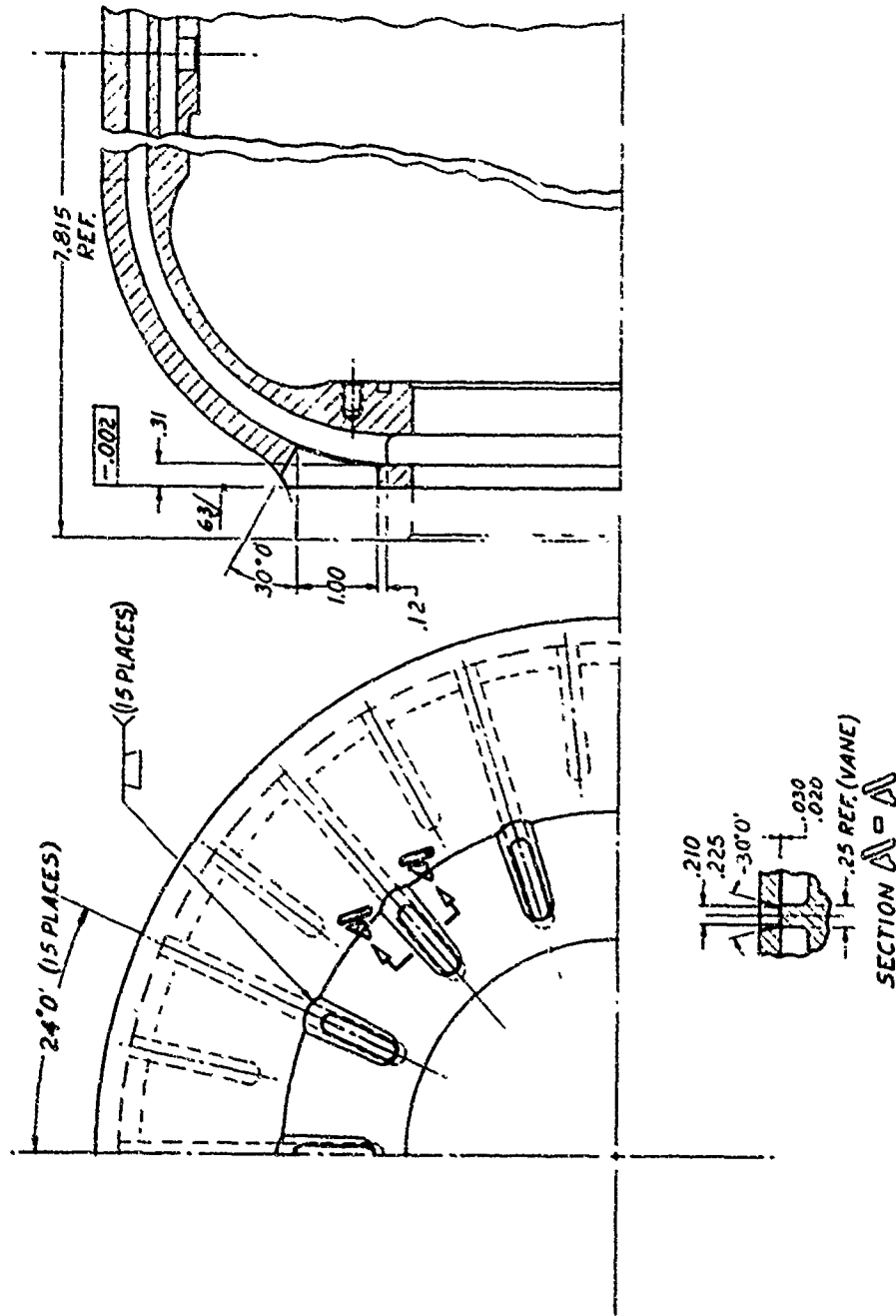
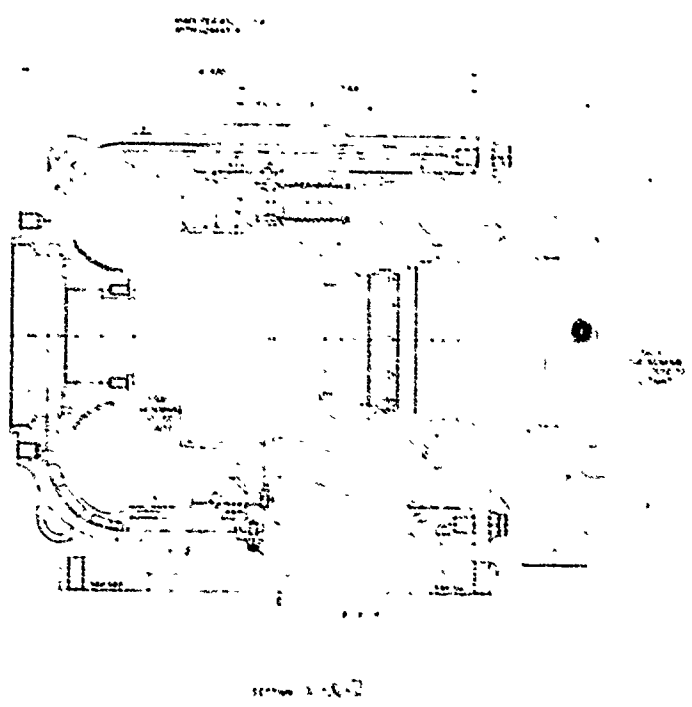


Figure VII-13

UNCLASSIFIED

Report 10830-Q-4

- 1. THIS DRAWING IS TO BE USED FOR THE DESIGN OF THE END PLUG FLANGE WELD OF THE HOUSING A-2 OXIDIZER DOME.
- 2. ALL DIMENSIONS ARE IN INCHES UNLESS OTHERWISE SPECIFIED.
- 3. MATERIAL AND TOLERANCE ARE AS SHOWN.
- 4. THE WELD SHALL BE AS SHOWN.
- 5. THE WELD SHALL BE MADE TO THE REQUIREMENTS OF MIL-W-8838, CLASS 1, AND SHALL BE INSPECTED AND ACCEPTED BY THE QUALITY CONTROL DEPARTMENT.
- 6. THE WELD SHALL BE MADE TO THE REQUIREMENTS OF MIL-W-8838, CLASS 1, AND SHALL BE INSPECTED AND ACCEPTED BY THE QUALITY CONTROL DEPARTMENT.



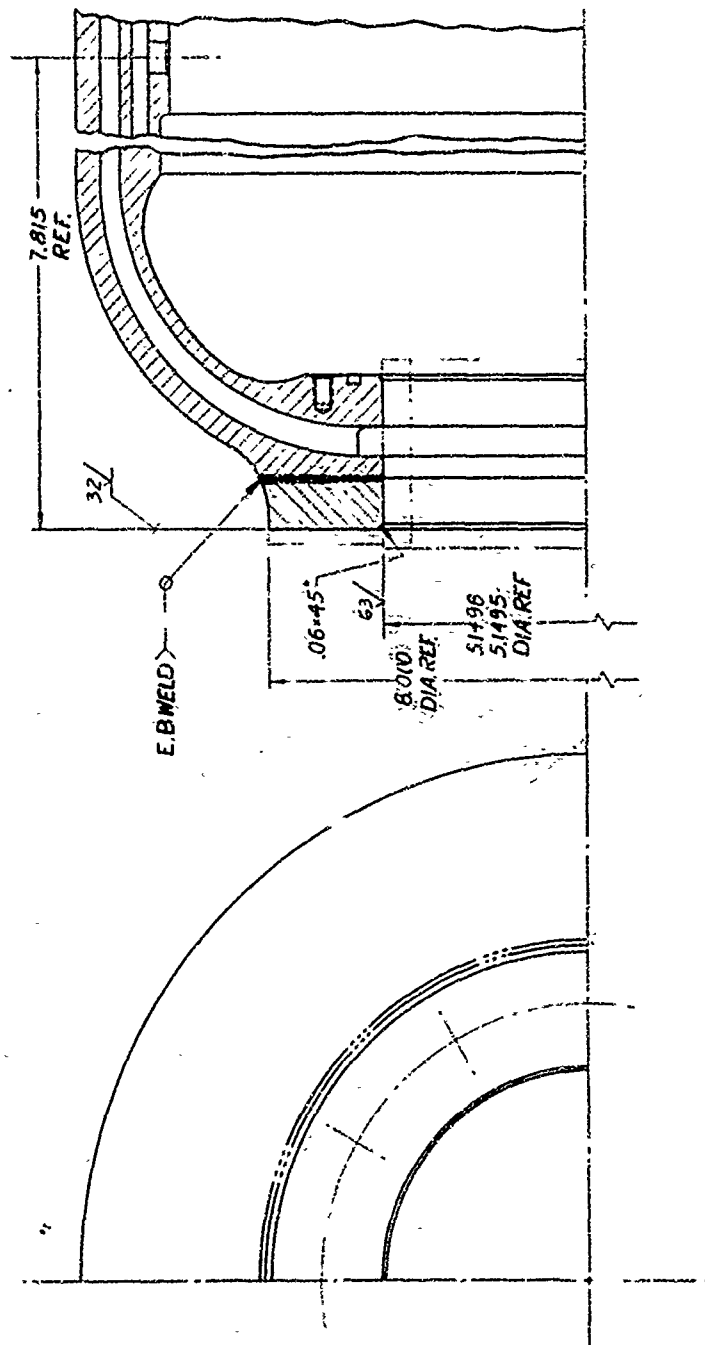
Housing A-2 Oxidizer Dome End Plug Flange Weld

Figure VII-14

UNCLASSIFIED

UNCLASSIFIED

Report 10830-Q-4



Housing B Assembly

Figure VII-15

UNCLASSIFIED

UNCLASSIFIED

Report 10830-Q-4

VIII.

TURBOPUMP BEARING DEVELOPMENT

A. GENERAL

(u) The ARES turbopump bearing development program consists of three phases: Phase I, 25,000-rpm N_2O_4 lubricated bearing tests to develop cage designs; Phase II, 40,000-rpm N_2O_4 and AeroZINE 50 lubricated bearing tests to demonstrate operation at the design requirement of the T-engine (advanced) turbopumps; and Phase III, 31,250-rpm N_2O_4 and AeroZINE 50 lubricated bearing tests to demonstrate operation at the design requirements of the inline (backup) turbopump. In addition to the normal load and speed requirements, the operation of misaligned roller bearings is being demonstrated during the 40,000-rpm tests.

(u) Testing at 25,000 rpm was completed successfully, as reported in the second quarterly report,* but tester and facility problems caused delays in both the 40,000- and 31,250-rpm test series. These problems have been solved, and demonstration of the following Work Statement objectives was completed in this quarter:

1. N_2O_4 lubricated roller bearing at 31,250 rpm
2. N_2O_4 lubricated roller bearing at 40,000 rpm (aligned)
3. N_2O_4 lubricated roller bearing at 40,000 rpm (misaligned)
4. N_2O_4 lubricated ball bearings at 31,250 rpm
5. N_2O_4 lubricated ball bearings at 40,000 rpm
6. AeroZINE 50 lubricated roller bearing at 31,250 rpm
7. AeroZINE 50 lubricated ball bearings at 31,250 rpm

(u) The remaining objective is to demonstrate the AeroZINE 50 lubricated bearings at 40,000 rpm. Although one successful test has been conducted for over seven minutes, some wear existed on the roller bearing in this test and two bearing cages failed in subsequent tests. The hardware is being modified and testing will resume early in the next quarter. The AeroZINE 50 lubricated ball bearings were in excellent condition after the seven-minute test.

B. BEARING DESIGN

(u) The Rulon-P inner-race-riding roller-bearing cages, modified as discussed in the third quarterly report* (removal of aluminum roller-retention stickout and the riveting of the aluminum shroud through each web), were used in the N_2O_4 tests. The alternative cages for ball and for roller bearings of the outer-race-riding thin-line design, which have been proven during 25,000-rpm testing, were received; however, because of the smaller size (series 108 versus 210) and because of the large number of rolling elements (15 rollers and 14 balls) these cages were flimsy. An outer-race-riding ball-bearing cage consisting of glass-filled Teflon molded around a stainless-steel "halo" ring was also received.

*Report TR-66-1, 15 January 1966

UNCLASSIFIED

Report 10830-Q-4

VIII, B, Bearing Design (cont.)

(u) The through-flow area of both of these outer-race designs is much greater and, therefore, much more desirable than the shrouded-inner-race design. Figures VIII-1 and VIII-2 show the ball-and the roller-cage designs both separately and installed in bearings so as to illustrate the comparative flow areas.

(u) The first two 40,000-rpm AeroZINE 50 lubricated bearing tests were conducted with bearings assembled with outer-race cages: the molded-Teflon "halo" design in the ball bearings and the thin-line design (as used in the 25,000-rpm tests) in the roller bearing. Both performed very well in the first test (Test 8), but the ball-bearing cages failed in the second test (Test 9).

(u) An aligning-type roller bearing incorporating rollers and an outer race, made from K-5-H carbide and an inner race made from 440C steel, operated successfully for over seven minutes at required speed and loads, but exhibited wear in the load zone of the K-5-H outer race.

(u) The testing at 40,000 rpm of AeroZINE 50 lubricated bearings (discussed in detail in Paragraph VIII,E) was temporarily suspended for a complete analysis of the testing problems. It was concluded that the thin-line outer-race-riding roller-bearing cage could be improved by eliminating two roller pockets. This will increase the web thickness by 50% and still allow the larger through-flow area not available in the shrouded-inner-race design. A thorough analysis revealed that critical speed would not be decreased significantly by reducing the number of rollers from 15 to 13.

C. BEARING TESTING AT 40,000 RPM in N_2O_4

(u) Work-Statement objectives were accomplished in two significant tests conducted on the same bearings. One test (Test 5A) was made with the roller bearing aligned and the other (Test 6B) with the roller bearing misaligned (see Figure VIII-3). This misalignment is equivalent to a radial displacement of 0.016 in. of the bearing bores of the advanced-turbopump housing, which is twice the maximum expected displacement.

(u) In addition to these two tests, three test attempts were made which did not generate significant data because of difficulties encountered in the test systems. Figure VIII-4 tabulates steady-state data points for all five N_2O_4 tests. Figures VIII-5 and VIII-6 are plots of significant parameters versus time for the significant tests (Tests 5A and 6B). Figure VIII-7 tabulates pretest and posttest inspection measurements of critical bearing dimensions.

(u) The inner race, the outer race, and the rolling elements were made from 440C steel for both the ball and the roller bearings. The ball and the roller cages were similar inner-ring-riding designs of Rulon-P shrouded on the outside diameter with aluminum. Figures VIII-1 and VIII-2 show these designs and alternative outer-race-riding designs.

UNCLASSIFIED

Report 10830-Q-4

VIII, C, Bearing Testing at 40,000 rpm in N_2O_4 (cont.)

All five tests are briefly discussed below.

(u) During Test 4 (the first test of this reporting period) a tester thrust-bearing disc failed at 38,000 rpm after a duration of 18 sec. This thrust-bearing disc failed in a classical burst pattern with brittle-type behavior. The test bearings were not damaged. A complete analysis of the tester failures was conducted and is reported briefly in Paragraph VIII,F, below.

(u) A new tester, with a redesigned thrust-bearing disc of AM-350 material, was assembled and installed for Test 5A. The test bearings from Test 4 were reinstalled for this and all subsequent 40,000-rpm N_2O_4 tests. The roller bearing was installed in the aligned position. Test duration was 297 sec, of which 269 sec was at speeds of 38,900 to 40,000 rpm (see Figure VIII-5). Minimum and maximum axial loads were 1170 and 2950 lb. The radial load for the entire duration was over 500 lb. The test was terminated prematurely during the radial-load increase to 870 lb due to a loss of the turbine speed signal. The bearings were removed, examined, and found to be in excellent condition.

(u) The same bearings were reinstalled for the next test. The roller bearing was installed in a misaligned position (see Figure VIII-3). Test 5B was a 1-sec-duration test attempt, which was terminated at 39,300 rpm when a safety diaphragm burst in the gas-supply line to the tester drive turbine failed. Test 6A was a 2-sec-duration test attempt terminated at 27,600 rpm due to a false over-speed signal caused by an instrument malfunction.

(u) The significant parameters for Test 6B are plotted in Figure VIII-6. Test duration was 350 sec, of which 522 sec was at speeds of 38,900 to 40,000 rpm. Minimum and maximum axial loads were 1450 and 2500 lb. Minimum and maximum radial loads were 500 and 1000 lb. The radial peak load of 1000 lb was applied twice during this test. The bearings were in very good condition after these tests, as shown in Figure VIII-8. Air Force representatives reviewed the data and examined the bearings. Test 6B combined with Test 5A completed the Phase-I Work-Statement requirements for 40,000-rpm N_2O_4 lubricated bearings.

D. BEARING TESTING AT 31,250 RPM IN N_2O_4

(u) Upon completion of the 40,000-rpm N_2O_4 lubricated bearing tests, a new set of bearings was installed for the 31,250-rpm N_2O_4 lubricated bearing test series. The ball-bearing set was of the same tandem load-sharing design as that used in the 40,000-rpm test series. The roller bearing was the same except that the outer race did not incorporate the self-aligning feature since self-aligning is not required in the inline TPA. Work Statement requirements were satisfactorily met in a single test. Figure VIII-4 tabulates steady-state data points, whereas Figure VIII-9 is a plot of significant parameters versus time for this test. Figure VIII-10 exhibits the excellent posttest condition of these bearings. The local Air Force representative inspected the bearings and the data and expressed satisfaction with the results.

UNCLASSIFIED

Report 10830-Q-4.

VIII, D, Bearing Testing at 31,250 rpm in N_2O_4 (cont.)

(u) The duration of Test 7 was 435 sec, of which 413 sec was at a speed of 31,250 to 32,000 rpm. Minimum and maximum axial load were 1770 and 4200 lb. The axial load was greater than 2200 lb for 6.17 min and was more than 4200 lb for 29 sec of the test duration. The radial load was greater than 500 lb during the entire test duration, and was between 980 and 985 lb for 33 sec.

E. BEARING TESTING AT 40,000 RPM IN AEROZINE 50

(u) Upon completion of the bearing testing with N_2O_4 as a lubricant, the tester was cleaned, reassembled, and installed for AeroZINE 50 lubricated bearing testing. Three tests (Tests 8, 9, and 11) were conducted. Figure VIII-11 tabulates steady state data points for these tests (Test 10 is reported in Paragraph VIII,F). Three separate and different types of bearing problems occurred, and the 40,000 rpm AeroZINE 50 lubricated bearing testing was therefore temporarily suspended on 23 May 1966. Testing is scheduled to resume in mid-July when improved bearing designs are available.

(u) The first AeroZINE 50 lubricated bearing test (Test 8) was completed satisfactorily; full duration of 450 sec was obtained, with about 429 sec of operation at 40,300 rpm. Minimum and maximum axial loads were 1820 and 2690 lb., whereas minimum and maximum radial loads were 500 and 1110 lb. Upon disassembly and inspection, it was found that wear had occurred in the loaded zone of the roller-bearing outer race (see Figure VIII-12). This bearing was of the self-aligning design with misalignment in accordance with Figure VIII-3. The rollers and the outer race were made from K-5-H (tungsten-titanium carbide), whereas the inner-race material was 440C steel. The roller-bearing cage was of the outer-race-riding thin-line design, made of 25% glass-filled Teflon supported by a machined aluminum containment ring (see Figure VIII-2). The ball-bearing tandem load-sharing set incorporated K-5-H balls in 440C races. The ball cages were both of the "halo" design of 25% glass-filled Teflon molded around a stainless-steel ring located at the pitch-circle diameter.

(u) Measurements of the K-5-H race and of roller wear were taken. Figure VIII-13 shows these posttest profilometer traces compared to a new K-5-H roller and to a new 440C roller. The K-5-H rollers were of poor quality; irregular crowning and eccentricity contributed partly to the outer-race wear. K-5-H material is most difficult to grind, and best results would be obtained if diamond wheels were used. However, the vendor could not justify the expense of these wheels for such a small development order. K-5-H had been selected for the outer race and for the rollers because of the excellent results obtained in four-ball wear tests conducted under Contract AF 04(611)-8548 (Reference, Report AFRPL-TR-65-150, Volume III).

(u) It was concluded that a finer grain material with a minimum of cobalt binder probably would be less prone to wear. Stress does not appear to be the primary cause of the wear since the bearings with K-5-H balls operated successfully at high stresses. Further testing with improved rollers will be necessary to determine the cause. Although the duration specified by the Work

UNCLASSIFIED

Report 10830-Q-4

VIII, E, Bearing Testing at 40,000 rpm in AeroZINE 50 (cont.)

Statement was not obtained, it should be noted that the bearings operated successfully for more than seven times the duration required in Phase II engine testing.

(u) Test 9 was conducted with (ball and roller) bearings of 440C steel for both the rolling elements and the races. The roller bearing was of the aligning type. The test was terminated prematurely, after 267 sec of operation at about 40,700 rpm, when the ball bearing cages failed. These cages were of the special molded Teflon "halo" design which had previously operated successfully in Test 8. The failure was attributed to excessive AeroZINE 50 flow (12 gal/min) and to higher friction of the 440C material. Based on calculations and previous test experience, a flow of 3 to 5 gal/min would have been sufficient. However, the tester and the test installation could not meet the lower flow requirements (for an acceptable pressure) and are therefore being modified. The failure caused considerable damage to all test bearing components (see Figure VIII-14). Loads during this test were similar to those of Test 8.

(u) A roller bearing failed during the start transient of Test 11 at 10,500 rpm. This failure was attributed to a combination of a slightly cocked inner race, excessive AeroZINE 50 flow, and a thin-profile cage of relatively flimsy design. The cage, of a design different from that used during successful N_2O_4 testing, had 15 roller pockets and was guided on the outer race.

(u) Cages of the same thin-profile design, but with 13 pockets which should significantly improve the strength of the cages, are presently on order and are due in mid-July. These units will more nearly duplicate the bearing cages used in the successful 90-mm bearing testing at 25,000 rpm. Critical-speed checks of the advanced turbopump indicated that critical speed would decrease only insignificantly if two rollers were eliminated. Heavy, shrouded, inner-race-riding cages with increased pocket clearance and flow slots at the inner bore have also been ordered. As soon as these cages are available, testing at 40,000 rpm with AeroZINE 50 as a lubricant will be resumed. Provisions are being made to reduce the bearing-tester propellant flows to 4 gal/min. Several other bearing designs with revised roller-guiding surfaces and revised clearances have also been ordered for future testing.

F. BEARING TESTING AT 31,250 RPM IN AEROZINE 50

(u) No problems were encountered in the AeroZINE 50 lubricated bearing testing at 31,250 rpm, and Work Statement Requirements were met in a single test (Test 10). Figure VIII-11 tabulates steady-state data points, Figure VIII-15 is a plot of significant parameters versus time, and Figure VIII-7 compares pre and posttest critical inspection measurements. Figure VIII-16 illustrates the excellent posttest appearance of these bearings. Duration at 32,000 rpm was 418 sec. The minimum axial load was 2700 lb, and an axial load of 4600 lb was maintained for 20 sec. A minimum radial load of 600 lb was maintained during the test, and a peak radial load of 1115 lb was kept for 18 sec.

UNCLASSIFIED

Report 10830-Q-4

VIII, Turbopump Bearing Development (cont.)

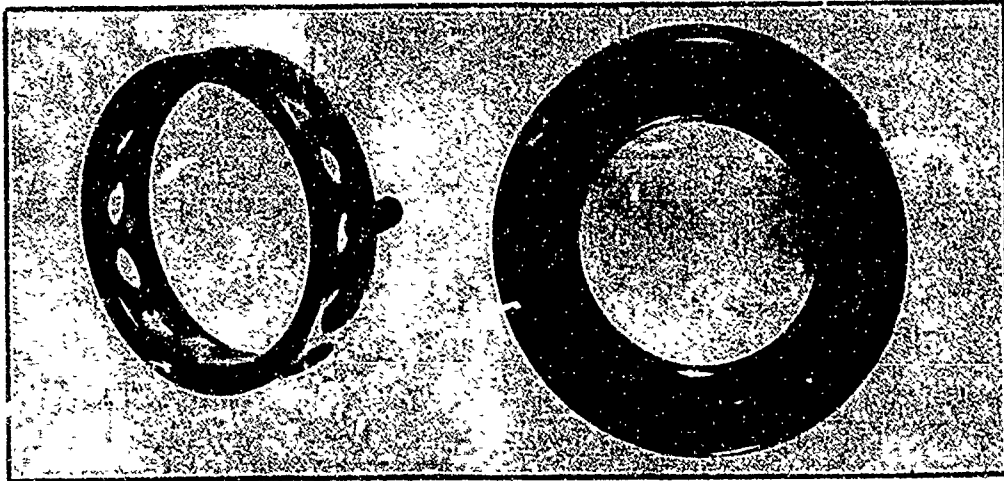
G. HYDROSTATIC THRUST-BEARING DISC FAILURE INVESTIGATION

(u) An oil-lubricated test thrust-absorbing hydrostatic bearing disc of 440C material failed on Bearing Test 4. This failure was similar to that reported in the third quarterly report,* even though the thrust-bearing disc had been retempered to a Rockwell hardness of $R_c 40$ (to improve ductility), the keyway radii had been enlarged to 0.030 in., and the new disc had been reinspected to ensure it had no cracks. Further analysis and investigation led to the conclusion that both failures can be explained by notch-disc burst theory: They will occur if the Charpy V-notch energy of the material is low and high stress concentrations exist. This theory, supported by extensive testing reported to the ASTM Task Force on brittle failure, would predict that notched discs, such as these discs of 440C steel with Charpy V-notch energy readings of 2 to 3 ft-lb, would fail when the average tangential stress in the disc is equal to about 10 to 20% of the ultimate tensile stress (Figure VIII-17). Based upon this theory, the thrust-bearing discs made from AM-350 and AM-355 steel, with Charpy V-notch energy loads of about 17 ft-lb, will withstand over 60,000 rpm without failure. An AM-350 thrust-bearing disc of new design was installed after Test 4 and performed satisfactorily on all subsequent tests.

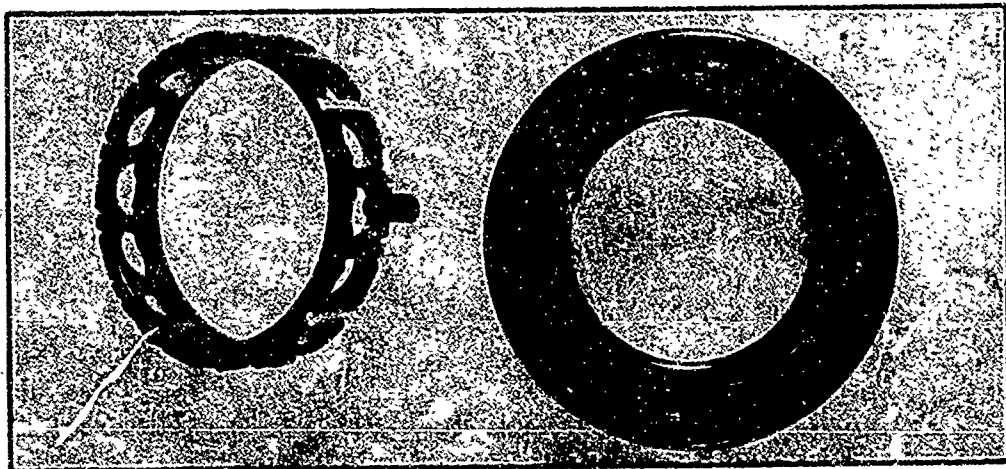
* Report TR-66-82, 15 April 1966

UNCLASSIFIED

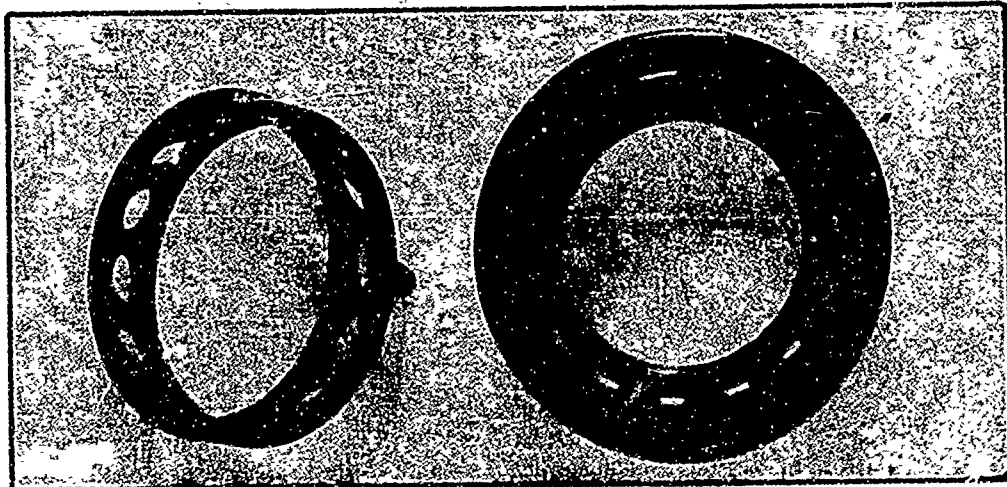
Report 10830-Q-4



SHROUDED INNER RACE RIDING BALL CAGE



"THIN LINE" OUTER RACE RIDING BALL CAGE



MOLDED "HALO" OUTER RACE RIDING BALL CAGE

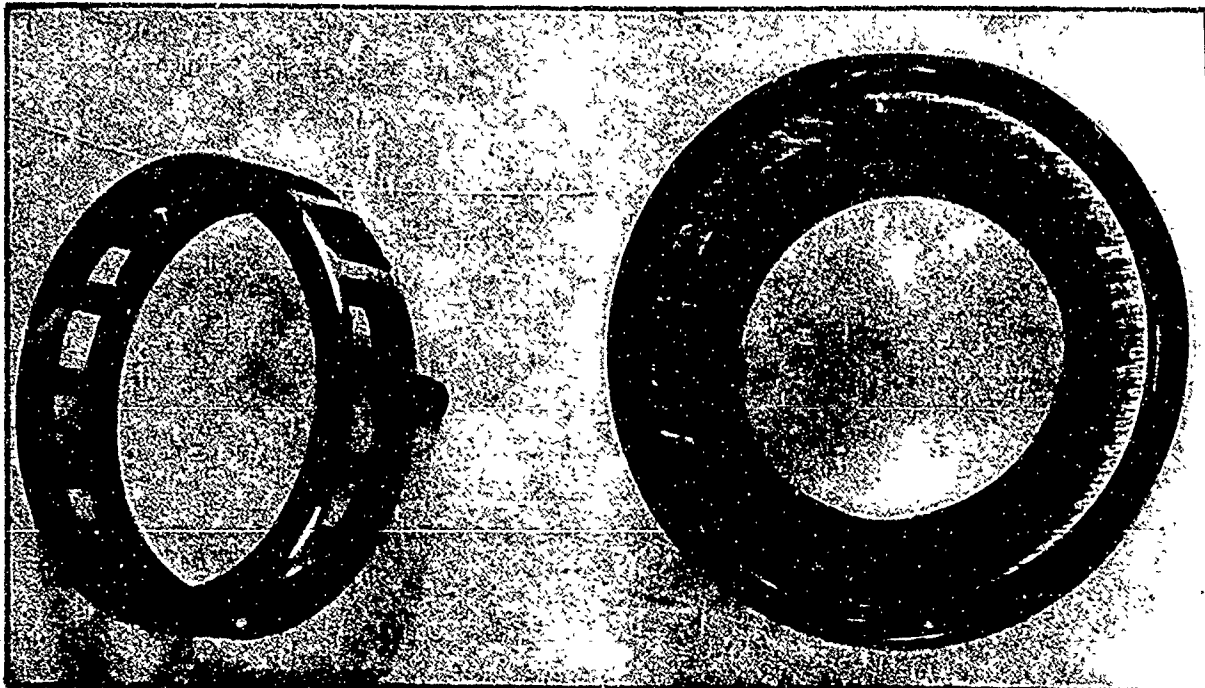
Ball Bearing Cage Design

Figure VIII-1

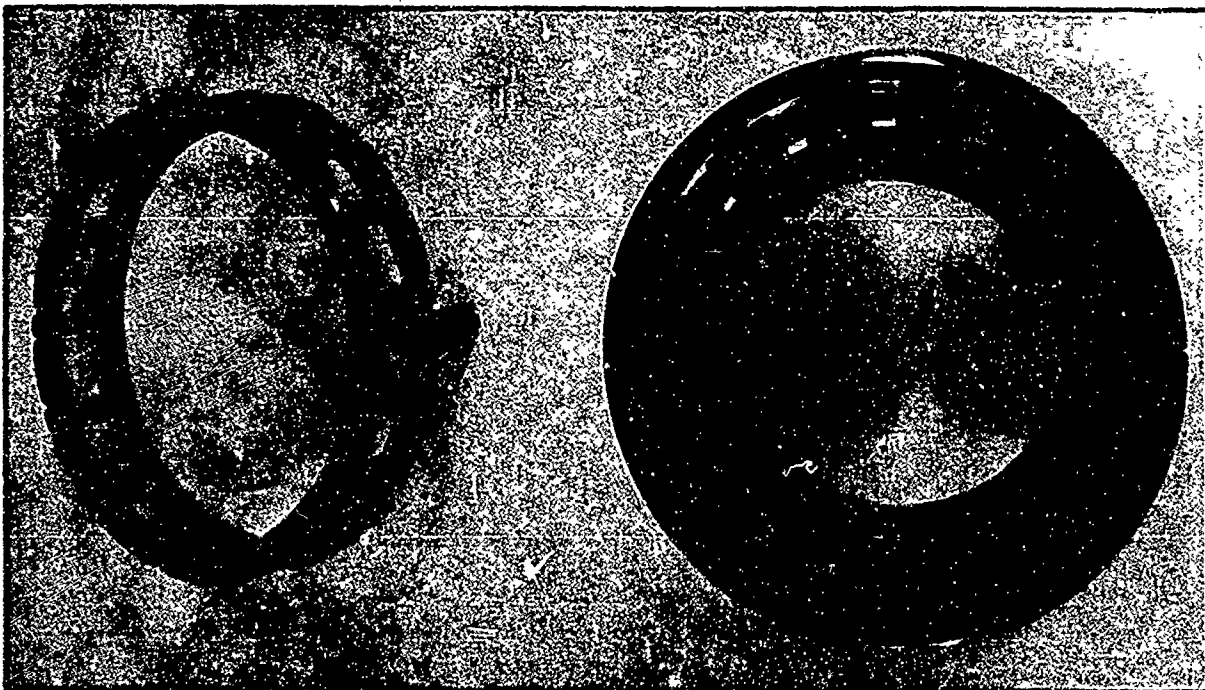
UNCLASSIFIED

UNCLASSIFIED

Report 10830-Q-4



SHROUDED INNER RACE RIDING ROLLER CAGE



"THIN LINE" OUTER RACE RIDING ROLLER CAGE

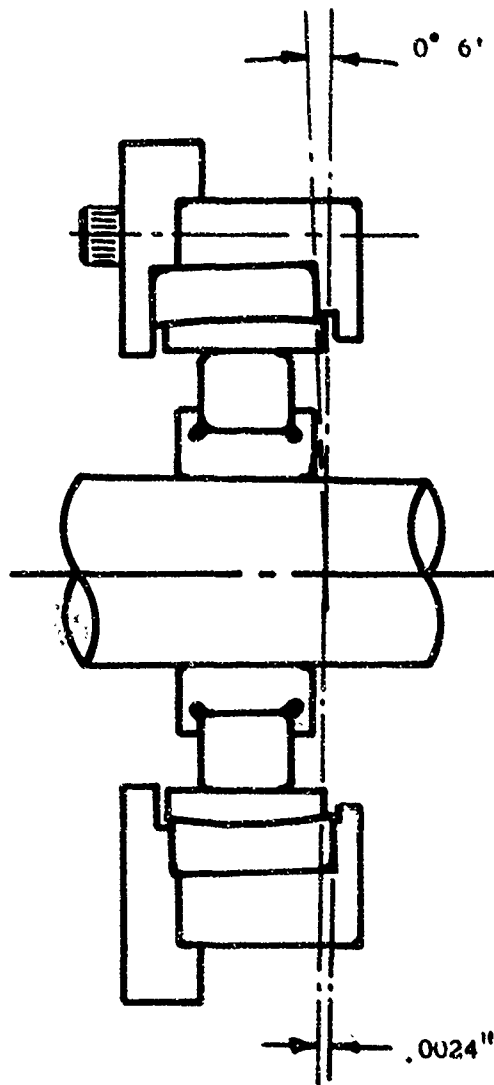
Roller Bearing Cage Design

Figure VIII-2

UNCLASSIFIED

UNCLASSIFIED

Report 10830-Q-4



The illustrated angular misalignment is equal to a shaft centerline deflection of .016 inches with ARES turbopump bearing span of 10.35 inches

Installation of Misaligned Roler Bearing for Test 1.2-03-WAW-006B

Figure VIII-3

UNCLASSIFIED

<u>Date</u>	<u>Run No.</u>	<u>Duration* Sec</u>	<u>Data Point** Sec</u>	<u>Speed N_T RPM</u>	<u>DN N_T x 10⁻⁶</u>	<u>Load</u>		<u>Propell.</u>	
						<u>Axial F_A Lb</u>	<u>Radial F_R Lb</u>	<u>Flow Q_P GPM</u>	<u>Temp</u>
4-7	004	2	2	38,700	1.55	2760	565	8.75	
4-22	005A	270	35	39,600	1.55	1170	525	9.6	
			245	39,100	1.56	2955	540	8.55	
			297	39,000	1.56	2350	880	8.2	
4-22	005B	1	1	39,300	1.57	835	551	9.6	
4-26	006A	1	1	27,600	1.1	1503	572	9.5	
4-27	006B	520	120	39,890	1.59	1810	560	9.0	
			340	39,435	1.58	2550	520	8.45	
			420	38,993	1.56	1840	1020	8.3	
4-28	007	410	35	32,212	1.29	2320	500	9.0	
			145	31,913	1.28	4200	500	9.2	
			200	31,575	1.26	2650	1010	8.6	

*Duration at full speed

**From turbine start

UNCLASSIFIED

Report 10830-Q-4

Propellant low	Temp. Rise	Rise of Outer Race Temperature			Remarks
		Ball Bearing	Ball Bearing	Ball Bearing	
QP GPM	ΔT_p °F	ΔT_{TB-1} °F	ΔT_{TB-2} °F	ΔT_{TB-3} °F	
8.75	11	22	22	32	Thrust disc failure
9.6	9	21	21	37	
8.55	22	22	22	41	
8.2	22.6	22	22	41	Speed probe malfunction
9.6	7	17.5	18.5		Burst diaphragm in GN ₂ line broke, terminating test, turbine inlet air.
9.5	-	-	-	-	False OST due to instrumentation malif.
9.0	24.1	23.9	23.9	33	
8.45	26	28.6	28	39	
8.3	26	29	28	40	Normal start & shutdown, all objectives met
9.0	12	10.8	13	20	
9.2	13	13.1	15.5	17	
8.6	13.2	15.5	15.8	24.1	Normal start & shutdown, all objectives met

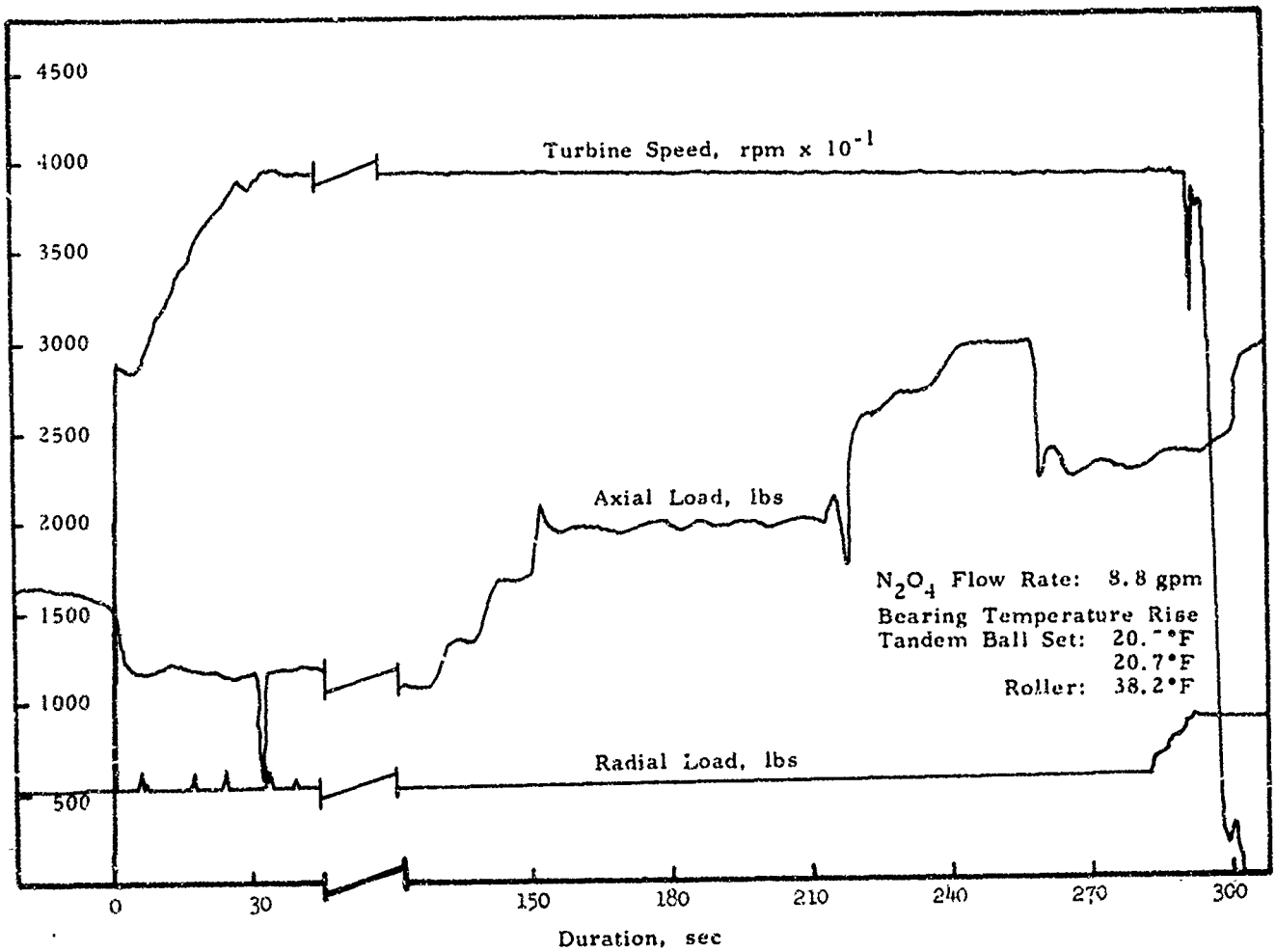
Tabulation of Steady-State Data Points of N₂O₄ Bearing Tests

Figure VIII-4

UNCLASSIFIED

UNCLASSIFIED

Report 10830-Q-4



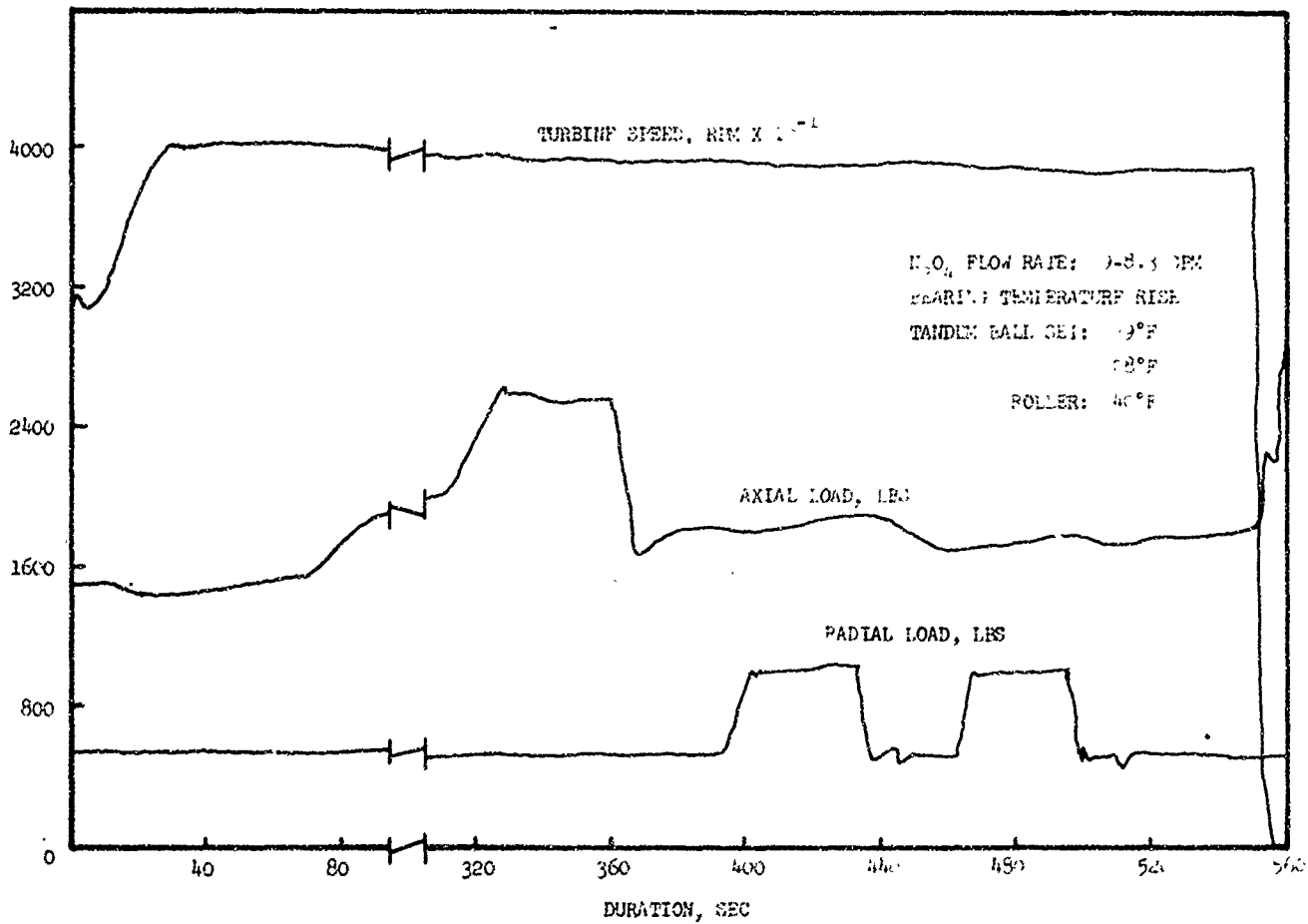
ARES Ball and Roller Test 1.2-03-WAW-005A

Figure VIII-5

UNCLASSIFIED

UNCLASSIFIED

Report 10830-Q-4



ARES Ball and Roller Test 1.2-03-WAW-006B

Figure VIII-6

UNCLASSIFIED

CAGE CLEARANCE

TEST	PART NO.	SERIAL NO.	SHAFT FIT	HOUSING FIT	POCKET	
					AXIAL	RADIAL
005A	1121349 ①	R005	-.0003	-.0003	.010	.020
006B	1121349	R005	-.0003	-.0002	.010	.020
007	1121350	R008	-.0002	+.0002	.010	.020
008	1121348 ④	R001	-.0003	-.0003	.010	.040
010	1121350	R011	-.00035	+.0003	.010	.020

BALL BEARING CRITICAL DIMENSIONS

TEST	PART NO.	SERIAL NO.	SHAFT FIT	HOUSING FIT	CAGE CLEARANCES	
					POCKET	DIAMETRAL
005A & 006B	1121347	R020	-.00016	+.00015	.015	.015 IRR
007	1121347	R018	-.0003	+.0001	.015	.015 IRR
008	1121347 ⑤	R016	-.0003	+.0004	.015	.010 ORR
010	1121347	R024	-.0003	+.00015	.015	.015 IRR

- ① P/N 1121349 & 1121348 INCORPORATE THE ALIGNING FEATURE
- ② INNER RACE RIDING CAGE & OUTER RACE RIDING CAGE
- ③ EXCESSIVE WEAR ON OUTER RACE & ROLLERS, NO POST INSPECTION
- ④ K-5-H ROLLERS & OUTER RACE
- ⑤ K-5-H BALLS

UNCLASSIFIED

Report 10830-Q-4

CAGE CLEARANCES

POCKET		DIAMETRAL	TOTAL RADIAL PLAY		PRETEST ROLLER END PLAY	POST TEST ROLLER END WEAR
AXIAL	RADIAL		PRE	POST		
.010	.020	.020 IRR (2)	.0010/ .0015		.001	NONE (LIGHT BURNISH)
.010	.020	.020 IRR	"	.0015	.0015	.0015
.010	.020	.020 IRR	.0011	.0014	.0007	NONE
.010	.040	.050 ORR (2)	.0016	(2)	.0014	NONE
.010	.020	.020 IRR	.00135	.00135	.0008	.0013

BEARING CRITICAL DIMENSIONS

CAGE CLEARANCES		TOTAL PLAY			
POCKET	DIAMETRAL	AXIAL		RADIAL	
		PRE	POST	PRE	POST
.015	.015 IRR	.0113	.0108	.0033	.0033
.015	.015 IRR	.0101	.0101	.0028	.0028
.015	.010 ORR	.0102	.0102	.0028	.0028
.015	.015 IRR	.0103	.0103	.0028	.0029

Tabulation of Ball and Roller Bearing Critical Dimensions

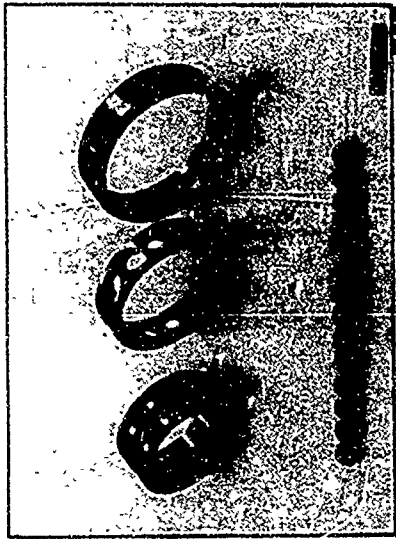
Figure VIII-7

UNCLASSIFIED

2

UNCLASSIFIED

Report 10830-Q-4



SPEED:	38,500 RPM		
DURATION:	791 sec, 13 min, 11 sec.		
		LOAD	DURATION
AXIAL, NOMINAL:	1500 + lbs		739 sec.
PEAK:	2500 + lbs		52 sec.
RADIAL, NOMINAL:	500 lbs		759 sec.
PEAK:	1000 lbs		32 sec.

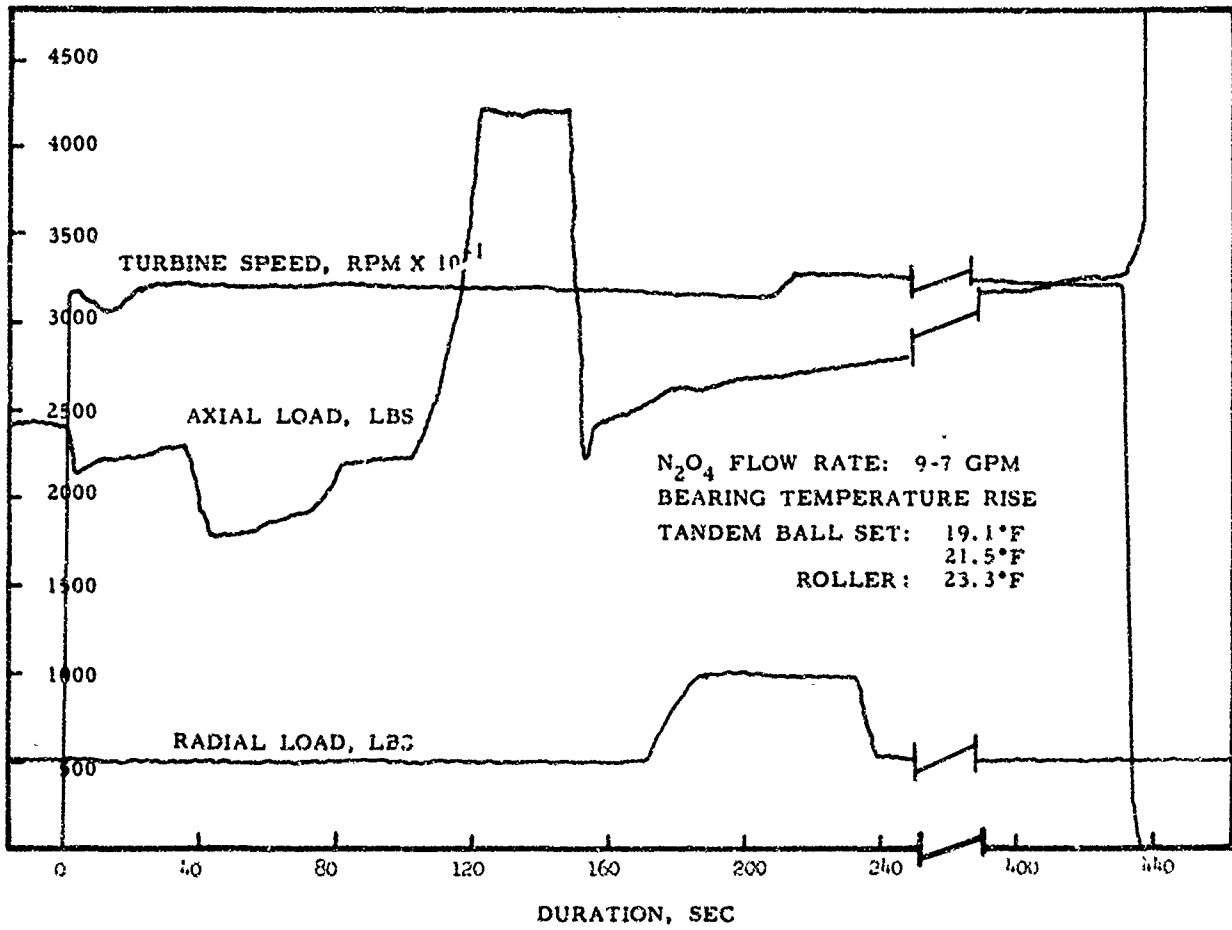
ARES Tandem Ball and Roller Bearings from N₂O₄ Test 1.2-03-MAW-006B

Figure VIII-8

UNCLASSIFIED

UNCLASSIFIED

Report 10830-Q-4

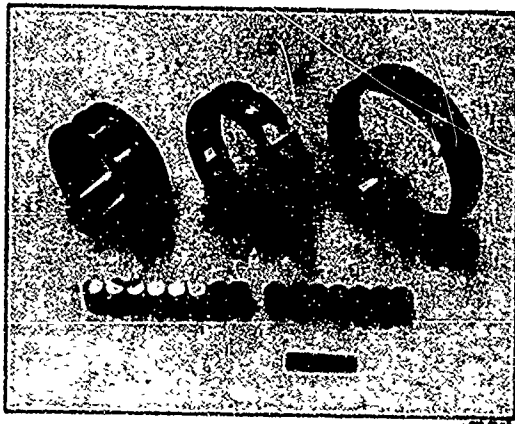
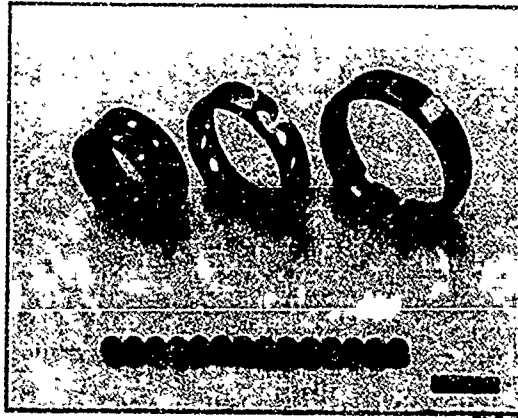
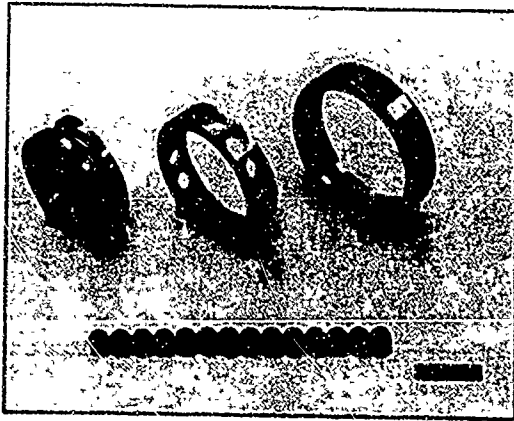


ARES Ball and Roller Bearing Test 1.2-03-WAW-007

Figure VIII-9

UNCLASSIFIED

UNCLASSIFIED
Report 10830-Q-4



SPEED : 31,250 RPM
DURATION : 413 sec, 6min. 53 sec.

	<u>LOAD</u>	<u>DURATION</u>
AXIAL, NOMINAL :	2200+ lbs	364 sec.
PEAK :	4200 lbs	29 sec.
RADIAL, NOMINAL :	500 lbs	368 sec.
PEAK :	985 lbs	45 sec.

ARES Tandem Ball and Roller Bearings from N_2O_4 Test 1.2-03-WAW-007

Figure VIII-10

UNCLASSIFIED

Date	Run No.	Duration* Sec	Data Point** Sec	Speed N _T RPM	DN N _T x 10 ⁻⁶	Load		Propellant	
						Axial F _A Lb	Radial F _R Lb	Flow Q _p GPM	Temp. ΔT _p
5-13	008	450	0	0	0	1970	554	15.2	.4
			70	40,300	1.61	2800	552	14.2	17
			100	40,400	1.62	600	552	13.9	18
			180	40,300	1.61	2060	1115	13.6	18
			440	40,300	1.61	1860	550	13.6	19
5-13	009	267	0	0		1940	551	14.8	1.
			85	40,700	1.63	1960	548	13.7	10
			107	40,800	1.63	2790	548	13.7	10
			200	41,200	1.65	2010	1118	13.4	10
			265	40,600	1.62	1690	560	8.1	10
5-20	010	418	0	0	0	2760	596	15.5	1.
			60	32,800	1.31	2790	595	14.2	10
			100	32,600	1.30	2840	1117	14.1	9.
			190	32,800	1.31	4690	605	14.1	9.
			415	32,200	1.29	2970	600	14.1	10
5-21	011	-	11	10,500	.42	2030	595	13.7	-

* Duration at full RPM

** From turbine start

UNCLASSIFIED

Report 10830-Q-4

Run No.	Propellant		Rise of Outer Race Temperature			Remarks
	Flow	Temp. Rise.	Ball Bearing	Ball Bearing	Ball Bearing	
	Q_p GPM	ΔT_p °F	ΔT_{TB-1} °F	ΔT_{TB-2} °F	ΔT_{TB-3} °F	
554	15.2	.4	0	0	0	Lube pump on, turbine not yet turning
552	14.2	17.6	12.4	12.3	17.9	Steady state
552	13.9	18.6	13.3	13.5	17.9	Axial Load Peak
1115	13.6	18.9	13.6	13.0	17.9	Radial load peak
550	13.6	19.2	13.1	13.3	19.1	Steady state prior to scheduled shutdown
551	14.8	1.1	0	0	0	Lube pump on, turbine not yet turning
548	13.7	10.3	24.5	25.1	30.2	Steady state
548	13.7	10.5	25.2	25.8	30.7	Axial load peak
1118	13.4	10.1	26.2	28.7	34.6	Radial load peak
560	8.1	10.5	33.1	32.8	51.6	Data prior to manual shutdown due to abnormal temperature rise in bearings
596	15.5	1.2	0	0	0	Lube pump on, turbine not yet turning
595	14.2	10.2	7	5.3	8.1	Steady state
1117	14.1	9.6	6.3	5.1	10.4	Axial load peak
605	14.1	9.7	6.0	4.4	9.4	Radial load peak
600	14.1	10.1	2.6	1.3	5.8	Data prior to scheduled shutdown
595	13.7	-	4	4	8	Roller bearing cage failure (misaligned, installation)

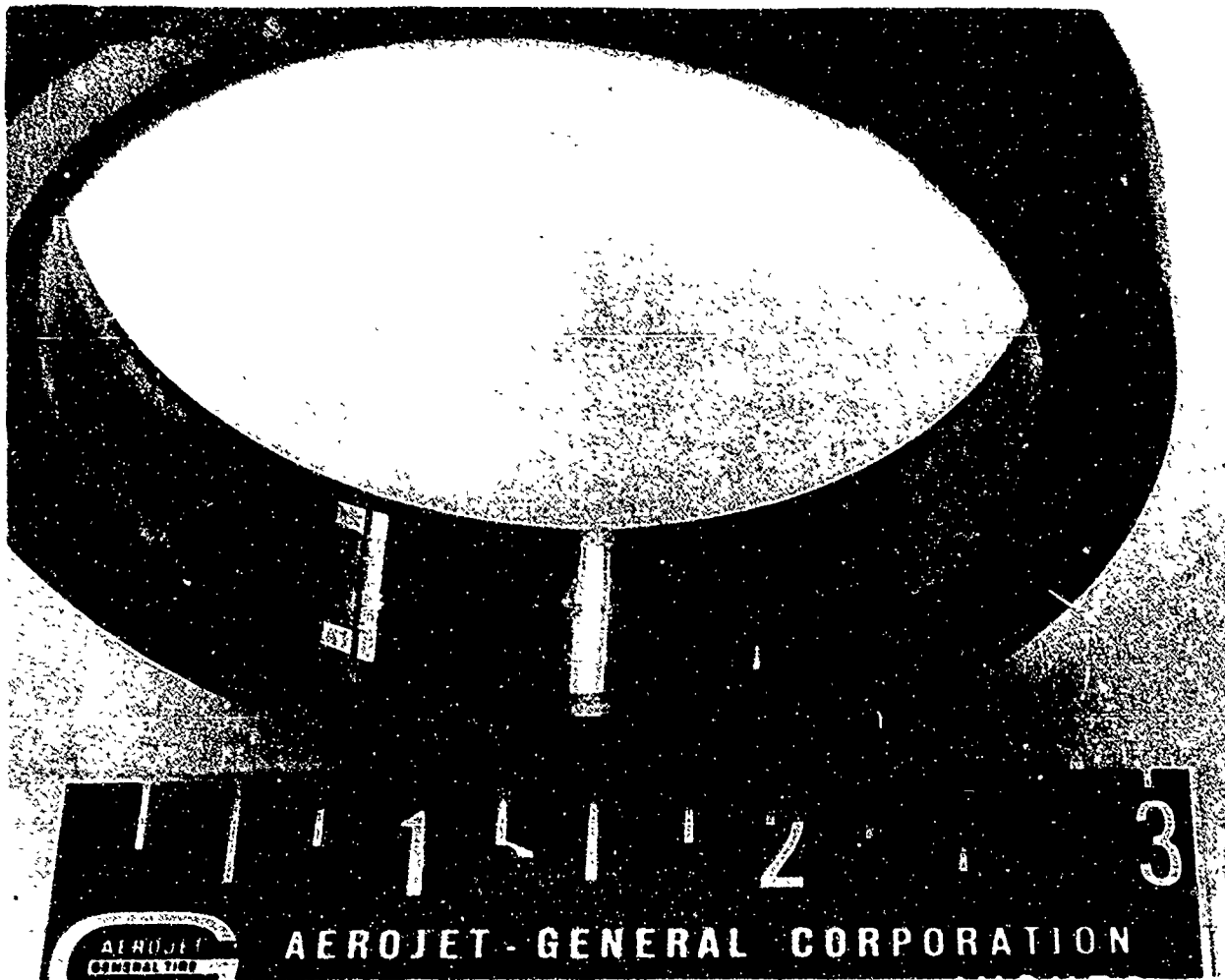
Tabulation of Steady-State Data Points of AeroZINE 50 Bearing Tests

Figure VIII-11

UNCLASSIFIED

UNCLASSIFIED

Report 10830-Q-4



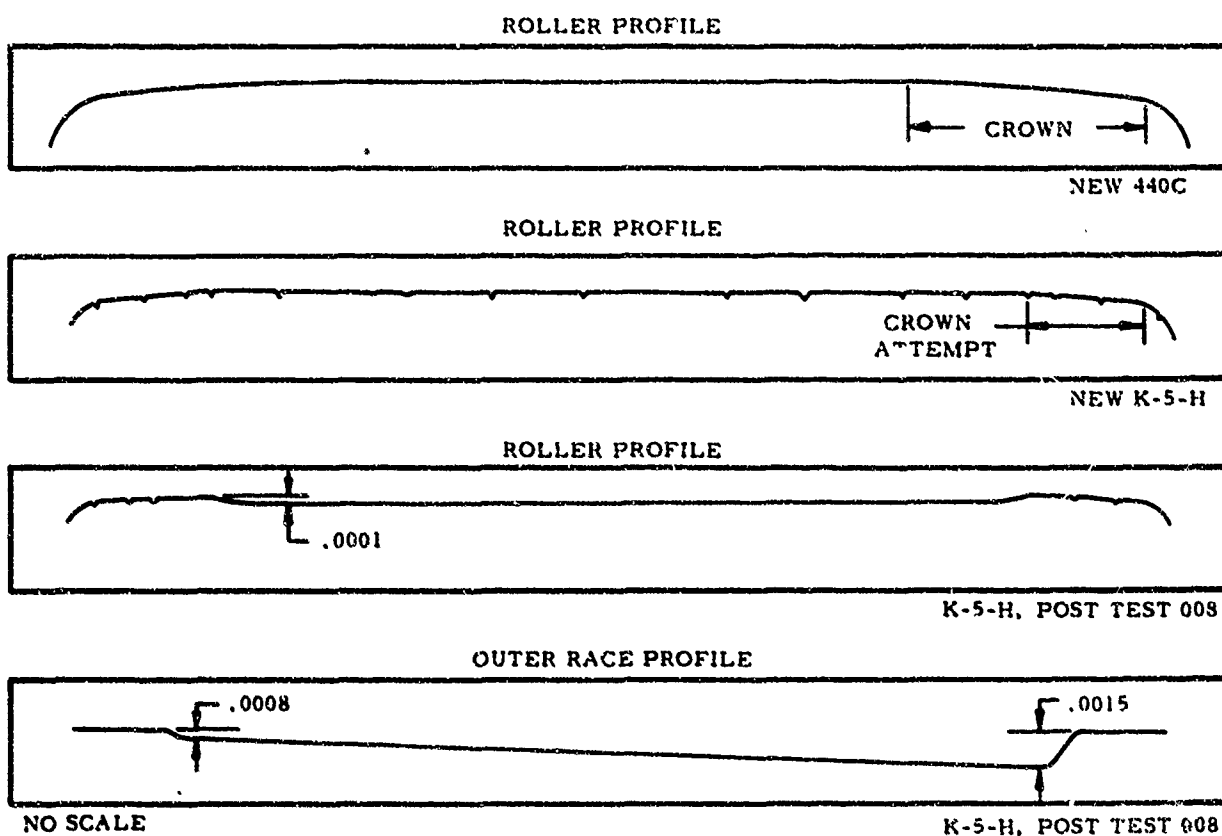
K-5-H Outer Race Wear. Posttest 1.2-03-WAW-008

Figure VIII-12

UNCLASSIFIED

UNCLASSIFIED

Report 10830-Q-4



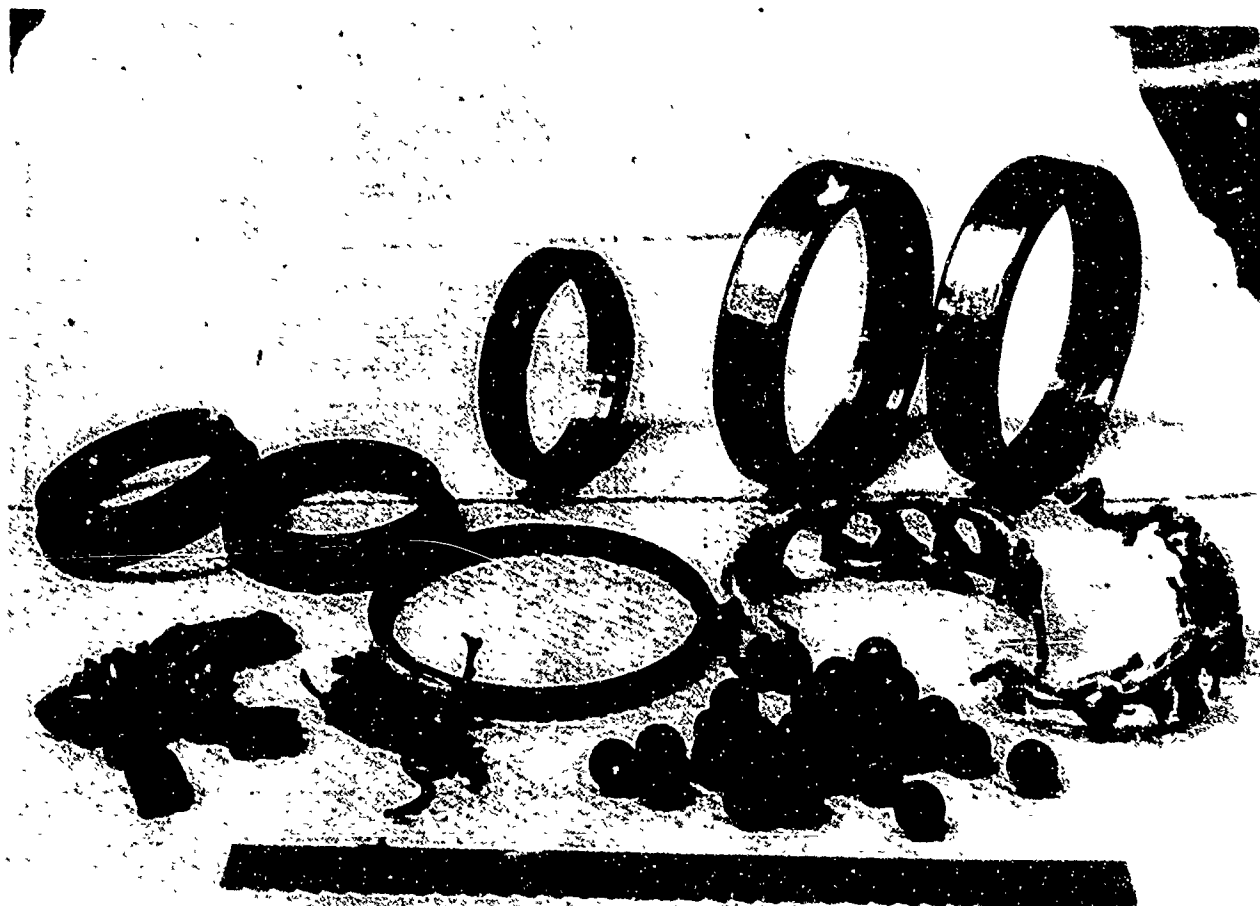
K-5-H Race and Roller Wear Measurements and Comparison to New K-5-H and 4400 Rollers

Figure VIII-13

UNCLASSIFIED

UNCLASSIFIED

Report 10830-Q-4



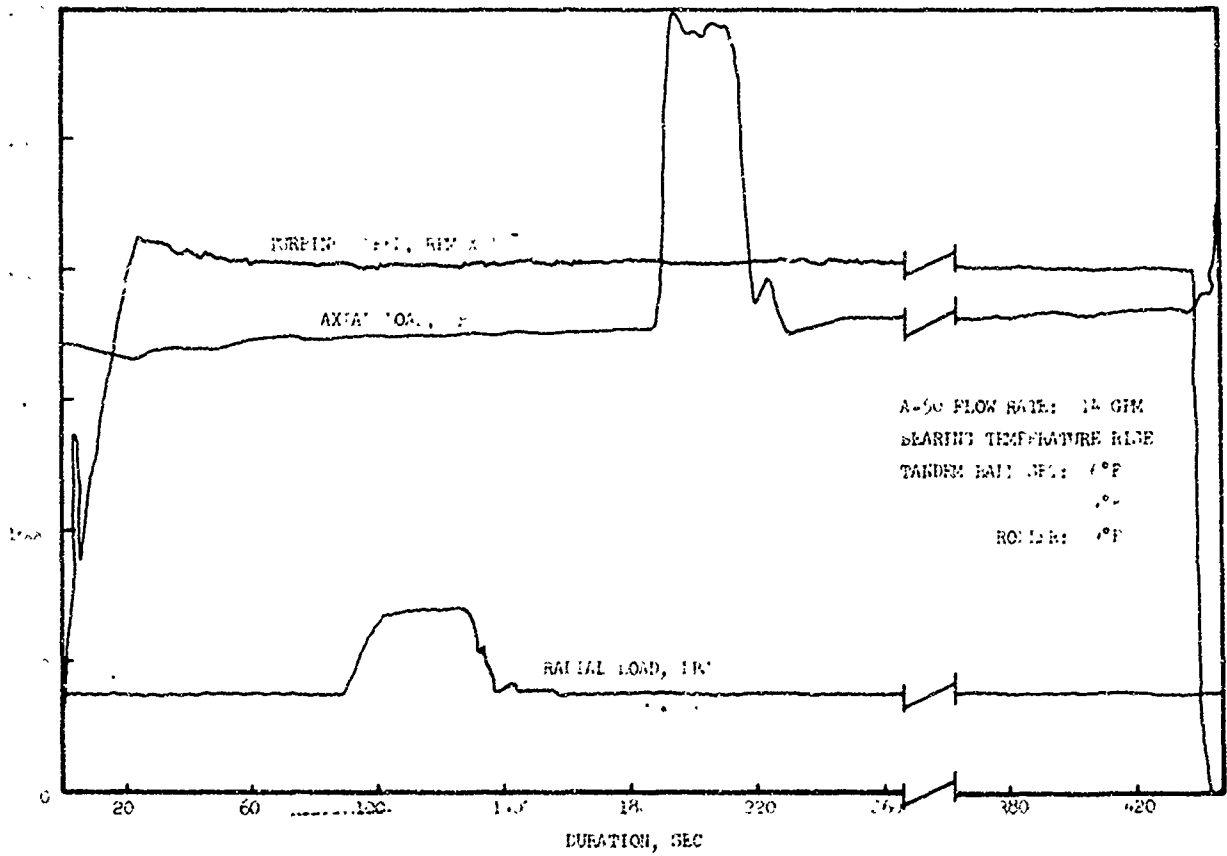
Ball Bearing Cage Failure, Posttest 1.2-03-WAW-009

Figure VIII-14

UNCLASSIFIED

UNCLASSIFIED

Report 10830-Q-4



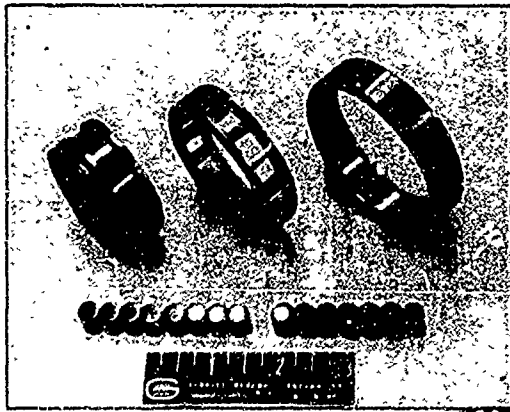
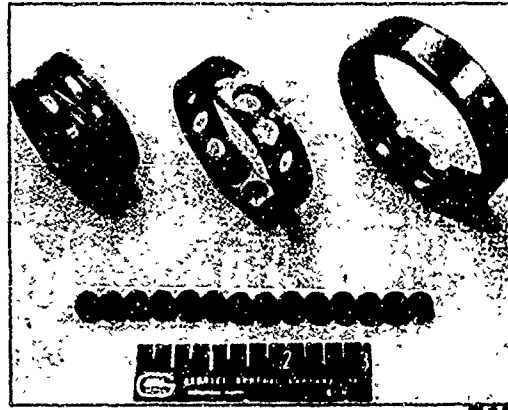
ARES Ball and Roller Bearing Test 1.2-03-WAW 010

Figure VIII-15

UNCLASSIFIED

UNCLASSIFIED

Report 10830-Q-4



SPEED: 31,250
DURATION: 418 sec, 6 min. 58 sec.

	<u>LOAD</u>	<u>DURATION</u>
AXIAL, NOMINAL:	2890 lbs	398 sec.
PEAK:	4650 lbs	20 sec.
RADIAL, NOMINAL:	600 lbs	403 sec.
PEAK:	1115 lbs	15 sec.

ARES Tandem Ball and Roller Bearings from AeroZINE 50 Test 1.2-03-WAW-010

Figure VIII-16

UNCLASSIFIED

UNCLASSIFIED

Report 10830-Q-4

IX.

TURBOPUMP WEAR-RING DEVELOPMENT

A. GENERAL

1. Objectives

(u) The objectives of the ARES turbopump wear-ring program are to design and develop wear rings that will (1) satisfactorily limit pump internal leakage and (2) operate safely and reliably with intermittent rubbing in both N_2O_4 and AeroZINE 50. The results of the wear-ring program will be applicable to both the advanced (T-housing) and the backup (inline) turbopump wear-ring designs as well as to other close-running components such as shaft labyrinths, axial thrust compensators, inducers, and boost pumps.

2. Approach

(u) Two approaches are being taken in solving the wear-ring sealing and explosion-hazard problems. The first approach is to allow intermittent rubbing of the impeller wear-ring on inert, compatible inserts; straight labyrinth seals incorporating these features are to be tested. The results are applicable to stepped labyrinth seals as well.

(u) The second approach is to allow low-speed transient rubbing, but to prevent high-speed contact by maintaining a fluid film between the impeller running surface and the seal itself. Tests will be conducted on axial and radial hydrostatic seals based on this concept. Experience with seals and bearings, obtained in Contracts AF 04(611)-7439, AF 04(611)-8548, and AF 04(611)-10784, indicate that this second approach is feasible. Analyses and designs of the four concepts to be tested were presented in Report TR-66-1.

3. Summary of Results

(u) Testing was delayed because of bearing rework after failure of a water-lubricated bearing during the first rotating test (see Report TR-66-82). Two successive failures of the hydrostatic thrust collar on the tester during the bearing test program (the first described in Report TR-66-82 and the second in Section VIII of this report) further delayed the resumption of wear-ring testing when the original wear-ring tester was converted into a bearing tester. A new tester was fabricated, and testing was resumed on 9 June 1966. Four tests utilizing stepped and straight labyrinths were conducted (two static flow checks and two rotating tests); the initial test in this series was reported previously. Wear-ring rubbing by test-heat displacement into the rotating labyrinth has been accomplished successfully. Another water-lubricated bearing failed during Test 3. This failure was found to be caused by the loss of water flow through the bearing at high speed. After the pressure differential across the bearing had been adjusted, the rotating rubbing test (Test 4) was conducted at 29,400 rpm with no difficulties.

UNCLASSIFIED

Report 10830-Q-4

IX, Turbopump Wear-Ring Development (cont.)

B. DESIGN

(u) In the design of the straight-labyrinth seals to withstand rubbing, much consideration has been given to the retention of the plastic inserts at high pressures and during rubbing. The following retention mechanisms are being evaluated.

1. Dovetail Insert

(u) This concept is illustrated in Figure IX-1, which also shows the essential components of the wear-ring test head. The plastic insert is sandwiched between a two-piece flange. The axial compression on the insert is established by the thickness of the Teflon shim and the torque on the bolts. The flange has pressure reliefs connecting the insert OD to the downstream side of the labyrinth to preclude forcing the insert out of the flange. This concept provides good pressure retention but requires several parts. Its main disadvantage is a wide axial clamp on the upstream side of the labyrinth, which requires locating the labyrinth teeth axially away from the impeller proper or reducing the number of teeth (and increasing the leakage). This concept has been tested successfully in water at 2500 psi.

2. Reinforced Dovetail Insert

(u) As a backup to the dovetail insert in the event of excessive pressure distortions, a reinforced dovetail concept has been fabricated (Figure IX-2) in which the Teflon insert is molded to a perforated steel ring and then machined to shape. The insert is then placed into the main flange, followed by the retaining ring. A thin lip of the main flange is then rolled over the retaining ring while an axial force is maintained on the assembly. This axial force ensures a tight lock-up of the parts and, in addition, deforms the perforated ring where it contacts the flange and retaining ring, providing a metal-to-metal seal against leakage between the parts. This concept has the same disadvantage as the dovetail insert.

3. Knurled Insert

(u) This simple design (Figure IX-3) has straight knurling on the ID of the flange which retains the plastic insert. However, it was found that the plastic insert would not deform sufficiently to fill the valleys between the crests of the knurls: the overall leakage rate of the labyrinth would therefore be excessive. Although the basic problem of excess leakage might be overcome by a better combination of knurl depth and flange/insert interference, and/or by using some type of compatible filler material in the knurled area, such an approach would involve time-consuming development that did not seem worthwhile. Instead, the knurled flanges were reworked to accept pressure-relieved inserts.

UNCLASSIFIED

Report 10830-Q-4

IX, B, Design (cont.)

4. Pressure-Relieved Insert

(u) This concept (Figure IX-4) consists of drilling a series of radial holes to connect the OD and the ID of the insert. A set of eight equally spaced holes are drilled in each of three planes, and each set of holes is connected by a circumferential groove. In this way the pressure gradients on the outside and inside of the insert are equalized and there is less tendency for the insert to be forced out under pressure.

5. Felt-Metal Insert

(u) This insert (Figure IX-5) consists of small nickel fibers that are sintered together to produce a material with a density controllable from 10 to 80% of that of a solid nickel insert. A density of 20% has been chosen for the water screening tests. For water testing, the insert is simply bonded to the flange with epoxy, but for use in propellants, the insert would be brazed to the flange. The material deforms when contacted and therefore has been used in high-speed turbocompressors as a labyrinth-sleeve material.

6. Shell-Reinforced Insert

(u) This concept (Figure IX-6) involves molding Teflon about a spun, perforated metal shell. The shell increases the strength of the part, whereas the perforations ensure a better adherence of the Teflon to the metal shell. This insert does not rely on an interference fit with the flange and thus should not be greatly affected by any time-rate changes in the Teflon properties. It is easy to assemble and replace.

(u) In the last quarterly report it was pointed out that impeller distortions significantly affect the operation of the hydrostatic wear rings. Any movement of the impeller that produces a diverging or converging flow path will change the overall flow of the seal, the seal stiffness, and the running clearance. Since the flow rates are low in comparison with other wear-ring types, any changes in flow rate are not in themselves too important. Changes to seal stiffness, and clearances are, however, very important, as shown in Figure IX-7 for the hydrostatic face seal. Figure IX-7 shows how the axial stiffness and the average running clearance of each land vary with the amount of coning of the seal faces. Data for two different seals are plotted. The only difference between the two seals is that one seal has a total face width of 0.150 in., whereas the other has a width of 0.300 in. Both seals have the same balance diameter (3.504 in.) and the same nominal running clearance (0.001 in. for zero face distortion). The 0.300-in.-wide face seal is the seal presently fabricated for water testing. From Figure IX-7 it can be seen that, for increasing divergence of the flow path (positive α), the axial stiffness increases, but the average running clearance across each land decreases. Thus, even though the seal stiffness is increasing, it appears that at some alpha the outer land (t_1) will contact the running surface. For the case of a convergent flow path, or negative α , the seal stiffness reaches a value where the seal response is inadequate to follow shaft movements and the seal is thus made inoperable. Hence, it is

UNCLASSIFIED

Report 10830-Q-4

IX, B, Design (cont.)

seen that limits exist to the amount of distortion that can be withstood by the seal. By comparing the data in Figure IX-7 for the two seals, it is seen that contact with the running surface occurs at larger distortions for narrower face widths. The narrower seal will also respond better to impeller wobble due to the fact that its mass can be reduced by about a factor of four (if its width is reduced to 1/2, then its length can also be reduced by 1/2), while seal stiffness decreases by only a factor of two (Figure IX-7); thus the response rate, which is proportional to $\sqrt{\frac{M}{K}}$, might be $\sqrt{4/2} = 1.4$ times that of the 0.300-in.-wide seal. It is therefore concluded that, as an aid in accommodating the impeller distortions, the face seal should be reduced in size. A size reduction of 50% is possibly a lower limit for ease in fabrication. If the water tests of the present wear ring with a face width of 0.300 in. are completed satisfactorily, additional seals of narrower width will be ordered.

C. FABRICATION

(u) All test hardware is now available for testing. Efforts to bond the Hystl resin to the stainless steel flange have not been successful; this concept therefore will not be tested.

D. TESTING

1. Setup

(u) A description of the basic test setup has been given in Report TR-66-82. Testing to date has required only one additional parameter to be monitored; i.e., inboard flow to determine the flow requirements for the water-lubricated roller bearing. Briefly, the basic test setup allows the pressures on each side of the wear rings to be monitored. In addition, the inflow, Q_1 , and the outboard flow, Q_3 , are measured (see Figure IX-1). The inboard flow, Q_2 , is simply $Q_1 - Q_3$. The inboard flow exits from the test head through two paths; since the path past the water-lubricated roller bearing is subsequently "contaminated" by a GN_2 purge, the other exit line is now monitored to yield, Q_2' , i.e., the inboard flow that does not pass through the bearing. The bearing flow then is $Q_1 - Q_3 - Q_2'$.

2. Test Results

(u) The second water test was conducted on 9 March 1966 to determine the leakage rate of the stepped labyrinth when run at close axial clearances; this test simulates an extreme condition that would be experienced during startup and shutdown of the turbopump. The results of this test, given in Figure IX-8, when compared with the results of Test 1 show that little change in flow occurs even though the axial clearance has been reduced from 0.050 to 0.022 and 0.012 in. on the outboard and inboard labyrinths, respectively. This means that little loss occurs from the bend or step proper, and that essentially all the loss is due to the primary restriction; i.e., the labyrinth teeth.

UNCLASSIFIED

Report 10830-Q-4

IX, D, Testing (cont.)

(u) Test 3 was conducted on 13 June 1966. Six-teeth straight labyrinths of 0.050-in. pitch were used. The inserts were made from Vespel SP-1 (outboard) and from TEC Fluorfil BF3 (inboard); both inserts were dovetail-retained (Figure IX-1). Vespel SP-1 is a DuPont tradename for parts fabricated from an aromatic polyimide resin. It is stronger than Teflon, has good friction and wear properties, and has been used for gears, ball-bearing separators, and sleeve bearings. The Fluorfil BF3 compound consists of Teflon with a proprietary fill material of Thermech Engineering Corp. (15% fiber glass and 10% metallic oxide). Preliminary compatibility testing shows it to be compatible with both N₂O₄ and AeroZINE 50. The test was conducted by increasing pressure to 2,500 psi, then increasing speed. At a speed of 27,000 rpm one of the radial loading bearings reached a temperature of 275°F and the tester was therefore shut down. Shaft-speed decay was normal until a speed of 10,000 rpm was reached, at which point the shaft seized. Disassembly of the tester revealed that the cage of the water-lubricated bearing had failed. In addition, the inner race spun on the shaft. Subsequent analysis of pressure and flow data (Figure IX-8) indicated the presence of large centrifugal pressure gradients that reduced the bearing flow to zero at about 15,000 rpm.

(u) Test 4 was conducted on 21 June 1966 with the same test pieces as Test 3. The inboard seal pressure was approximately doubled over that of Test 3 to increase the flow through the bearing and to reduce the effect of the centrifugal pressure gradient. Speed was increased to 15,000 rpm then reduced to zero, and the bearing flow was determined to be about 6 gal/min. The same procedure was followed at 25,000 rpm and the bearing flow was found to be about 3 gal/min. Speed was then increased to 29,400 rpm and the test head was misaligned radially 0.007 in. to induce rubbing (outboard and inboard radial clearances were 0.0045 and 0.005 in., respectively). Both flows and downstream pressures were momentarily affected by the rubbing but returned to normal after the rubbing ceased. Approximately two seconds after misalignment, the test head was realigned, and about six seconds later the test was terminated. Examination of the plastic inserts showed them to be in good condition (Figures IX-9 and -10). No damage was observed except where rubbing had occurred. The water-lubricated bearing can be partially examined without disassembly of the tester and was found to be in good condition. Preliminary data, presented in Figure IX-8, are being analyzed. These preliminary data permit the computation of the flows to be expected in the turbopump if this particular labyrinth design is used (Figure XI-11). Comparing the predicted oxidizer pump leakage of 143.7 gal/min with the previously estimated leakage of 121 gal/min (Ref Figure VI-7, Report TR-66-82) shows a difference of 19%. The total fuel-pump leakage with the thrust balancer near the null position has been estimated previously to be 143 gal/min (Ref Figure VI-12, Report TR-66-82); the value of 154.4 gal/min of Figure IX-11 correlates within 8%.

(u) The estimated oxidizer-pump leakage of 121 gal/min is for a labyrinth design with seven teeth, instead of six as in the test hardware. This explains most of the difference in oxidizer leakages. The rest of this difference, and the difference between the estimated fuel-pump leakage and the test-data-correlated leakage (143 versus 154.4 gal/min), can probably be explained by a

UNCLASSIFIED

Report 10830-Q-4

IX, D, Testing (cont.)

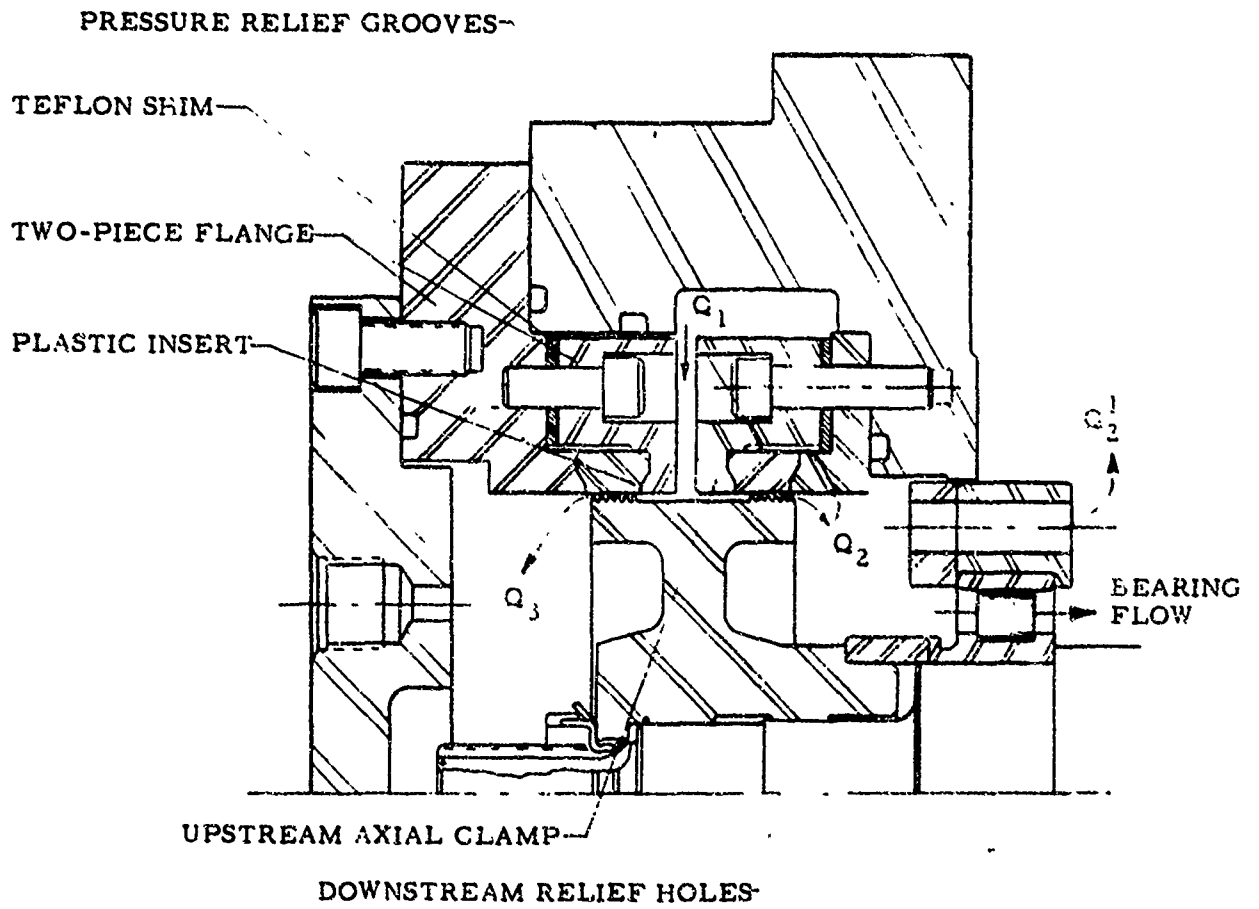
deviation from the flow coefficient originally assumed for the leakage calculations. No absolute flow coefficient value was known during the labyrinth design-and-analysis period. The assumed coefficient deviated by less than 10% from the measured test data. It may be concluded from this correlation that the leakage expected with this labyrinth design will not significantly change the pump efficiencies used in the cycle analysis (Ref Figure VI-7 of Report TR-66-82).

(u) Concept-screening testing in the Hydrolab is expected to be completed late in July, at which time testing in AercZINE 50 will be initiated.

UNCLASSIFIED

UNCLASSIFIED

Report 10830-Q-4



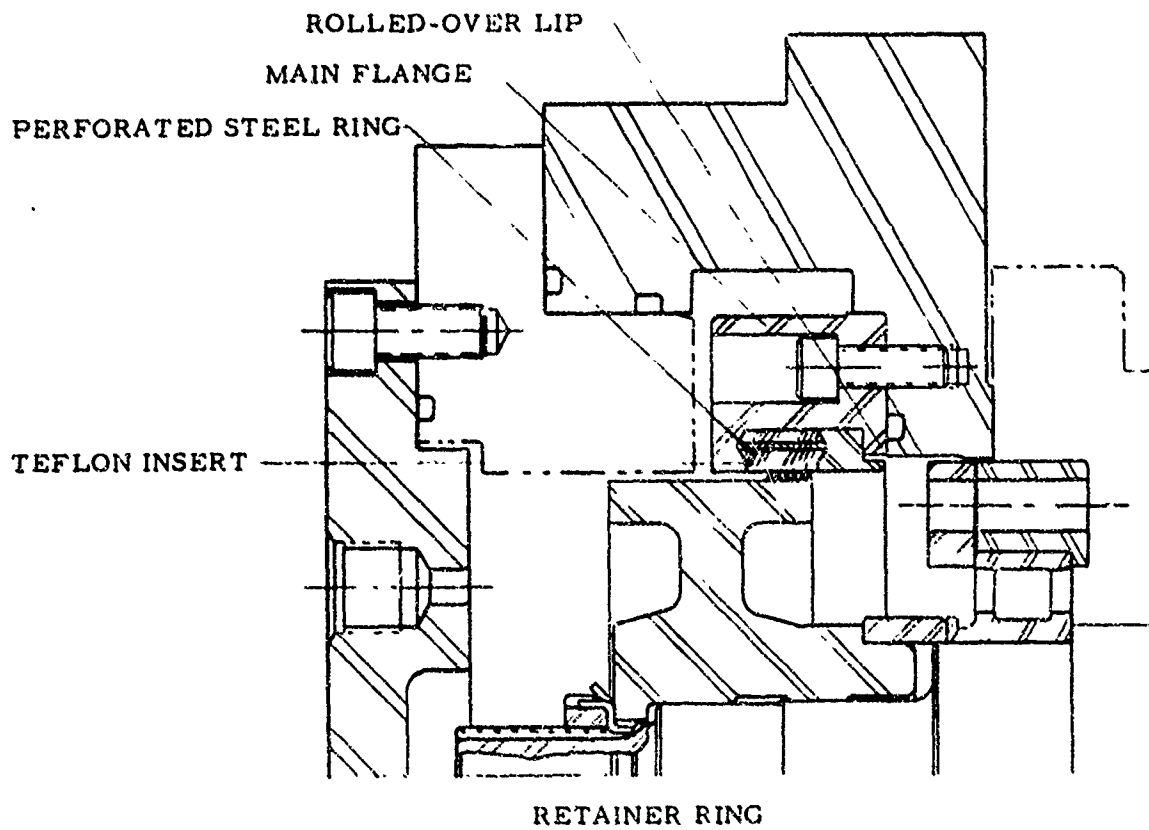
Dovetail Insert for Impeller Wear Rings

Figure IX-1

UNCLASSIFIED

UNCLASSIFIED

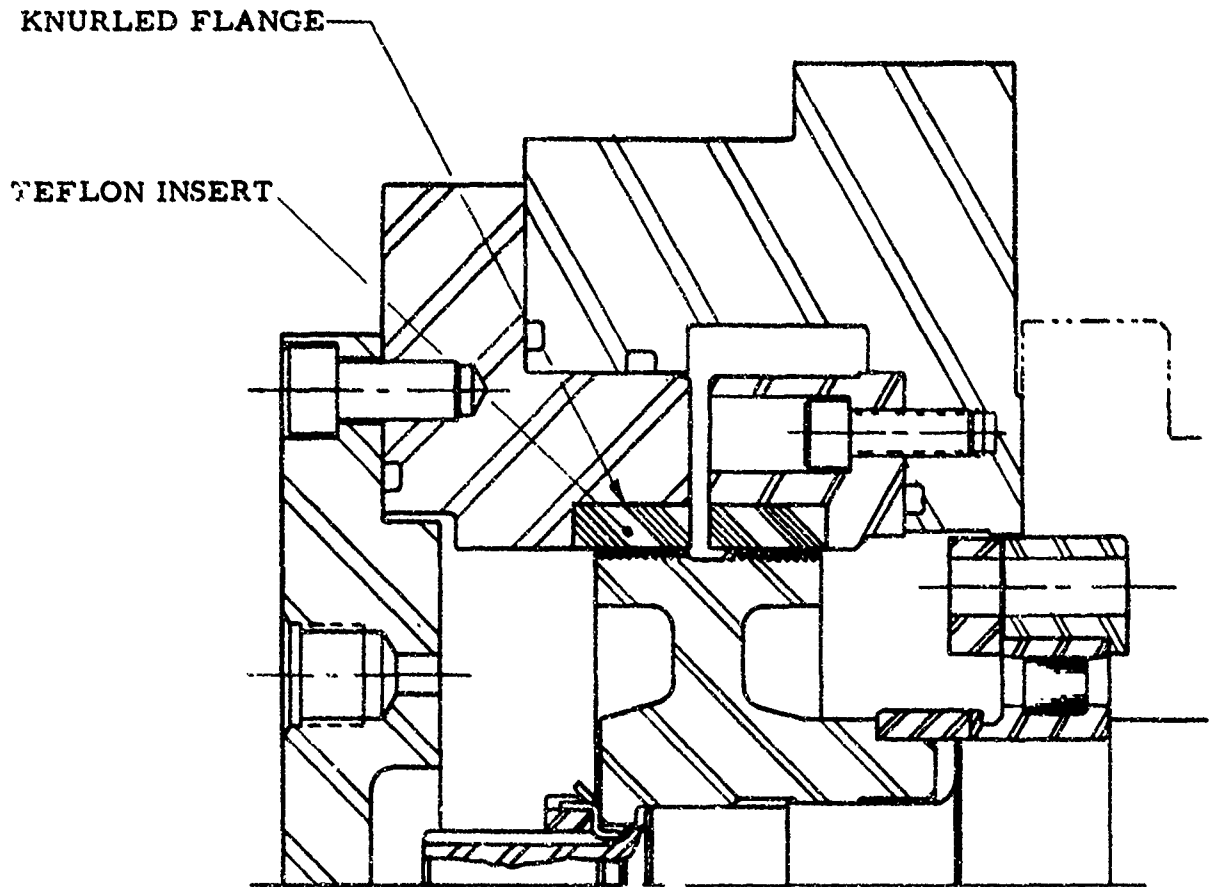
Report 10830-Q-4



Reinforced Dovetail Insert for Impeller Wear Rings

Figure IX-2

UNCLASSIFIED

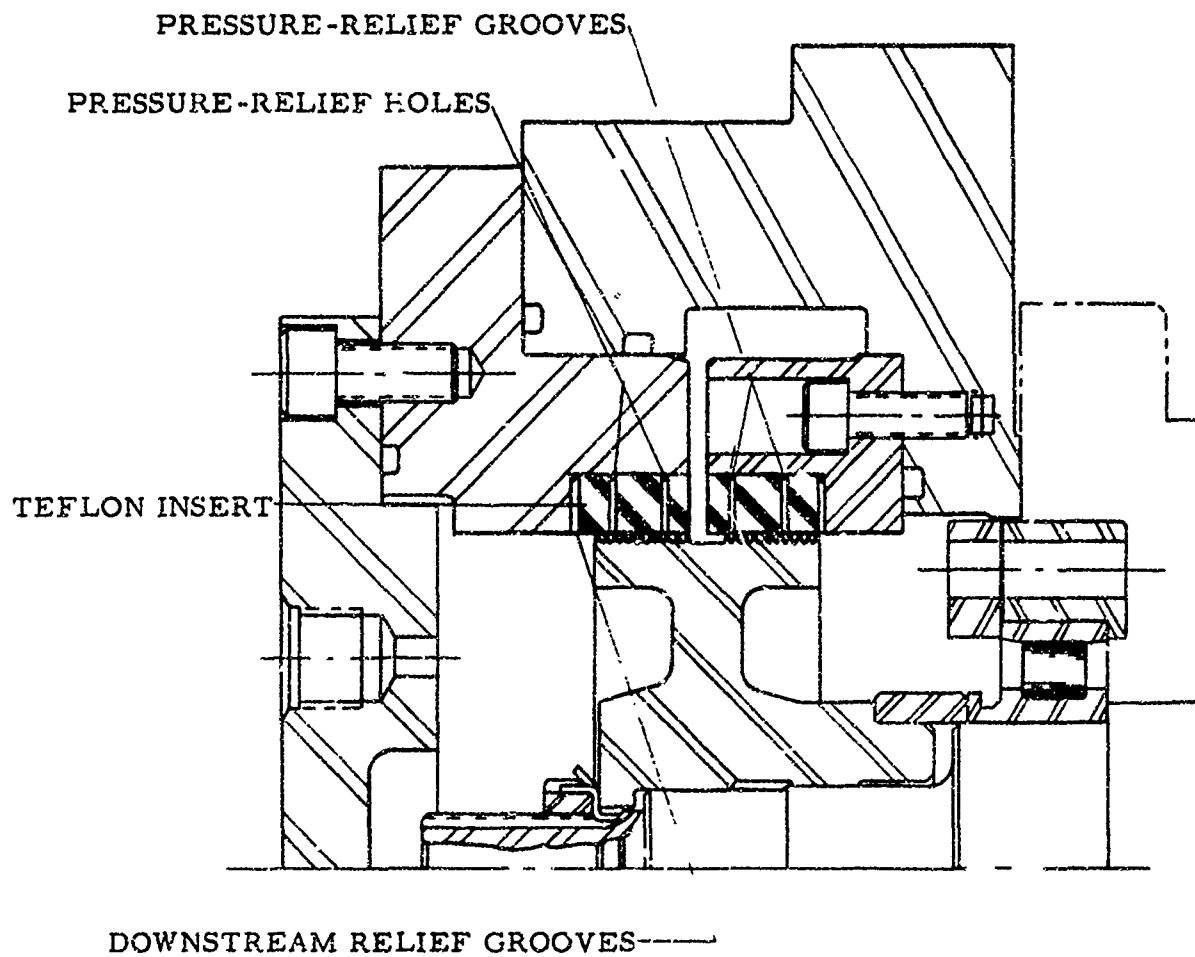


Knurled Insert for Impeller Wear Rings

Figure 1X-3

UNCLASSIFIED

Report 10830-Q-4



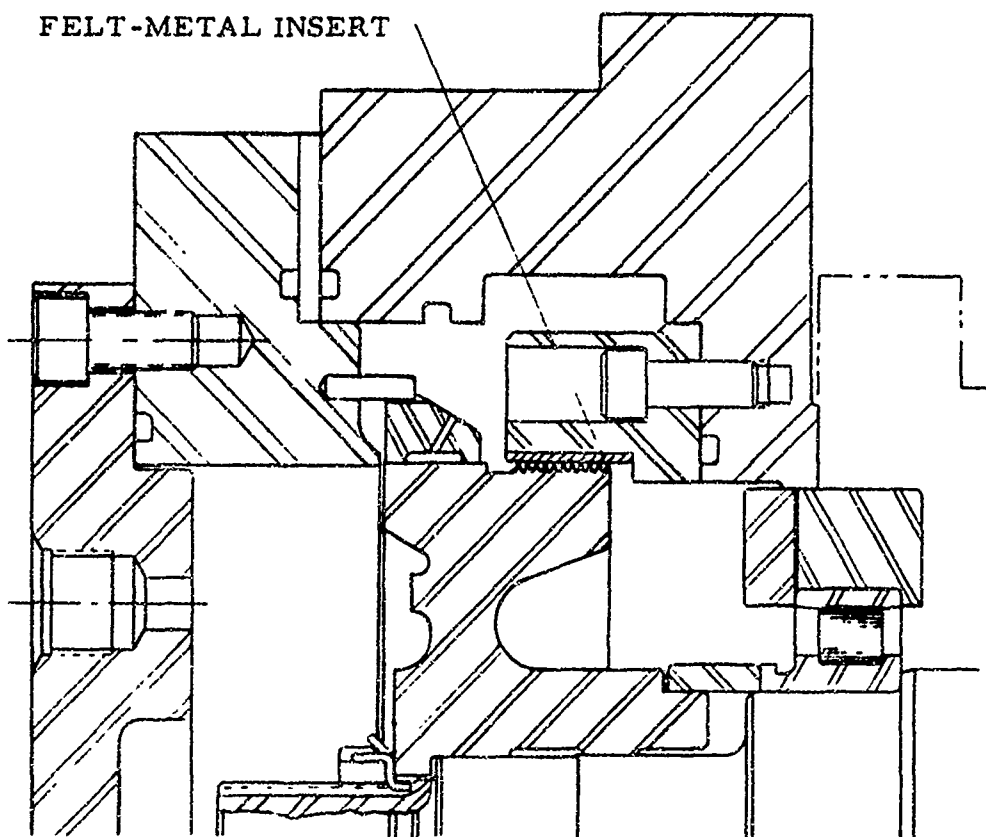
Pressure-Relieved Insert for Impeller Wear Rings

Figure IX-4

UNCLASSIFIED

UNCLASSIFIED

Report 10830-Q-4



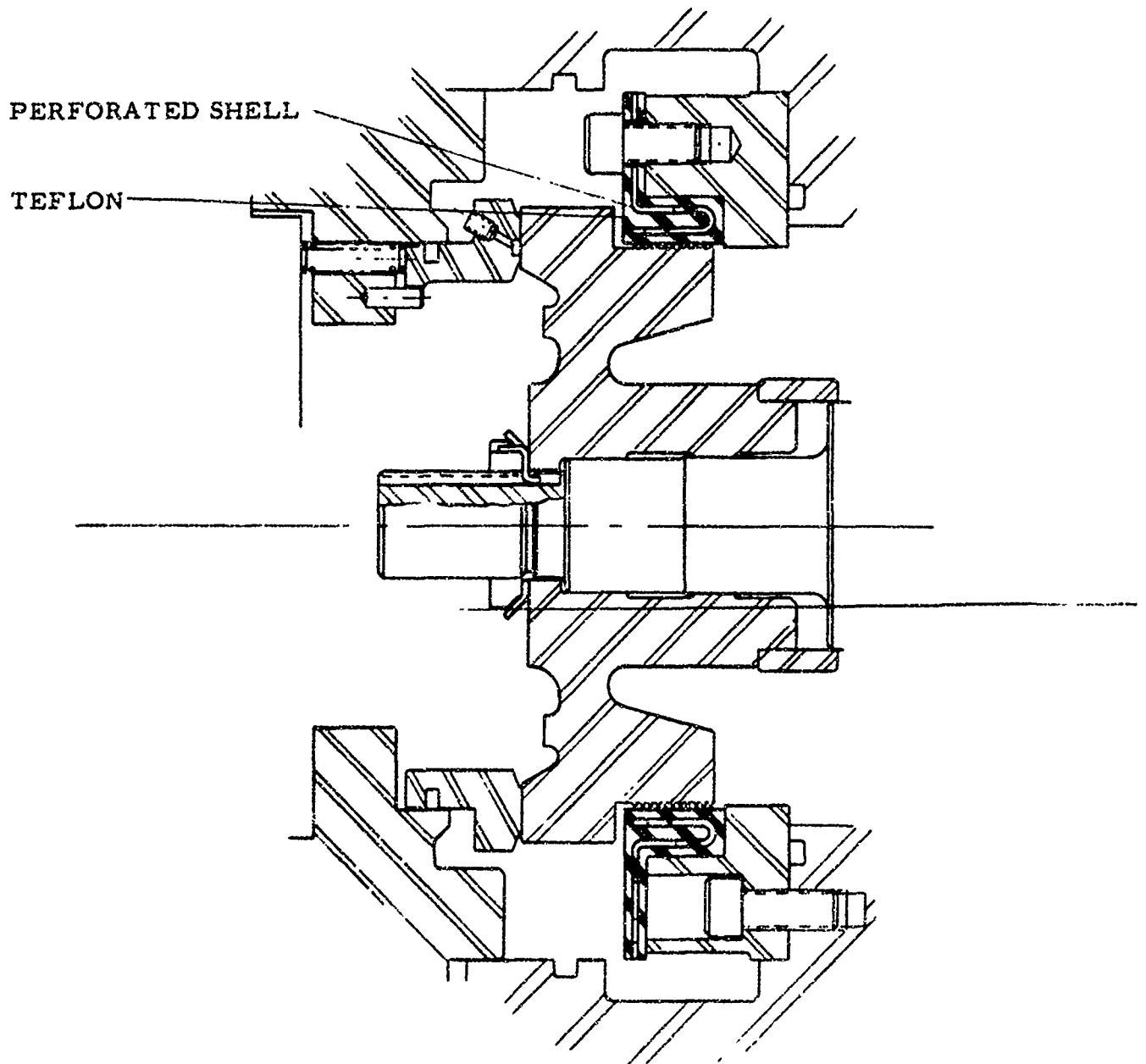
Felt-Metal Insert for Impeller Wear Ring

Figure IX-5

UNCLASSIFIED

UNCLASSIFIED

Report 10830-Q-4



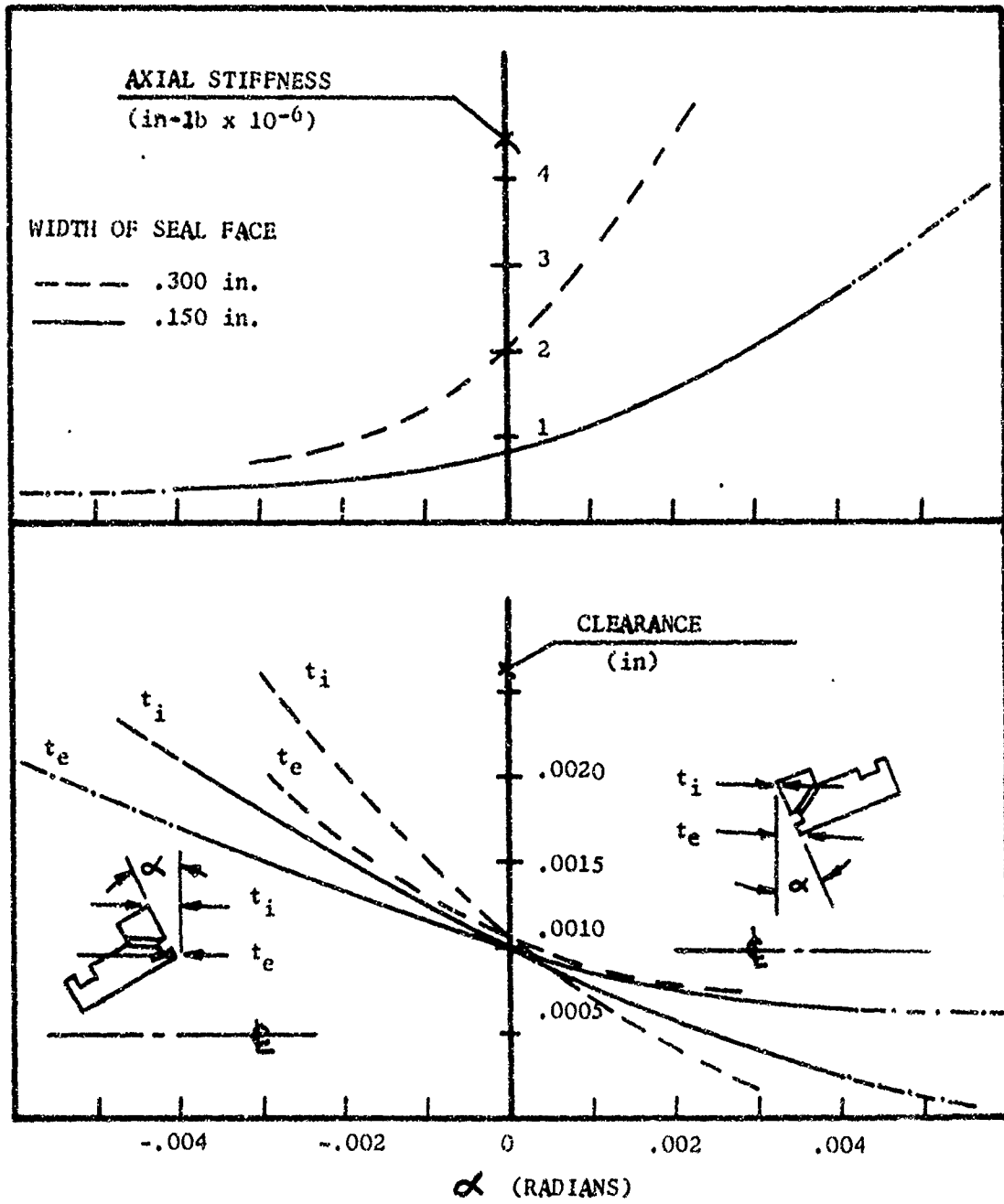
Shell-Reinforced Insert for Impeller Wear Ring

Figure IX-6

UNCLASSIFIED

UNCLASSIFIED

Report 10830-Q-4



Hydrostatic Face-Seal Stiffness and Clearance vs Impeller Angular Deflections

Figure IX-7

UNCLASSIFIED

UNCLASSIFIED

Report 10830-Q-4

TEST NO.	P ₁ ' PSI	P ₃ ' PSI	P ₂ ' PSI	N, RPM	Q ₁ ' GPM	Q ₃ ' GPM	Q ₂ ' GPM	Q ₂ ' GPM	BEARING FLOW, GPM	REMARKS
1	2440	88	53	0	94.6	55.2	39.4	NA	NA	STEPPED LABYRINTHS; OUTBOARD AND INBOARD AXIAL CLEARANCE, 0.056 IN. OUTBOARD DIAMETRAL CLEARANCE 0.020 IN. ZERO-SPEED TEST, Q ₂ NOT MONITORED. INBOARD DIAMETRAL CLEARANCE, 0.011 IN.
2	2355	86	46	0	99.0	63.6	35.4	33.3	2.1	SAME AS TEST 1, EXCEPT THAT OUTBOARD AXIAL CLEARANCE IS 0.022 IN. AND INBOARD AXIAL CLEARANCE IS 0.012 IN.
3	2444	89.7	53.0	0	87.0	44.5	42.5	37.7	4.8	STRAIGHT LABYRINTHS, SIX-TEETH/LABYRINTH, 0.056-IN. PITCH; DOVETAIL RETAINED INSERTS, VESPEL SP-1 OUTBOARD, TEC FLUORFIL BF3 INBOARD; OUTBOARD DIAMETRAL CLEARANCE, 0.069 IN.; INBOARD DIAMETRAL CLEARANCE, 0.019 IN.; NEGATIVE BEARING FLOWS ARE DUE TO GN, CONTAMINATING Q ₂ , AND/OR DATA-REDUCTION ERRORS.
	2444	84.5	62.2	10,000	86.4	46.4	40.0	37.7	2.3	
	2444	79.3	67.7	14,860	84.	45.8	38.2	38.5	-0.3	
	2444	39.7	73.7	27,220	73.5	37.1	36.5	37.9	-1.2	
4	2475	150	112	0	82.5	40.8	41.7	35.9	5.8	SAME AS TEST 3 EXCEPT P ₁ AND P ₃ ARE INCREASED TO MAINTAIN HIGHER BEARING FLOWS AT SPEED.
	2460	120	114	15,000	78.0	38.1	39.9	34.5	5.4	
	2425	143	112	0	82.5	40.3	42.2	35.0	7.2	
	2450	120	117	25,370	71.4	35.8	35.6	33.0	2.6	
	2450	142	130	0	82.5	40.3	42.2	35.3	6.9	
	2475	90	125	29,400	71.4	38.1	33.3	32.1	1.2	
	2375	178	185	29,280	95.8	47.0	48.8	41.6	7.2	
	2500	90	105	29,640	66.9	38.1	28.8	30.2	-1.4	
	2475	150	90	0	78.0	41.5	36.5	30.2	6.3	

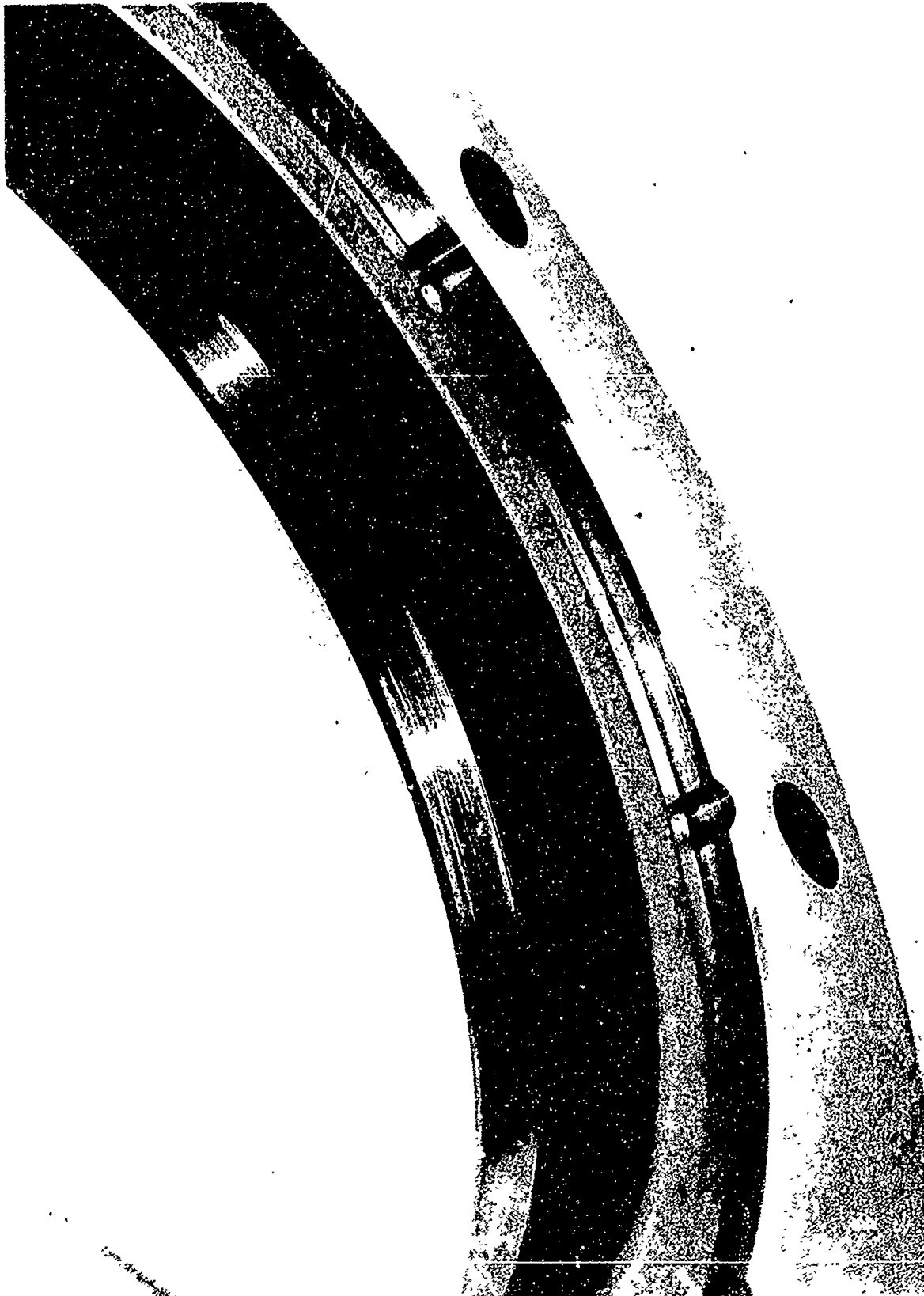
- Tabulation of Steady-State Hydrostatic Test Data Points

Figure IX-8

UNCLASSIFIED

UNCLASSIFIED

Report 10830-Q-4

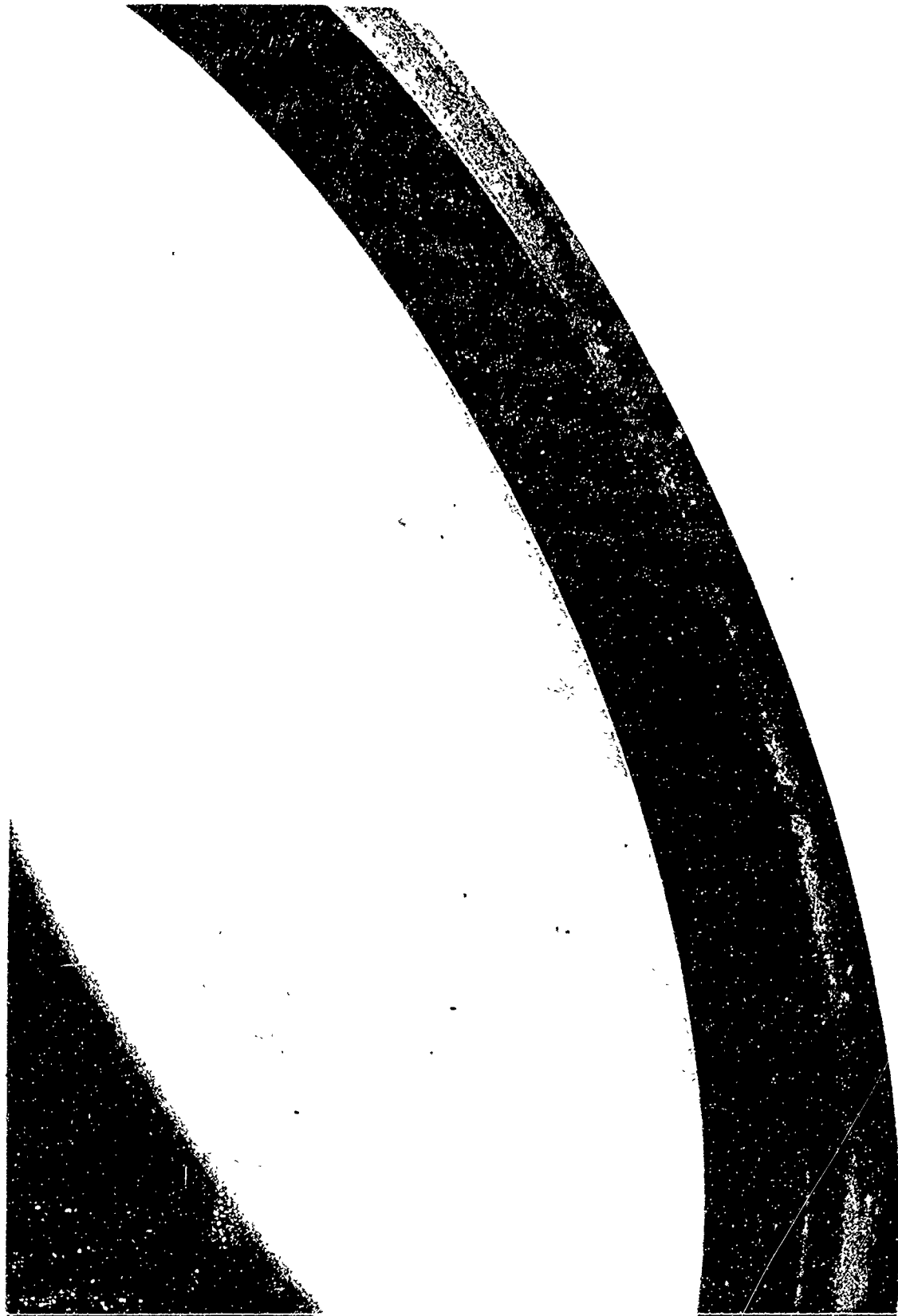


Vespe1 SP-1 Insert in Flange after Rubbing Hydrostatic Test 4

Figure IX-9

UNCLASSIFIED

UNCLASSIFIED
Report 10830-Q-4



TEC Fluorfil BF₃ Insert after Rubbing Hydrostatic Test 4

Figure IX-10
UNCLASSIFIED

UNCLASSIFIED

Report 10830-Q-4

CASE NO.	SEAL LOCATION	DIAMETRAL CLEARANCE, IN.	SEAL MEAN DIAMETER, IN.	DIFF. PRESSURE, PSI	FLUID DENSITY, LB/IN. ³	FLOW RATE, GPM	REMARKS
1	HYDROTEST, OUTBOARD*	0.009	3.592	2308	0.0361	40.3	DATA FROM OUTBOARD SEAL, TEST 4 (6/21/66)
2	OXIDIZER PUMP, INBOARD	0.014	4.000	3443	0.052	71.0	
3	OXIDIZER PUMP, OUTBOARD	0.014	4.000	3623	0.052	72.7	
143.7 DURING RUBBING CONDITIONS THIS FLOW MAY INCREASE TO ABOUT 170 GPM							
4	FUEL PUMP, INBOARD	0.014	4.720	1757	0.0325	75.0	
5	FUEL PUMP, OUTBOARD	0.014	4.720	1907	0.0325	76.8	
154.4 DURING RUBBING CONDITIONS THIS FLOW MAY INCREASE TO ABOUT 180 GPM							

* SIX-TOOTH STRAIGHT LABYRINTH OF 0.050-IN. PITCH

Pump Leakage Rates Based upon Preliminary Test Data of Hydrostatic Test 4

Figure IX-11

UNCLASSIFIED

CONFIDENTIAL

Report 10830-Q-4

X.

TPA SEAL DEVELOPMENT

A. GENERAL

1. Background

(c) The ARES T-engine will require a rotating shaft seal between the fuel pump and the oxidizer-rich gas. This sealing will be accomplished by either (a) a hydrostatic seal in which fuel acts as the operating fluid, with out-flow entering and combusting in the oxidizer-rich turbine exhaust gas, or (b) a hydrostatic seal in which an inert purge fluid is introduced to separate the fuel from the oxidizer.

(u) Previous work completed on Contract AF 04(611)-10784, "Hydrostatic Combustion Seal Feasibility Demonstration Program," included the design of a hydrostatic combustion seal and test equipment, feasibility demonstrations of the seal while rotating in water, and combustion tests of a thin, representative cross-section of the seal (2D tests). This work was satisfactorily completed and is described in Final Report AFRPL-TR-66-79.

2. Objectives

(u) The Phase-I portion of the ARES program requires a 60-sec demonstration of both a hydrostatic combustion seal and a purge seal while operating at 40,000 rpm under temperatures and pressures simulating those expected in the ARES engine.

3. Test Program

(u) The following test series have been planned to attain the program objectives:

a. Additional 2D tests, in which combustion is further examined with the modified cross-section of the seal developed on Air Force Contract AF 04(611)-10784, but with a clearance of 0.001 in.

b. Preburner checkout, completed during the previous quarter.

c. Cold rotating tests to 40,000 rpm, wherein the seal-fuel flows and the tester operating characteristics are evaluated while using fuel only, without combustion.

CONFIDENTIAL

CONFIDENTIAL

Report 10830-Q-4

X, A, General (cont.)

d. Hot rotating combustion tests, in which the combustion-seal objective is to be reached.

c. Purge-seal tests, which will evaluate operation, while cold, hot, static, and rotating. These tests will culminate in the demonstration of the purge-seal program objective.

4. Summary of Work Completed

(u) Work during this quarter included:

a. Completion of the 2D test program.

b. Completion of the cold-rotating hydrostatic-seal tests.

c. Design, fabrication, and testing of a modified hydrostatic combustion-seal bellows.

d. Selection of a purge fluid and the design of pressurizing equipment for purge-seal testing.

B. HYDROSTATIC COMBUSTION SEAL

1. 2D Tests

(u) The 2D test series, completed during this quarter, were an extension to the tests conducted under Contract AF 04(611)-10784.

a. Description of Hardware

(u) The tester (described in detail in Report AFRPL-TR-66-79, Figure III-1) was designed to produce oxidizer-rich gas at conditions simulating the ARPS engine, except that facility limitations restricted the operating pressure to 1000 psi. Combustion in the seal test zone was observed by closed-circuit television and photographed through a quartz window in the side of the tester.

(u) The test segment (Figure X-1) duplicated the cross section of the hydrostatic combustion seal at the point of fuel introduction. Temperatures were monitored at a point 0.1 in. below the surface and 0.1 in. upstream of the fuel inlet, and also at two points along the downstream ramp. Formation of a 0.001-in.-thick slot was successfully accomplished by fabricating the seal in two parts, using a 0.001-in.-thick shim to separate the parts at the required gap. The parts were gold-brazed in a vacuum furnace.

Page X-2

(This page is Unclassified)

CONFIDENTIAL

UNCLASSIFIED

Report 10830-Q-4

X, B, Hydrostatic Combustion Seal (cont.)

b. Description of Tests

(u) The tester was installed in accordance with the flow diagram shown in Figure IV-23 of Report AFRPL-TR-66-79. A total of 11 seal-segment tests were attempted during eight firings. A summary of these tests is shown in Figure X-2. During the first three firings, two segments were tested simultaneously but, because of technical difficulties with the bottom segments, it was decided that more expeditious testing could be accomplished by eliminating the bottom segments in the later tests. Two segments were tested for total durations of 8.3 and 40.5 sec, respectively. No damage occurred to any test hardware, as evidenced by Figure X-3.

(u) An inert purge fluid was initially used for filling the fuel-segment tubing to reduce the possibility of interpropellant contamination. Because of the time required to expel this fluid at the close clearances, it was necessary to extend the duration of the tests. A significant development during the last three tests was the introduction of fuel to the segment before the preburner was activated. During the engine startup transient, fuel at low pressure may leak from the seal prior to precombustor ignition, which poses the possibility of damage to hardware during this time. However, the 2D test results show that there will be no hardware damage if the fuel and oxidizer flows to the seal precede combustor ignition.

c. Test Results

(u) During 2D testing, the flow of fuel to the test segment was to be representative of the reduced seal flow rate. This resulted in a lower fuel flow rate through a smaller slot than had been accomplished during the 2D tests on Contract AF 04(611)-10784. Examination of test data revealed that the seal-segment fuel-circuit pressure-drop increased markedly within about 1.5 sec after stable preburner combustion had been attained, reducing fuel flow to about one-third of the nominal value. The added restriction was not permanent, and occurred only during preburner operation. Figure X-4 presents plots of pertinent data from Test 30, in which a typical flow restriction developed. An examination of possible causes led to the conclusion that this flow restriction had been caused by surface thermal expansion. This condition will be less aggravated on the hydrostatic seal since this seal can automatically adjust its average clearance.

(u) Temperatures 0.1 in. below the surface of the upstream half of the segment rose steadily during all tests, but surface temperatures along the downstream ramp were less than 200°F. These data are plotted in Figure X-5.

UNCLASSIFIED

Report 10830-Q-4

X, B, Hydrostatic Combustion Seal (cont.)

(u) The 2D test program led to the following observations:

a. It is not necessary to reduce fuel flow to the lowest possible value to protect downstream hardware.

b. Mixture ratios in the range of 10 to 20:1 appear to be acceptable.

c. Average axial seal operating clearances of about 0.001 in. appear to be practical. If the initial seal operating clearance is reduced to lesser values, the seal distortion due to temperature of the rotating portion may cause rubbing. If the initial seal clearance is increased to more than 0.0015 in., the fuel flow rate will be excessive.

d. Additional oxidizer cooling and shielding of the rotating ring should be investigated. Such investigations are presently under way.

2. Cold Rotating Tests in AeroZINE 50

(u) A total of 12 tests were attempted to complete the cold rotating testing. The objectives of these tests were:

a. Determination of fuel fill time at 60 psi.

b. Determination of the drive-turbine gas pressure necessary to rotate the tester at 40,000 rpm.

c. Tester component evaluation.

d. Determination of tester acceleration and deceleration rates.

e. Determination of fuel flow from the seal at operating speed for two axial clearances and two seal-to-gas operating pressure differentials.

f. Test installation checkout and evaluation.

(u) The tester shown in Figure X-6 was used for the cold test series. The same tester will be used for hot tests, except that the internal shielding and the velocity-control equipment were removed for the cold tests.

CONFIDENTIAL
Report 10830-Q-4

X, B, Hydrostatic Combustion Seal (cont.)

(u) The test seal is shown in Figure X-7. Essentially the same seal will be used in hot testing. For hot testing, a burnoff shield will be added and the rotating face will be designed for upstream oxidizer admission.

(u) The tester was installed in accordance with Figure X-8. Pertinent test data from the hydrostatic seal testing are tabulated in Figure X-9.

(u) Two nonrotating tests were conducted to establish fuel flow rates and fill times. These tests were made during the third quarter, and are described in the last quarterly report.

(u) The first cold-rotating test attempt failed when a bearing thermocouple was forced from its housing at 3000 psi. The AeroZINE 50 escaping to the atmosphere through this opening ignited and destroyed exterior instrumentation wiring. During shutdown, the seal bellows was subjected to external overpressure and consequently collapsed. A malfunction during the next test caused overpressurization of the chamber and, during shutdown, a bellows was again destroyed by a pressure reversal.

(c) The test head was removed for the next three tests while a technique was developed which would prevent a pressure reversal on the bellows. The following pressurizing procedure was finally developed:

- a. Seal fuel-supply pressure was set at 200 psi.
- b. Chamber gas pressurization was initiated by opening a valve, and the computer which controlled the fuel-intensifier pressure immediately increased seal-fuel pressure to 500 psi.
- c. The computer, responding to the chamber pressure, increased the intensifier pressure at a ratio of 51:31 until chamber pressure reached 3100 psi and seal supply pressure reached 5600 psi.
- d. Shutdown was likewise controlled in the reverse order.

(u) Five attempts were then made with a rotating seal. All attempts were aborted because of various system malfunctions. Partial success was obtained on Tests-007 and 010B where shutdown occurred before the desired rotation was reached. Damage to the test seal occurred in Test-008 when the valve that internally pressurized the seal failed to open. The lack of internal pressure caused the seal to contact the rotating face for 4 sec at 28,000 rpm. The seal faces consequently welded together, causing an abrupt loss in speed. During disassembly, the rotating face had to be cut from the seal face as shown in Figure X-10.

CONFIDENTIAL

Report 10830-Q-4

X, B, Hydrostatic Combustion Seal (cont.)

(u) The first successful rotating test (Test 011) achieved a total rotating-time of 84 sec, 60 sec of which were at a speed above 38,000 rpm. All test parameters were met except speed, which was 2-1/2% low. Seal external flow was 0.27 lb/sec, which resulted in an operating clearance of 0.00076 in. Data from this test are plotted in Figure X-11. To reduce fuel flow to a minimum, this seal was designed for a pocket-to-chamber pressure of 200 psi instead of the original 500 psi. One 0.025-in. orifice was used in each seal pocket. Axial runout of the rotating face was 0.0004 in. This is the closest clearance and the least fuel flow that will be considered for the hydrostatic combustion seal. The seal was installed with 0.019 in. axial compression-- the expected installed compression in the ARES engine. There was no damage to the test hardware and no evidence of seal-face contact, as evidenced by the excellent condition of the seal shown in Figure X-12.

(u) Turbine power was insufficient to reach the desired speed of 40,000 rpm. The highest speed was 39,400 rpm and average speed about 39,000 rpm. The turbine nozzle diameters were therefore increased from 0.269 to 0.300 in. to increase gas flow for the last test of the series. The seal used for a pocket-to-chamber differential pressure of 500 psi was installed for the final test of the series, and two 0.030-in.-dia orifices were used for each seal pocket. This was done to increase seal-face clearance to 0.001 in. in anticipation of warpage that might occur in future hot tests. Axial runout of the rotating face was 0.0005 in. Bellows compression was 0.020 in.

(u) The procedure followed in Test-012 was identical to that of Test-011. All objectives were met; seal fuel flow was 0.43 lb/sec and speed was 40,000 rpm. Total rotating time was 78 sec, with a duration of 63 sec at 40,000 rpm. Surface velocity was about 600 ft/sec and the pressure on the installed face was 19.5 psi. The test results are plotted in Figure X-13. There was no evidence of seal contact and no damage, as evidenced by the excellent posttest appearance of the hardware (Figure X-14).

(u) The following conclusions may be reached from the cold rotating tests:

a. Seal operation at fuel flows to combustion from 0.27 up to 0.43 lb/sec has been demonstrated. This covers the expected range of operating clearances and ΔP .

b. Axial wobble of 0.0004 in. at operating speeds can be accommodated with an average clearance of 0.00076 in.

CONFIDENTIAL

Report 10830-Q-4

X, B, Hydrostatic Combustion Seal (cont.)

c. The tester components have been checked-out at specified operating speeds and pressures for the desired duration of 60-sec tests.

d. Fill times, turbine gas pressures, acceleration and deceleration rates, and pressure drops have been established.

3. Hot Rotating Tests

(u) Various components were modified in preparation for the hot rotating tests.

(u) The seal was redesigned to optimize heat transfer to the burnoff shield downstream of the seal by providing an annulus approximately 0.018 in. thick below the shield surface (Figure X-15). Oxidizer, flowing in this annulus at a velocity of 50 ft/sec will improve the cooling at that point.

(u) The original rotating face was designed to be screwed onto the shaft to prevent interpropellant leakage. This made it impossible to lock the ring to the shaft. Additionally, it was impossible to attain the desired interference fit to offset expansion caused by centrifugal force. The rotating face was therefore redesigned (Figure X-15) so that the face is shrunk on the shaft and held by a nut, which is locked to the shaft with a key. A cover plate retains the key and also seals against leakage. As a further precaution against leakage, the interior is filled with RTV potting compound during assembly.

(u) A circulation ring (Figure X-15) has been designed to fit within the seal test chamber and serves to improve gas circulation within the test head.

(u) Computer studies of seal-tester performance during combustion indicated the possibility of pressure instability between the preburner and the test housing. To prevent flow reversal, the preburner will operate at a pressure about 1000 psi higher than that in the test housing. This will be accomplished by installing six nozzles in the gas-diffuser flange at the junction of the preburner and the test housing.

4. Special Problems

(u) The connection between the bellows and the seal has been redesigned to increase the reliability of the bellows in case of pressure reversal. Instead of being welded along the opposing faces of the seal components, the bellows attachment point has been moved to the inside circumference of the seal and the flange (Figure X-16). This will facilitate weld inspection and will increase the resistance to external pressurization by about 400%. The new bellows design was tested in cold rotating Test 012.

Page X-7

(This page is Unclassified)

CONFIDENTIAL

CONFIDENTIAL

Report 10830-Q-4

X, B, Hydrostatic Combustion Seal (cont.)

(u) The strength of the bellows will be further increased by fabricating the bellows from two 0.006-in.-thick plies of Inconel 718 (Figure X-16), thus providing redundant protection from bellows failure. For normal operation, the redesigned bellows will further increase resistance both to external and internal pressures by 100%. The net result of the two-ply bellows will therefore result in an eight-fold improvement in resistance to pressure reversal.

b. Effect of Low Internal Pressure

(c) Because the seal faces contacted and welded together during Test-008, the effect of low internal seal-cavity pressure on seal clearance was investigated to determine an allowable tolerance on the internal seal pressure. The plots shown in Figure X-17 indicate that reducing the internal pressure (P_3) tends to reduce the seal clearance. In Figure X-17, the clearance (t) is computed excluding the effect of seal distortion, and t_{min} is computed taking into account the distortion caused by a reduced P_3 . In cold rotating Test-008, a valve malfunction resulted in a P_3 of only 170 psi instead of 2800 to 3100 psi as intended. From Figure X-17, the minimum clearance corresponding to a P_3 of 170 psi is 0.00004 in. This extremely close clearance resulted in the rubbing and welding together of the seal faces during Test-008 at a shaft speed of 28,000 rpm.

(u) Figure X-18 is a plot of several seal parameters calculated from the theoretical TPA start transient. The plot indicates that the pressure differential between seal pocket (P_2) and inner cavity (P_3) does not exceed 700 psi during the start transient. During the start transient, the seal will therefore not be subjected to the conditions that caused the failure during Test-008.

c. PURGE SEAL

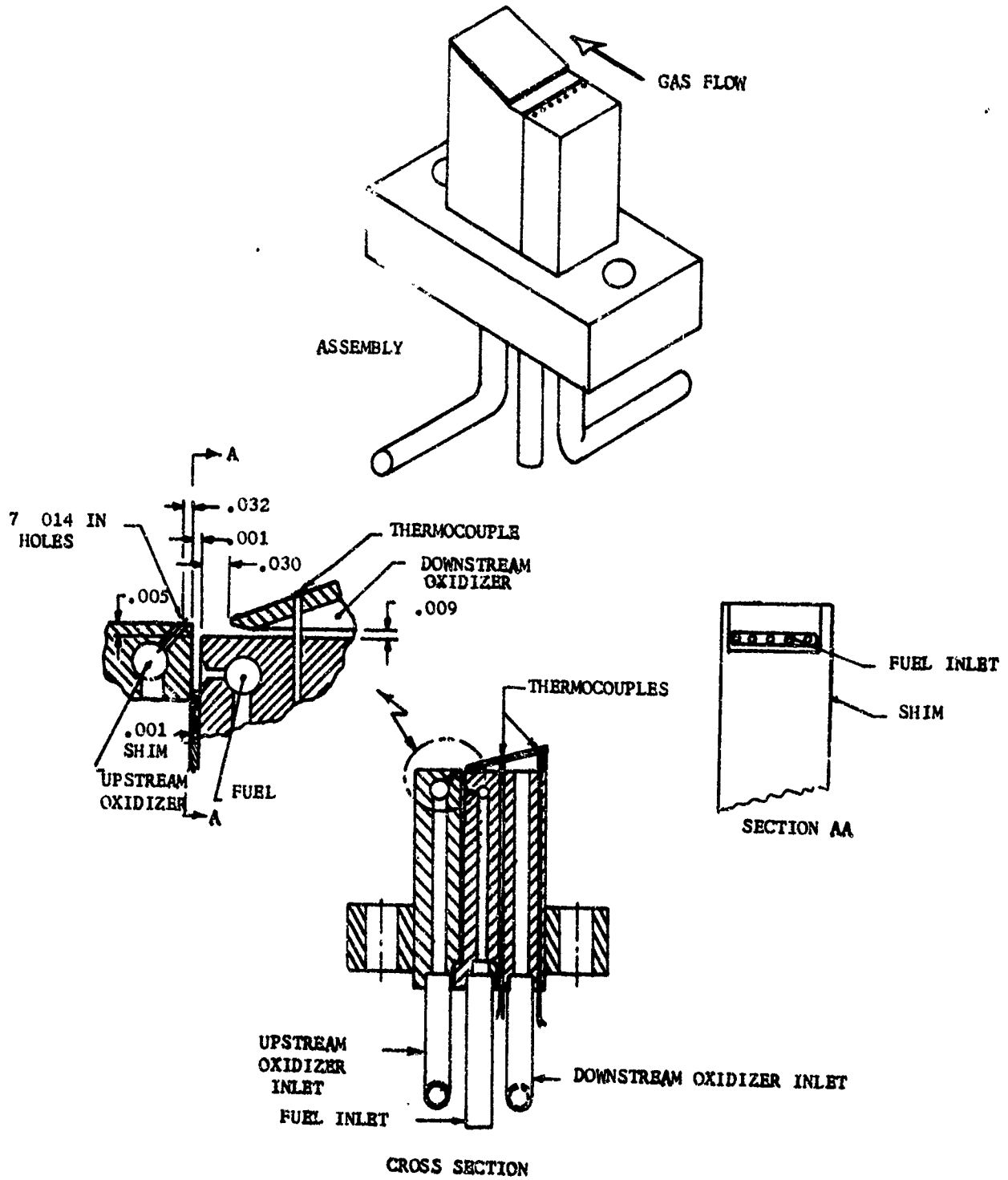
(u) The purge seal is being designed as an alternative to the hydrostatic combustion seal.

(u) Fabrication of all tester and seal parts is nearing completion. The purge fluid selected, is duPont PR-143AB, an inert material that meets the viscosity requirements of the purge seal.

(u) The pressurizing system will simulate anticipated APRES engine conditions. The fuel will pressurize one end of a vertical cylinder and a floating piston will pressurize the purge fluid on a 1:1 ratio. Fabrication of this pressure vessel has started.

UNCLASSIFIED

Report 10830-Q-4



2D Test Segment

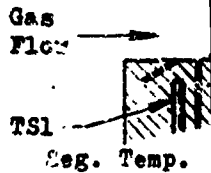
Figure X-1

UNCLASSIFIED

UNCLASSIFIED

Report 10830-Q-4

Test	Seal-Segment Type and Serial No.	Representative Full-Scale-Seal			Segment MR	Segment Duration Sec	Seg. Temp.	
		Fuel, A-50	Oxidizer, N ₂ O ₄				TS 1*** °F	TS 2**** °F
			Upstr.	Downstr.				
24	A-3, #1	-	1.75	3.50	-	1.7	273	122
25	"	-	0.89	3.71	-	1.6	220	121
26	"	-	0.93	2.22	-	1.6	246	160
27	A-3, #1	0.093	1.82	2.96	51.5	3.4	404	145
28	A-3, #3	0.218* 0.064**	1.78	2.21	18.3* 62.3**	1.5* 8.5**	200	150
29A	A-3, #3	0.267* 0.036**	1.82	2.07	14.6* 10.8**	1.2* 8.8**	220	145
29B	A-3, #3	0.268* 0.054**	1.82	2.32	15.4* 76.6**	1.0* 9.0**	360	170
30	A-3, #3	0.303* 0.089**	1.71	2.32	13.3* 45.3**	1.2* 8.8**	380	170

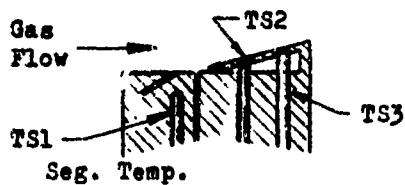


- *condition after preburner start before increase in fuel gap resistance.
- **condition after fuel gap resistance adjusted to a higher stable level.
- ***maximum reached at end of test - thermal steady state not reached.
- ****maximum reached during thermal steady state.

2D Test Summary

Figure X-2

UNCLASSIFIED



Seg. Temp.			Preburner Gas Conditions			Remarks
TS 2**** °F	TS 3**** °F	Press., psia	Temp. (Av), °F	Velocity ft/sec		
122	152	1000	1150	300	No apparent fuel flow at segment.	
121	151	995	1150	300		
160	200	990	1150	300		
145	169	995	1150	300	Intermittent fuel flow	
150	190	980	1130	300		
145	150	980	1130	300	Segment fired and visually noted approx. 2.5 sec prior to preburner start. Procedure previous to these tests was to lag segment start after preburner	
170	210	970	1130	300		
170	215	970	1130	300		

UNCLASSIFIED
Report 10830-Q-4

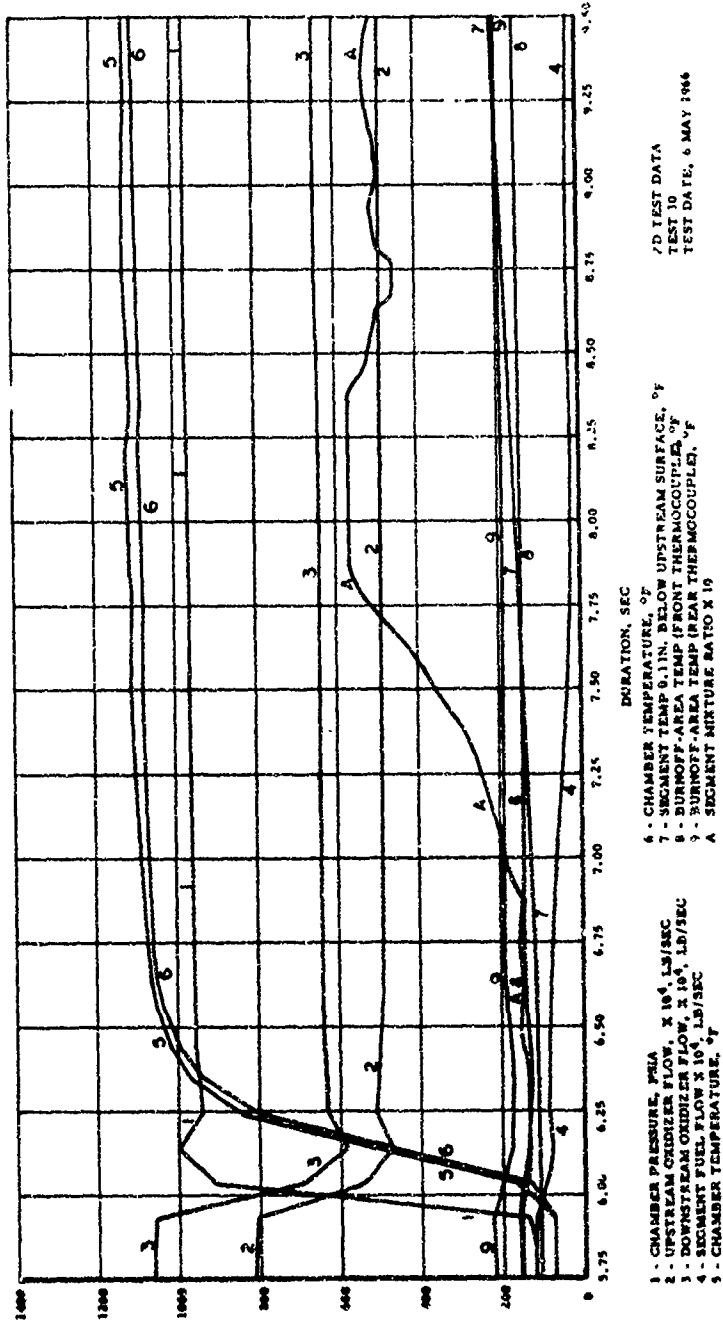


LEFT SEGMENT
0.3 SEC. TOTAL OPERATING TIME

RIGHT SEGMENT
40.5 SEC. TOTAL OPERATING TIME

2D Seal Segments after Testing

Figure X-3
UNCLASSIFIED

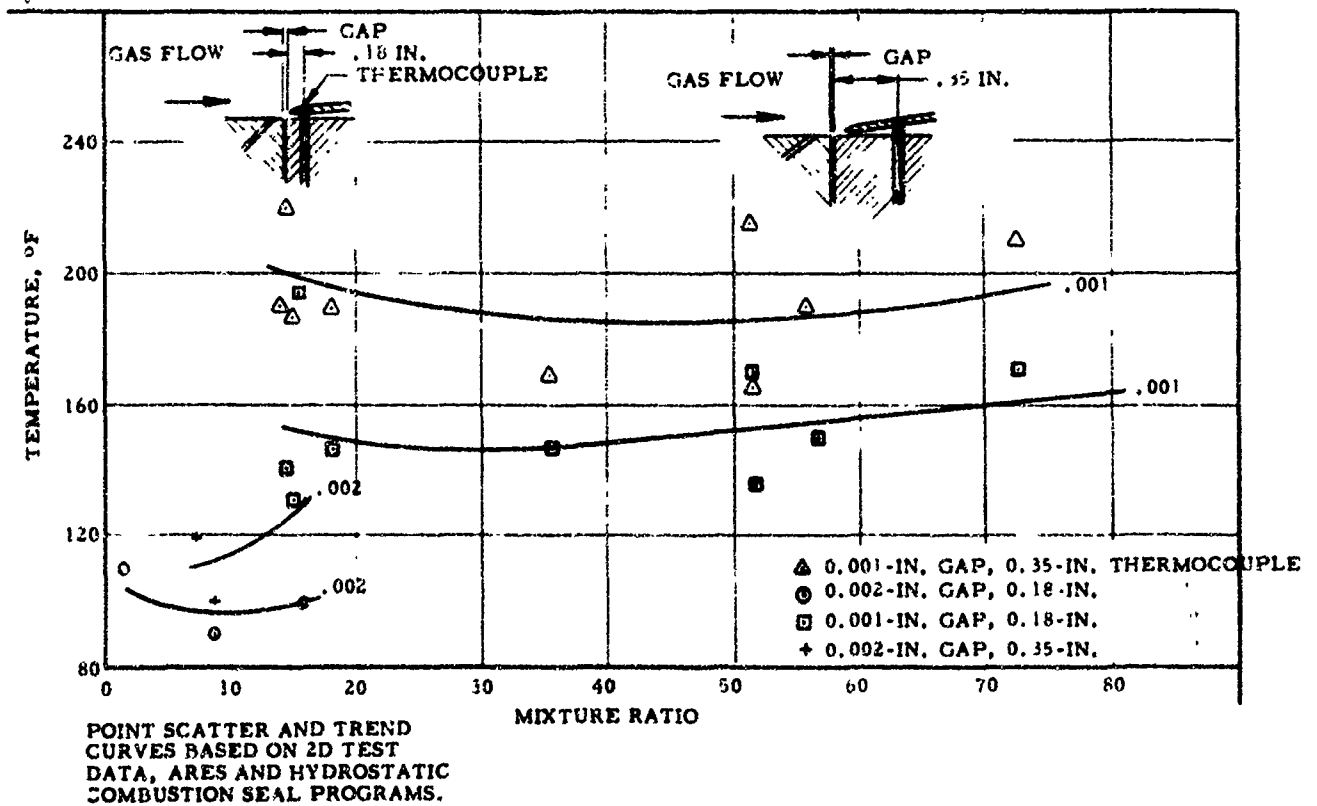
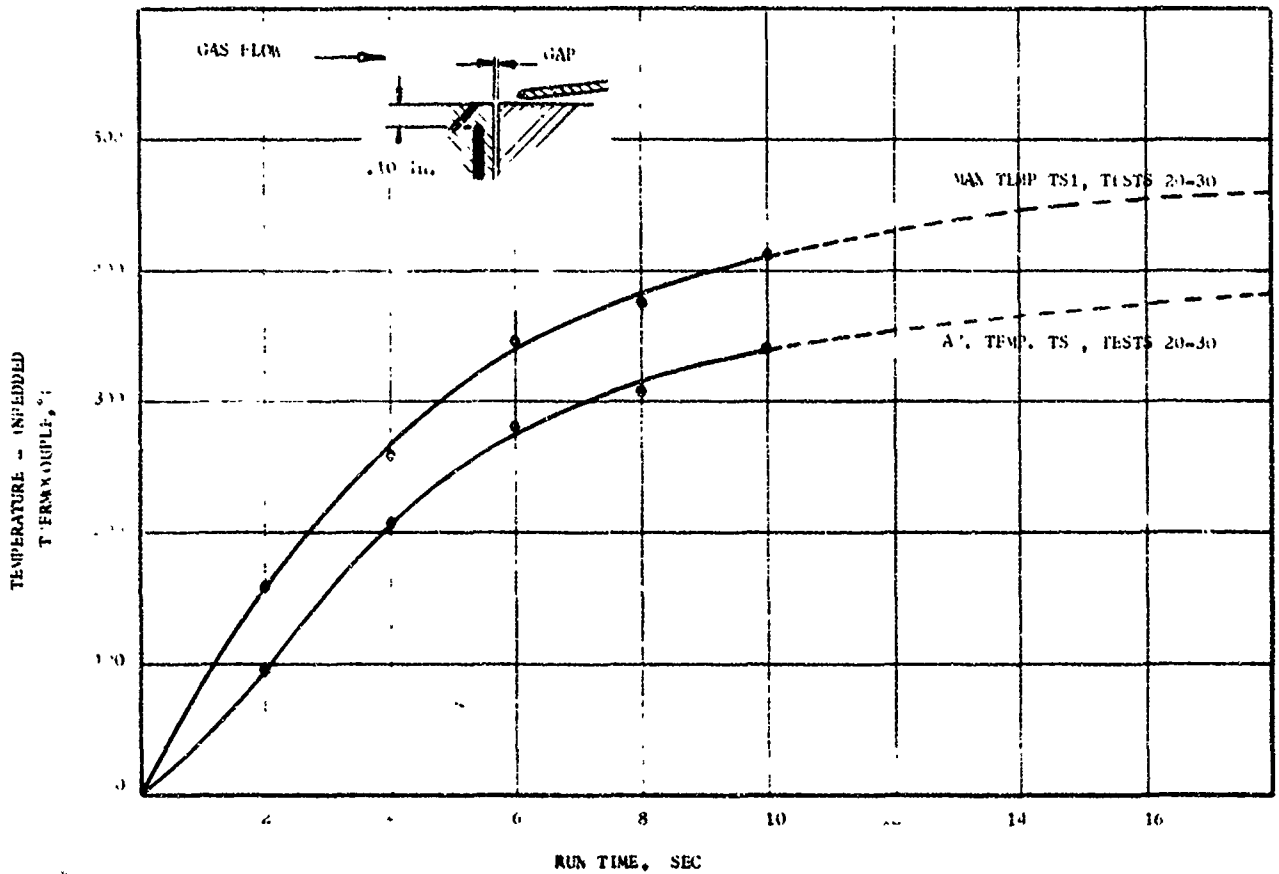


2D Test Data, Test 030

Figure X-4

UNCLASSIFIED

Report 10830-Q-4



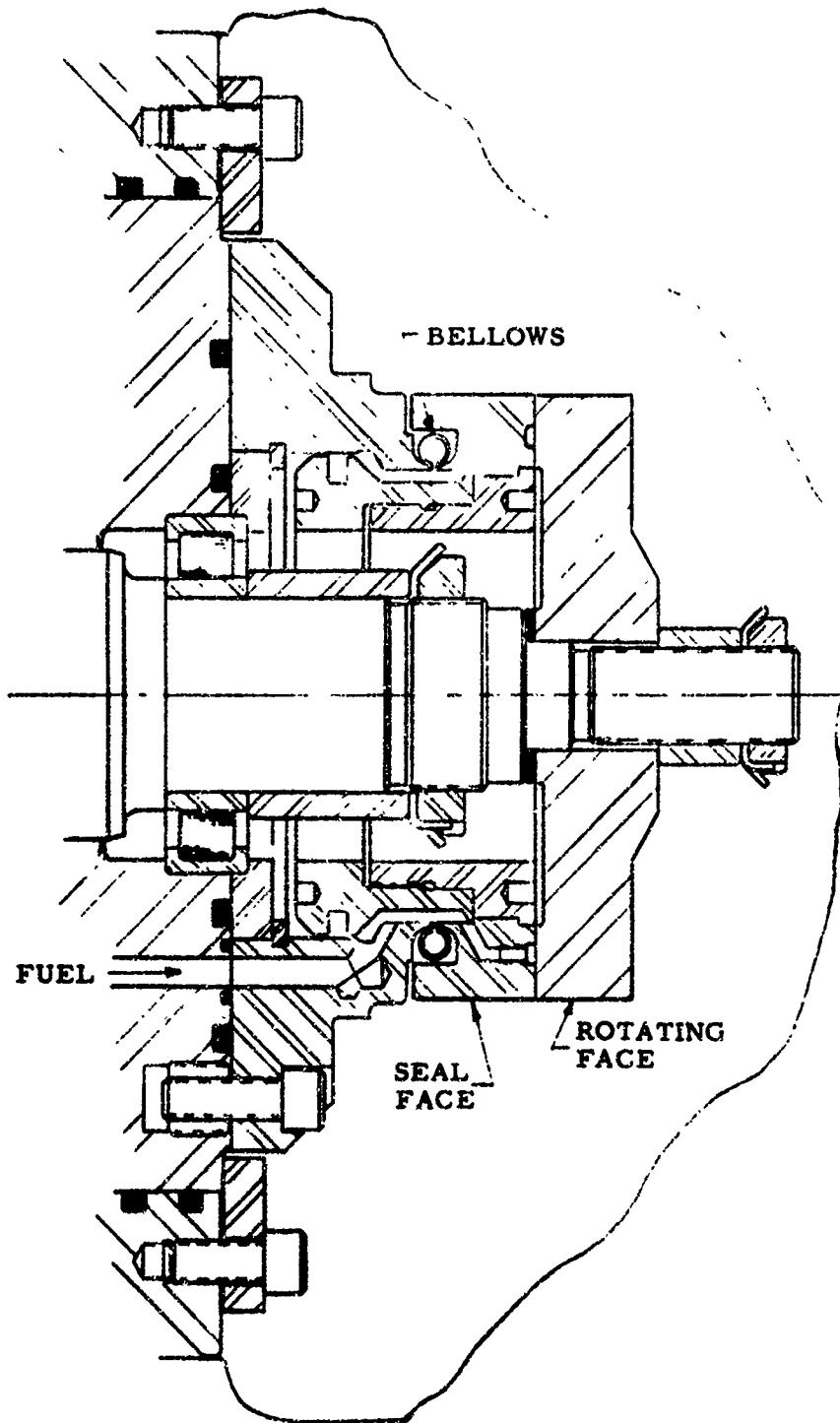
Imbedded-Thermocouple Temperature versus Run Time and Shield Surface Temperature versus Combustion-Seal Mixture Ratio

Figure X-5

UNCLASSIFIED

CONFIDENTIAL

Report 10830-Q-4



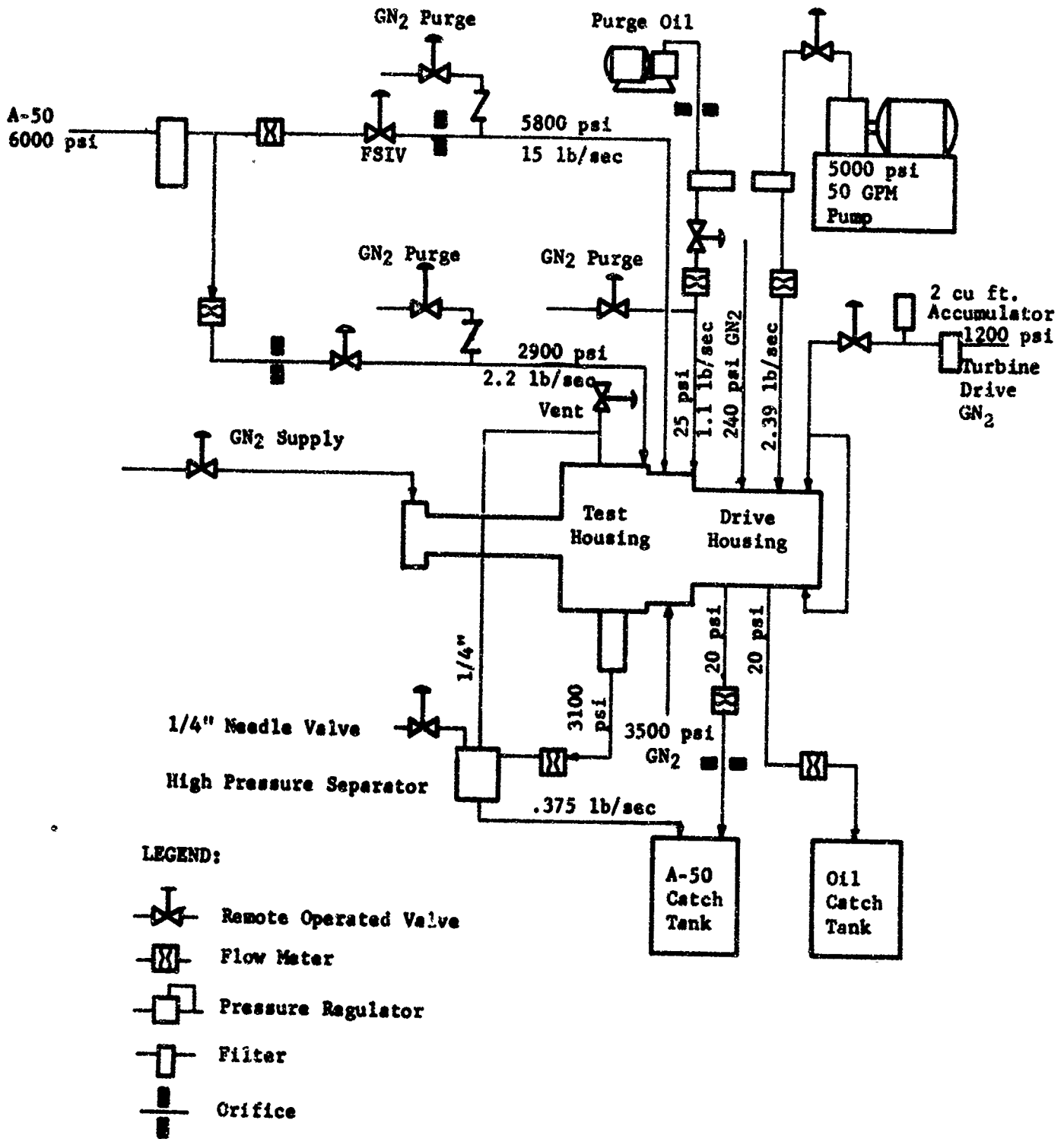
Hydrostatic Combustion Seal in Tester--Cold AeroZINE 50 Tests

Figure X-7

(This page is Unclassified)

CONFIDENTIAL

CONFIDENTIAL
Report 10830-Q-4



Flow Diagram, Rotating Fuel-Calibration Tests, ARES Hydrostatic Combustion-Seal Program (u)

Figure X-8

CONFIDENTIAL

TEST SERIES	TEST NO.	DATE 1966	OBJECTIVE	DUR. SEC. (FS ₁ TO FS ₂)	FLOWS, LB/SEC						MIXTURE RATIO		
					PREBURNER		SEALS				PRE-BURNER	SEAL	
					FUEL	OXID.	FUEL		OXIDIZER				
							TOTAL	COMP.	UP-STREAM	DOWN-STREAM			
PREBURNER CHECKOUT NO. SEAL	1.2-02-WAW 001	2-8	OXID FLOW CALIB	73	0	9.5	0	0	0	0	0	NA	NA
	002	2-8	FUEL FLOW CALIB	18	0.88	0	0	0	0	0	0	NA	NA
	003	2-8	FUEL FLOW CALIB	112	0.88	0	0	0	0	0	0	NA	NA
	004	2-17	HOT-START AT 600 PSI	4	0.8	10.5	0	0	0	0	0	13.1	NA
	005	2-18	HOT-START AT 250 PSI	.8	-	-	0	0	0	0	0	-	NA
	006	2-18	HOT-START AT 250 PSI	10	0.45	9.4	0	0	0	0	0	20.9	NA
	007	2-18	HOT-START AT 60 PSI	15	0.9	10.5	0	0	0	0	0	11.7	NA
COLD A-50 TESTS CHAMBER PRESSURIZED WITH CH ₂	1.2-04-WAW 001	3-23	FUEL FLOW CALIB	45	0	0	0.20	0.17	0	0	0	NA	NA
	002	3-24	" "	45	0	0	0.12	0.095	0	0	0	NA	NA
	003A	5-4	COLD ROTATION	15	0	0	1.23		0	0	0	NA	NA
	003B	5-10	COLD ROTATION	47	0	0	1.1		0	0	0	NA	NA

CONFIDENTIAL

Report 10830-Q-4

M	MIXTURE RATIO			CHAMBER PRESSURE, PSIG		TEMPERATURE, °F				SPEED, RPM	RAMP TIME, SEC	COMMENTS	RATING
	DOWN-STREAM	PRE-TURNER?	SEAL	GOAL	ACTUAL	PRE-TURNER	CHAMB	SHUTOFF AREA					
								MAX	MIN				
0	NA	NA	NA	NA	NA	NA	NA	NA	NA	0	0.7	CORRECTED CAVIT. VENTURI	SUCCESS
0	NA	NA	NA	NA	NA	NA	NA	NA	NA	0	0.9	LEAK IN SYSTEM	PARTIAL SUCCESS
0	NA	NA	NA	NA	NA	NA	NA	NA	NA	0	0.75	CORRECTED CAVIT. VENTURI	SUCCESS
0	13.1	NA	3100	3600	1140	1050	NA	NA	NA	0	0.7	SMOOTH OPERATION	SUCCESS
0	-	NA	3100	-	-	-	NA	NA	NA	0	-	SAFETY SHUTOFF TOO LOW	PARTIAL SUCCESS
0	20.9	NA	3100	2000	550	500	NA	NA	NA	0	0.7	LOW FUEL CLOGGED VENTURI	PARTIAL SUCCESS
0	11.7	NA	3100	3200	1300	1150	NA	NA	NA	0	0.7	ALL OBJECTIVES REACHED	SUCCESS
0	NA	NA	3100	3000	NA	NA	NA	NA	NA	0	3.5	INSUFFICIENT DATA	PARTIAL SUCCESS
0	NA	NA	3100	3200	NA	NA	NA	NA	NA	0	5.5	SEAL BELLOWS BROKE	SUCCESS
0	NA	NA	3100	3050	NA	NA	NA	NA	NA	0	4.5	FUEL IGNITION BECAUSE OF THERMO-COUPLE VENT. REVERSE PRESSURIZATION DURING SHUTDOWN FAILED BELLOWS.	FAILURE
0	NA	NA	3100	3680	NA	NA	NA	NA	NA	0	8	SHUTDOWN BECAUSE OF HIGH CHAMBER PRESS. MALFUNCTION IN SHUTDOWN FAILED BELLOWS	FAILURE

CONFIDENTIAL

ARES Seal Test Data Sheet (u)

Figure X-9, Sheet 1 of 2

CONFIDENTIAL

TEST SERIES	TEST NO.	DATE 1966	OBJECTIVE	DUR SEC (FS ₁ TO FS ₂)	FLOWS, LB/SEC						MIXTURE RATIO		GCR
					PREBURNER		SEALS				PRE-BURNER	SEAL	
					FUEL	OXID	FUEL		OXIDIZER				
							TOTAL	COMB.	UP-STREAM	DOWN-STREAM			
COLD A-50 TESTS. CHAMBER PRESSURIZED WITH GN ₂	004	5-26	SYSTEM CHECKOUT NO SEAL	80	0	0	0	0.40	0	0	NA	NA	310
	005	5-26	" "		0	0	0	0.05	0	0	NA	NA	310
	006	5-27	" "		0	0	0	0.40	0	0	NA	NA	310
	007	6-3	COLD ROTATION	ROTATION 2	0	0	0.936	0.225	0	0	NA	NA	310
	008	6-3	" "	4	0	0	0.76	0.045	0	0	NA	NA	310
	009	6-10	" "	0	0	0	-	-	0	0	NA	NA	310
	010A	6-15	" "	0	0	0	1.30	0.17	0	0	NA	NA	310
	010B	6-16	" "	ROTATION 5.5	0	0	1.24	0.30	0	0	NA	NA	310
	011	6-17	" "	ROTATION 84	0	0	1.30	0.27	0	0	NA	NA	310
	012	6-24	" "	ROTATION 78	0	0	2.14	0.43	0	0	NA	NA	310

CONFIDENTIAL

Report 10830-Q-4

MIXTURE RATIO		CHAMBER PRESSURE PSIG		TEMPERATURE, °F				SPEED RPM	RAMP TIME SEC	COMMENTS	RATING
PRE-BURNER	SEAL	GOAL	ACTUAL	PRE-BURNER	CHAMB	BURNOFF AREA					
						MAX	MIN				
NA	NA	3100	3100	NA	NA	NA	NA	0	5	80 PSI PRESSURE REVERSAL	PARTIAL SUCCESS
NA	NA	3100	3100	NA	NA	NA	NA	0	20	NO IMPROVEMENT	FAILURE
NA	NA	3100	3100	NA	NA	NA	NA	0	24	NO PRESSURE REVERSAL	SUCCESS
NA	NA	3100	3100	NA	NA	NA	NA	23,000	34	SEAL OK N-SPEED SHUT DOWN	PARTIAL SUCCESS
NA	NA	3100	3130	NA	NA	NA	NA	28,000	24	PRESSURIZING FUEL FAILURE RUINED SEAL	FAILURE
NA	NA	3100	3100	NA	NA	NA	NA	0	24	VALVE FAILED TO OPEN	FAILURE
NA	NA	3100	3100	NA	NA	NA	NA	0	24	INTENSIFIER OVERPRESSURE INTERLOCK STOPPED TEST BEFORE ROTATION	FAILURE
NA	NA	3100	3100	NA	NA	NA	NA	30,000	24	SHUTDOWN BECAUSE OF FAILURE OF SPEED SIGNAL NO TESTED OR SEAL DAMAGE	QUALIFIED SUCCESS
NA	NA	3100	3200	NA	NA	NA	NA	38,000 39,400	24	0.002" CLEARANCE 200 PSI Δ P 60 SEC. AT 38000 + RPM SEAL OK	SUCCESS
NA	NA	3100	3200	NA	NA	NA	NA	40,000	27	0.001" CLEARANCE 500 PSI Δ P 63 SEC AT 40,000 RPM SEAL OK	SUCCESS

CONFIDENTIAL

ARBS Seal Test Data Sheet (11)

Figure X-9, Sheet 2 of 2

CONFIDENTIAL

2

CONFIDENTIAL

Report 10830-Q-4



Posttest 1.2-04-WAW-008 Seal Faces after Welding during Contact

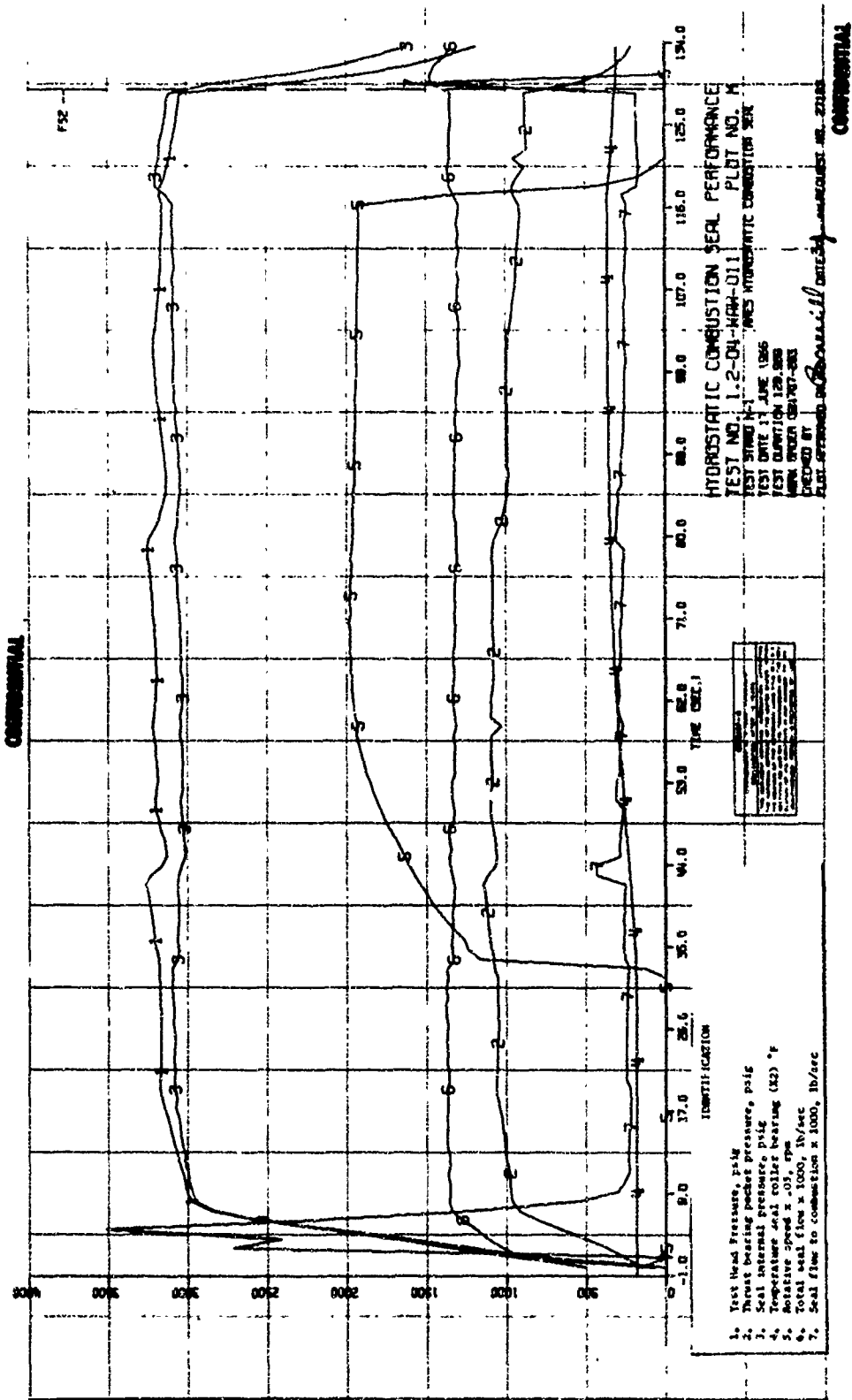
Figure X-10

(This page is Unclassified)

CONFIDENTIAL

CONFIDENTIAL

Report 10830-Q-4



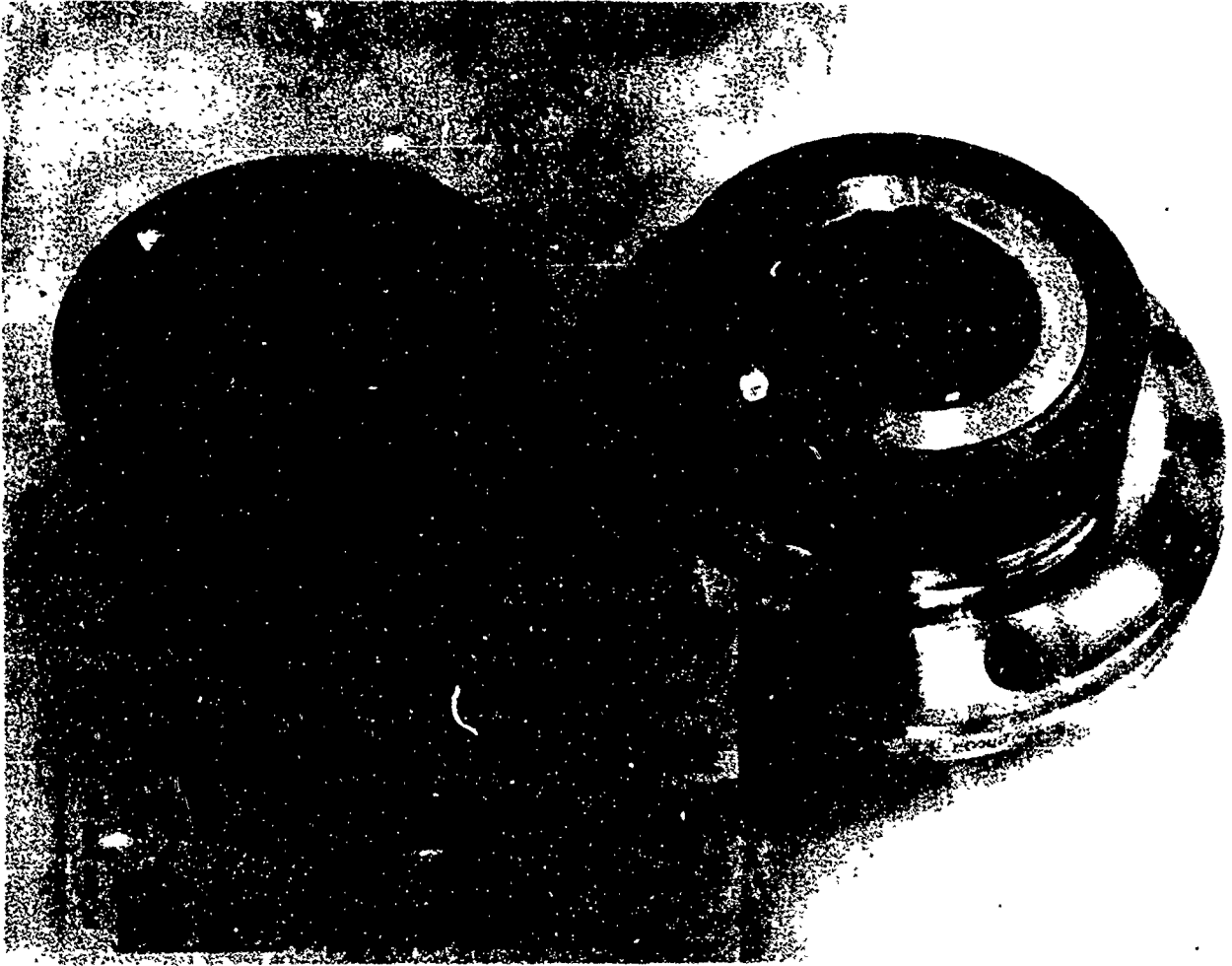
Hydrostatic Combustion-Seal Performance, Test 1.2-04-MAW-011 (u)

Figure X-11

CONFIDENTIAL

CONFIDENTIAL

Report 10830-Q-4



Hydrostatic Combustion Seal after Test 1.2-04-WAW-011

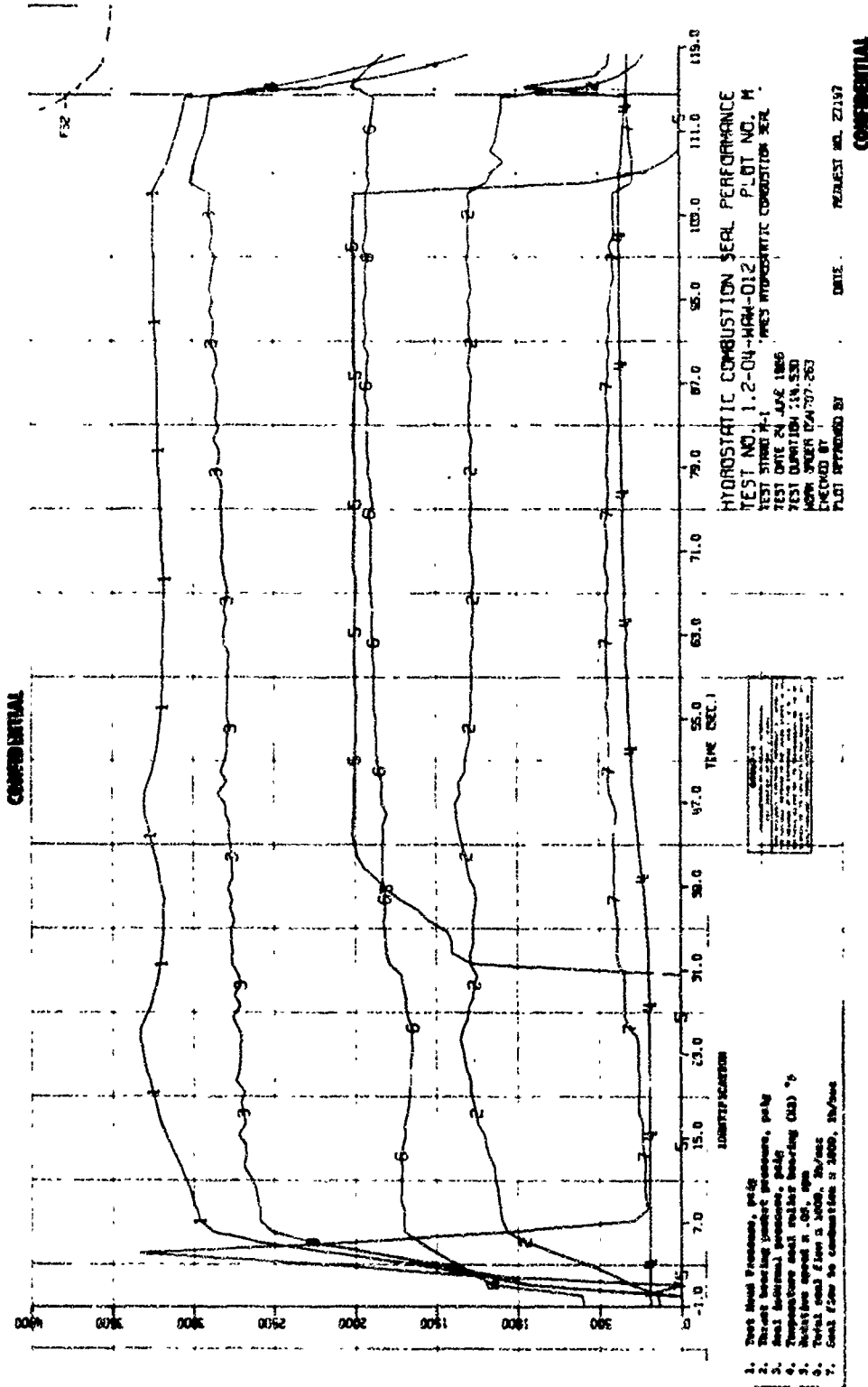
Figure X-12

(This page is Unclassified)

CONFIDENTIAL

CONFIDENTIAL

Report 10830-Q-4



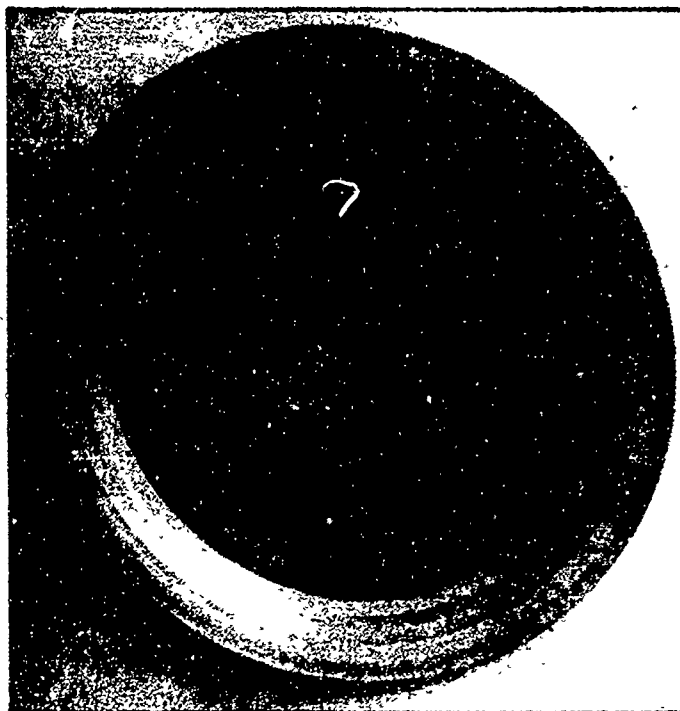
Hydrostatic Combustion-Seal Performance, Test 1.2-04-WAW-012 (u)

Figure X-13

CONFIDENTIAL

UNCLASSIFIED

Report 10830-Q-4



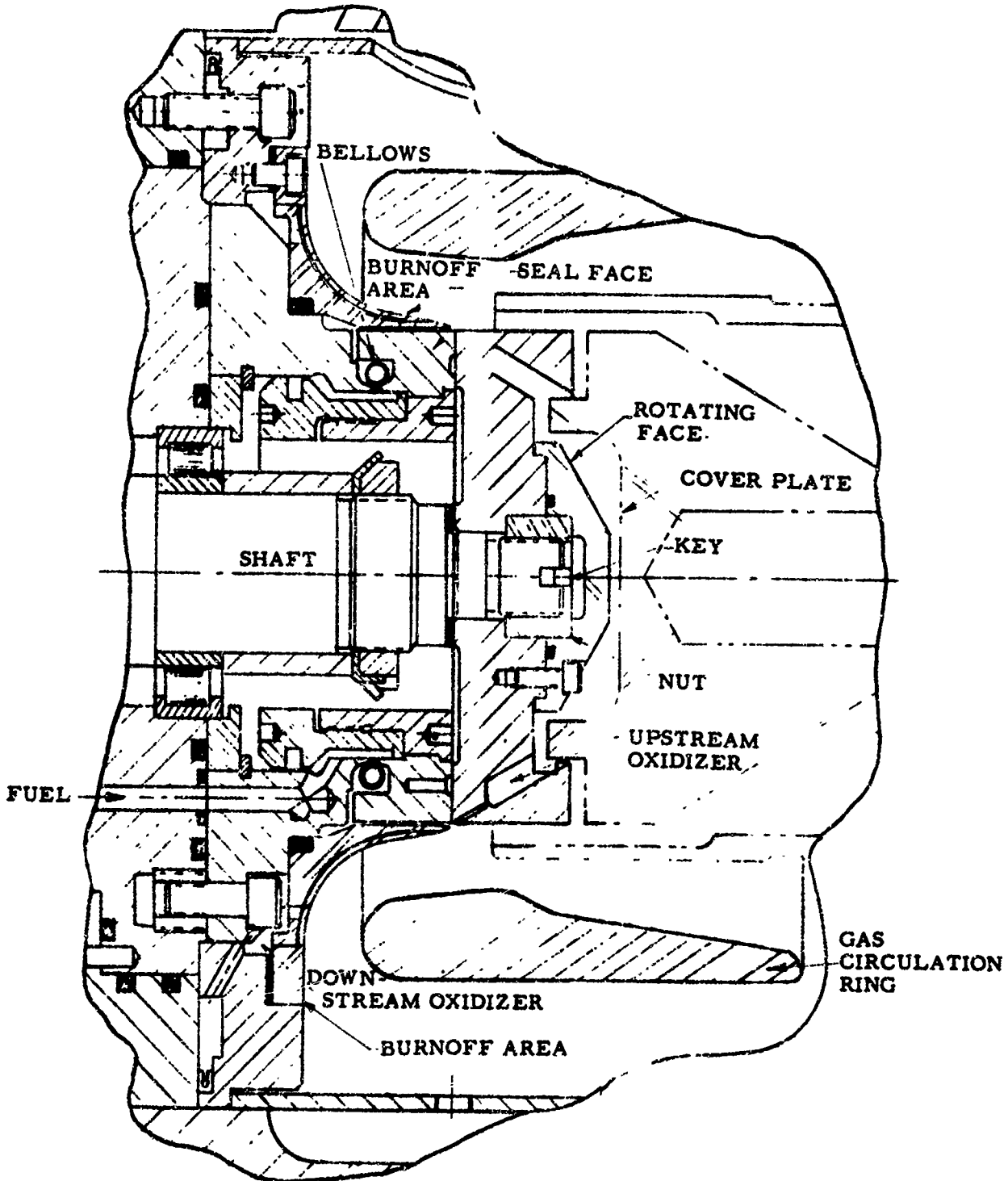
Hydrostatic Combustion Seal after Test 1.2-04-WAW-012

Figure X-14

UNCLASSIFIED

UNCLASSIFIED

Report 10830-Q-4

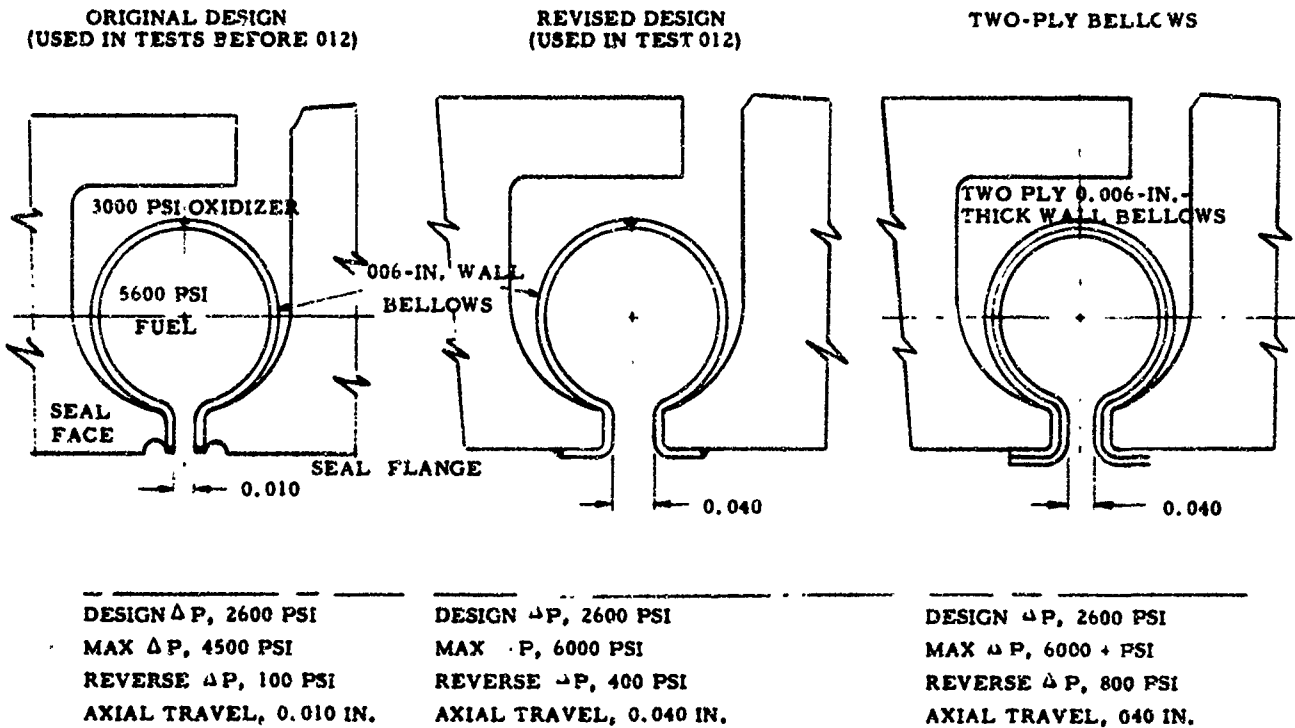


Hydrostatic Combustion Seal in Tester (Hot Testing)

Figure X-15

UNCLASSIFIED

CONFIDENTIAL
Report 10830-Q-4



Hydrostatic Combustion-Seal Bellows Redesign

Figure X-16

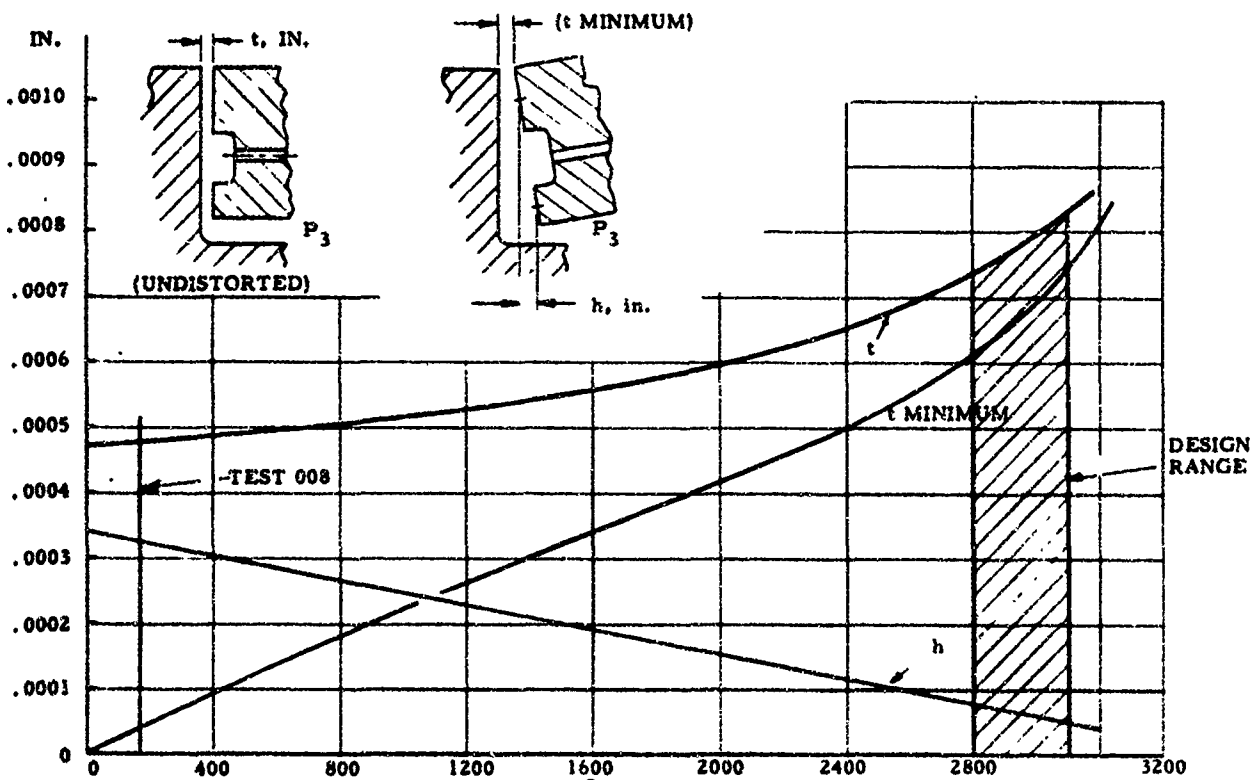
(This page is Unclassified)

CONFIDENTIAL

CONFIDENTIAL
Report 10830-Q-4

SEAL CLEARANCE & DISTORTION VS. INTERNAL PRESSURE (P_3)

ALL OTHER PRESSURES NOMINAL, 40,000 RPM
 $D_o = 0.030$, $P_{RO} = 2.886$ (500 PSI ΔP), t (NOMINAL)
 $= 0.0008$ IN.



CONFIDENTIAL

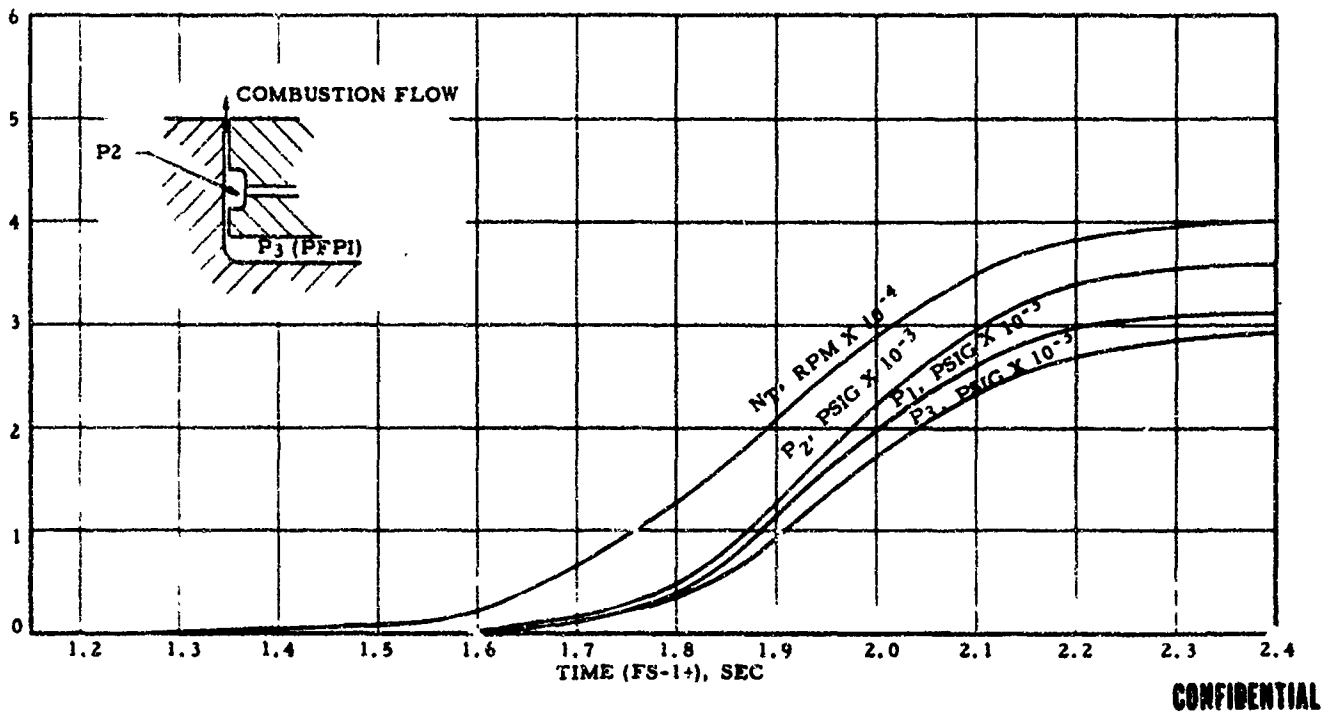
Seal Clearance and Distortion vs Internal Pressure (u)

Figure X-17
CONFIDENTIAL

CONFIDENTIAL

Report 10830-Q-4

**SEAL SUPPLY TAKEN DOWNSTREAM
FROM PRIMARY COMBUSTOR FUEL VALVE**



Hydrostatic Combustion-Seal Parameters during Engine Start Transient (u)

Figure X-18

CONFIDENTIAL

UNCLASSIFIED

Report 19830-Q-4

XI.

SUCTION VALVES

A. GENERAL

(u) The purpose of the suction valves is to control the admission of fuel and oxidizer from the propellant tanks to the main pump inlets of the engine module. The valves provide a positive, long-term, welded, shear-disc storage seal and a secondary seal to effect a positive shutoff of the propellant after initial activation. The construction of the valves provides a straight-through uninterrupted flow passage in the fully open position, which permits a close-coupled installation at the main pump inlets.

B. DESIGN

(u) The suction-valve gate is a segmented ball, which lifts from the seat and rotates completely out of the flow passage when fully open. The action of the gate (i.e., to lift from the seat and then to rotate out of the flow path) is controlled by the interaction of two cams--one rotating, the other stationary. The cam design permits closure and positive shutoff of the valve at reasonably high inlet pressures with a minimum operating torque. Additionally, the initial linear lifting action upon opening provides the motion required to shear the long-term storage seal.

(u) The design concept has been effectively proven by testing of two experimental valves.

(u) A prototype design (Figure XI-1), which approaches flight-weight and envelope requirements, has also been completed and four units are in fabrication.

(u) The design of a satisfactory method of welding the shear disc in place to ensure long-term storage capability has been completed, and an electron-beam-welding technique to accomplish the installation has been developed.

(u) Static and dynamic stress analyses were made to ensure the functional and structural capability of the valve, and the integrity of the analyses has been demonstrated by initial testing on experimental units.

C. FABRICATION AND TESTING

(u) Two experimental valves were completed early in May and have been subjected to extensive development testing.

UNCLASSIFIED

Report 10830-Q-4

XI, C, Fabrication and Testing (cont.)

(u) Proof-pressure testing demonstrated the structural integrity of the housing with the valve open and with the gate in the shut-off position.

(u) External leakage requirements were met. However, internal leakage testing indicated a need to provide additional support for the lip-type secondary seal. A design change has been made and new seal-support rings have been fabricated and are being tested. This new design has also been incorporated in the prototype valve.

(u) Flow testing demonstrated that the predicted flow characteristics are being met except that the flow factor (K_v) in the fully open position was 133 rather than 120 as predicted, indicating smoother-than-anticipated flow conditions through the valve.

(u) Response tests were made at opening and closing rates faster than 0.300 sec, and endurance cycling tests were made against inlet pressures exceeding 300 psi. No degradation or excessive wear was noted when the valve was disassembled and examined.

(u) Fabrication of the four prototype suction valves is expected to be completed by mid-July, and testing of these units is scheduled to begin immediately thereafter. After proof-pressure and functional testing of the secondary seal, the shear-disc seal assemblies will be welded into the valves. Demonstration of the completed valves to meet contractual requirements is scheduled for late August and early September 1966.

UNCLASSIFIED

Report 10830-Q-4

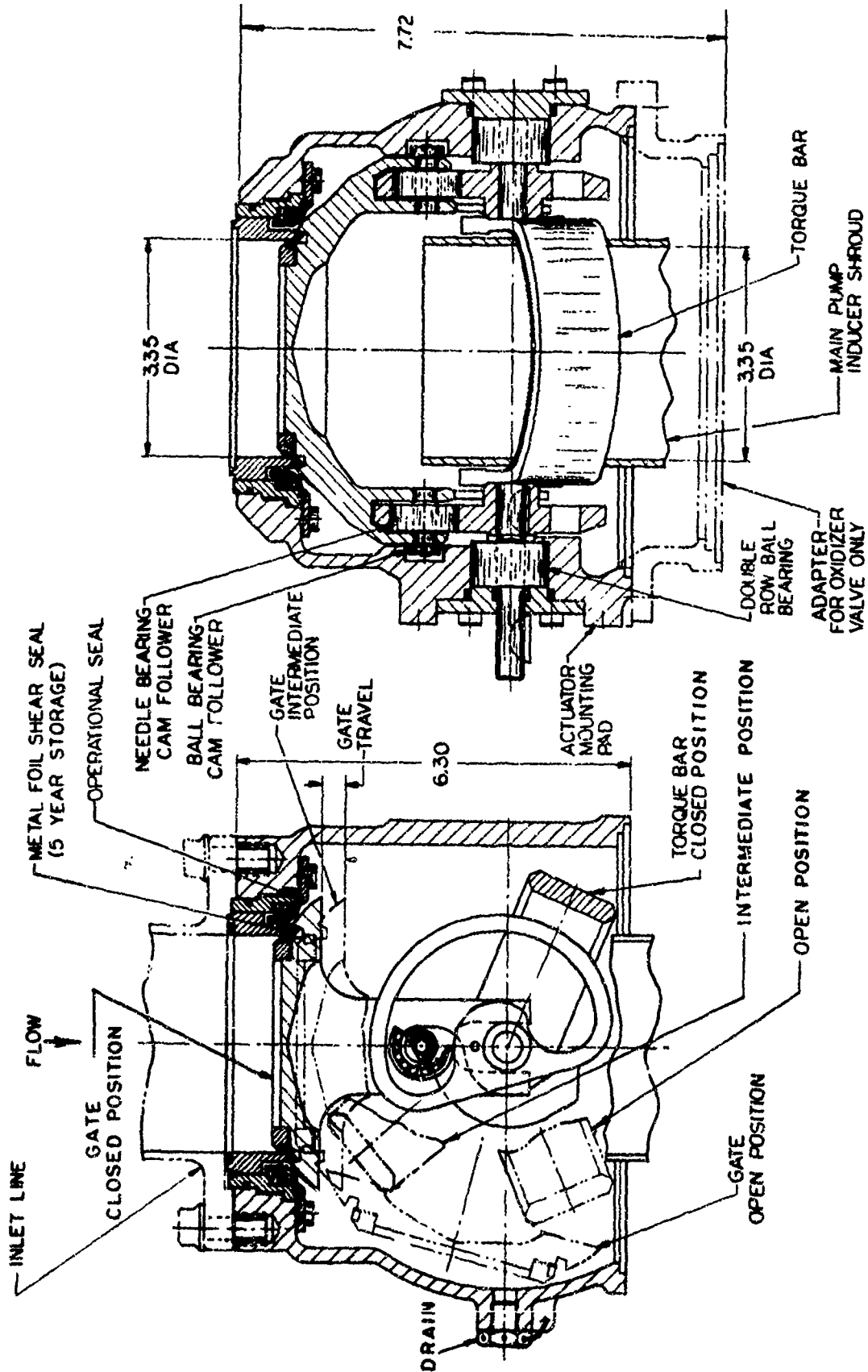


Figure XI-1

UNCLASSIFIED

UNCLASSIFIED

Report 10830-Q-4

XII.

FUEL-CONTROL VALVES

A. GENERAL

(u) The purpose of the primary and secondary combustor fuel-control valves (PCFCV and SCFCV, respectively) is to control the fuel flow to these combustors during all phases of module operation. The digital computer analysis of module performance indicated the necessity for closely coordinating the operation of the PCFCV and the SCFCV, particularly during module startup and shutdown. A reliability study, made to determine the need for actually interlocking the two fuel-control valves, led to the conclusion that an interlock was not warranted during engine development if residual components are used during Phase-II module testing. Based on this analysis and in the interest of maintaining maximum control flexibility during the development testing phase, the valves will be servocontrolled with individual position-feedback. The control signals will be subordinated to time and TPA speed during startup and shutdown, with provision for manual signal override to effect simultaneous shutdown of both valves in an emergency.

B. PRIMARY COMBUSTOR FUEL-CONTROL VALVE (PCFCV)

1. Design

(u) Figure XII-1 shows the configuration of the PCFCV as it will be installed in the module. A development test valve having an identical configuration at the control ports and simulating the module inlet and outlet port configuration has been designed and is scheduled for testing in July. Testing conducted on the PCFCV for the high-feed-pressure intensifier tests demonstrated that the control-orifice inlets should be chamfered if the range of design flow factor (K_v) is to be met. This change has been incorporated in the development test valve.

2. Fabrication and Testing

(u) All fabrication on the PCFCV is complete unless future testing indicates the need for modifications to obtain the desired control and flow characteristics.

(u) Testing of the PCFCV intended for the intensifier tests of the primary combustor was completed. A K_v control range from 0.01 to 1.25 was attained, which will meet all requirements for these combustor tests. The desirable K_v control range for the module PCFCV is from 0.01 to 1.40, and it is anticipated that this range will be attained with the development test valve.

UNCLASSIFIED

Report 10830-Q-4

XII, Fuel-Control Valves (cont.)

C. SECONDARY COMBUSTOR FUEL-CONTROL VALVE (SCFCV)

1. Design

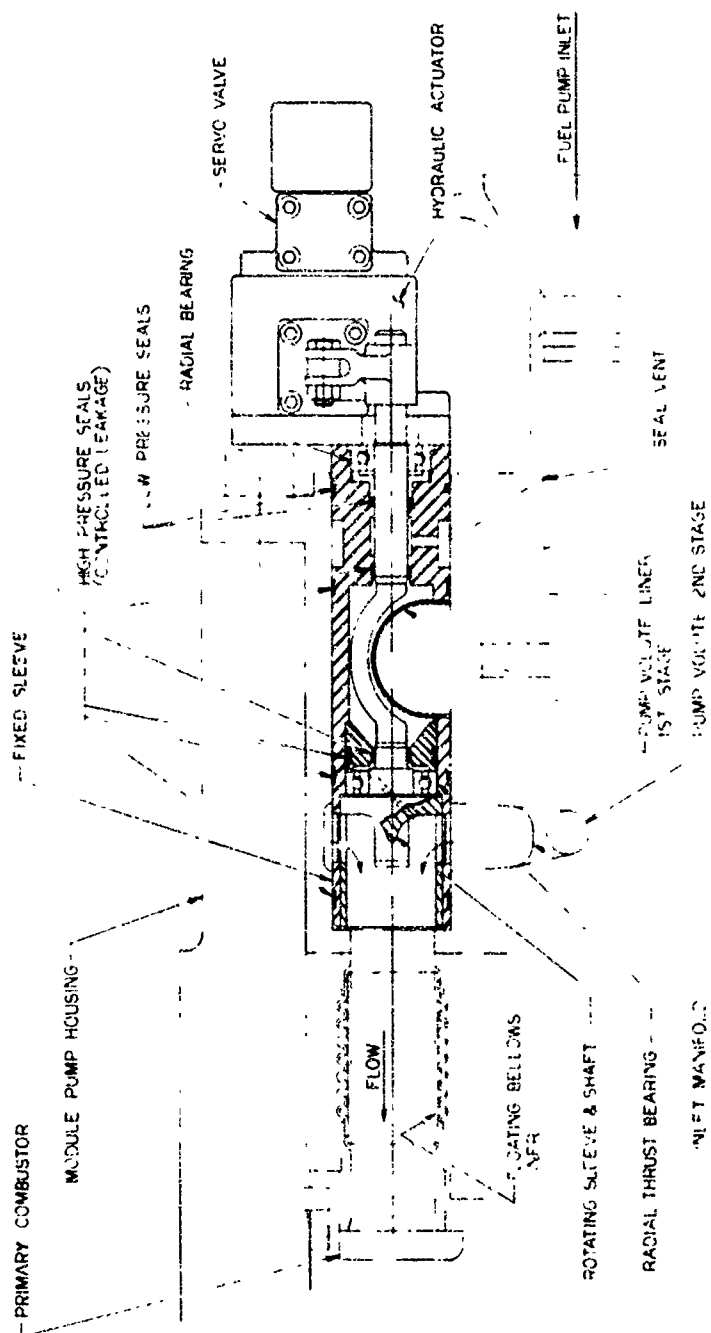
(u) Figure XII-2 shows the configuration of the SCFCV as it will be installed in the module. A development test valve (Figure XII-3) has been designed to duplicate the control ports and to simulate closely the configuration of the module inlet and outlet ports. An additional SCFCV has been designed for high-pressure intensifier testing of the secondary combustor. Both SCFCV configurations incorporate the design modifications developed during PCFCV testing to obtain a maximum K_v control range.

2. Fabrication and Testing

(u) Fabrication of both SCFCV configurations was completed, and testing has been completed on the development configuration. The control capability of the valve was within $\pm 3\%$ over the full design range.

UNCLASSIFIED

Report 10830-Q-4



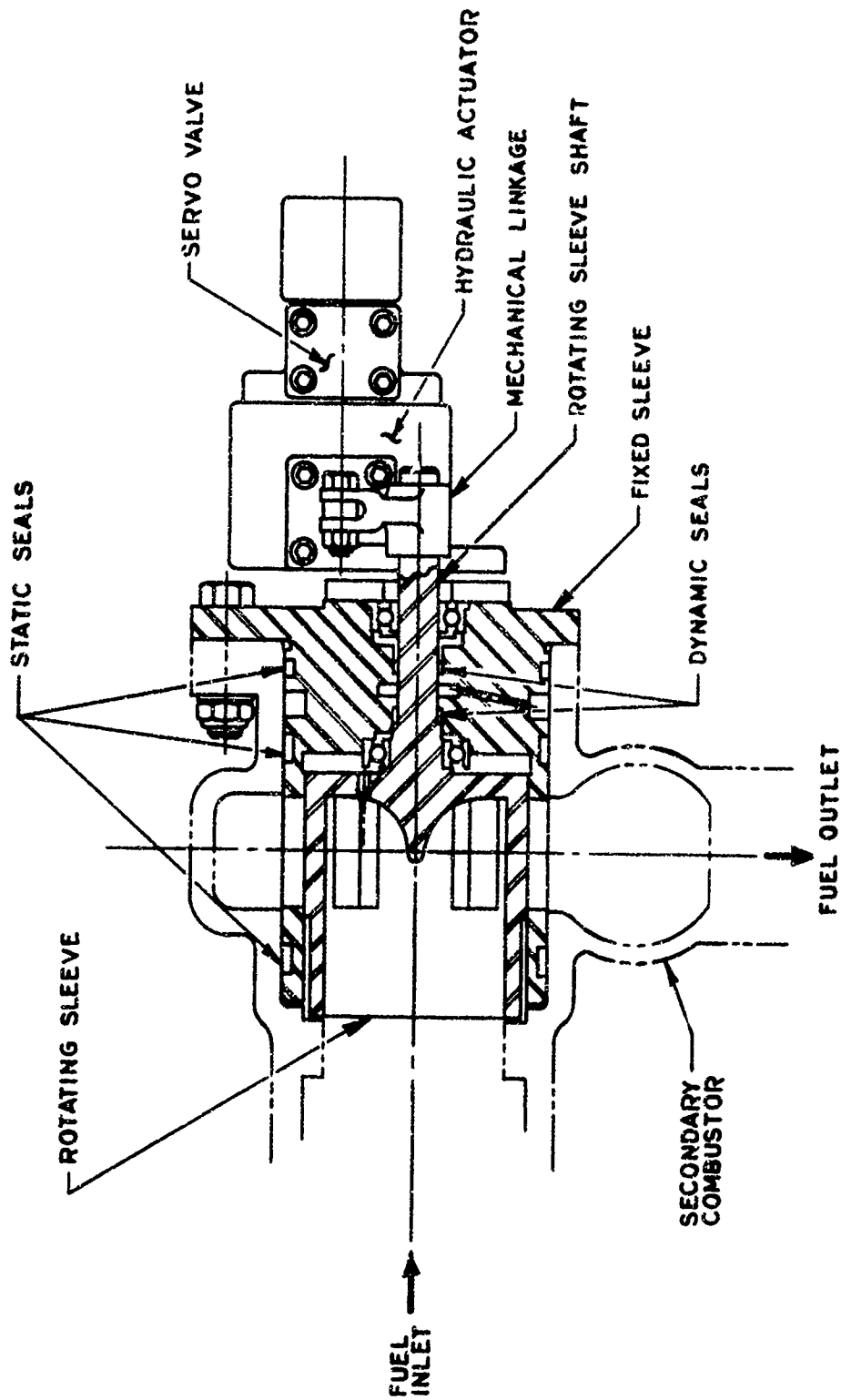
Primary Combustor Fuel Control Valve (Module)

Figure XII-1

UNCLASSIFIED

UNCLASSIFIED

Report 10830-Q-4



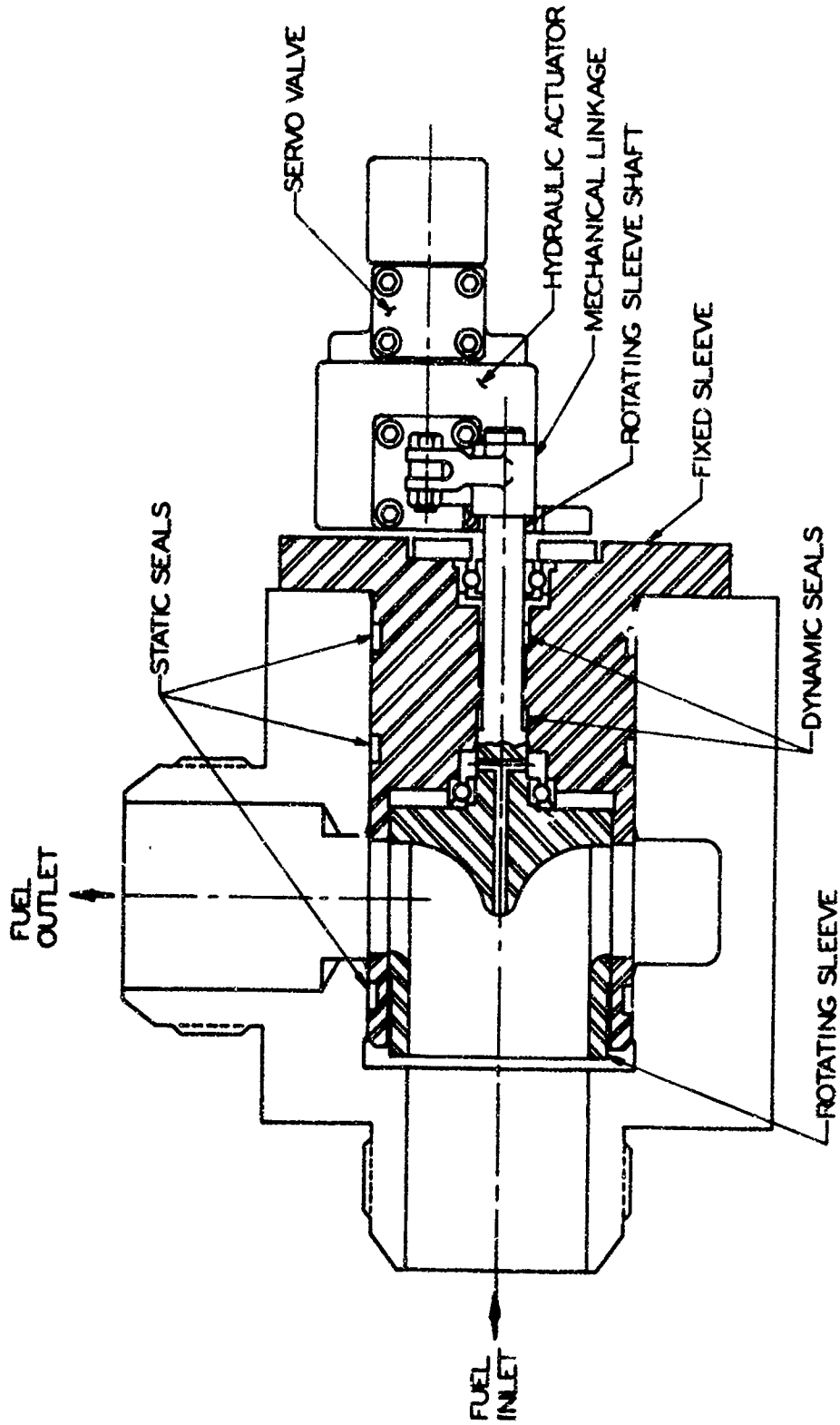
Secondary Combustor Fuel Control Valve (Module)

Figure XII-2

UNCLASSIFIED

UNCLASSIFIED

Report 10830-Q-4



Secondary Combustor Fuel Control Valve (Test)

Figure XII-3

UNCLASSIFIED

UNCLASSIFIED

Report 10830-Q-4

XIII.

SUCTION LINES AND AUXILIARY SYSTEMS

A. GENERAL

1. Main-Pump Suction and Boost-Pump Suction and Feed Lines

(u) The suction lines provide the connection from the boost-pump outlet to the suction-valve inlet. These lines are subjected to a relatively low pressure (150 and 350 psi for the fuel and oxidizer, respectively). Conversely, the boost-pump feed lines provide high-pressure propellants from the main-pump first-stage discharge to the boost-pump fluid-drive turbine inlets. These oxidizer- and fuel-turbine feed lines operate at main-pump first-stage discharge pressures.

2. Servo-Control System

(u) The servo-control system is intended to provide a flexible and reliable control for the primary and secondary fuel valves. Available electro-hydraulic servo actuators will be used to operate the fuel-control valves, which have position-feedback to close the minor loop.

B. DESIGN

1. Suction and Feed Lines

(u) The preliminary design analysis for sizing the suction and feed lines has been completed. The sizing was based on line lengths of 6 ft and on the module differential-pressure allocations shown in Figure XIV-2. Tentative interfaces for the suction and feed lines have been established.

2. Servocontrol System

(u) An all-solid-state control system has been designed to sequence and provide closed-loop position control to the primary and secondary fuel valves. The solid-state approach was selected because it offers the highest flexibility of any system proposed.

(u) This high degree of flexibility is obtained through the use of basic modules, which can be interconnected from a patch panel for a given sequence. If a different sequence is desired, only the patch cords need be changed. Flexibility is also increased by the ability to change sequence times and rates electronically, without any other modification.

(u) The basic modules utilized in the control system consist of a NOR gate, NAND gate, flip-flop, timer, integrator, and amplifier.

UNCLASSIFIED

Report 10830-Q-4

XIII, B, Design (cont.)

(u) The existing electrohydraulic servoactuators, which have been integrated with the PCFCV and SCFCV, are an integral part of the control system. Positional accuracy of each control valve is expected to be well within 1.0% of steady-stage operating position. Additionally, the actuators have built-in fail-safe devices, which will close the fuel valves in the event that either electric or hydraulic control power is lost.

C. FABRICATION AND TESTING (SERVOCONTROL SYSTEM)

(u) The preliminary circuits for the modules have been fabricated, and are presently under intensive tests. The servo amplifier for the position-control loop has been designed, and initial units have been fabricated. Initial testing demonstrated a variable-voltage gain from 1 to 100v, which will meet all anticipated demands for either the PCFCV or the SCFCV.

(u) Two control units have been fabricated for use in Phase-I development testing and have been integrated with the electrohydraulic servoactuators. The servocontrol units with the integrated servoactuators and respective fuel-control valves will be calibrated in July so that a precise fuel-valve operating K_w value can be remotely preselected and obtained at a predetermined valve opening rate.

UNCLASSIFIED

Report 10830-Q-4

XIV.

PROPULSION SYSTEM

A. GENERAL

(u) The propulsion-system effort is directed toward expediting and coordinating the design of major components to meet the Work Statement objective of demonstrating the engineering practicality and the performance of the entire engine module. The Phase-I design effort will ensure that components designed for testing are compatible with the engine modules for both single and clustered module applications. The module can be used either in conventional clusters or autonomous units or arranged to discharge through a common plug or forced-deflection type nozzle. A 20-module forced-deflection nozzle propulsion system has been defined for establishing the overall envelope requirements for the module.

B. SUMMARY

(u) The following tasks were performed:

1. The design pressure schedule was revised.
2. The pressure-drop allocations for the propellant passages were revised slightly.
3. The operating point of the engine module was updated.
4. The steady-state mathematical model of the module assembly was updated.
5. A design review and an evaluation study were initiated on the flow distribution and pressure drops in the oxidizer flow passages.
6. An operating envelope was defined for the Work Statement specification.
7. Module influence coefficients were computed.
8. A tolerance study was initiated to determine the effect on engine performance of anticipated component variations.
9. The net restoring torque of the turbine was computed.
10. The effort of determining and documenting the interfaces between major components was continued.
11. A test-instrumentation study was made.
12. Drawings of the internal and external views of the main engine assembly were updated.
13. A drawing was made of the external view of the engine assembly showing the interface locations.
14. Drawings were prepared showing external and internal views of the overall module arrangement and the test arrangement.

UNCLASSIFIED

Report 10830-Q-4

XIV, Propulsion System (cont.)

C. MODULE ASSEMBLY (ADVANCED TPA CONFIGURATION)

(u) The design pressure schedule was required as shown in Figure XIV-1 to include hydraulic turbine inlet pressures.

(u) The pressure drops that are allocated to the module propellant and gas passages were revised slightly and are presented in Figure XIV-2.

(u) The operating point of the engine module was adjusted to include the effects of propellant density variations and the latest adjustments of pump performance and passage pressure drops. An operating-point summary is shown in Figure XIV-3.

(u) Analysis continued on module operation including the following: (1) the steady-state mathematical model was updated, (2) a design review and evaluation study was made on the flow distribution and pressure drops in the oxidizer circuit, (3) a Work Statement operating envelope was defined for the module and its major components, and preliminary module component operating limits were specified, (4) influence coefficients were computed to determine engine module sensitivity of engine operating parameters to variations in component performance and variations in propellant inlet conditions, (5) a tolerance study was initiated to determine the effect on engine performance of anticipated component variations and to further define engine component operating limits, and (6) the net restoring torque of the turbine, in the spectrum of the engine module steady-state operating region, was computed and found to be satisfactory.

(u) The determination of interfaces between major components was continued. Detailed drawings of the following interfaces were submitted for engineering approval:

1. Main propellant suction lines to main suction valves.
2. Boost-pump discharge flanges to main suction lines.
3. Thrust pad and handling pads on engine assembly.
4. Primary combustor fuel valve to fuel housing.
5. Secondary combustor fuel valve to secondary combustor injector.
6. Fuel pump outlet to fuel coupling.
7. Fuel coupling to secondary combustor injector.

(u) Drawings of the internal and external views of the main engine assembly were updated and a drawing was made of the external view of the engine assembly showing the interface locations between the major components and the overall dimensions of the assembly. This external view is shown in Figure XIV-4.

UNCLASSIFIED

Report 10830-Q-4

XIV, C, Module Assembly (Advanced TPA Configuration)

(u) A test instrumentation study was made for the module testing, and a preliminary test-instrumentation requirements list and drawing were prepared showing the test-instrumentation locations and types required for the engine module test program. The study was made to determine component design requirements.

(u) The overall module arrangement with the engine assembly interconnected with the boost pumps and propellant lines was documented with internal and external view drawings. In addition, a preliminary drawing was made of the test arrangement including the interconnections of the controls with the test stand as well as purge and drain provisions. This drawing, which also shows the overall module arrangement as well as the test arrangement, is presented in Figure XIV-5.

CONFIDENTIAL

Report 10830-Q-4

This pressure schedule is based on (1) allocated flow-passage, K_w , values to determine ΔP , (2) minimum allocated turbopump efficiencies, and (3) target module performance. These pressure values define target operating requirements for Phase-I design purposes, and will remain in effect unless an increase in module operating pressures becomes incompatible with existing design margins of safety.

Location	Pressure, psia *				
	Liquid Oxidizer		Hot Gas	Liquid Fuel	
Boost Pump Inlet	36.6**	75		19.5**	75
Boost Pump Discharge	310	340		170	225
Main Pump Inlet	255	295		135	190
Main Pump Discharge		6025			3750
Boost Pump Turbine Inlet		5600			3440
2nd Stage Fuel Pump Inlet					3400
2nd Stage Fuel Pump Discharge					5765
Cooling Jacket Inlet		5900			
Film Cooling Manifold		5900			
Cooling Jacket Exit		5125			
PC Injector Inlet		5000			5100
PC Injector Face			4700		
Turbine Inlet			4575		
Turbine Exit (Blade), Static			3050		
Turbine Exit (Blade), Total			3100		
SC Injector Inlet			3010		3200
SC Injector Face			2885		
SC Chamber (P_o)			2800		

* Total pressure unless otherwise indicated

** Corresponds to minimum NPSH per work statement

CONFIDENTIAL

ARBS Module Pressure Schedule, Advanced Turbopump Configuration (u)

Figure XIV-1

CONFIDENTIAL

CONFIDENTIAL

Report 10830-Q-4

Hydraulic Passages:	Flow Factor $K_W = \frac{f}{\Delta P \times S.G.}$	Reference ΔP , Flow and Spec. Grav. (used to es- tablish min.allocated K_{f1})		
	Minimum Allocated K_W	ΔP , psi	\dot{W} , lb/sec	S.G.
Oxid. Suction Line	34	51.5	291.8	1.433
Oxid. Suction Valve	130	3.5	291.8	1.433
Oxid. Outer Housing Passage (Pump to Cooling Jacket)	18.6	125	248.2	1.433
Oxid. Cooling Jacket	6.9	775	217.2	1.282
Oxid. Inner Housing Passage (Cooling Jacket to PC Injector)	17.2	125	217.2	1.282
Oxid P.C. Injector	10.9	500	213.3	1.282
Oxid. Pump Disch. to Hyd. Turb. Port	2.50	170	39	1.433
Oxid. Hyd. Turb. Line & Check Valve	2.30	200	39	1.433
Oxid. Hyd. Turb. Orif. (Nominal)	4.39	55	39	1.433
Fuel Suction Line	20.6	34.8	115.2	.9
Fuel Suction Valve	110	1.2	115.2	.9
Fuel S.C. Valve and Passage (valve full open)	7.01	146	80.3	.9
Fuel S.C. Manifold and Injector	4.16	415	80.3	.9
Fuel Stage 2 Suction Passage	-	350	23.8	.9
Fuel P.C. Valve and Passage (valve wide open)	1.19	271	18.6	.9
Fuel P.C. Line to Injector	2.77	50	18.6	.9
Fuel P.C. Injector	0.98	400	18.6	.9
Fuel Pump Disch. to Hyd. Turb. Port	1.54	120	16	.9
Fuel Hyd. Turb. Line & Check Valve	1.51	125	16	.9
Fuel Hyd. Turb. Orif. (Nominal)	2.09	65	16	.9
Gas Passages:				
P.C. Injector Face to Turbine Inlet	2.02**	125	231.9	106*
Turbine Exit to S.C. Injector	3.01**	90	239.6	70.7*
S.C. Gas Injector	2.60**	125	239.6	68.2*
S.C. Injector Face to Plenum	$P_{Inj}/P_c = 1.03$	85	-	-

* Spec. grav. of gas = $\frac{\rho_{gas}}{\rho_{air}} = \frac{P_s / RT_s (\text{avg. gas})}{.0808}$. ** For gas passages, Flow Factor K_g is used instead of K_w , where effective K_g includes heat addition losses.

NOTES:

1. ΔP , flow, and specific gravity values are for reference only. For latest predicted pressures and flows, see ARES Module Operating Point.
2. Pressure drop alone does not establish a firm requirement for a passage since pressure will vary with minor changes in flow, and to a lesser degree with density. Wherever practical, the K flow factor should be used in place of ΔP as design criteria, since the measured K of a given piece of hardware will not change with operating conditions.

CONFIDENTIAL

ARES Module Flow-Passage Design Requirements (u)

Figure XIV-2

CONFIDENTIAL

CONFIDENTIAL

Report 10830-Q-4

<u>Parameter</u>	<u>Symbol</u>	<u>Units</u>	<u>Value</u>
<u>Module Assembly</u>			
Thrust	F	lb	100,000
Specific Impulse (Sea Level)	I_s	sec	285
Mixture Ratio, Module	M.R.	-	2.407
Total Weight Flow	\dot{W}_T	lb/sec	350.9
Oxidizer Weight Flow	\dot{W}_{OS}	lb/sec	247.9
Fuel Weight Flow	\dot{W}_{FS}	lb/sec	103.0
Oxidizer Suction Total Pressure	P_{OSBP}	psia	36.6
Fuel Suction Total Pressure	P_{FSBP}	psia	19.5
Oxidizer Net Positive Suction Head, Minimum	$NPSH_{OSBP}$	ft	30
Fuel Net Positive Suction Head, Minimum	$NPSH_{FSBP}$	ft	43
<u>Secondary Combustor</u>			
Chamber Pressure, Plenum	P_C	psia	2,800
Mixture Ratio, Injector	M.R. _{SC}	-	2.20
Oxidizer Film Cooling Flow (1)	\dot{W}_{OFC}	lb/sec	21.3
<u>Primary Combustor & Turbine</u>			
Mixture Ratio	M.R. _{PC}	-	11.56
Turbine Inlet Total Pressure	P_{TIT}	psia	4623
Turbine Inlet Total Temperature	P_{TIT}	°F	1215
Shaft Speed	N_T	rpm	40,038
<u>Main Pumps</u>			
Total Discharge Pressure, Oxidizer	P_{ODM}	psia	6075
Total Discharge Pressure, Fuel First Stage	P_{FDM-1}	psia	3789
Total Discharge Pressure, Fuel Second Stage	P_{FDM-2}	psia	5879
<u>Boost Pumps</u>			
Total Discharge Pressure, Oxidizer	P_{ODBP}	psia	312
Total Discharge Pressure, Fuel	P_{FDEP}	psia	179

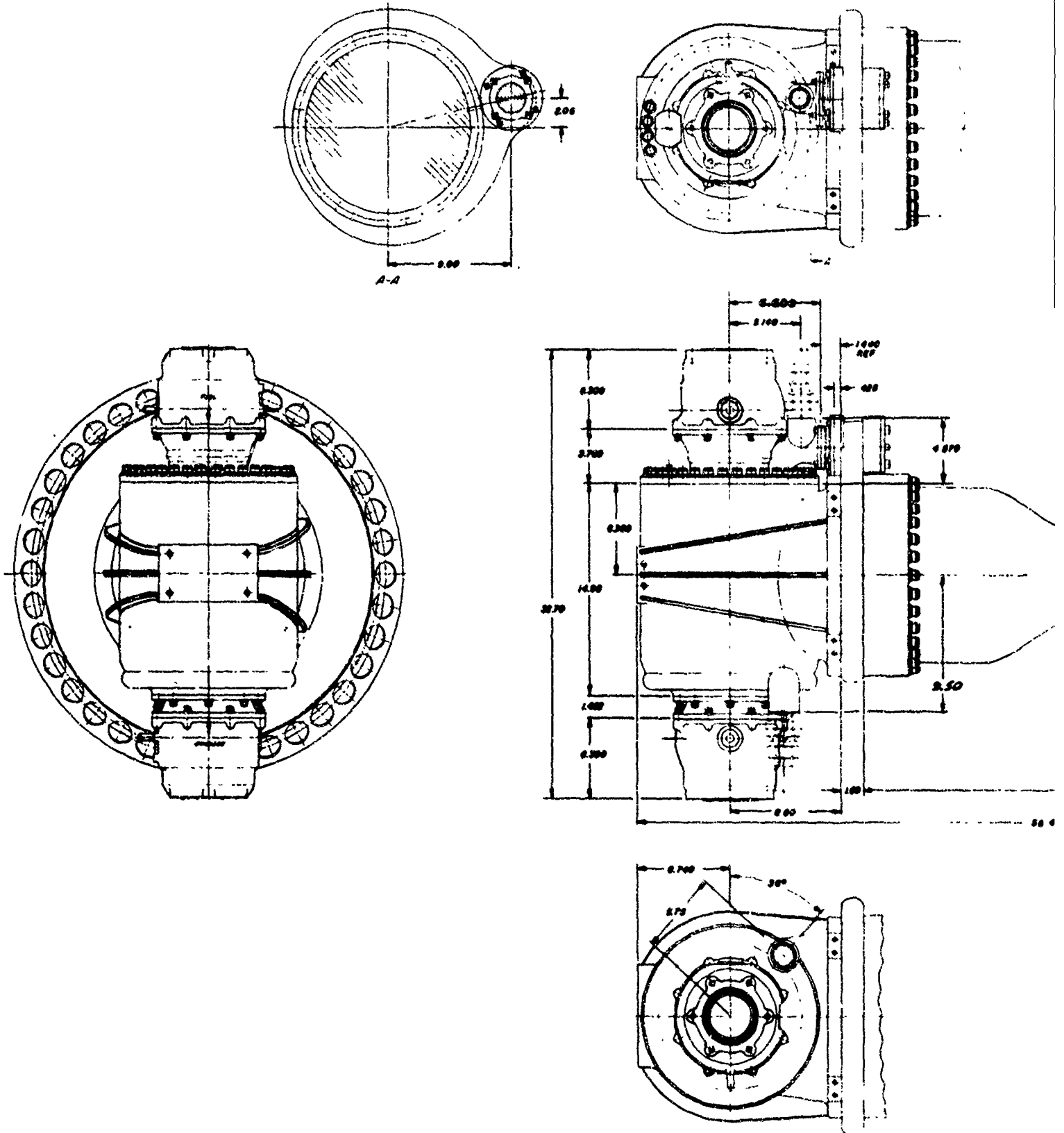
CONFIDENTIAL

Summary of ARES Module Operating Point (u)

Figure XIV-3

CONFIDENTIAL

CONFIDENTIAL
Report 10830-Q-4



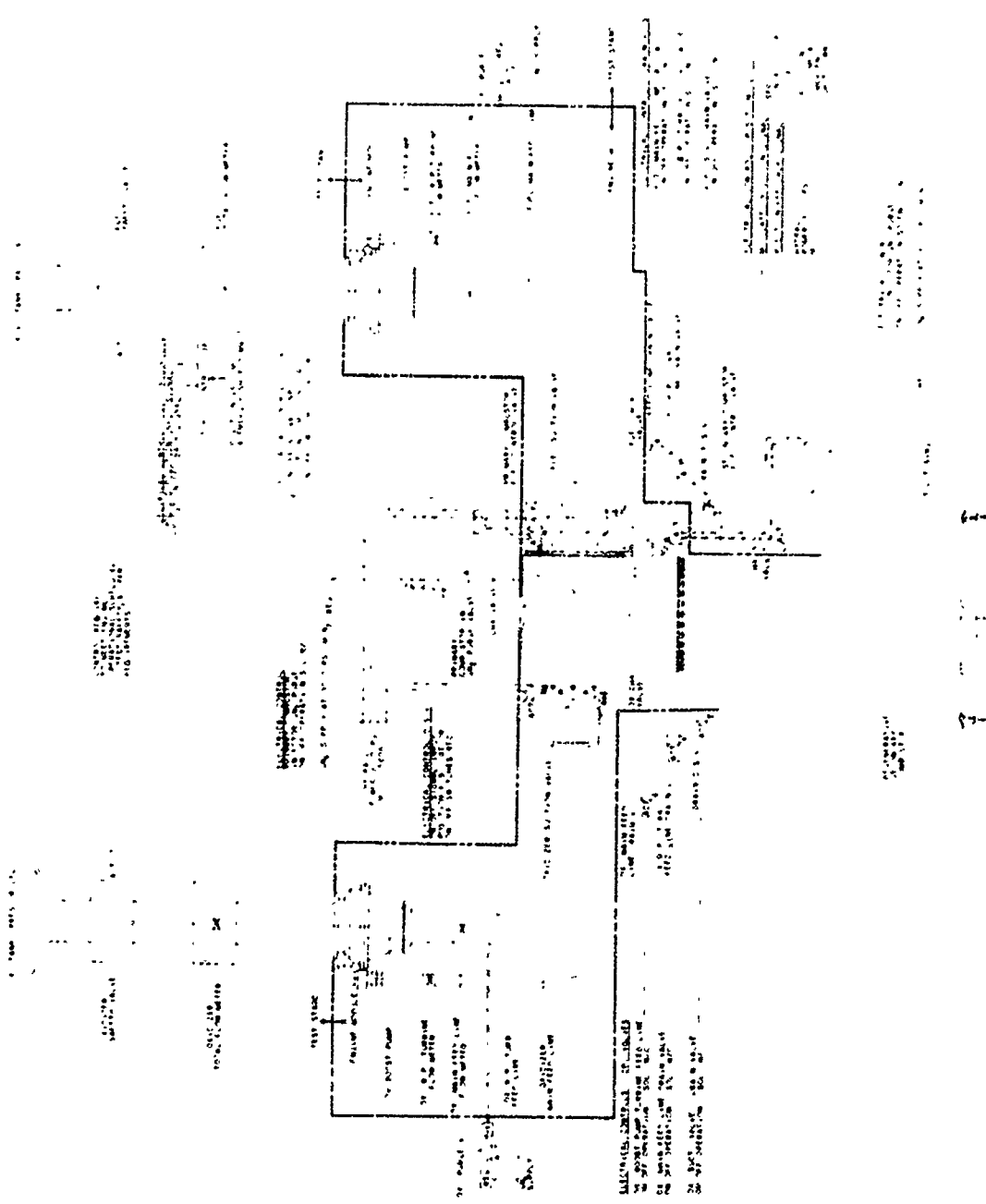
ARES Engine Module, External View (u)

Figure XIV-4

CONFIDENTIAL

CONFIDENTIAL

Report 10830-Q-4



Test Installation Interface (u)

Figure XIV-5

CONFIDENTIAL

UNCLASSIFIED

Report 10830-Q-4

XV.

ENGINE ANALYTICAL MODELS

A. GENERAL

(u) The engine analytical models include an engine module steady-state model, a module start and shutdown transient model, a burnoff-seal-tester start and shutdown transient model, and a low-frequency-stability model of the engine module. The steady-state model is currently operational. The engine module start-transient model has been completed and checked-out and is being used to obtain a revised engine start and shutdown sequence. The burnoff-seal-tester model has been completed, checked-out, and used to obtain a tester system start transient including manifold fill times. The results are being used in planning of valve sequencing and intensifier ramping for the hot tests. The burnoff-seal tester shutdown transient analysis will be completed in July. Checkout has continued on the low-frequency-stability model. The transfer-function program was completed but the technical results obtained appear to be in error and further effort will be required to ensure correct results.

B. START AND SHUTDOWN TRANSIENTS

(u) Programing and checkout of the combustion chamber-turbopump sub-routine was completed. Preliminary results indicate that the engine would operate at mixture ratios (MR) from 25 to 150 or higher during the low-speed portion of the start transient. This required that the gas properties for mixture ratios up to 150 be determined on a basis other than that of extrapolating the data available at a mixture ratio of 25. This was done by assuming that at $MR = 25$ (partial equilibrium), the enthalpy is determined by reacting 2 lb of oxidizer and 1 lb of fuel, and by diluting this mixture with another 23 lb of oxidizer. The reduction in enthalpy per pound of mixture, caused by the addition of more oxidizer, was then used in conjunction with a temperature entropy diagram with constant enthalpy lines at a pressure of 14.7 psia to determine the temperatures for the higher mixture ratios. The gas constant at high mixture ratios was determined by using the specific volume read from a P, V, T diagram at 14.7 psia in the equation of state. Further analytical investigation and test-data verification will be initiated if the engine start transient continues to indicate this requirement.

(u) The results of the start transient prior to ignition show that the oxidizer pump and the second-stage fuel pump operate at high Q/N values where the pump acts as a turbine (i.e., positive flow, with suction pressure higher than discharge pressure). This occurs while the oxidizer is filling the manifold downstream of the pump. The pump head and torque curves were revised to have head-torque relationships as indicated in Figure 13.1 of Centrifugal and Axial Flow Pumps, by A. J. Stephanoff, New York, John Wiley & Sons, 1957. A rerun of

UNCLASSIFIED

Report 10830-Q-4

XV, B, Start and Shutdown Transients (cont.)

the transient using the extended pump curves indicated that head losses through the pumps were higher than on previous transients; therefore, the oxidizer manifold filling time was extended from 1.2 to about 2.6 sec at a tank pressure of 60 psia. Further references are being sought to obtain a better definition of the pump performance curve at high Q/N values. It is interesting to note that the pumps and the turbine accelerate to 600 rpm due to torque produced by the oxidizer head loss during manifold filling.

(u) An approach to obtaining the shutdown transient prior to obtaining the startup transient was initiated. This involved minor programing changes to the main subroutine to input and store past time values. An approximation to the engine steady-state point with only the major flow rates included was run on the steady-state balance program and the results were then input into the transient program. This system is now working, and a steady-state point has been achieved with the transient program. Shutdown transients are being investigated. This procedure was beneficial because it revealed programing and logic errors which otherwise would not have been evident until the start transient reached steady state. In the future, this procedure will be adopted as a standard checkout technique.

C. BURNOFF SEAL TESTER TRANSIENT

(u) The startup sequence of the combustion-seal tester has been simulated on the IBM 7094 digital computer. Pressures and flow rates in the seal as well as seal clearances have been obtained for the entire start transient from initial valve opening to steady state.

(u) Conditions in the seal were calculated by using steady-state equations. Flows in the propellant lines were computed by means of the water-hammer equations. The combustion process in the preburner and in the turbopump housing was simulated with the instantaneous mixing model described in previous reports. Also included in the simulation was a line- and manifold-filling model.

(u) The valves were sequenced in such a way that the oxidizer entered the combustors 0.2 sec earlier than the fuel. The liquid in the intensifiers was kept at 60 psi until after ignition. Then the liquid pressures were raised to their final values in 0.7 sec, with the oxidizer pressure rise initiated 0.05 sec sooner than that of the fuel. This sequence of operation gave a satisfactory start transient.

UNCLASSIFIED

Report 10830-Q-4

XV, Engine Analytical Models (cont.)

D. LOW-FREQUENCY-STABILITY ANALYSIS

(u) Checkout of the low-frequency engine module model was continued. Several logic and programing errors have been corrected in the program for matrix derivation of transfer functions. The results obtained still do not appear technically correct, and the model equations as well as the program are therefore being rechecked.

(u) The subroutine for calculating and plotting the frequency response functions (Bode plots) has been completed and is operational in the program for matrix derivation of transfer functions. Programing the real-time-response subroutine and plotter was completed. The subroutine is being checked-out separately prior to integration in the main program.

(u) The checkout of the system equations for the engine model is being facilitated by use of an existing program for the solution of large systems of simultaneous linear equations. When the derivatives are set to zero in the module differential equations, a system of linear algebraic equations results that can be solved for the steady-state gains or influence coefficients of the engine. The system gains obtained by this approach must agree with the gains obtained by the transfer-function program, thereby providing a cross-check on the results.

(u) In summary, the system equations for the low-frequency model are complete, the program for matrix derivation of transfer functions is complete, the frequency response subroutine is complete, and the transient response subroutine is programed and being checked out. Preliminary results indicate some technical problems either as a result of errors in the system equations or errors in the transfer-function program. Present efforts are being directed toward isolating and correcting these errors.

UNCLASSIFIED

Report 10830-Q-4

XVI.

NOZZLE AERODYNAMICS

A. SUMMARY

(u) All experimental cold-flow testing in the subscale nozzle program was completed by the subcontractor (FluidDyne Engineering Corporation) on 12 May 1966. These data have been prepared for presentation and inspection in the order in which the program objectives are enumerated in the Program Plan*. Discussion has been limited to comments of a qualitative nature because the data are not final. The FluidDyne final report is expected to be released in August. Preliminary results, in general, were as predicted with the exception of those from the ARES prototype model where sea-level performance was considerably lower than anticipated.

(u) Warm-flow testing in the subscale nozzle program was completed on 10 June 1966. Reduced data are expected to be available by 15 July 1966, and their analysis will begin immediately thereafter.

B. COLD-FLOW PROGRAM

1. ARES Prototype Model Performance

(u) Results from experimental testing of Cold-Flow Model 2, the ARES prototype performance-simulation model, are presented in Figure XVI-1. These results include data obtained both with and without ambient base bleed as well as predicted performance data based upon results from previous cold-flow programs.** Three features are immediately apparent upon inspection of this graph. First, ambient bleed increases sea-level performance about 2-1/2%--an amount that appears consistent with the bleed-passage area ratios and performance improvements of previous programs (see Report AFRPL-TR-65-150). Second, the performance differential extends well beyond design conditions, a fact also reflected in former programs. And third, the difference between predicted and actual results, especially at sea level, is substantial, amounting to about 3%. No explanation can be advanced for this deviation and none will be sought until the final data have been received; however, even these data are not expected to radically alter the results. Thus, the error is undoubtedly in the prediction procedure, and a review of the technique outlined in Report AFRPL-TR-66-82*** is indicated.

* ARES Program Plan, Revision I (u), Aerojet-General Corporation Report 10830-PP, February 1966 (Confidential).

** Integrated Components Program -- Phase I, Final Report (u), Technical Report RPL-TDR-64-99, prepared by Aerojet-General Corporation for the United States Air Force, 20 January 1965 (Confidential) and, Integrated Components Program, Final Report, Technical Report AFRPL-TR-65-150, prepared by Aerojet-General Corporation for the United States Air Force, September 1965 (Confidential).

*** Advanced Rocket Engine--Storable (u), Quarterly Technical Report AFRPL-TR-66-82, prepared by Aerojet-General Corporation for the United States Air Force, April 1966 (Confidential).

UNCLASSIFIED

Report 10830-Q-4

XVI, B, Cold-Flow Program (cont.)

2. Prospective Nozzles for ARES Application

(u) Two types of external expansion nozzles, i.e., plug and forced-deflection nozzles, are being considered for ARES application. Within this broad classification, both contoured-wedge and DeLaval internal-expansion sections (IES) may be used. Therefore, possible prototype nozzles in each of these configurations were designed, and cold-flow performance-simulation models were built for three: a DeLaval IES forced-deflection configuration, a contoured-wedge IES forced-deflection configuration, and a contoured-wedge IES plug-nozzle model. Results from experimental testing of these models are presented in Figure XVI-2. The chosen ARES prototype nozzle, a DeLaval IES forced-deflection configuration, exhibits the best design performance, whereas the contoured-wedge plug nozzle, with 13% of isentropic length, out performs the others at sea level (no base bleed). The lower design performance of the contoured-wedge forced-deflection nozzle is probably caused by the greater base area required to fit this nozzle into the available envelope.

3. IES Area-Ratio Variation

(u) The postulation, for plug nozzles, that the aerodynamically optimum IES area ratio will result in maximum performance at the particular pressure ratio under consideration led to an investigation of similar effects in forced-deflection nozzles. Cold-Flow Model 3 was designed with a sea-level optimum area ratio (9.7), and its performance is compared with that of the ARES prototype model in Figure XVI-3. Sea-level performance of Model 3 is indeed higher, although the exact source of this improvement cannot be derived from the graph. However, design performance was degraded by an almost equal amount, and further analysis is required before a definite statement can be made as to whether these effects have been caused by IES area-ratio variation or by related side effects.

4. Skirt Contour Variations

a. Module-to-Skirt Merging Study

(u) Difficulty in matching aerodynamically designed forced-deflection nozzle skirts to DeLaval internal-expansion sections necessitated a review of techniques for merging or joining these two nozzle components. In particular, a sharp or abrupt compression corner at the IES exit into the skirt would be convenient from a fabrication viewpoint. Testing of two models having a smooth and an abrupt juncture, respectively, shows that this proposed solution to the problem will result in no measurable performance degradation (Figure XVI-4).

UNCLASSIFIED

Report 10830-Q-4

XVI, B, Cold-Flow Program (cont.)

b. Shortened-Skirt Study

(u) Among the techniques considered for improving payload performance is that of reducing nozzle weight without proportionately reducing performance. Since the skirt contour of a forced-deflection nozzle with DeLaval IES usually is very approximate, aerodynamically speaking, an arbitrary decrease in skirt length and weight may not seriously affect nozzle performance. The skirt of Model 2b, therefore, was arbitrarily shortened about 18%, equivalent to a theoretical 1% reduction in design performance, and the results of its testing were compared to that of Model 2a (Figure XVI-4). Inspection of this graph reveals that sea-level performance is unaffected by the change in skirt length, reflecting the significance of IES area ratio on this performance parameter. However, design performance did indeed drop, but not in the amount predicted, indicating that the nozzle skirt could probably be shortened by almost 25% before design performance would suffer as much as a 1% decline.

5. Cant-Angle Study

(u) Mention was made, in the preceding section, of the approximation in forced-deflection nozzle-skirt design when DeLaval IES are employed. A further area of uncertainty surrounds the selection of module cant-angle, a parameter clearly defined only when expansion is purely external and the throat is annular. It is current practice to set this angle at the Prandtl-Meyer turning angle for the equivalent annular IES area ratio, that is,

$$\theta_{ei} = \theta_e + v_e - v_{ei}$$

Cold-Flow Model 2a was designed in this manner, but in Models 2c and 2d the cant angle was arbitrarily reduced and increased five degrees, respectively. Results (Figure XVI-5) indicate that performance might be improved slightly if the cant angle were reduced, but that performance is definitely impaired if the module cant angle is increased. These results were expected and tend to verify the predictions made by Dr. G.V.R. Rao in a review of the program plan. (Dr. Rao is a consultant to the Aerojet-General Corporation.)

6. Forced Base Bleed

(u) Review of ambient base-bleed data from previous programs indicates that the model bleed flow passages have been choked at the lower pressure ratios, usually up to those around 300, above the point of minimum P_0/P_a . Data also indicates that the secondary weight-flow ratio, in these instances, varies downward from a maximum at sea level to about 3 or 4% at a pressure ratio of 250, depending upon bleed-passage size. An attempt to simulate flight total pressures along a typical trajectory, for the forced bleed portion of this program, did not significantly

UNCLASSIFIED

Report 10830-Q-4

XVI, B, Cold-Flow Program (cont.)

increase these bleed flow ratios since vehicle velocities were relatively low and total pressure losses, if any, were small. Thus, secondary weight-flow ratios of 1, 3, and 5%, were selected, regardless of the bleed-flow total pressure, to bracket available ambient base-bleed data. Results were not expected to vary greatly from those experienced with ambient bleed, as confirmed by Figure XVI-6. As expected, performance improvement at a pressure ratio of 1000 is lower than at 250, and further analysis of the similarity of the data at the 5% bleed flow ratio will probably confirm that the wake was closed at both pressure ratios.

7. Module Failure

(u) Previous module failure testing (Figure IV-37, Report AFRPL-TR-65-150) has fairly well established the performance of an eight-module forced-deflection nozzle when one or two modules fail. By increasing the number of modules from 8 to 20, the effect of module failure should be minimized, even when the modules are adjacent. Figure XVI-7 verifies this; in fact, sea-level performance (thrust efficiency) degradation is now only about 1% instead of more than 5% encountered with an eight-module configuration. Design performance losses are also smaller, reflecting the smaller increase in overall area ratio when only 1 or 2 of 20 modules fail. At the same time, thrust-vector misalignment remained under one degree (Figure XVI-8)--a standard established during previous testing (Figure IV-38, Report AFRPL-TR-65-150).

8. Engine Throttling

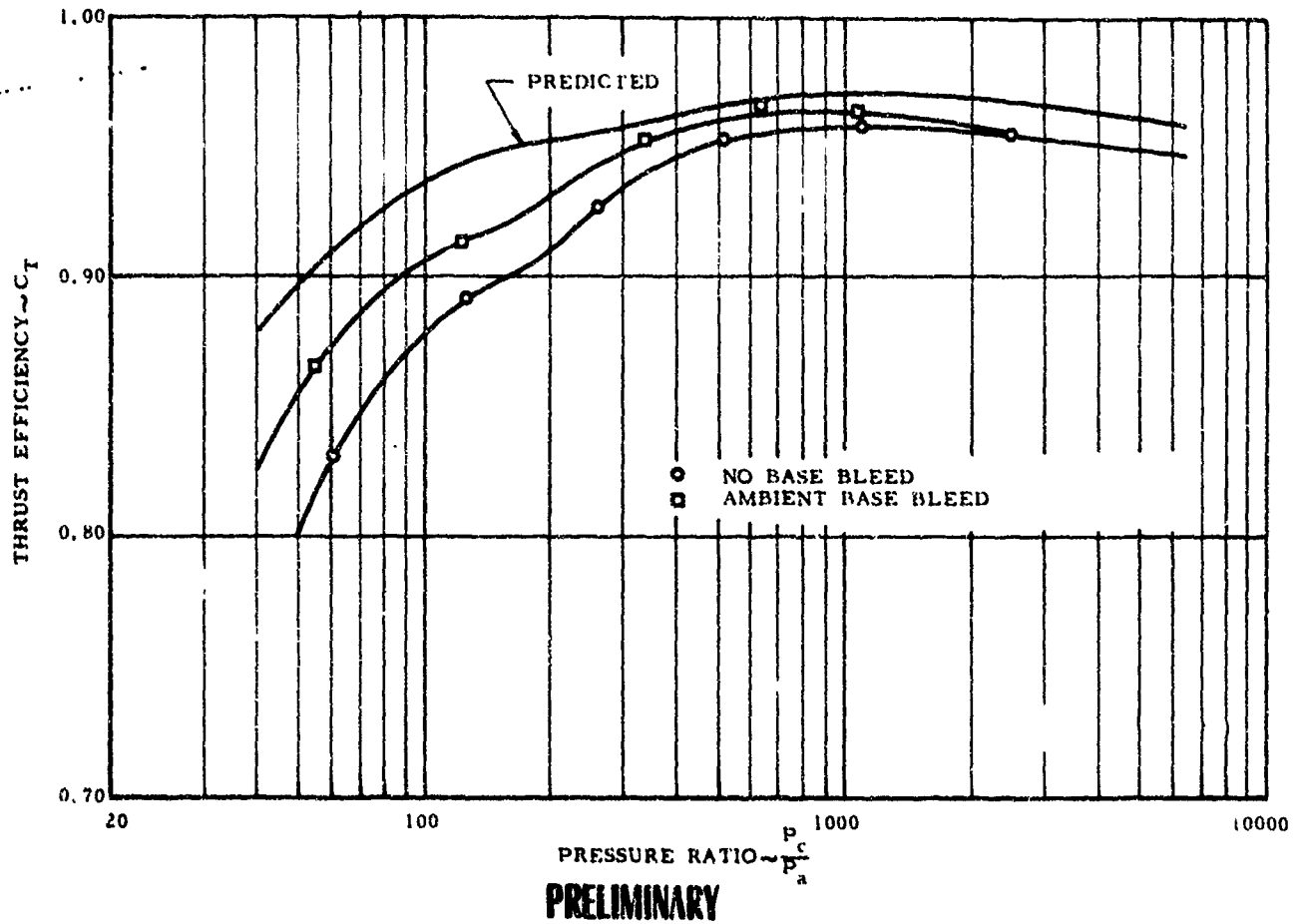
(u) Engine throttling by module shutdown was shown to be an efficient method of thrust-level control during previous testing (Figure IV-39, Report AFRPL-TR-65-150) in that the vacuum thrust coefficient was relatively unaffected by throttling, at least to a throttle ratio of 0.5. Extension of these results, during this program, to a throttle ratio of 0.8 indicates that the previous conclusions are still valid, that is, the vacuum thrust coefficient is not significantly altered when as many as 16 of 20 modules are shut down (see Figure XVI-9).

C. WARM-FLOW PROGRAM

(u) The warm-flow part of the subscale nozzle program was completed on 10 June 1966, with the two-dimensional visual portion finished earlier, on 21 May. Shadowgraphs and Schlieren photographs of the flow are available, but no quantitative data have yet been received, primarily because the volume of data and the extensive reduction procedure required more time to present them in usable form. Reduced data are expected to be available about 15 July 1966.

UNCLASSIFIED

Report 10830-Q-4



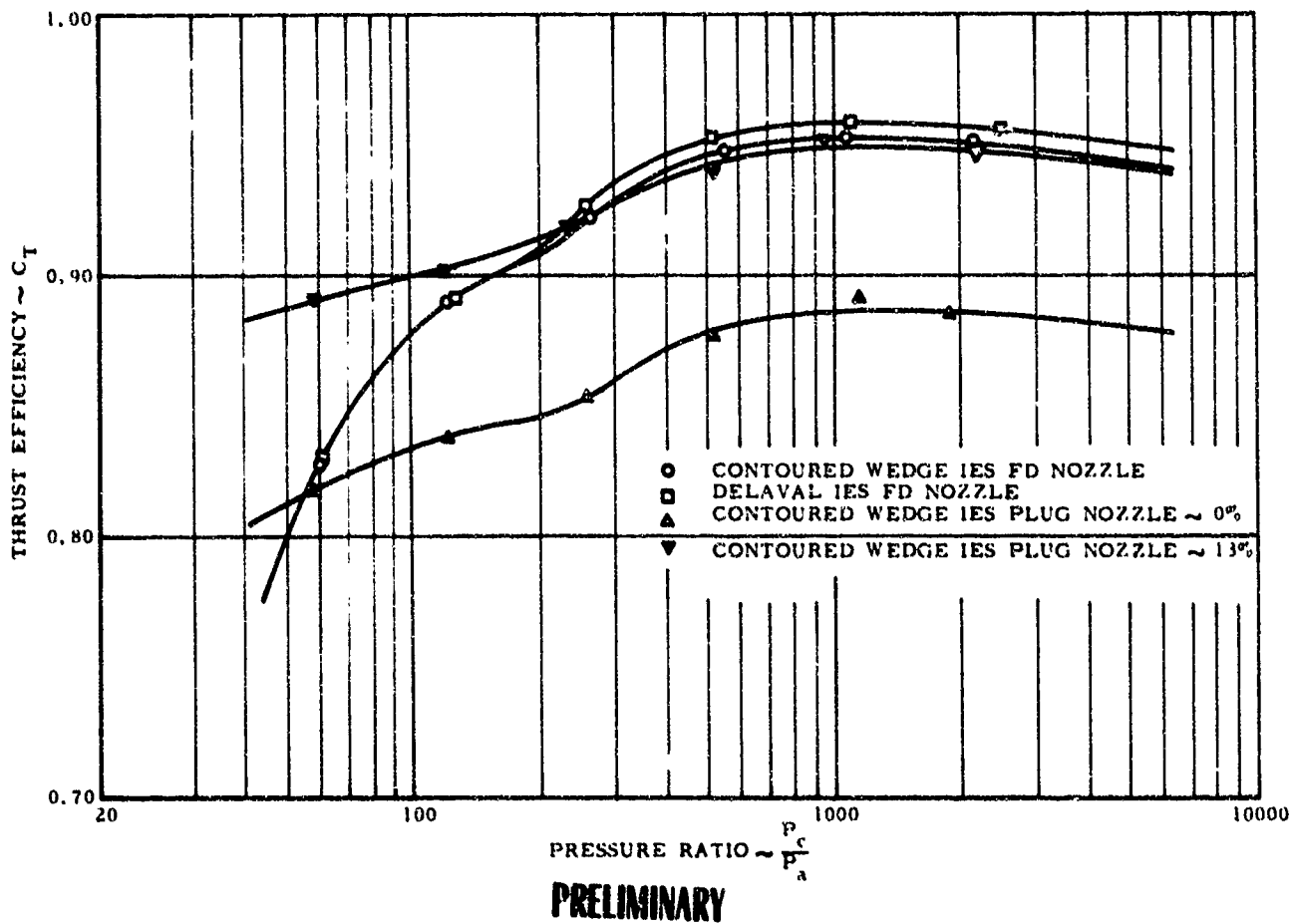
ARES Prototype Model Performance

Figure XVI-1

UNCLASSIFIED

UNCLASSIFIED

Report 10830-Q-4



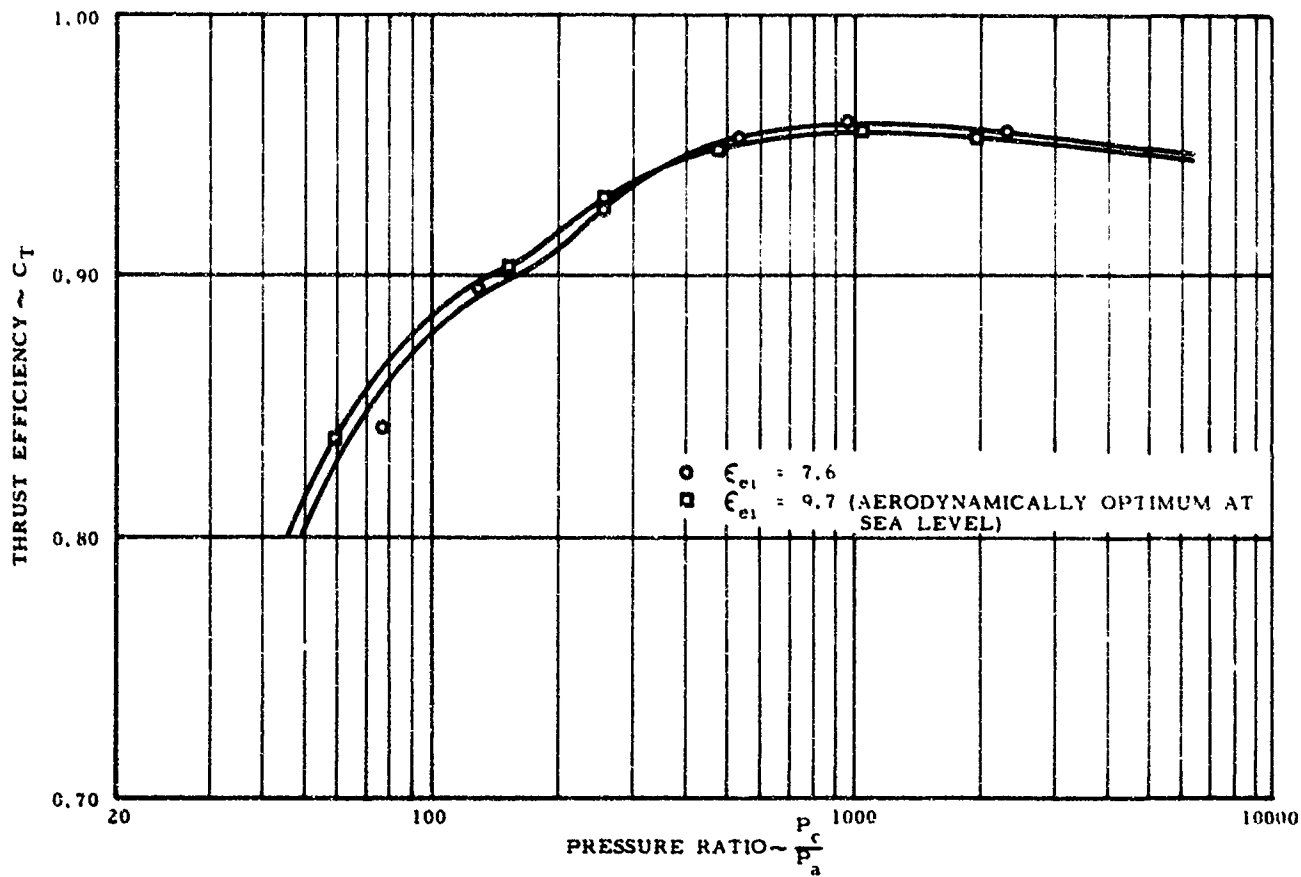
Performance of Several Nozzles Suitable for ARES Application

Figure XVI-2

UNCLASSIFIED

UNCLASSIFIED

Report 10830-Q-4



PRELIMINARY

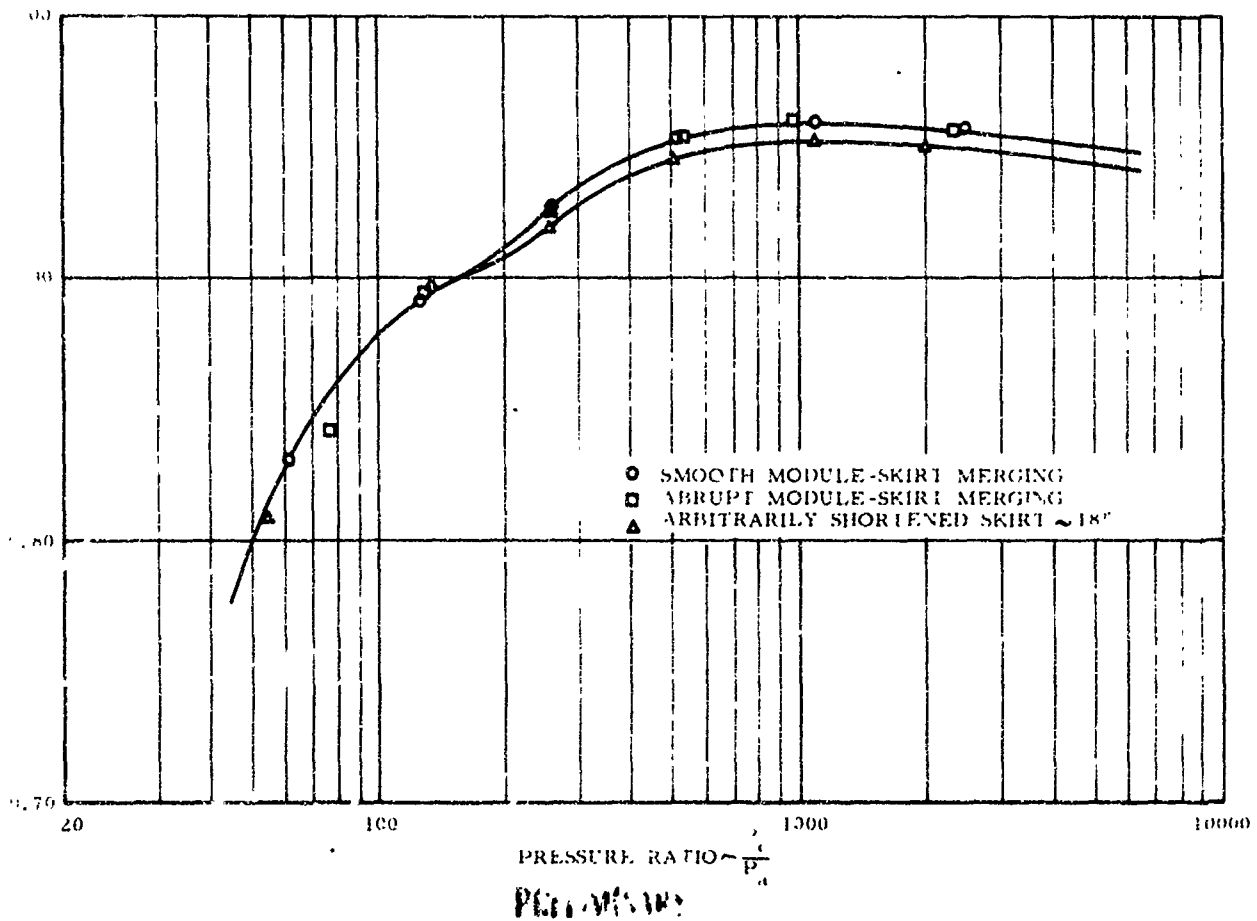
Effect of IBS Area Ratio Variation

Figure XVI-3

UNCLASSIFIED

UNCLASSIFIED

Report 10830-Q-4



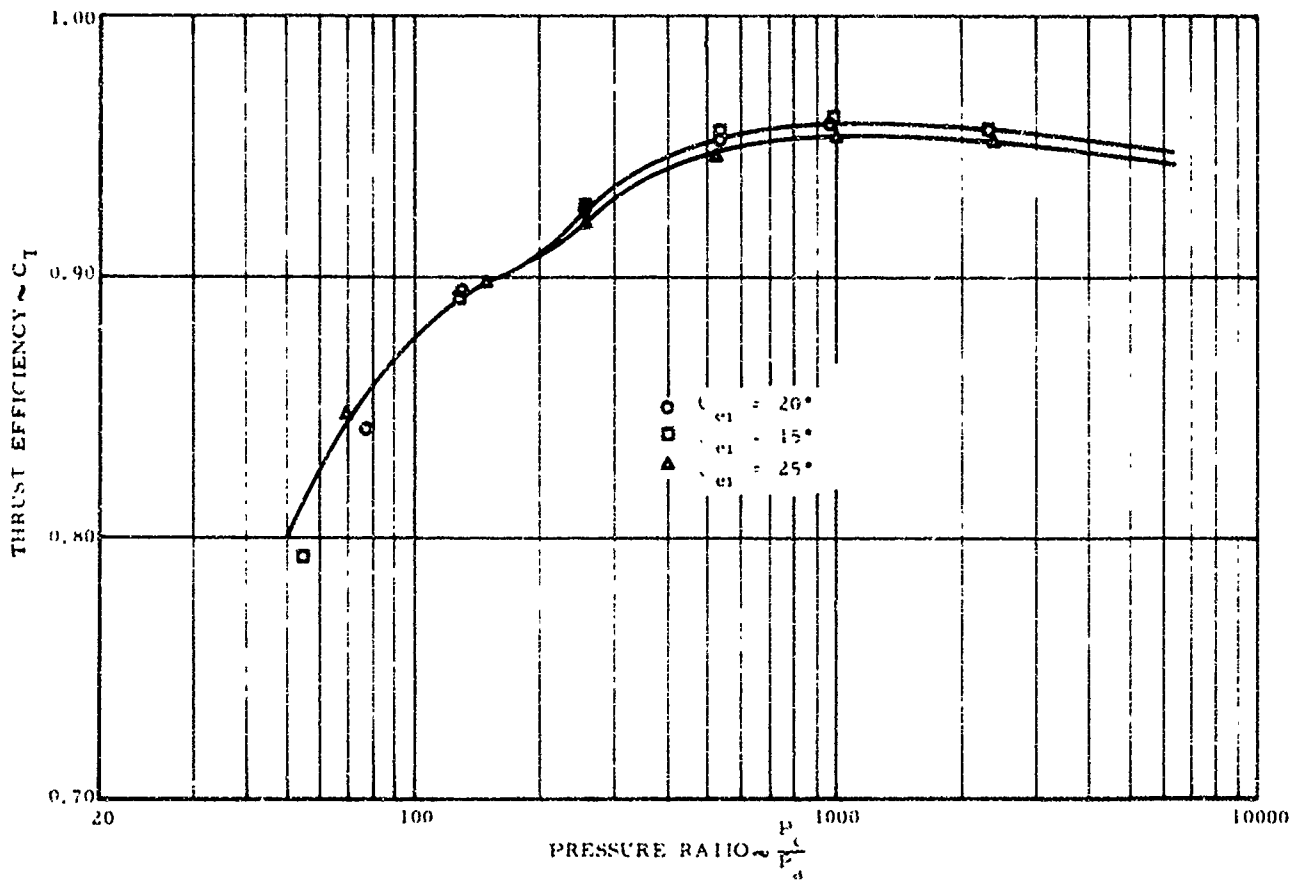
Results of Module-Skirt Merging Study and Effect of Arbitrarily Shortened Nozzle Skirt

Figure XVI-4

UNCLASSIFIED

UNCLASSIFIED

Report 10630-Q-4



PRELIMINARY

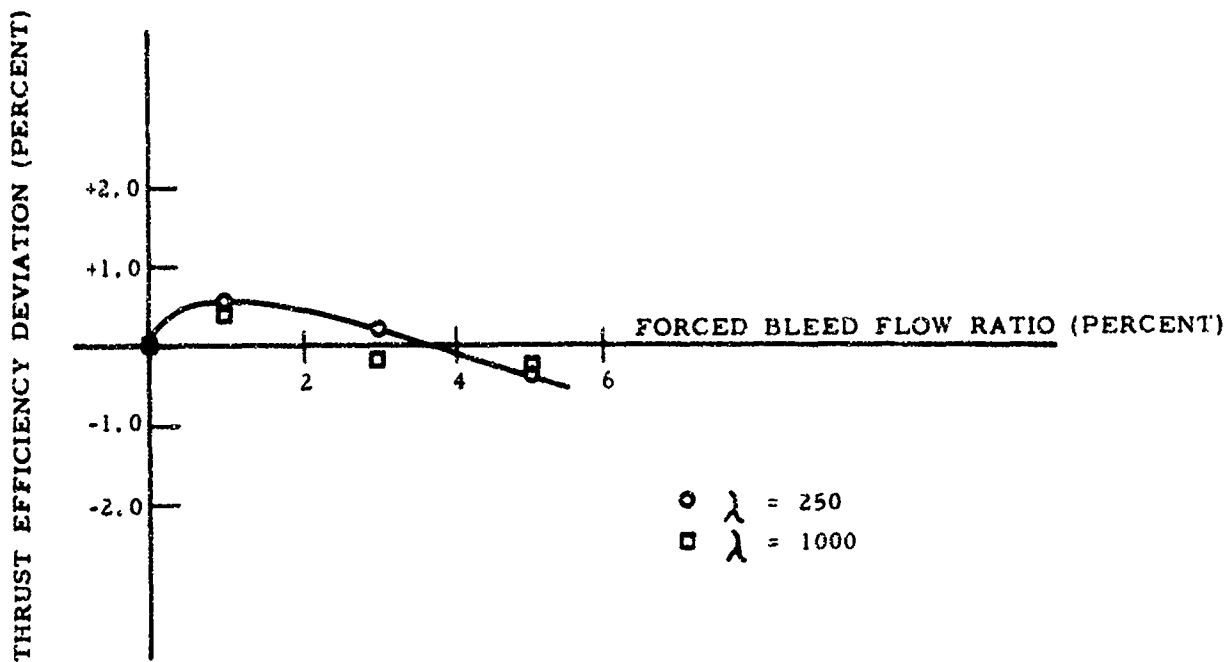
Results of Cant Angle Study

Figure XVI-5

UNCLASSIFIED

UNCLASSIFIED

Report 10830-Q-4



PRELIMINARY

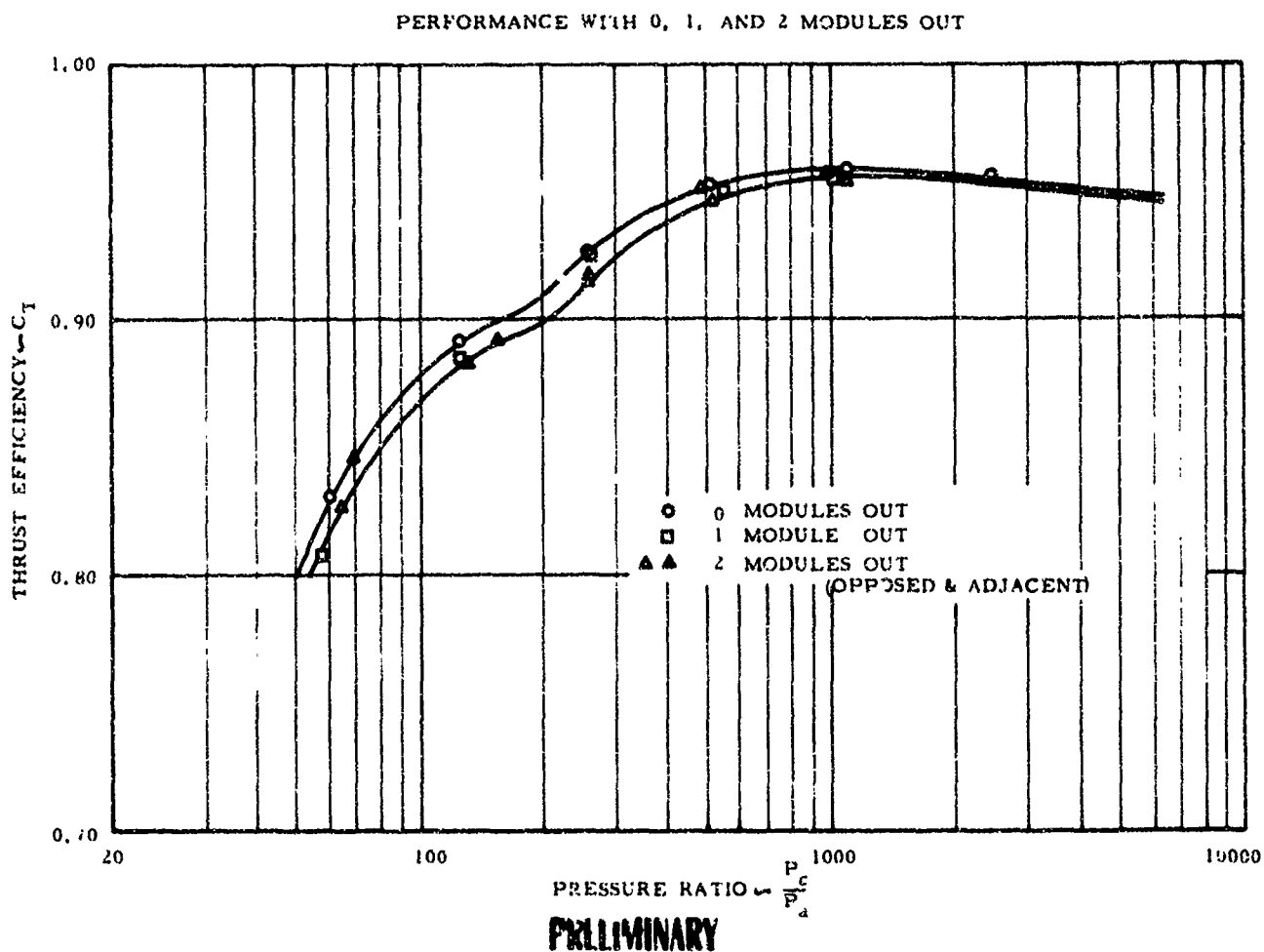
Effect of Forced Base Bleed on Forced Deflection Nozzle Performance

Figure XVI-6

UNCLASSIFIED

UNCLASSIFIED

Report 10830-Q-4



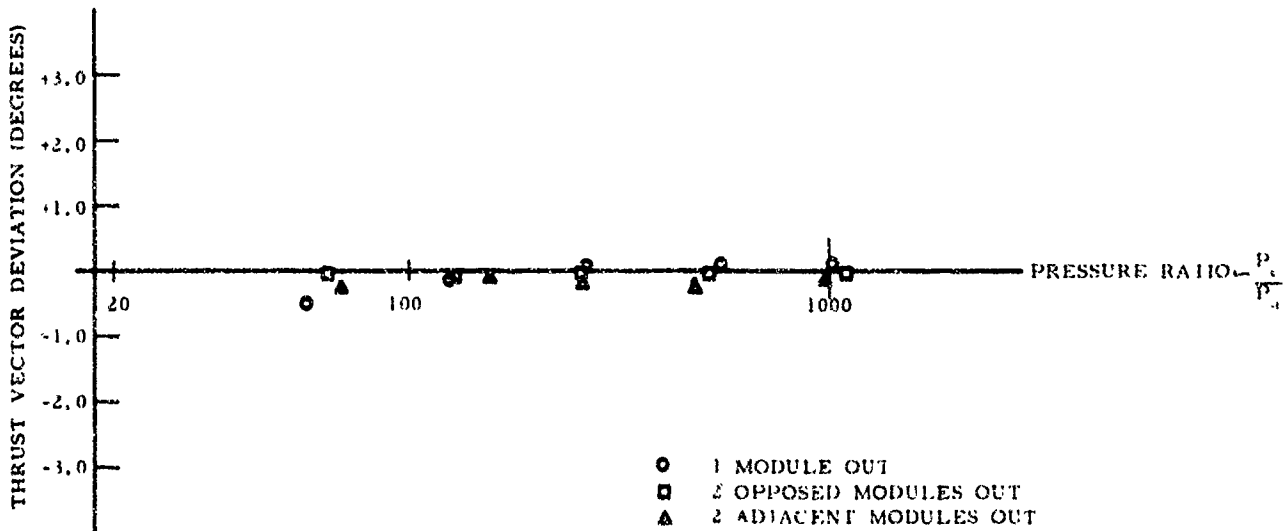
Performance with 0, 1, and 2 Modules Out

Figure XVI-7

UNCLASSIFIED

UNCLASSIFIED

Report 10830-Q-4



PRELIMINARY

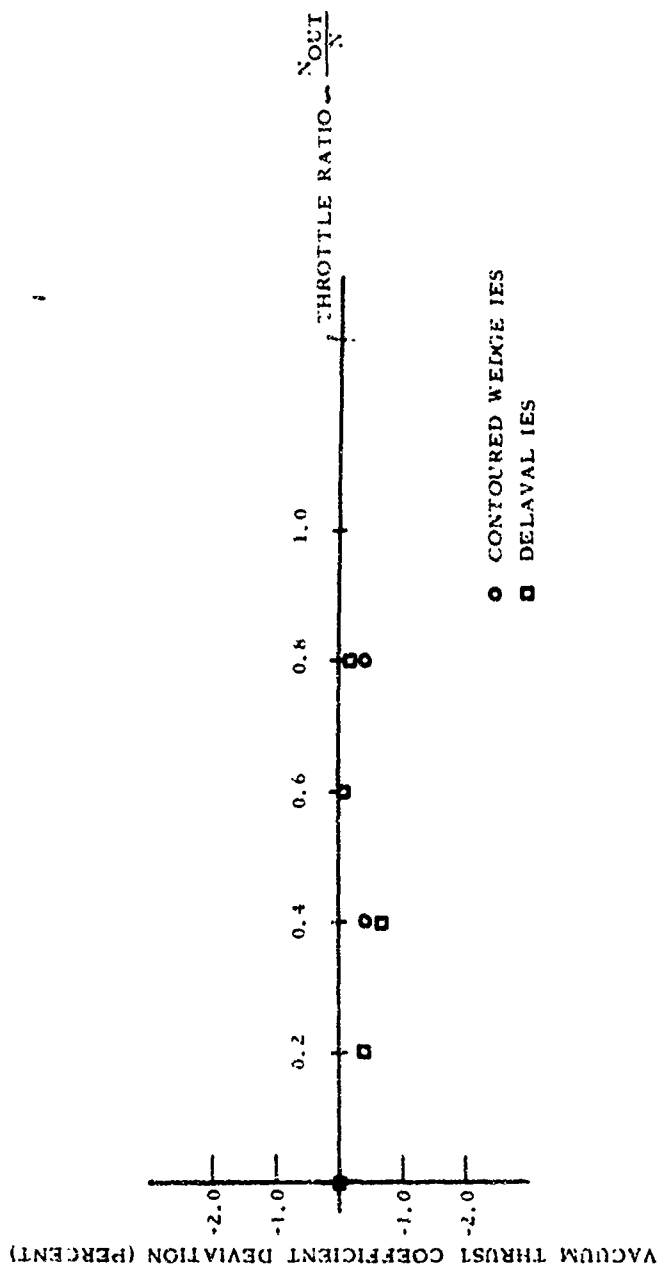
Thrust Vector Misalignment with 1 and 2 Modules Out

Figure XVI-8

UNCLASSIFIED

UNCLASSIFIED

Report 10830-Q-4



Effect on Vacuum Performance of Engine Throttling by Module Shutdown

Figure XVI-9

UNCLASSIFIED

UNCLASSIFIED

Report 10830-Q-4

XVII.

AIR-FLOW MODEL TESTING

A. GENERAL

(u) A simplified cold flow model of the primary combustor was constructed and tested to obtain qualitative data for the effects on flow distribution of turbulators and large-radius centerbodies. These tests revealed a significant effect of turbulator positioning and also showed that large-radius centerbodies are effective in eliminating flow separation at the turbine nozzle inlet.

(u) Testing at the Monterey Naval Postgraduate School of the turbine inlet passage model was completed, and the final report is being prepared. Fabrication of the liquid-oxidizer-passage models was completed and testing has begun. Preliminary data for the oxidizer-passage model are included in this report. Installation of the oxidizer return passage was started and testing will begin in July. Fabrication of the turbine exhaust model was completed, and fabrication of the Mod-I and Mod-II ARES turbine models is on schedule.

B. PRIMARY COMBUSTOR STUDIES

(u) Previous studies of the primary combustor flow field indicated the presence of an adverse pressure gradient in the direction of flow along the inner wall (see Report TR-65-189). These results were obtained using a conducting graphite paper to construct an electrical analog of the flow field. The assumptions of potential flow and no flow separation are inherent in the analogy. However, the presence of an adverse pressure gradient is indicative of the possible existence of a region of flow separation.

(u) The initial results have been extended to include two large-radius centerbody configurations. The two large-radius centerbodies, in addition to the basic configuration, are illustrated in Figure XVIII-1. The potential flow dynamic pressure profiles obtained for both the inner and outer walls of the primary combustor are shown in Figure XVII-2. In a potential flow field, the total pressure of the flow is a constant and the static pressure at any point in the flow field is the total pressure minus the dynamic pressure. Therefore, a higher dynamic pressure corresponds to lower static pressure. The peak dynamic pressure which occurs at the tip of the inner wall corresponds to the minimum static pressure and, as the flow continues around the 180° bend, the dynamic pressure decreases, resulting in an adverse pressure gradient. The large-radius centerbodies are effective in reducing the adverse pressure gradient and, hence, the probability of flow separations and flow distortions.

(u) A simple air-flow model was constructed to check the potential flow results and to further investigate the flow-field effects when turbulence-producing devices (turbulators) are placed in the primary combustor. The model

UNCLASSIFIED

Report 10830-Q-4

XVII, B, Primary Combustor Studies (cont.)

was a full-scale ten-degree wedge section of the primary combustor. The ten-degree wedge was selected to provide a nearly two-dimensional configuration, which facilitated visual flow studies and yet provided a flow field of sufficient thickness not to be significantly distorted by the viscous effects from the bounding radial plates. The model was constructed of wood with a removable 5/8-in.-thick lucite window as one radial plate. The other radial plate was lacquered white to provide a contrasting background. The Mach number of flow was regulated by a sonic nozzle discharging to atmosphere. The model was tested at 30 psia with ambient-temperature air.

(u) Lamp-black and oil-streak photography was used for flow visualization. This technique consists of spraying fine droplets of an oil-and-lamp-black mixture uniformly over the white radial plate. The model, with the streak plate horizontal, is then flowed with air. The resulting oil and lamp-black streaks are recorded photographically. The streaks are not a "picture" of the main flow streamlines, but are a "picture" of the flow streamlines in the boundary layer on the radial plate. The boundary layer streamlines are distorted from those in the main stream due to viscous effects. The boundary layer flow loses a large portion of its momentum to the plate through friction and, therefore, has a greater tendency to flow in the direction of maximum pressure gradient. Although the streak technique cannot be used to indicate the exact flow streamlines (except in the case of one-dimensional flow with favorable pressure gradient), the streak plates can be used to identify gross flow distortions, regions of flow separation, regions of adverse pressure gradient, and relative flow velocities.

(u) The basic model was constructed in the configuration of the primary combustor, and modeling clay was used to simulate large-radius centerbodies and turbulators. Figure XVII-3 shows the resulting streak photographs obtained for three large-radius centerbodies. The basic primary combustor streak plate is shown in Figure XVII-4. The first two large-radius centerbodies, shown in Figure XVII-3, are similar to those assumed in the electrical analog work. The third centerbody is similar to that tested at the Monterey Naval Postgraduate School and was tested at Sacramento for comparison of results. The streak plate of the basic primary combustor, Figure XVII-4, shows the high velocities present at the tip of the centerbody and the region of flow separation just downstream of the turn. The streaks are at a large angle to the outer wall after the turn, and it must be remembered that this is not the true flow direction. The angularity of the streaks is due to the large pressure difference radially from the outer to the inner wall. Tufts have been used to confirm that the true flow direction is very nearly parallel to the outer wall at this point. The streak plates for the large-radius centerbodies, L_2 and L_3 , clearly show some improvement in the flow, i.e., elimination of the regions of flow separation and less distortion of streaks due to pressure difference across the channel. The third centerbody, L_4 , eliminates the region of flow separation but clearly produces higher velocities than necessary at the minimum cross-section of the flow which would result in increased total pressure losses.

UNCLASSIFIED

Report 10830-Q-4

XVII, B, Primary Combustor Studies (cont.)

(u) Figure XVII-4 show the results of an investigation conducted to determine the effect of turbulator positioning, in addition to the basic primary combustor flow effects. It is interesting to note that the B-configuration produces a flow field similar to that obtained with a large-radius centerbody. The region of flow separation does not exist and the streaks are very nearly parallel to the channel walls at the turbine inlet. The B-configuration produces extensive regions of flow separation with attendant high velocities. The C-configuration would produce the most violent turbulence, as expected.

(u) Figure XVII-5 shows the retest results of the final turbulator design. In addition, each turbulator was tested separately to simulate the effect of staggered blades, which more nearly corresponds to the actual design. The individual blade tests show mixed results with respect to effect on flow around the 180-degree bend. It is clearly evident that significant flows in the circumferential direction would be present in the actual combustor.

C. FLUID DYNAMIC TESTING (TPA)

(u) Model tests with air were completed on the turbine inlet passage. Testing was conducted on a full-scale model installed as shown in Figure XVII-6. The Plexiglas test section can be seen on the right side of the model with traversing Pitot probes installed in three locations.

(u) The initial design tested, as specified by turbopump and primary combustor drawings, produced severe flow separations ahead of the turbine nozzles. Flow separation proved to be independent of the centerbody position or of the relative distance between the outer contour of the primary combustor passage and the centerbody.

(u) On the basis of flow visualization studies, an improved centerbody was design and tested. The resulting flow channel can deflect the flow from the primary injector to the turbine inlet by 180° without flow separation and gives nearly uniform turbine inlet conditions.

(u) The loss in total pressure (ΔP_t) of the modified passage is expressed by

$$\frac{\Delta P_t}{P_{t_0}} = 0.0003 \left[\frac{\dot{w} \sqrt{T_0}}{P_{t_0}} \sqrt{\frac{R}{g}} \right]^2$$

where: w = Flow rate, lbm/sec
 P_{t_0} = Total inlet pressure, psia
 T_0 = Total inlet temperature, °R
 R = Gas constant, ft-lb/lbm-°R
 g = 32.2 ft/sec²

UNCLASSIFIED

Report 10830-Q-4

XVII, C, Fluid Dynamic Test (TPA) (cont.)

(u) A perforated plate, simulating the primary injector, did not affect the flow conditions ahead of the turbine nozzles.

(u) Fabrication of all the components for the liquid-oxidizer passage models was completed. The Oxidizer Discharge Passage Model (a) is shown disassembled in Figure XVII-7, prior to installation of the guide vanes. The Oxidizer Return Passage Model (b) is shown disassembled in Figure XVII-7, also prior to installation of the guide vanes.

(u) Preliminary testing of Model (a) was completed and data were provided on the passage pressure drops and outlet flow distribution to the thrust-chamber cooling tubes. Typical flow-distribution results are shown in Figure XVII-8 as a function of the 52 holes which simulate the cooling-tube entrance.

(u) Installation of the Oxidizer Return Passage Model (b) was started, and testing will be conducted during the next reporting period. Following these tests, the two models will be assembled and the complete liquid-oxidizer circuit tested. These tests will provide the primary injector outlet as well as measurements of the flow distribution in the thrust-chamber cooling tubes and from the primary injector.

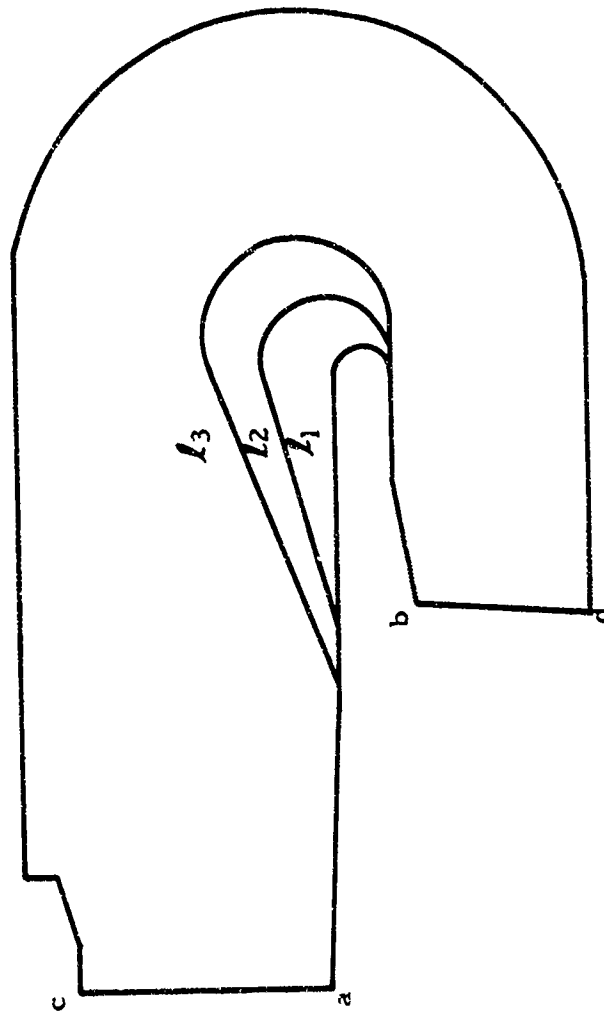
(u) Fabrication of the Turbine Exhaust Passage Model (1) was completed. Testing of this model will be conducted following preliminary testing of the liquid oxidizer passage models now in process.

(u) Fabrication of all components for Mod-I and Mod-II ARES turbines is proceeding on schedule.

(u) Design of the Pump Inlet Housing Model (1) for the back-up TPA was delayed by fabrication and testing priorities on the other models.

UNCLASSIFIED

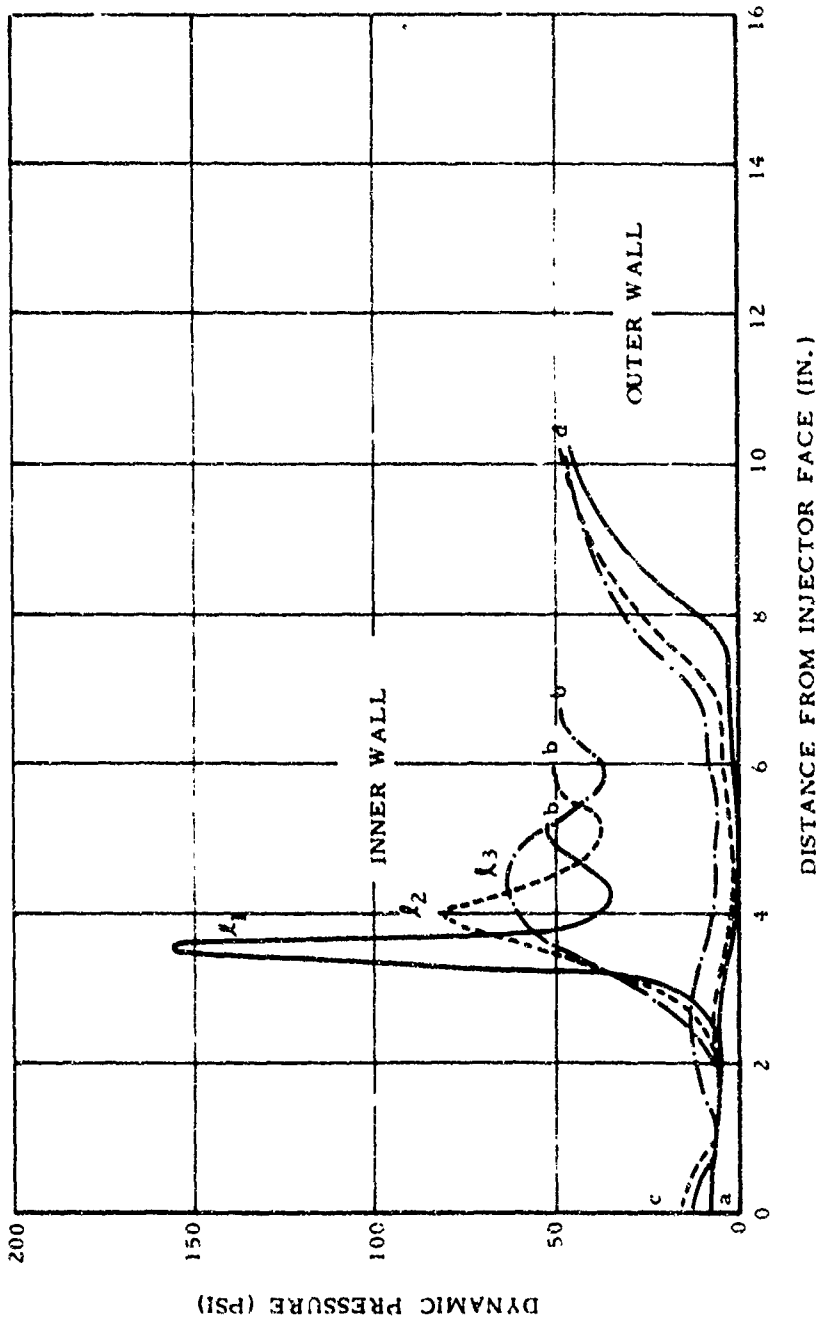
UNCLASSIFIED
Report 10830-Q-4



Large Radius Primary Combustor Centerbodies

Figure XVII-1

UNCLASSIFIED



Large Radius Centerbody Potential Flow Dynamic Pressures

UNCLASSIFIED

Report 10830-Q-4



CENTER BODY L2



CENTER BODY L3



CENTER BODY L4

Streak Plate Results for Large Radius Centerbodies

Figure XVII-3

UNCLASSIFIED

UNCLASSIFIED

Report No. 30-Q-5



TURBULATOR CONFIGURATION A



TURBULATORS, CONFIGURATION C



REFERENCE PRIMARY COMBUSTOR



TURBULATORS, CONFIGURATION B

Streak Plate Results for Various Turbulator Positions

Figure XVII-4

UNCLASSIFIED

UNCLASSIFIED

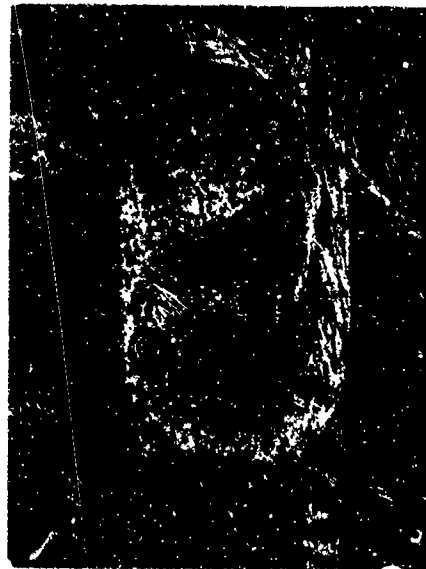
Report 10230-12-4



TURBULATORS, SELECTED CONFIGURATION



OUTER TURBULATOR ONLY



INNER TURBULATOR ONLY

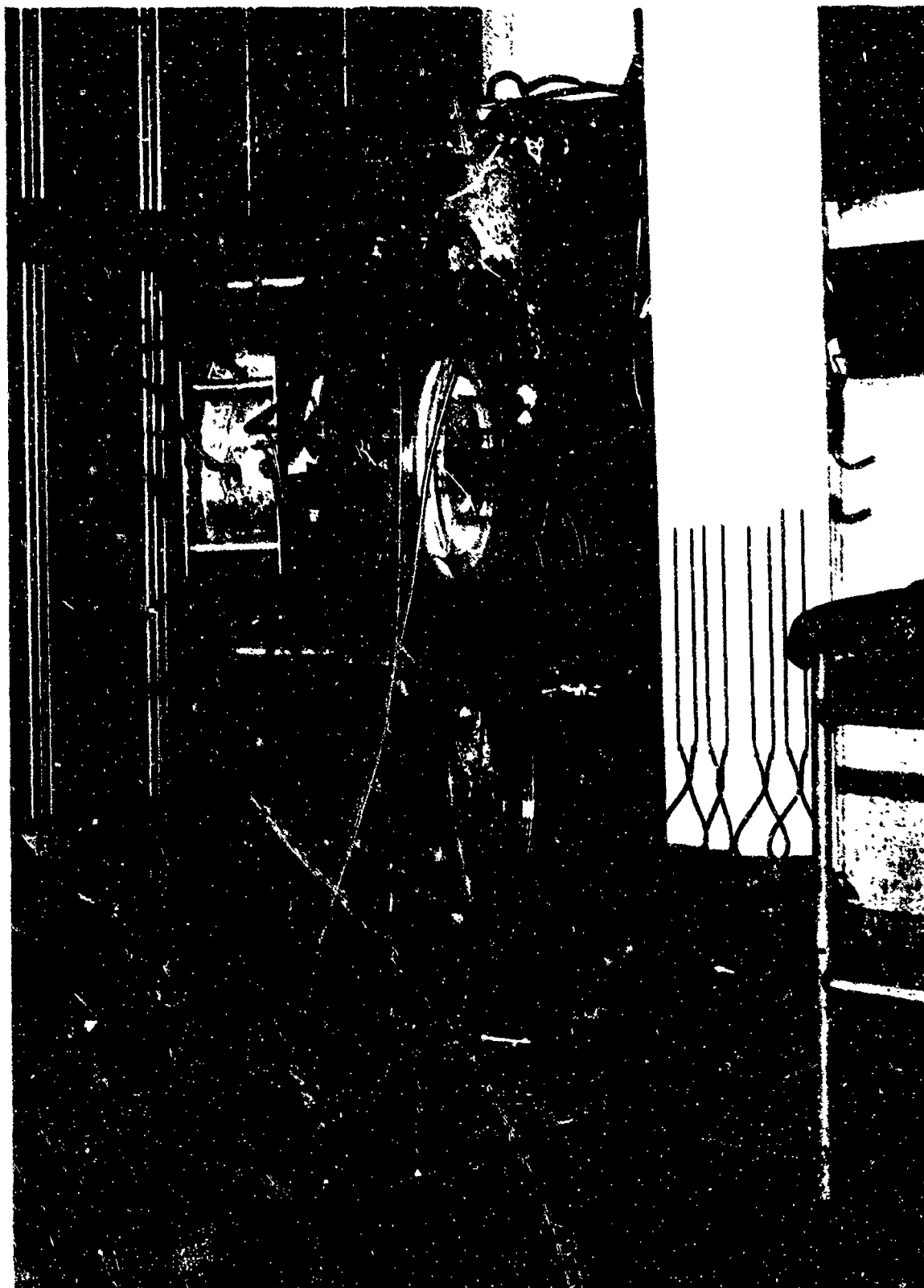
Streak Plate Results for Selected Configuration

Figure XVII-5

UNCLASSIFIED

UNCLASSIFIED

Report 10830-Q-4



Turbine Inlet Passage Model (L) Installation

Figure XVII-6

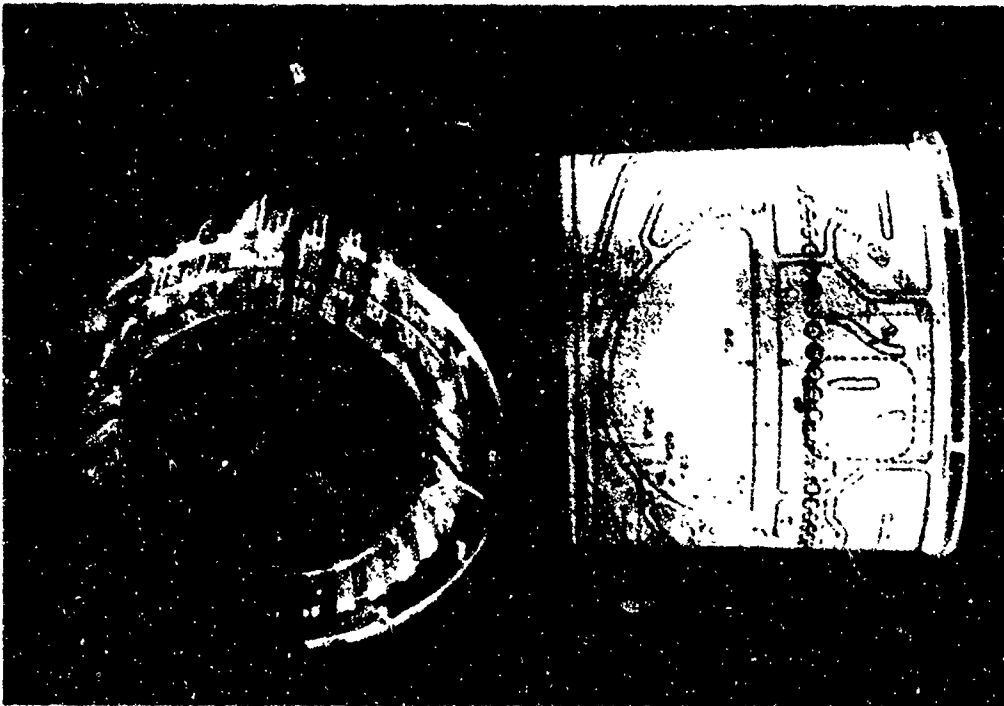
UNCLASSIFIED

UNCLASSIFIED

Report 10830-Q-4



OXIDIZER DISCHARGE PASSAGE MODEL (a) WITHOUT VANES - EXPLODED VIEW



OXIDIZER RETURN PASSAGE MODEL (b) WITHOUT VANES - EXPLODED VIEW

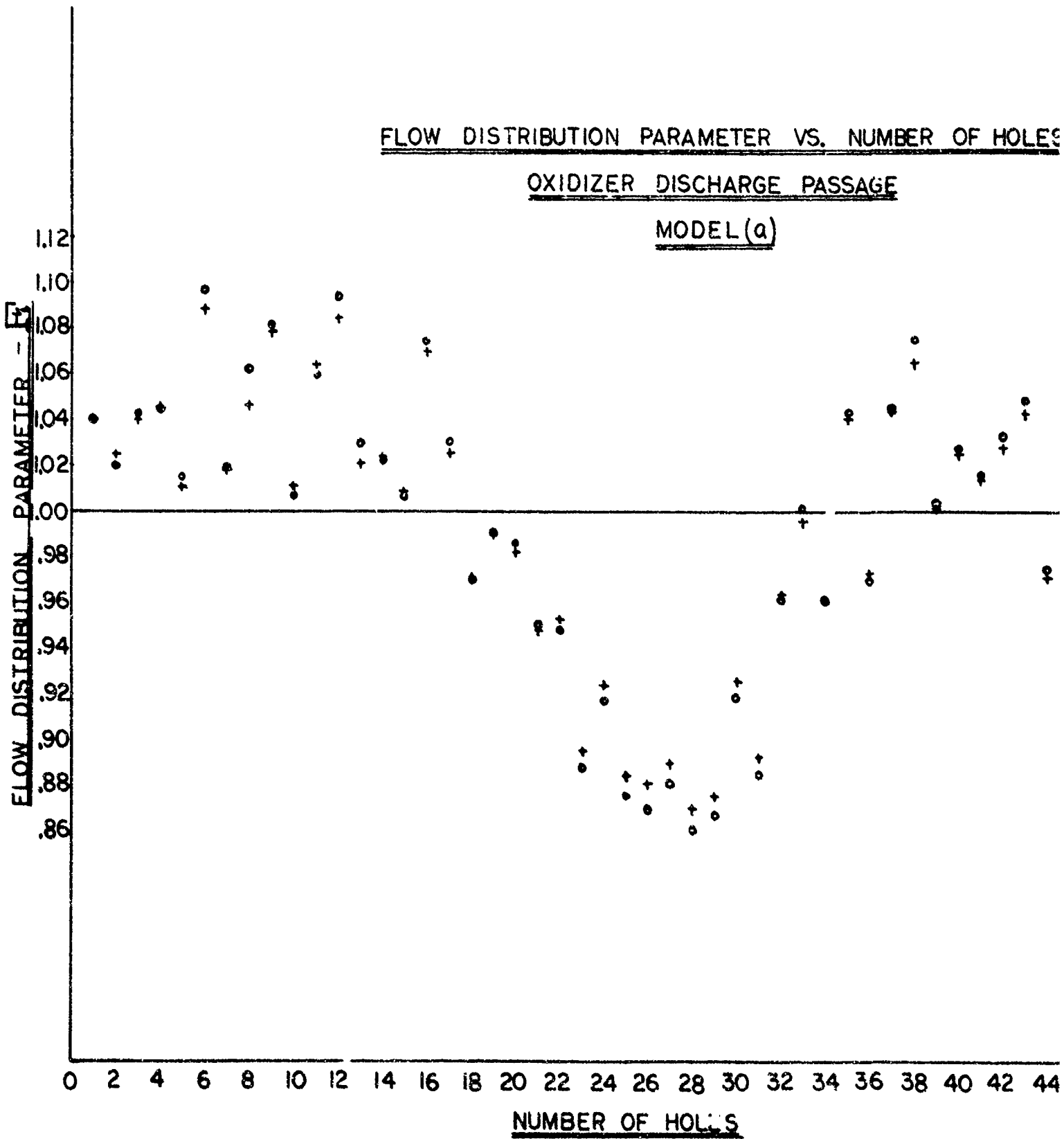
Oxidizer Passage Models

Figure XVII-7

UNCLASSIFIED

UNCLASSIFIED

Report 10830-Q-4



Flow Distribution Parameter--Oxidizer Discharge Passage

Figure XVI-8

UNCLASSIFIED

NUMBER OF HOLES

E

$$F_i = \frac{52\sqrt{q_i}}{\sum_{i=1}^n \sqrt{q_i}} \quad \text{WHERE:}$$

$$q_i = \Delta H_{\text{static}} \text{ (cm. H}_2\text{O)}$$

$$W_u^* = 7.313 Y_1 \sqrt{\frac{P_u - P_b}{P_u}}$$

$$W_{\text{IN}}^* = W_u^* \frac{P_u}{(P_{\text{TOT}})_{\text{IN}}}$$

$$Y_1 = 1 - .369 \left(\frac{P_u - P_b}{P_u} \right)$$



Run No.	Pt. No.	W_{IN}^* in ²	$(P_{\text{TOT}})_{\text{IN}}$ cm. H ₂ O absolute	T_{IN} °F	P_u cm. H ₂ O absolute	$P_u - P_b$ cm. H ₂ O	
+	5	1	.624	1300	76	1308.25	9.71
o	5	2	.525	1196.5	76	1201.08	6.11

6 38 40 42 44 46 48 50 52

UNCLASSIFIED

Report 10830-Q-4

XVIII.

HEAT-TRANSFER ANALYSIS

A. GENERAL

(u) The objectives of the heat-transfer effort are to provide the necessary analysis for the design of both the regeneratively and the transpiration-cooled thrust chambers and other engine components, including analyses of test data to aid in the design of such chambers. The development of a satisfactory thermal barrier, optimization of film-cooling for the ARES environment, and special thermal analysis to support component designs are also part of this effort.

(u) The accomplishments of the heat-transfer effort during this reporting period are itemized below.

1. Two additions have been made to the "Regeneratively and Film Cooled Thrust Chamber" computer program: (a) the capability of analyzing pressure drop in tubes of various absolute roughnesses and (b) the capability of evaluating the effect of film cooling carryover in two-point injection chambers.

2. The utilization of capillary tubes in the regeneratively cooled chamber has been re-evaluated to consider the effect of heat addition and the true absolute roughness.

3. A series of heated tube tests to determine the burnout-heat-flux characteristics of high-pressure (up to 6000 psia) N_2O_4 in small tubes (0.019 in. ID) has been completed.

4. The analytical effort pertaining to the design and first test of the transpiration-cooled chamber and has been completed.

5. The second phase of the thermal-barrier investigation including experimental evaluation of braze bonding, techniques of plasma-process improvement, and sprayed Hastelloy-X has been completed.

6. Support of the component design efforts continued, including heat-transfer analysis of the advanced TPA housing and stator and hydraulic analysis of the primary combustor fuel circuit.

B. ARES THRUST CHAMBERS

1. Regeneratively Cooled Chambers

a. Computer Program Modification

(u) Two modifications have been incorporated in the "Regeneratively and Film Cooled Thrust Chamber" computer program. The first modification was made to facilitate the evaluation of multiple-point film-coolant injection

UNCLASSIFIED

Report 10830-Q-4

XVIII, B, ARES Thrust Chamber (cont.)

by providing a means of approximating the coolant carryover effect downstream of the second film-coolant injection port. It is anticipated that this could be accomplished in a two-step procedure. Initially, only the first injection point would be considered to establish the temperature of the N_2O_4 film, which, subsequently, heats the coolant injected from the second injection point. These temperatures would then be input in a second computer run as the mainstream gas temperatures. The heat-transfer coefficient at the interface between the two N_2O_4 streams would be calculated internally using the Colburn equation:

$$h_g = \frac{0.027K}{D} (Re)^{0.8} (Pr)^{0.4}$$

where:

- h_g = Heat-transfer coefficient between N_2O_4 layers
- K = Conductivity of N_2O_4 at average temperature of layers
- D = Chamber diameter
- Re = Reynolds Number of N_2O_4 from first injection point
- Pr = Prandtl Number of N_2O_4 from first injection point

This modification to the program necessitated the inclusion of the following options:

- (1) Inputting the mainstream temperature at each station or calculating a recovery temperature based on the gas stagnation temperature and local velocity.
- (2) Calculating the gas-side heat-transfer coefficient for a film-cooled case based on N_2O_4 properties or mainstream gas properties.

The above modification to the computer program is currently being checked out to determine the best means of utilizing this capability.

(u) The second modification to the computer program consists of a refinement to the method of calculating the pressure drop due to friction in the coolant tubes. Previously, the pressure drop in the tubes was calculated based on a constant relative roughness (ϵ/D) in the tubes of 0.0001. With the modification, the absolute roughness (ϵ) is input and held constant throughout the tubes. The relative roughness is calculated for each tube-length increment based on the local tube hydraulic diameter. The corresponding friction factor, f , is then calculated based on the empirical relation:

UNCLASSIFIED

Report 10830-Q-4

XVIII, B, ARES Thrust Chambers (cont.)

$$f = 0.0055 [1 + (2 \times 10^4 \epsilon/D + 10^6/Re)^{1/3}]$$

where:

- f = Friction factor
- ϵ = Absolute roughness of tube
- D = Hydraulic diameter of tube
- Re = Reynolds Number

The above equation is an algebraic representation of the Moody diagram.*

(u) The equation for pressure drop between stations remains unchanged:

$$\Delta P = \frac{f \rho \Delta L V^2}{D 2g}$$

where:

- ΔP = Pressure drop between stations
- f = Friction factor
- ΔL = Distance between stations
- V = Velocity mid-way between stations
- D = Hydraulic diameter mid-way between stations
- ρ = Fluid density mid-way between stations
- g = Gravitations constant

b. Capillary Tube Studies

(u) The absolute roughness of two modified ICP capillary tubes was investigated experimentally. The tubes (PN 1129150-5 and -7) had uniform inside diameters of 0.044 and 0.055 in., respectively. Each had a uniform wall thickness of 0.004 in. and a length of 9 in. These tubes were flow-tested with water in the hydraulics laboratory.

* L. F. Moody, "Friction Factors for Pipe Flow," Trans. ASME, November, 1944.

UNCLASSIFIED

Report 10830-Q-4

XVIII, B, ARES Thrust Chambers (cont.)

(u) The flow-test data consisted of inlet and outlet pressures and flow rates for two test conditions: (1) a constant inlet pressure of 2800 psia with varying back pressure (400 to 2300 psia); and (2) varying inlet pressure (2000 to 2800 psia) with a constant back pressure of 300 psia. These data were used to evaluate the friction factors and corresponding absolute roughnesses for the two tubes.

(u) The evaluation revealed absolute roughness values of about 90μ for the 0.044-in.-dia tube and of 200 to 300μ for the 0.055-in.-dia tube. These values correspond to a friction-factor variation of about 0.023 to 0.032 in the present capillary tube design. Utilizing the new computer-program capability described above, the results of the capillary tube study presented in Report TR-66-82 (third quarterly report) were reviewed. The increased pressure drop which could be anticipated in the selected 0.045-in.-ID capillary tubes indicated that a larger tube might be a better selection. As a result, a 0.055-in.-ID tube with a nozzle exit diameter of 0.035 in. was evaluated for use in the first capillary tube chamber (SN 3). Enough tubes of this configuration for one chamber are available from the ICP program. This larger tube satisfies the criteria established earlier for the 0.045-in.-ID tube, i.e., a capability range which encompasses the high flow rates desired for initial tests as well as the flow rate associated with the total allowable flow for Phase I. Additionally, the nozzle exit provides the high injection velocities desired for increasing film-cooling effectiveness.

(u) The effects of heat addition to the uncoated capillary tubes of both sizes were evaluated. The fluid bulk temperature is increased substantially by heat addition over the 8 in. of heated length. As a result, the film coolant required from these tubes to cool the convergent portion of the chamber of the throat is increased from those values previously reported. A minimum film-coolant flow rate of 24.7 lb/sec is required from heated 0.045-in.-ID tubes as compared with 13.8 lb/sec for unheated tubes. The minimum required from the heated 0.055-in.-ID tubes is 20.5 lb/sec. The effect of film cooling carryover from the first injection station is not considered in these numbers. The capability of analyzing the effect is now available in the computer program used for these analyses, and the final predicted requirements will take this effect into account.

(u) The maximum flow rate available through the 0.055-in.-ID tubes is 25 lb/sec compared to the conservative requirement of 20.5 lb/sec, whereas the maximum available through the 0.045-in.-ID tubes is 22 lb/sec compared to the conservative requirement of 24.7 lb/sec. This situation led to the selection of the 0.055-in.-ID capillary tube for use in the first capillary tube chamber.

(u) The additional consideration of the heat addition to the capillary tubes and the effect of the resulting outlet velocity and temperature did not change the selection of a point 8 in. axially downstream of the injector face as the location for the second point of film-coolant injection.

UNCLASSIFIED

Report 10830-Q-4

XVIII, B, ARES Thrust Chambers (cont.)

c. Heated-Tube Tests

(u) Heat-transfer tests were conducted to determine experimentally the heat-transfer characteristics of nitrogen tetroxide (N_2O_4) in very small tubes at ARES combustion-chamber conditions. Test data have not yet been analyzed and therefore will be included in a future report. These tests will provide information as to the feasibility of self-cooling capillary tubes and/or a microflow liner. The effects of small tube diameter, high velocities, high pressures, and high bulk temperatures on the burnout heat flux of N_2O_4 will be determined.

(u) A previous investigation* evaluated the burnout heat flux of supercritical N_2O_4 using 0.13-to-0.40-in.-ID tubes at velocities of 11 to 180 ft/sec, pressures of 1700 to 2500 psia, and bulk temperatures of 100 to 285°F. Certain prospective ARES chamber designs include very small tubes (ID as small as 0.019 in. for the microflow liner) in which velocities to 600 ft/sec, pressures to 5000 psia, and bulk temperatures to 500°F are expected. Estimation of the burnout heat flux at these conditions from the existing data is difficult. Therefore, a series of six tests was conducted to evaluate the relative effects of these conditions.

(u) The test sections were straight, 304 stainless-steel tubes of circular cross section and constant flow area. Each had an inside diameter of 0.019 in. and a wall thickness of 0.006 in.

(u) The first test was essentially a repeat of the flow conditions at which burnout was observed previously in a 0.13-in.-ID tube (Test D-110-LC-3, reported in the reference**). The results of this test should indicate the effect of the small tube diameter.

(u) Subsequent tests simulated flow conditions expected in the proposed ARES microflow-liner chamber. These conditions correspond to total weight flows up to 30 lb/sec for film-cooling the convergent portion of the chamber downstream of the microflow liner.

(u) Details of the test setup, individual test conditions, and results will be documented at the completion of data analysis.

* W. R. Thompson, E. L. Gerry, and J. F. Harkee, An Experimental Study of the Heat Transfer Characteristics of Nitrogen Tetroxide at Supercritical Pressures, Technical Memorandum 163-64-39, Aerojet-General Corporation, Azusa, California, 12 June 1964

** Ibid

UNCLASSIFIED

Report 10830-Q-4

XVIII, B, ARES Thrust Chamber (cont.)

2. Transpiration-Cooled Chamber

a. Comparison of the Boundary Layer Mixing Model with the Hatch and Papell Film Cooling Model

(u) The approach made in determining the gas-side convective boundary conditions was to consider each individual platelet as a distinctly separate film-cooling entity. This means that each platelet would be affected externally only by the fluid which had passed through the platelet on the upstream side, and that film-coolant carryover from adjacent upstream platelets would not be considered. This approach is admittedly unrealistic, but was necessary to keep the hand calculations within reason.

(u) The currently accepted film-cooling model utilized is that developed by Hatch and Papell*. It evolved from a very simple model which basically consists of an adiabatic flat plate on which it was assumed that the coolant film exists as a discrete layer, that the temperature profile in the coolant film does not change rapidly in the flow direction, that the temperature gradient through the coolant is small, and that conditions are uniformly normal to the flow direction. It can be readily seen that few, if any, of these restrictions are met for the conditions assumed in the ARES analysis. First, the chamber surface is exposed to a very severe pressure gradient and is not at all adiabatic from the standpoint of an individual platelet regardless of how small the energy loss from the mainstream to the individual platelets is relative to the total energy existing within the mainstream. Furthermore, when this model is used, the temperature does change rapidly in the flow direction over an individual platelet and the temperature difference in the flow direction is equivalent to that normal to the flow direction. The extent to which this model is forced can be appreciated when one considers that on the average the boundary layer momentum and the thermal thicknesses are of the same order of magnitude as the width of an individual platelet.

(u) The heat-transfer coefficients between the mainstream and the coolant were taken from the ARES regeneratively cooled chamber analysis for which heat-transfer coefficient factors, or Bartz factors, were applied ranging from 1.5 within the cylindrical portion of the chamber, varying with chamber diameter to a factor of 1.0 at the throat section and through the divergent section. These heat-transfer coefficients do not take into account the thermodynamic properties associated with the mass addition of the H_2O_4 into the mainstream. The heat-transfer coefficients assumed to exist between the coolant and the wall are the same as those assumed between the hot gas stream and the coolant stream, except that no heat-transfer coefficient factors are applied. Figure XVIII-1 shows in schematic form the relationships of the hot-gas convective exchange with the platelet.

* J. E. Hatch and S. S. Papell, Use of a Theoretical Flow Model to Correlate data for Film Cooling or Heating an Adiabatic Wall by Tangential Injection of Gases of Different Fluid Properties, NASA TN D-130, Nov. 1959

UNCLASSIFIED

Report 10830-Q-4

XVIII, B, ARES Thrust Chamber (cont.)

(u) Figure XVIII-2 shows results typical of the Hatch and Papell film-cooling model. The first group of curves indicates the differences in the effective film temperature for a constant initial film temperature and various Bartz factors. The second group of curves shows the difference in the effective film temperature predicted for a constant Bartz factor of 1.5 and various initial film temperatures. Since the one-dimensional conduction model requires a constant film-temperature input as one of the thermal-boundary conditions, the "Beta Curves" are integrated over the platelet surface for an average effective film temperature. Modifications to the existing film-cooling program to provide a direct printout of the average effective film temperatures are being made.

(u) Since the Hatch and Papell film cooling model is fundamentally an empirically adjusted control-volume energy-balance approach, it was decided to utilize an approach which would take into account the physical characteristics of the boundary layer and paradoxically neglect the coolant carryover from upstream adjacent platelets. The analysis chosen was that advanced by Stollery and El Ehwany* modified by LaBotz** to extend the range of Reynold's number for which it could be applied.

(u) This boundary-layer mixing model, as it will be referred to, considers the mass profile of the boundary layer and differentiates as to its composition. The total mass of the injected coolant is assumed to remain within the boundary layer, and the difference between this quantity and that predicted for the entire boundary layer is assumed to be entrained from the mainstream flow. The analysis further assumes that the temperature of this resultant mixture is obtained by means of an energy balance between the injected coolant and the entrained mainstream gas required to satisfy a mass balance on the boundary layer. The effect of pressure gradient is not considered in this analysis, but can be included when the history of the entire boundary layer is to be considered.

(u) Stollery and El Ehwany assume that the mass-velocity power law holds to the 1/7 power to give the relationship:

$$\frac{\rho u}{\rho_\infty u_\infty} = \left(\frac{y}{\delta}\right)^{1/7} \quad (\text{Eq 1})$$

The mass flow rate in the boundary layer is:

$$\dot{M}_{bL} = \int_0^\delta \rho u dy \quad (\text{Eq 2})$$

* J. L. Stollery and A. A. M. El Ehwany "A Note on the Use of a Boundary-Layer Model for Correlating Film Cooling Data", Int. Journ. of Heat Mass Transfer, Vol. 8, pp 55-65, 1965

** R. J. LaBotz, "Boundary Layer Mixing Analysis," unpublished Correspondence, Department 9648, LRO, Aerojet-General Corporation.

UNCLASSIFIED

Report 10830-Q-4

XVIII, B, ARES Thrust Chamber (cont.)

substituting (Eq 1) into (Eq 2) and integrating,

$$\dot{M}_{bL} = \frac{7}{8} \rho_{\infty} u_{\infty} \delta$$

LaBotz now solves for the boundary-layer thickness in a more general manner so as to avoid the restrictions imposed by the relationship used by Stollery and El Ehwany: namely, $\delta = 0.37 X Re_x^{-1/5}$, and the 1/7 power velocity law.

(u) LaBotz follows Schlichting's development* of the velocity distribution as a function of the Blasius law of friction which is applicable to both the fully developed turbulent flow in a pipe and the turbulent flow along a flat plate. From this basic law, generalized relationships between the friction velocity and other flow parameters are developed. Then, the wall shear stress is related to the growth of the boundary-layer-momentum thickness and subsequently, the ratio of momentum thickness to boundary-layer thickness for a flat plate with a generalized profile is developed. After some substitution and rearranging, LaBotz arrives at a generalized expression for the boundary-layer thickness

$$\delta = X^{\frac{n+1}{n+3}} \left[\frac{n C_n^{\frac{2n}{n+1}}}{(n+3)(n+2)} \left(\frac{\rho_{\infty} u_{\infty}}{\mu_{\infty}} \right)^{\frac{2}{n+1}} \right]^{-\frac{n+1}{n+3}}$$

where n is an exponent in the dimensionless velocity profile and is a function of the Reynold's number referenced to the chamber diameter. C_n is a function of n and is given on Page 507 of Schlichting*. X is the distance downstream of the coolant injection slot.

(u) LaBotz's form of the boundary layer mass relationship is now

$$\dot{M}_{bL} = \frac{n}{n+1} \rho_{\infty} u_{\infty} \delta [f(n)] \quad \text{and}$$

$$\dot{M}_{bL} = C (\rho_{\infty} u_{\infty})^{\frac{n}{n+1}} X^{\frac{n+1}{n+3}} \left[\frac{n C_n^{\frac{2n}{n+1}}}{(n+3)(n+2)} \left(\frac{\rho_{\infty} u_{\infty}}{\mu_{\infty}} \right)^{\frac{2}{n+1}} \right]^{-\frac{n+1}{n+3}}$$

where C is a constant (0.82) employed to bring the results more in line with experimental data.

* H. Schlichting Boundary Layer Theory, McGraw Hill, Fourth Edition, New York, 1960, p. 506.

UNCLASSIFIED

Report 10830-Q-4

XVIII, B, ARES Thrust Chamber (cont.)

(u) The analysis now considers that the mass within the boundary layer which is entrained from the mainstream is:

$$\dot{M}_e = \dot{M}_{bL} - \dot{M}_c$$

Furthermore, an energy balance on a small section of the boundary layer yields:

$$T_F = \frac{(T_{Fi} \dot{M}_c C_{pc}) + T_o (\dot{M}_{bL} - \dot{M}_c) C_{pg}}{\dot{M}_c C_{pc} + (\dot{M}_{bL} - \dot{M}_c) C_{pg}} = f(X)$$

(u) T_F can be plotted as a function of the distance along the platelet in a manner similar to that of Hatch and Papell. Figure XVIII-2 shows a comparison of the boundary-layer mixing model with the Hatch and Papell model for similar conditions. It can be seen that the integrated average of the boundary-layer mixing model compares quite well with the Hatch and Papell model employing a 1.5 Bartz factor, which is the design value. However, in the throat region, a difference of some 15% is predicted, with the boundary-layer mixing model indicating the higher wall temperatures for a given coolant flow rate.

(u) It is inappropriate to consider whether the boundary-layer mixing model is more realistic than the Hatch and Papell film-cooling model in predicting the wall temperatures that will occur for a given flow rate since neither analysis includes the effect of coolant carryover. It is believed that if the total boundary-layer history, including carryover, were considered, the boundary-layer mixing model would provide the most realistic approach to the problem solution. Some treatment of the effort of coolant carryover similar to that which is advanced by Sellers* would be a good first approach to the problem. Ultimately, a comprehensive boundary-layer analysis is required which will consider the total boundary-layer history of mass transport and chemical reaction. The other and perhaps more expedient approach is to obtain valid data and empirically determine correlative relationships between the mass transfer to the boundary layer and the resultant wall temperatures. Hopefully, valid data in conjunction with more realistic hydrodynamic, thermal, and chemical reactive models will provide the best solution to the heat-transfer analysis of this advanced cooling concept.

b. Radial Wall-Temperature Distribution

(1) 0.021-in. Platelets

(u) Figure XVIII-3 shows the radial wall-temperature distribution calculated using the advanced thermal model shown in Figure XVIII-1

* J. P. Sellers, Jr. "Gaseous Film Cooling with Multiple Inspection Stations," AIAA Journal, Vol I, No. 9, Sept. 1963

UNCLASSIFIED

Report 10830-Q-4

XVIII, B, ARES Thrust Chamber (cont.)

for 0.021-in. platelets located within the cylindrical chamber section operating with coolant flow rates which establish surface temperatures of 1500 and 1830°F. The plot gives the metal temperature as a function of the distance into the platelet from the hot gas side. It can be seen that the thermal influence zone is a scant 0.250 in. into the platelet from the hot gas side, which means that there is a very short time available for the internal coolant heat exchange to take place. This delineates the need for a material of high conductivity to obtain a less steep temperature profile and, as a result, to extend more deeply into the platelets for greater thermal effectiveness.

(2) 0.011-in. Platelets

(u) Figure XVIII-4 shows the radial temperature distributions for three arbitrary surface temperatures of 1900, 1500, and 1100°F for 0.011-in. platelets located within the throat region. The thermal influence zone is only about 0.150 in. for all three surface-temperature conditions. The coolant flow rates and temperature rises within the platelets in the throat region reflect the very short thermal influence zone available for energy transfer.

(3) Radial Temperature Distribution of 0.021-in. Instrumented Platelet Located in the Throat Region

(u) Figure XVIII-4 also shows the radial temperature distribution within a 0.021-in. platelet located at the throat with a maximum flow metering platelet indexed at the Number 1 location, experiencing the same effective gas-recovery temperature as the adjacent 0.011-in. platelets operating at a surface temperature of 1900°F. The corresponding surface temperature of the 0.021-in. platelet would be 2175°F. It can be seen that there is a substantial longitudinal temperature gradient (over 150°F) between the 0.011-in. and the 0.021-in. platelets. This means that the instrumented platelet will record temperatures in excess of these the 0.011-in. platelets should be experiencing, but lower than that which would exist in the 0.021-in. platelet if it were thermally isolated from the cooler 0.011-in. platelets. The actual deviation in recorded temperature within the 0.021-in. platelet from the adjacent 0.011-in. platelets must be determined by a more comprehensive analysis which would allow both radial and longitudinal conduction effects.

c. Hydraulic Analysis

(u) The hydraulic analysis described in the previous quarterly report is summarized in Figures XVIII-5, -6, and -7, which show pressure drop as a function of N_2O_4 coolant flow rate for each of the twelve compartments.

(u) Figures XVIII-5 through 7 also indicate, for each individual flow-control compartment, the point at which the transition from laminar to turbulent flow can be expected to begin. These transition points are given for both the primary and secondary metering passages and are indicative of the flow regime existing in the Number-1 index position for all compartments with the exception of Compartment 9, for which the transition point is for flow conditions within platelets oriented in the Number-2 index position.

CONFIDENTIAL

Report 10850-Q-4

XVIII, B, ARES Thrust Chamber (cont.)

d. Tri-Chloroethylene Flow Requirements for Reynold's Number Similarity with N_2O_4 Flow

(u) Because the prototype chamber will be flow tested with trichloroethylene as the working fluid, it is desirable to know the normalizing flow relationships between the two fluids. Since the transition from laminar to turbulent flow will probably be reached during the first firing it is desirable to know at what nominal Reynold's number the transitory flow occurs. This can be done if the Reynold's number range anticipated with N_2O_4 is duplicated with tri-chloroethylene. For Reynold's number similarity

$$Re = \left[\frac{2\dot{V}}{\mu(A+B)} \right]_{N_2O_4} = \left[\frac{2\dot{V}}{\mu(A+B)} \right]_{C_2HCl_3}$$

Since the fluid flow passages are identical in both cases, Reynold's number similarity requires that:

$$\dot{V}_{C_2HCl_3} = \frac{\mu_{C_2HCl_3}}{\mu_{N_2O_4}} \dot{V}_{N_2O_4}$$

Figure XVIII-8 gives the trichloroethylene flow rates required to duplicate the Reynold's number range that will be characteristic of the predicted N_2O_4 flow rates.

(u) For an equal pressure drop the relative flow rates are found to be

$$\frac{\Delta P}{x} = \left[\frac{\dot{V}\mu}{8c^3 p} \frac{(A+B)^2}{2A^3 B^3} (fRe) \right]_{N_2O_4} = \left[\frac{\dot{V}\mu}{8c^3 p} \frac{(A+B)^2}{2A^3 B^3} (fRe) \right]_{C_2HCl_3}$$

since the geometry and the geometry-related factors are constant,

$$\left(\frac{\dot{V}\mu}{\rho} \right)_{N_2O_4} = \left(\frac{\dot{V}\mu}{\rho} \right)_{C_2HCl_3}$$

and

$$\dot{V}_{N_2O_4} = \left(\frac{\rho}{\mu} \right)_{N_2O_4} \cdot \left(\frac{\mu}{\rho} \right)_{C_2HCl_3} \cdot \dot{V}_{C_2HCl_3}$$

is the weight flow relationship for equal pressure drop for the two fluids.

CONFIDENTIAL

Report 10830-Q-4

XVIII, B, ARES Thrust Chamber (cont.)

e. Thermocouple Locations

(1) Radial Locations

(u) Based upon the platelet radial temperature distributions it was decided to locate the thermocouple junctions at the hot gas surface, 0.010 and 0.050 in. below the hot gas surface. There will be a total of 72 thermocouples of which 57 will be surface junctions, ten will be 0.010 in. below the surface, and five will be 0.050 in. below the surface. For any given test, 40 of the 72 thermocouples will be recording data due to availability of test area instrumentation channels.

(2) Axial Locations

(u) With respect to the chamber axial location, special 0.021-in. platelets with six thermocouples, oriented in multiples of 60° intervals peripherally, separate each flow-control compartment. One exception to the 60° peripheral orientation is made for the instrumented platelet separating compartments 2 and 3. The reason for this anomaly is to obtain midpoint and onpoint spacing of the thermocouples with respect to the injector fuel discharge pattern for either a 12-sector or a 32-sector injector configuration. The thermocouples will be nominally located opposite a central flow groove of a flow sector except for specific dual-point groove-land installations.

C. THERMAL BARRIER DEVELOPMENT

1. Summary and Conclusions

a. Recommended Liner

(c) The thermal barrier recommended for the first ARES chamber is a tungsten cermet of the following composition and thickness in the as-sprayed condition:

<u>Location</u>	<u>Thickness, in.</u>	<u>Composition</u>
Primer Layer	0.005	95W-5 Nicoro 80
Thermal Barrier	0.020	82W-12 ZrO ₂ -3 Nicoro 80 - 3 Si
Topcoat	0.005	Si

b. Nicoro-80 Substitution

(c) The substitution of 3% Nicoro 80 (82 Au-16 Cu-2 Ni) for 3% copper previously used was found to provide equivalent oxidation resistance and will resist corrosion attack between test firings from residual N₂O₄ absorbed into the liner.

CONFIDENTIAL

Report 10830-Q-4

XVIII, C, Thermal Barrier Development (cont.)

c. Braze Bonding

(c) Braze bonding of the tungsten cermet thermal barriers in Inconel 718 was accomplished in a braze treatment of 2 hr in vacuum at 1750°F, as illustrated in Figures XVIII-9 and -10. An excellent bond is achieved by diffusion of the gold through the pores of the liner into the surface of the Inconel 718. An additional layer of liner, which is desiliconized, was found necessary for preventing embrittlement of the bond zone during the braze cycle. Unfortunately, the Inconel 718 cannot be aged prior to braze-bonding the liner and, in the compositions studied, the aging treatment of 8 hr at 1350°F, furnace-cooling to 1200°F, and 20 hr total time, caused embrittlement of the bond zone between primer layer and the thermal barrier. Consequently, at this time, braze bonding is not recommended for ARES Inconel 718 chambers. It is believed that braze bonding on stainless-steel or Hastalloy-X chambers will be practical with some additional development.

d. Hastelloy X

(c) Sprayed Hastelloy X was found to possess insufficient bond strength to Inconel 718 for use in the ARES chamber. Braze-bonding of Hastelloy X to Inconel 718 resulted in some improvement, but not enough to recommend its use. The primer coat contained 95% Hastelloy X and 5% Nicoro 80. It is now believed that a primer coat of 95 MO-5 Nicoro 80 or 95W-5 Nicoro 80 would result in a better bond since the gold alloy is insoluble in the molybdenum and tungsten and would diffuse preferentially to the Inconel-718 bond zone as it does with the tungsten cermet liners. As it was, the gold diffused into the Hastelloy X matrix without concentrating at the Inconel 718 bond zone.

e. Topcoat Improvement

(c) The braze-bond cycle of 2 hr at 1750°F did not cause significant diffusion of the silicon topcoat into the thermal barrier, and a hoped-for improvement in oxidation protection from this treatment failed to occur. Torch-fusing of the silicone topcoat either with or without a furnace-braze cycle did not improve these properties. A topcoat composed of 70 Si-30(Au-6Si eutectic) also did not significantly improve oxidation protection in as-sprayed, braze-bonded, torch-fused, or torch-fused and braze-bonded conditions. Further studies of topcoat improvement are recommended as the best way to gain oxidation resistance.

f. Plasma-Process Improvement

(u) Experiments were conducted with the objective of increasing the strength of the deposit by raising the impingement velocity of the particles. Various powder-feed port-injection methods were investigated, which fed the powder into the plasma at angles close to the direction of the flame rather than at the conventional right angle. The idea was to raise the initial velocity of the particles. Also, a tungsten nozzle shroud was used to restrict the expansion of the plasma to raise impingement velocities and to reduce overspray. The near-parallel injection had a secondary purpose of eliminating deposit buildup on the tungsten nozzle by aiming the powder down the center line.

CONFIDENTIAL

Report 10830-Q-4

XVIII, C, Thermal Barrier Development (cont.)

(u) Powder buildup on the tungsten nozzle was a major problem which was not solved. The most promising means for eliminating the buildup would consist of using a water-cooled feed port of sufficient miniaturization and cooling to feed powder along the center line of the flame. In bend tests, the strongest coating was obtained by spraying the powder through a water-cooled feed tube at an impingement angle of 16° , from a distance of about 0.150 in. from the center line of the flame. However, the deposition efficiency with this arrangement was too low. At this time, right-angle powder injection is recommended for regeneratively cooled Chamber SN-1.

(u) A means was devised for continuously cleaning part of the overspray contamination. The device consists of a copper tube bent into a 1.5-in. ID ring, mounted 1/2 in. from the chamber surface and drilled with a series of holes pointed at the coating at a 45° angle away from the flame. Argon gas at 100 psig continuously blows loose powder and dust from the region of the flame. Bend tests showed some strength improvement and this technique is therefore recommended for the fabrication of ARES chamber.

2. Discussion

(u) A series of three-tube thermal shock tests and a series of bend tests were completed to late in the quarter to be included in this report. These recent tests are significant and were summarized in Paragraph 1, above. However, it is felt that a complete discussion of earlier results at this time would be lacking in meaning and continuity. Therefore, a very brief summary of the earlier work is shown in Figures XVIII-9, 10, -11, and -12.

(u) Complete documentation of the thermal-barrier development work for the past quarter will be included in the next quarterly report.

D. COMPONENT DESIGN SUPPORT

1. Advanced TPA

(u) An analysis was conducted to predict the temperature distribution in a portion of the B-design housing adjacent to the stator blades. Isothermal plots are presented in Figures XVIII-13 and 14 for 20-sec firing duration and thermal steady-state conditions, respectively.

(u) The boundary conditions used in the analysis of the stator are shown schematically in Figure XVIII-15. The heat-transfer coefficient in the curved annulus (upper left in Figure XVIII-15) was calculated on the basis of an N_2O_4 flow rate of 39.3 gal/min. The discrete holes shown by a dotted line in the figure, leading from the curved annulus to the shaft, were ignored for this analysis due to their localized cooling effect.

Page XVIII-14

(This page is Unclassified)

CONFIDENTIAL

UNCLASSIFIED

Report 10830-Q-4

XVIII, D, Component Design Support (cont.)

(u) The calculation of the heat-transfer coefficient between the housing and the liquid N_2O_4 flowing along the shaft and based on a velocity equal to half the tangential velocity of the shaft. However, in the plenum inboard of the nozzle stator, the heat-transfer coefficient was assumed to vary over a wide range. There is considerable uncertainty regarding the velocity of the fluid in this area due to the relatively large annular gap and also due to the effect of the stationary bolt heads protruding into the plenum. Therefore, the most conservative conditions, that of free convection, were assumed for the outboard wall of the plenum, as indicated in the figure. As the fluids approach the restricted door area adjacent to the turbine hub, it was assumed to again accelerate to a velocity equal to one-half the tangential velocity of the shaft.

(u) The calculation of the heat-transfer coefficient between the liner and the housing was based on a gas velocity of 1 ft/sec. This is believed to be conservative because no continuous flow path exists behind the liner. The temperature in this area was assumed equal to the stagnation temperature of the gas, i.e., 1500° F.

(u) The heat-transfer coefficient on the stator hub was calculated in an identical manner as for the rotor hub. That is, a single composite heat-transfer coefficient was calculated to represent both conduction and convection to the stator hub. Details of the analysis are reported in Section XIX,E,2 of the previous quarterly report.

(u) The convective heat-transfer coefficient between the gas and the stator hub was calculated to be 5000 Btu/ft²-hr °R. The conductive coefficient, representing heat transferred between the blades and the hub, was calculated to be 3650 Btu/ft²-hr-°R. A single composite coefficient, representing both convection to the hub and conduction through the blades to the hub, was calculated to be 4525 Btu/ft²-hr-°R using the area weighting technique described in the previous quarterly report.

(u) The average recovery temperature on the blades and on the hub was attained at 1481° F based on a stagnation temperature of 1500° F.

(u) The temperature distributions were obtained using the thermal-analyzer computer programs. The interfacial thermal resistance between adjacent parts have been ignored for this analysis. The presence of the bolt and of the bolt hole was ignored, i.e., a section between bolt holes was analyzed.

(u) The stator was composed of a number of parts made from different materials. The materials are identified on the schematic diagram of Figure XVIII-15, and the corresponding physical properties which were used in the thermal analysis are tabulated below:

UNCLASSIFIED

Report 10830-Q-4

XVIII, D, Component Design Support (cont.)

<u>Material</u>	<u>Thermal Conductivity, Btu/ft-hr-°F</u>	<u>Specific Heat, Btu/lb-°R</u>	<u>Density, lb/in.³</u>
Udimet 100	12.0	0.105	0.286
Inconel 718	9.0	0.14	0.296
Hastelloy	12.0	0.10	0.297
Porous Metal (Primarily Ni)	0.79	0.008	0.161
Teflon	0.14	0.25	0.776

(u) The results of the transient analysis of the stator indicated that the stator hub, with a relatively small mass, reaches steady-state temperature very quickly. In contrast, the adjacent thicker section of the housing has not yet reached steady-state temperature after 20 sec. The latter area is heated primarily by convection from the hot gas between the housing and the flow liner. The heat-transfer coefficient on this surface, based on an assumed gas velocity of 1 ft/sec, is therefore the controlling factor affecting the temperature in the housing.

(u) As stated previously, there was some uncertainty about the flow velocity along the liquid side of the arm connecting the hub with the main portion of the housing; therefore, a very conservative heat-transfer coefficient was used along this surface. The results of the analysis of the stator show that very little heat is conducted along the connector arm from the hub to the housing. This clearly indicated that the assumed flow conditions in the N₂O₄ plenum will not materially affect the temperature distribution in the vicinity of the bolt holes in the housing.

(u) The thermal gradient in the stator hub is minimized by a low-conductivity porous-metal strip on the inboard side of the hub. However, the porous metal does not extend around the corner to protect the end surface of the hub. Thermal stresses may be significant in this localized area because the temperature on the exposed surface of the hub is as low as 100°F compared to 1400°F at 0.3 in.

2. Primary Combustor Fuel Circuit Pressure Drop

(u) An analysis was conducted to determine the circumferential variation in mass flow in the primary fuel injector due to pressure variations in the fuel manifold. The results of the analysis are presented in Figure XVIII-16 and are based on a nominal pressure drop across the injector of 400 psig.

(u) The fuel enters an annular manifold through a single pipe and then passes through the injector into the combustion chamber. The mass flow of fuel entering the chamber varies directly with the pressure in the manifold according to the following relationship:

UNCLASSIFIED

Report 10830-Q-4

XVIII, D, Component Design Support (cont.)

$$\dot{W} + \sqrt{2g \rho A^2 (P_M - P_C)}$$

where:

\dot{W} = Local mass flow rate of fuel

g = Gravitational constant

ρ = Density of fuel

A = Area of injection port

P_C = Pressure in primary combustion chamber

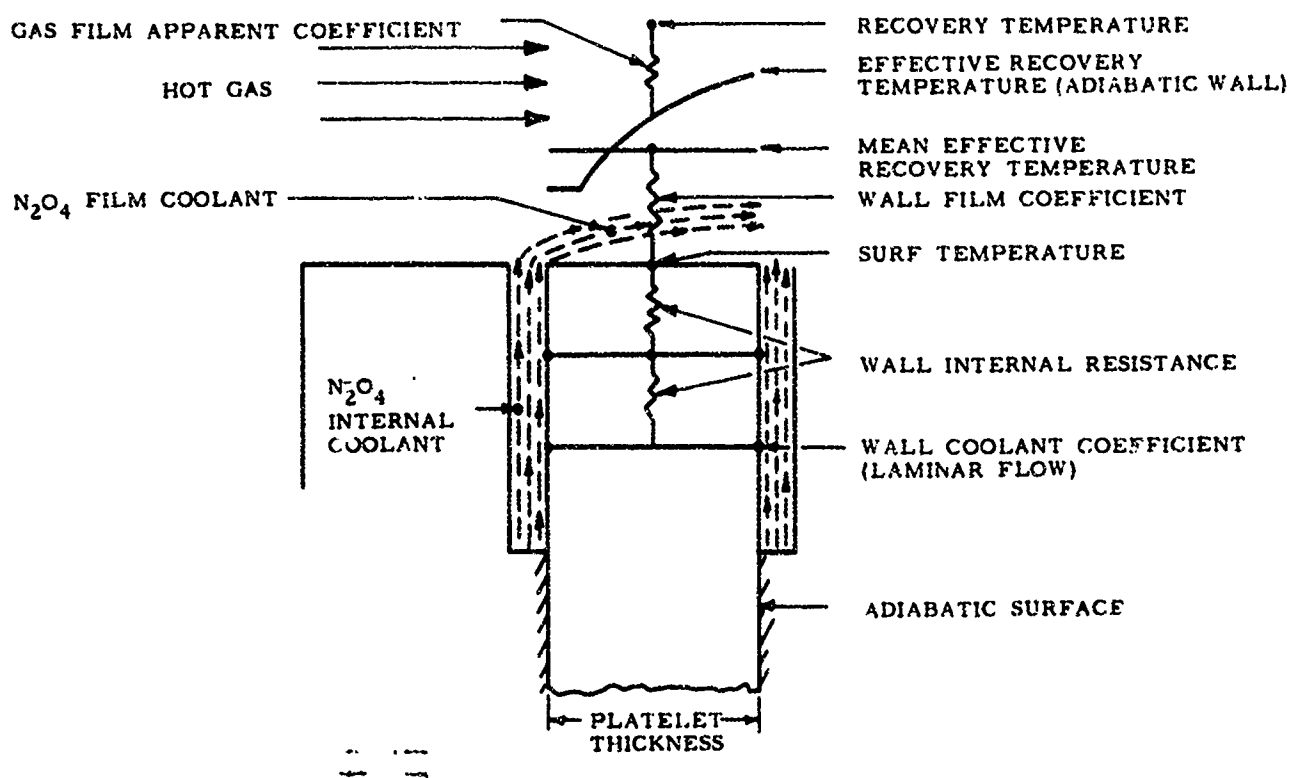
P_M = Local pressure in fuel manifold

(u) The pressure in the manifold varies circumferentially around the manifold due to differences in fluid velocity and also due to friction in the manifold. The fuel mass flow immediately opposite the inlet pipe in the manifold is considerably higher (5%) than the mass flow rate at adjacent locations since the former will be exposed to the total pressure in the pipe. Adjacent stations in the manifold will see a lesser pressure due to the loss in pressure associated with the 90° turn at the mouth of the feed pipe.

(u) Ignoring the local high mass flow at the pipe inlet, which would probably affect only one set of injector holes, the maximum variation in mass flow rate is 2%, as may be seen from Figure XVIII-16.

UNCLASSIFIED

Report 10830-Q-4



Advanced Thermal Model

Figure XVIII-1

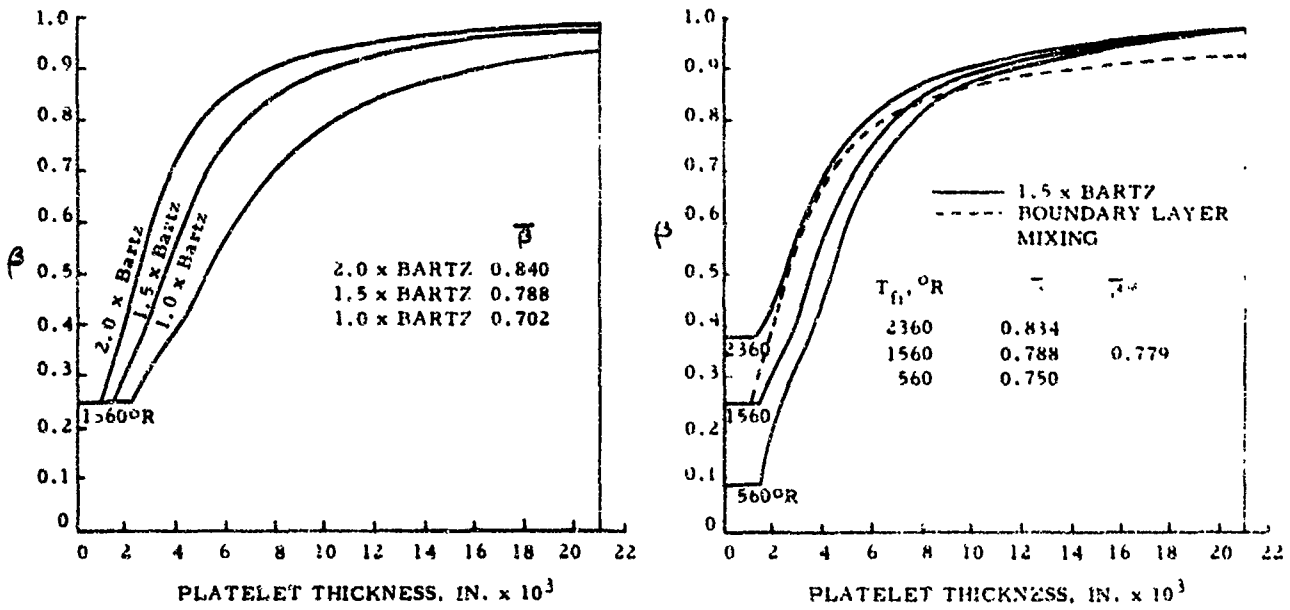
UNCLASSIFIED

UNCLASSIFIED
Report 10830-Q-4

$$\dot{W}_c = 0.0188 \text{ LB/SEC-IN.}^2$$

$$T_0 = 6229^{\circ}\text{R}$$

$$T_c = \frac{T_F}{T_0}$$



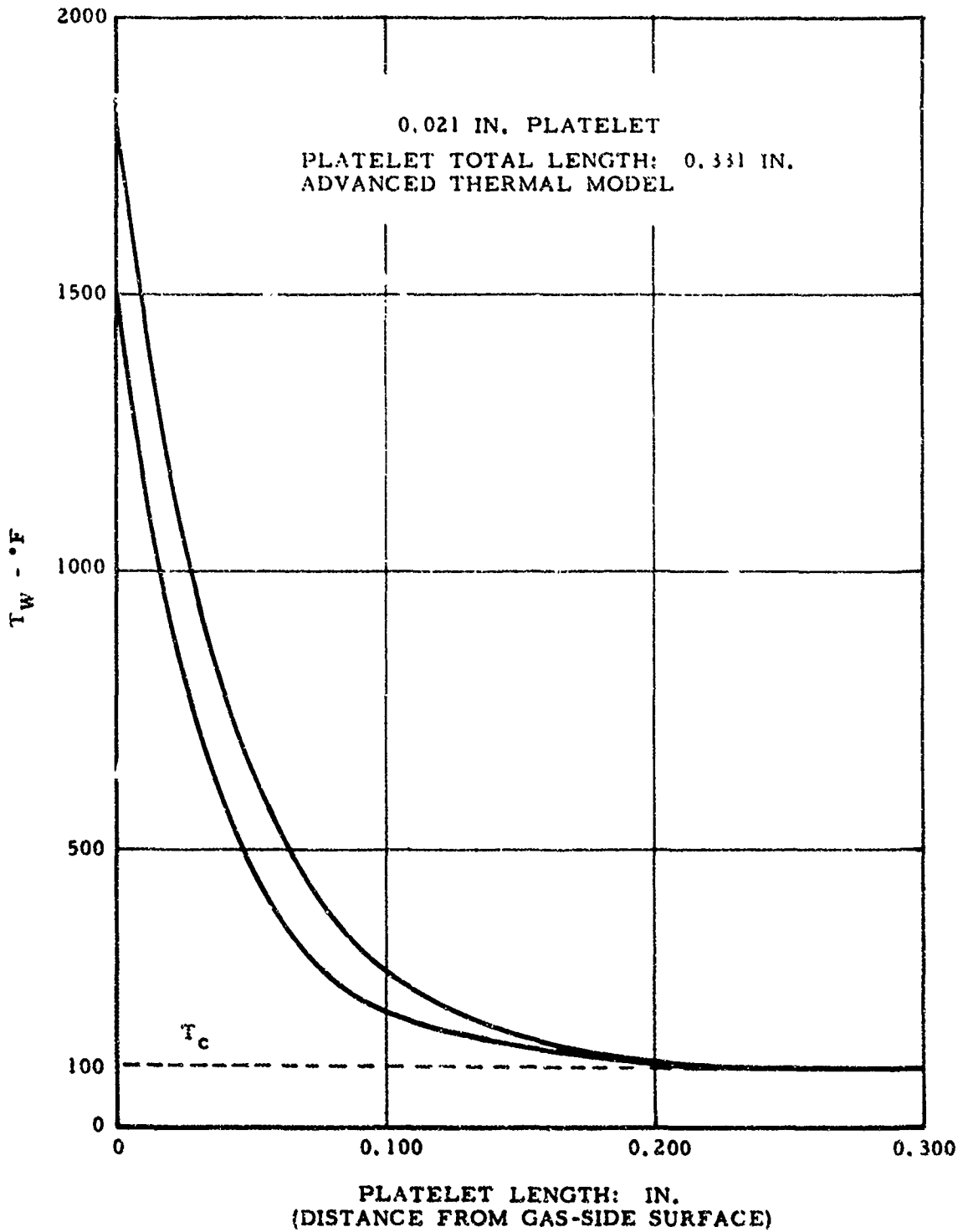
ARES Prototype Transpiration-Cooled Chamber (Chamber Region) Individual Platelet Film Cooling Effectiveness (Hatch and Papell Model)

Figure XVIII-2

UNCLASSIFIED

UNCLASSIFIED

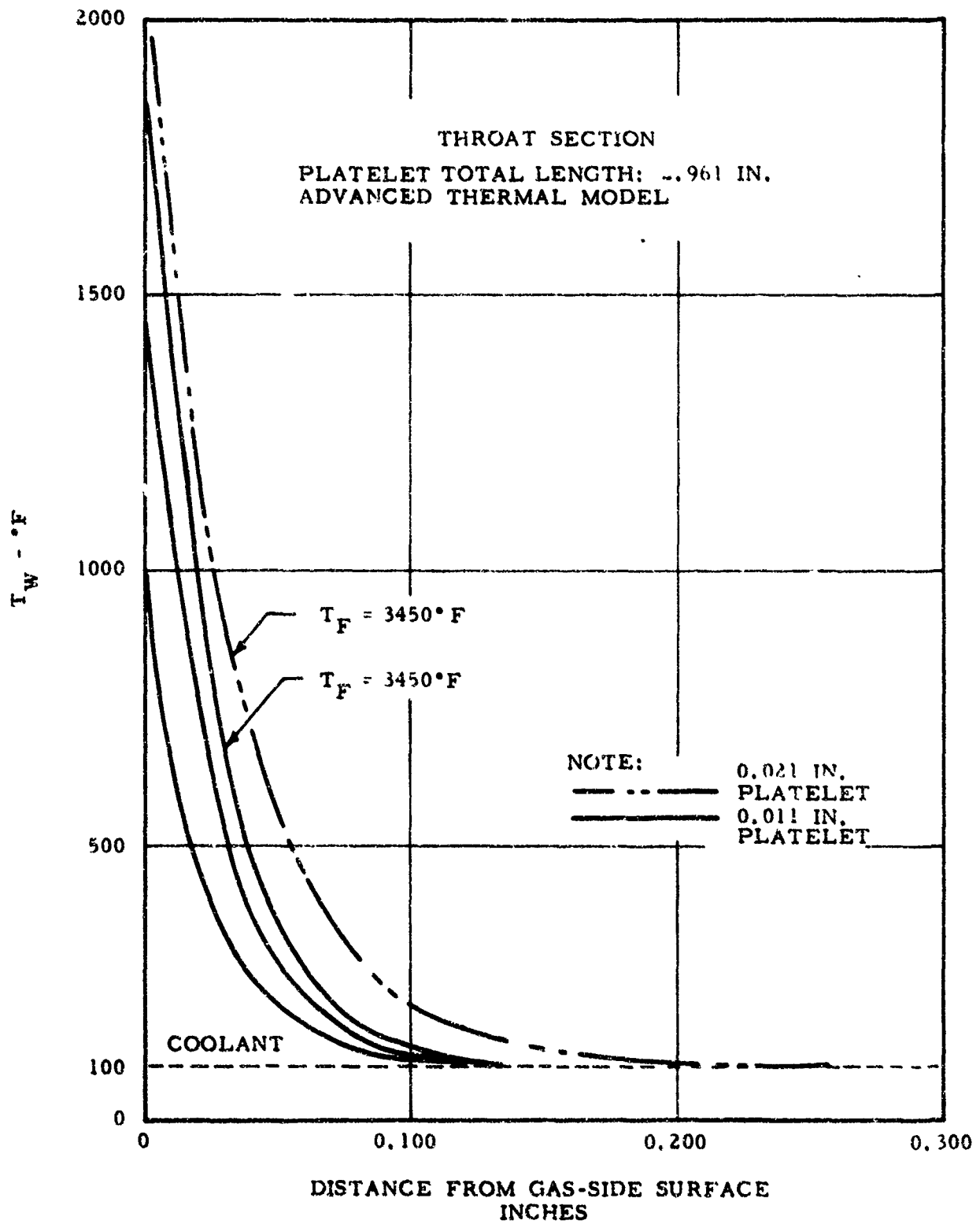
Report 10830-Q-4



ARES Prototype Transpiration-Cooled Chamber Chamber Wall Temperature vs Length (0.021 in. Platelet)

Figure XVIII-3

UNCLASSIFIED

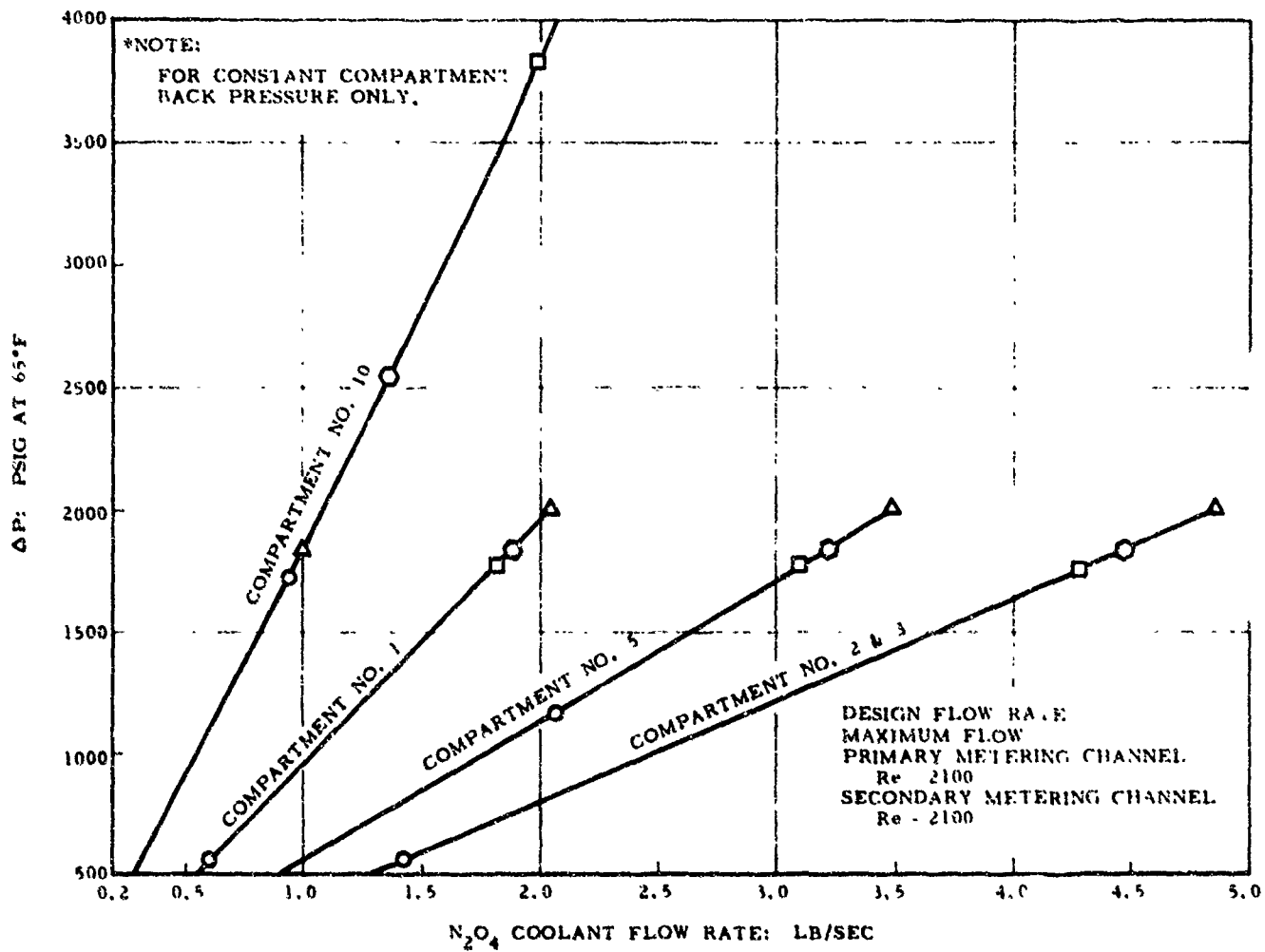


ARES Prototype Transpiration-Cooled Chamber Chamber Wall Temperature vs Length (Throat Section)

Figure XVIII-4

UNCLASSIFIED

Report 10830-Q-4



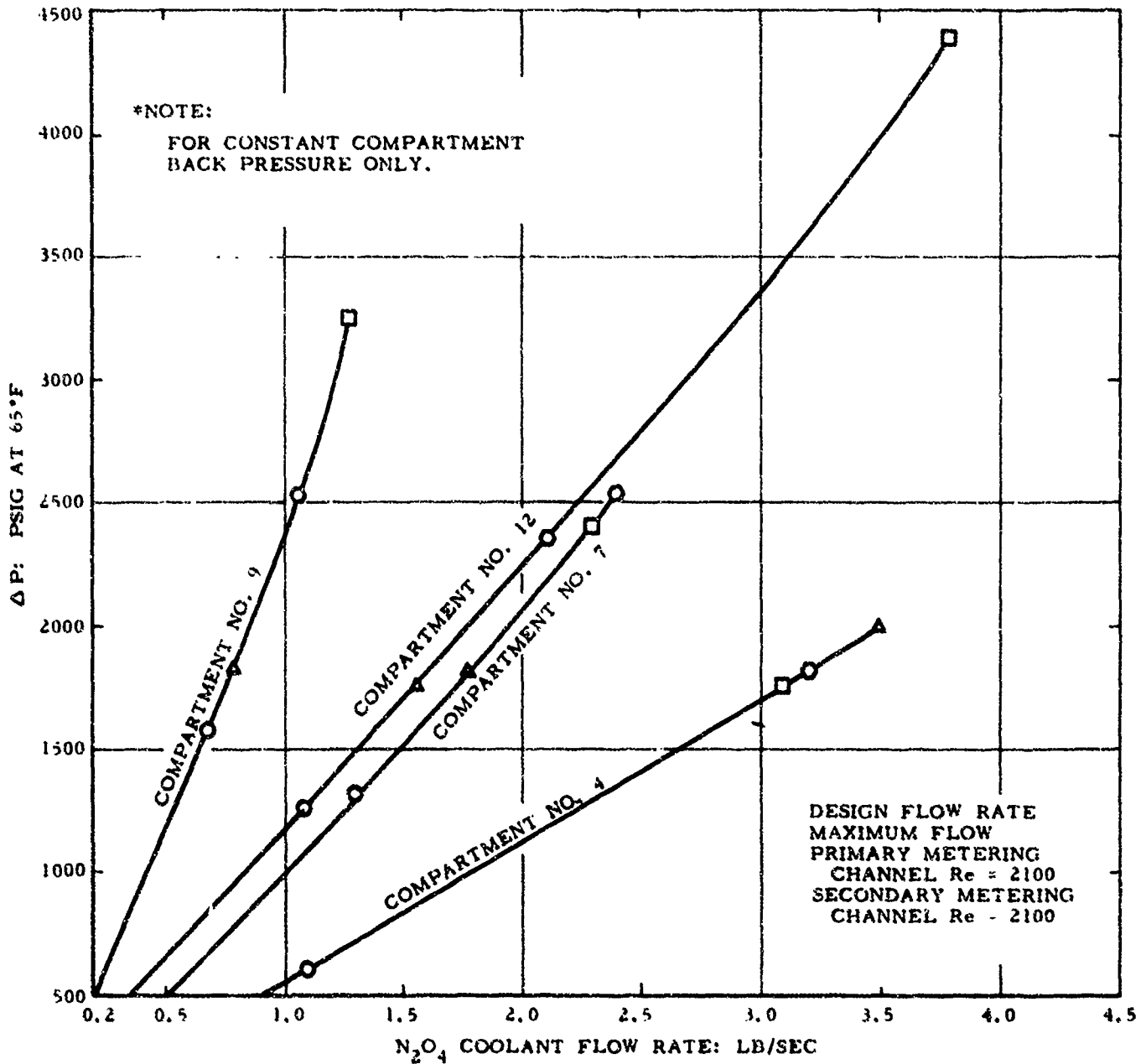
N₂O₄ Coolant Pressure Drop vs Flow Rate*, Compartments 1, 2, 3, 5, and 10

Figure XVIII-5

UNCLASSIFIED

UNCLASSIFIED

Report 10830-Q-4



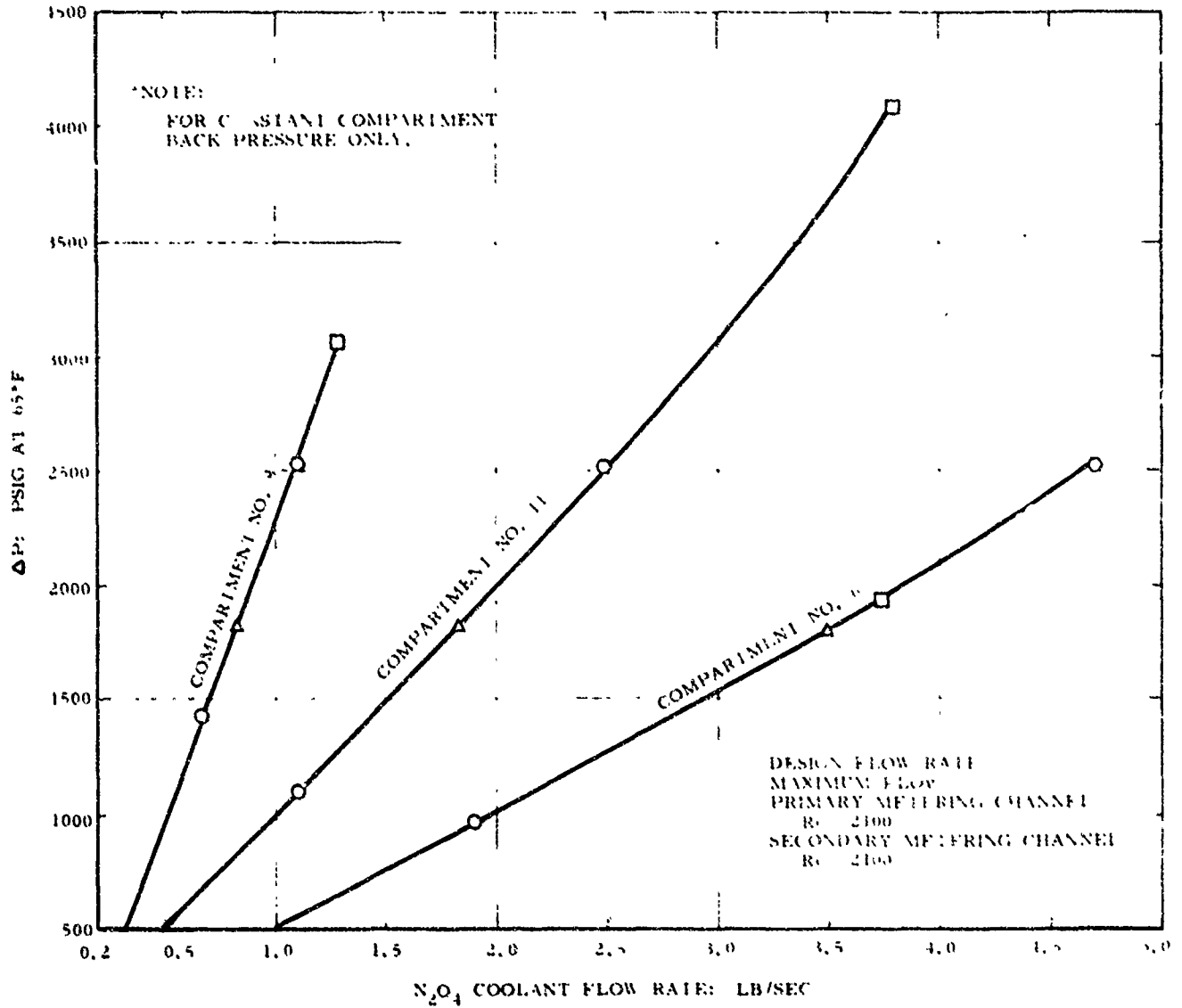
N_2O_4 Coolant Pressure Drop vs Flow Rate*. Compartments 4, 7, 9, and 12

Figure XVIII-6

UNCLASSIFIED

UNCLASSIFIED

Report 10830-Q-4



N₂O₄ Coolant Pressure Drop vs Flow Rate*, Compartments 6, 8, and 11

Figure XVIII-7

UNCLASSIFIED

UNCLASSIFIED

Report 10830-Q-4

COMPARTMENT NUMBER	N ₂ O ₄		C ₂ HCl ₃ *	
	MIN.	MAX.	MIN.	MAX.
1	0.60	1.83	0.82	2.52
2	1.42	4.28	1.95	5.89
3	1.42	4.28	1.95	5.89
4	1.11	3.10	1.52	4.26
5	2.06	3.10	2.83	4.26
6	2.24	3.73	3.08	5.12
7	1.37	2.28	1.88	3.13
8	0.65	1.28	0.89	1.76
9	0.69	1.28	0.95	1.76
10	0.95	1.99	1.30	2.74
11	1.11	3.79	1.52	5.20
12	1.19	3.90	1.63	5.36

$$*\dot{W}_{C_2HCl_3} = \dot{W}_{N_2O_4} \left(\frac{\rho_{C_2HCl_3}}{\rho_{N_2O_4}} \right) = 1.373 \dot{W}_{N_2O_4}$$

FOR REYNOLDS NUMBER SIMILARITY AT 70°F

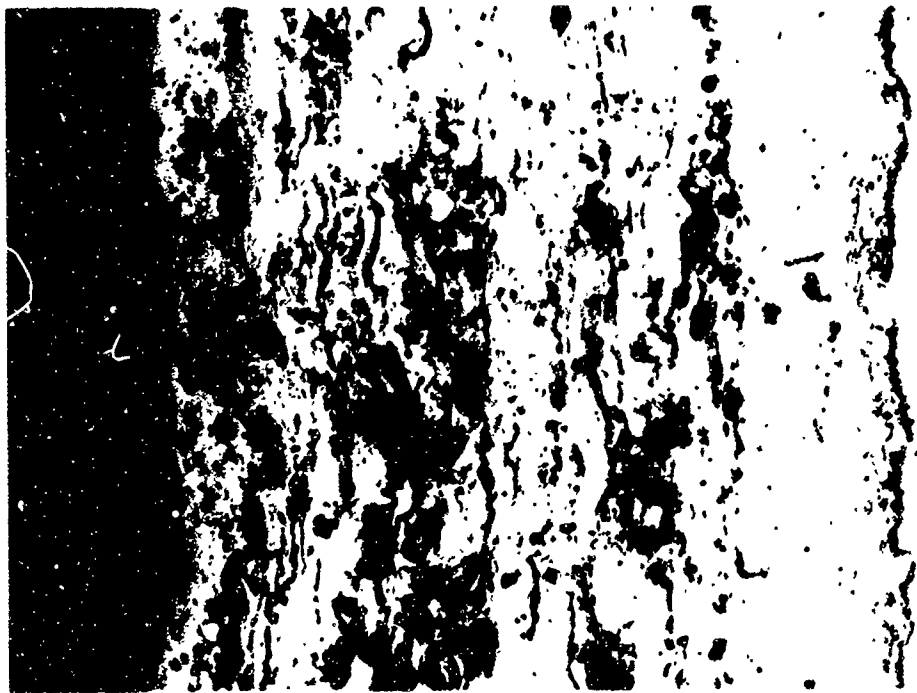
Trichloroethylene Estimated Flow-Rate Ranges (lb/sec) for Reynolds
Number Similarity

Figure XVIII-8

UNCLASSIFIED

CONFIDENTIAL

Report 10830-Q-4



LAMINATES:

100 Silicon	Topcoat
82 Tungsten	Thermal Barrier
12 Zirconia	
3 Gold Alloy	
3 Silicon	
85 Tungsten	Desilicized Layer
12 Zirconia	
3 Gold Alloy	
95 Tungsten	Bonding Layer
5 Gold Alloy	
Stainless Steel Substrate	

150X

Adjacent to area which was thermal cycled 45 times

Braze Bonded Laminated Tungsten Cermet Thermal Barrier (u)

Figure XVIII-0

CONFIDENTIAL

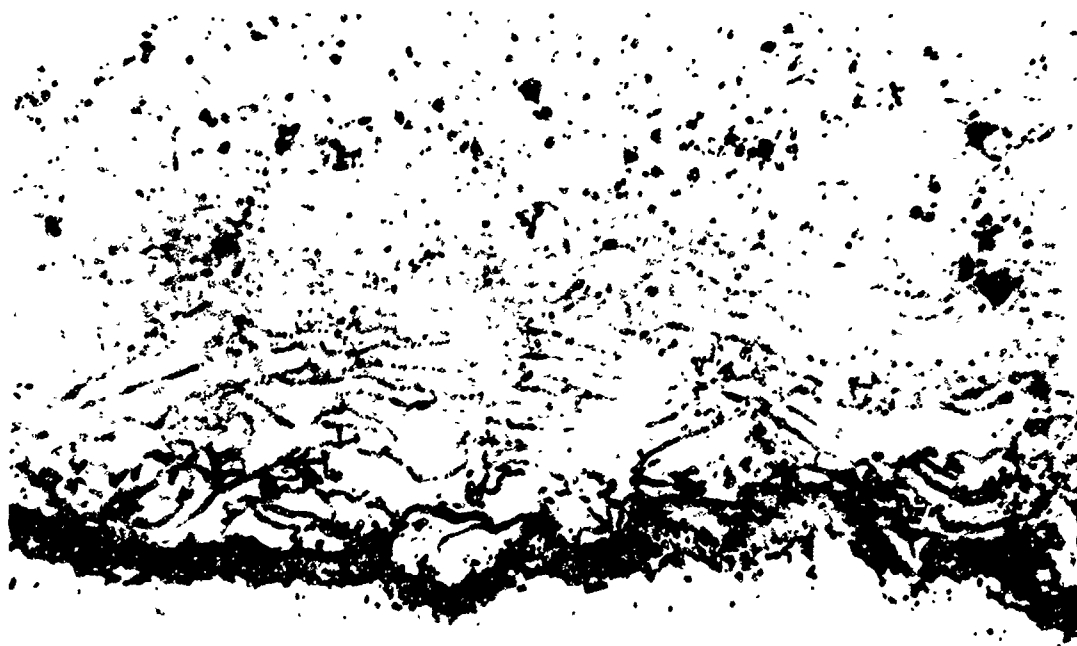
CONFIDENTIAL

Report 10830-Q-4



As sprayed 95W-5 gold alloy on stainless steel

400X Iodine Etch



Braze bonded two hours at 1730°F in vacuum

400X Iodine Etch

Braze Bonding Microstructure (u)

Figure XVIII-10

CONFIDENTIAL

CONFIDENTIAL
Report 10830-Q-4

SPECIMEN NO.	COMPOSITION* THICKNESS, MILS					
	<u>A</u>	<u>C</u>	<u>D</u>	<u>F</u>	<u>G</u>	<u>Si</u>
1	6	5	--	15	--	6
2	5	6	--	17	--	9
3	5	5	--	17	--	7
4	5	--	5	--	13	7
5	5	--	5	--	16	8
6	6	--	5	--	14	7
7	5	--	19	--	--	6
8	5	--	20	--	--	9
9	5	--	19	--	--	6
10	--	--	19	--	--	7
11	--	--	20	--	--	6
12	--	--	20	--	--	7
13	--	--	--	19	--	6
14	--	--	--	--	20	7
15	--	--	--	--	20	7
16	--	--	--	--	20	7

***COMPOSITION KEY**

- A = 95W - 5 NICORO 80
- C = 85W - 12 ZrO₂ - 3 Cu
- D = 85W - 12 ZrO₂ - 3 NICORO 80
- F = 82W - 12 ZrO₂ - 3 Cu - 3 Si
- G = 82W - 12 ZrO₂ - 3 NICORO 80 - 3 Si
- Si SILICON

CONFIDENTIAL

Composition of Braze Bond Test Specimens (u)

Figure XVIII-11

CONFIDENTIAL

CONFIDENTIAL

Report 10830-Q-4

SPECIMEN NUMBER	COMPOSITION	HEAT TREAT	RESULTS OF HEAT TREAT	NO. TEST CYCLES (1)	REGRESSION RATE	
					MAXIMUM	MINIMUM
1	ACFSi	NONE		32	50	50
2	"	H ₂	SOUND	43	4.6	0
3	"	VACUUM	SOUND	60	8.3	0
4	ADGSi	NONE		45	14	0
5	"	H ₂	PARTING	-	-	-
6	"	VACUUM	SOUND	45	8.9	0
7	ADSi	NONE		15	30	0
8	"	H ₂	PARTING	-	-	-
9	"	VACUUM	SOUND	15	60 ⁽³⁾	60 ⁽³⁾
10	DSi	NONE		15	23	0
11	"	H ₂	PARTING	-	-	-
12	"	VACUUM	SOUND	15	47	47
13	FSi	NONE		45	11	11
14	GSi	NONE		45	10	0
15	"	H ₂	PARTING	-	-	-
16	"	VACUUM	PARTING	-	-	-

(1) 3500°F SURFACE TEMPERATURE
OXIDIZING PLASMA GASES
20 SEC. HEATING CYCLES.

(2) NOT VALID, TEMP.
EXCESSIVE IN
TESTING.

(3) TOPCOAT LOST IN
FIRST TEST CYCLE.

CONFIDENTIAL

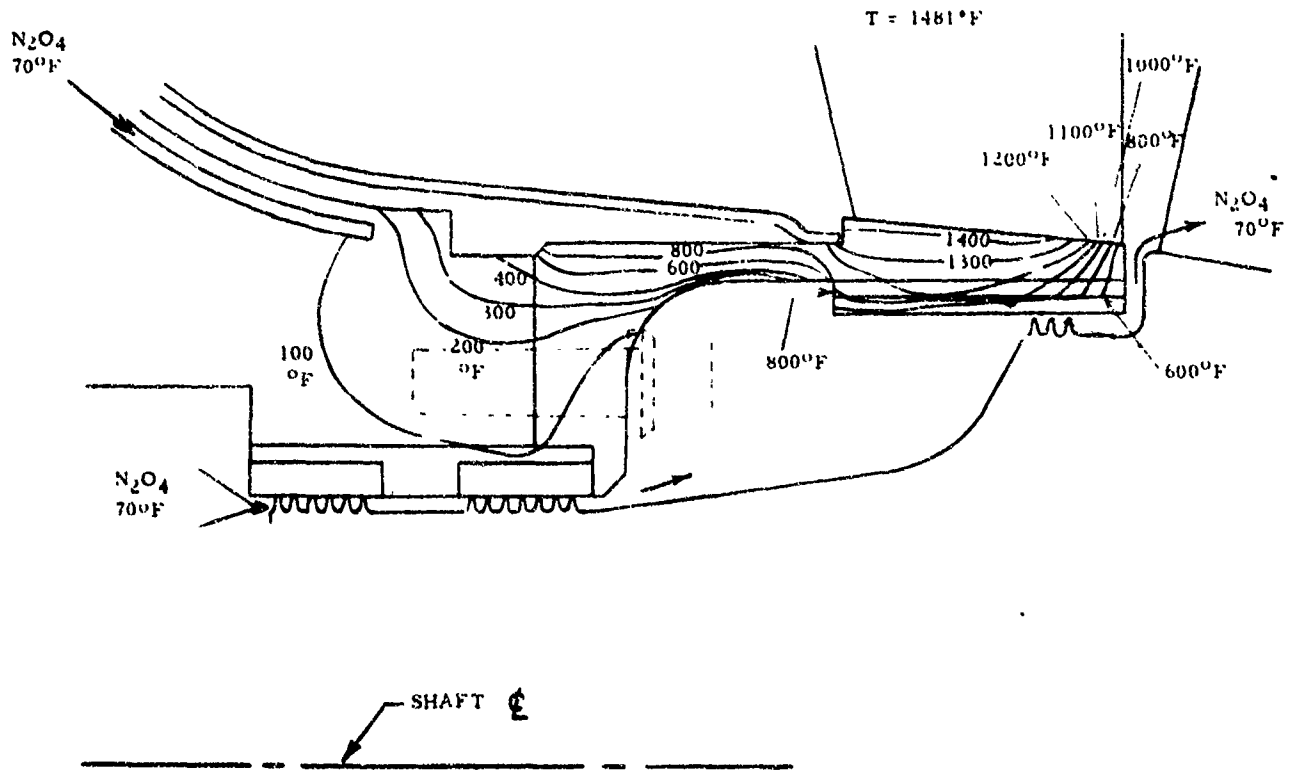
Braze Bonding Test Results (u)

Figure XVIII-12

CONFIDENTIAL

UNCLASSIFIED

Report 10830-Q-4



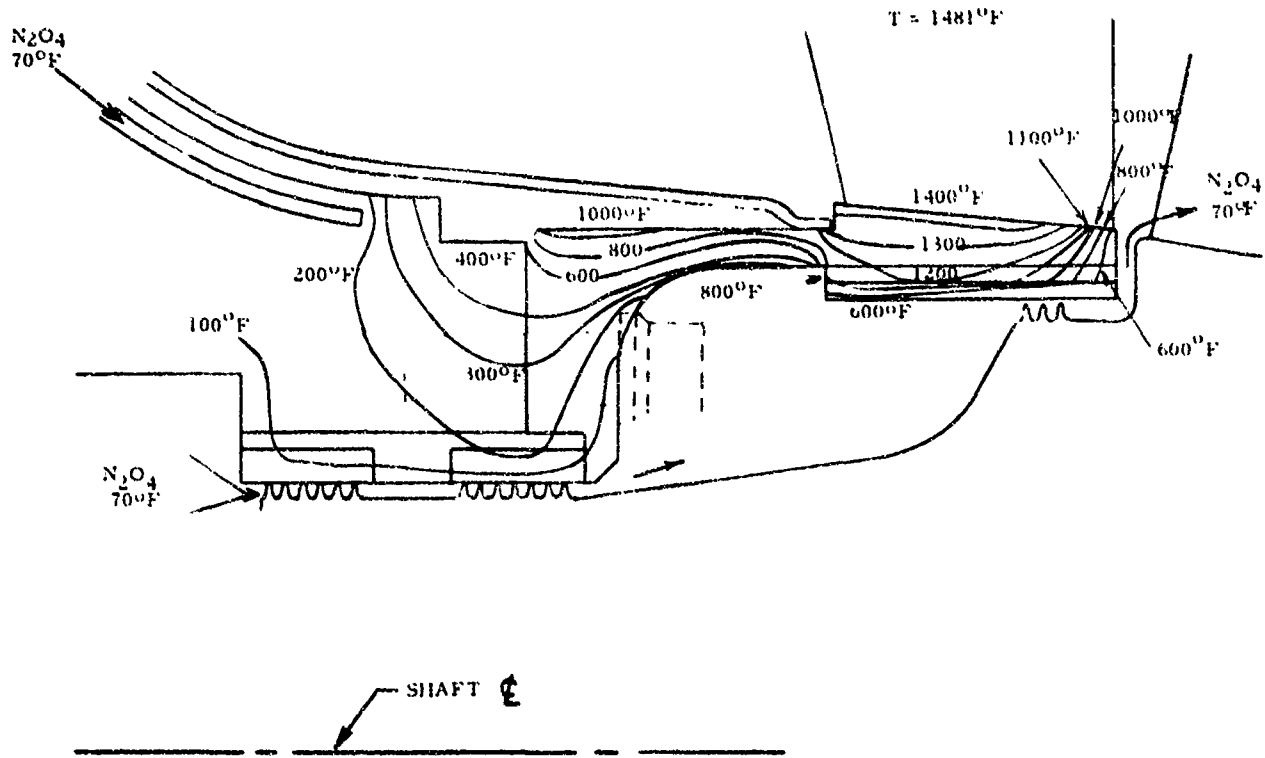
Advanced TPA B-Design Stator, Time = 20 sec

Figure XVIII-13

UNCLASSIFIED

UNCLASSIFIED

Report 10830-Q-4



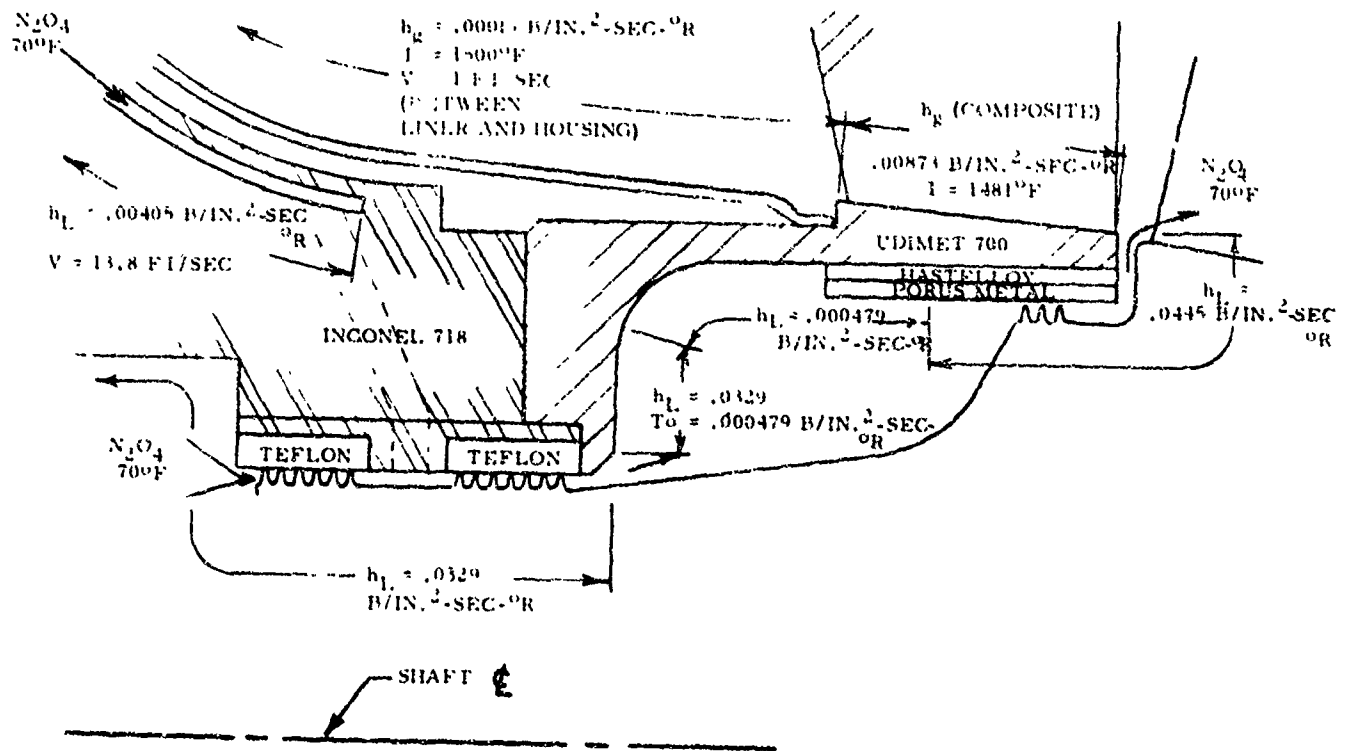
Advanced TPA B-Design Stator Steady State

Figure XVIII-14

UNCLASSIFIED

UNCLASSIFIED

Report 10830-Q-4



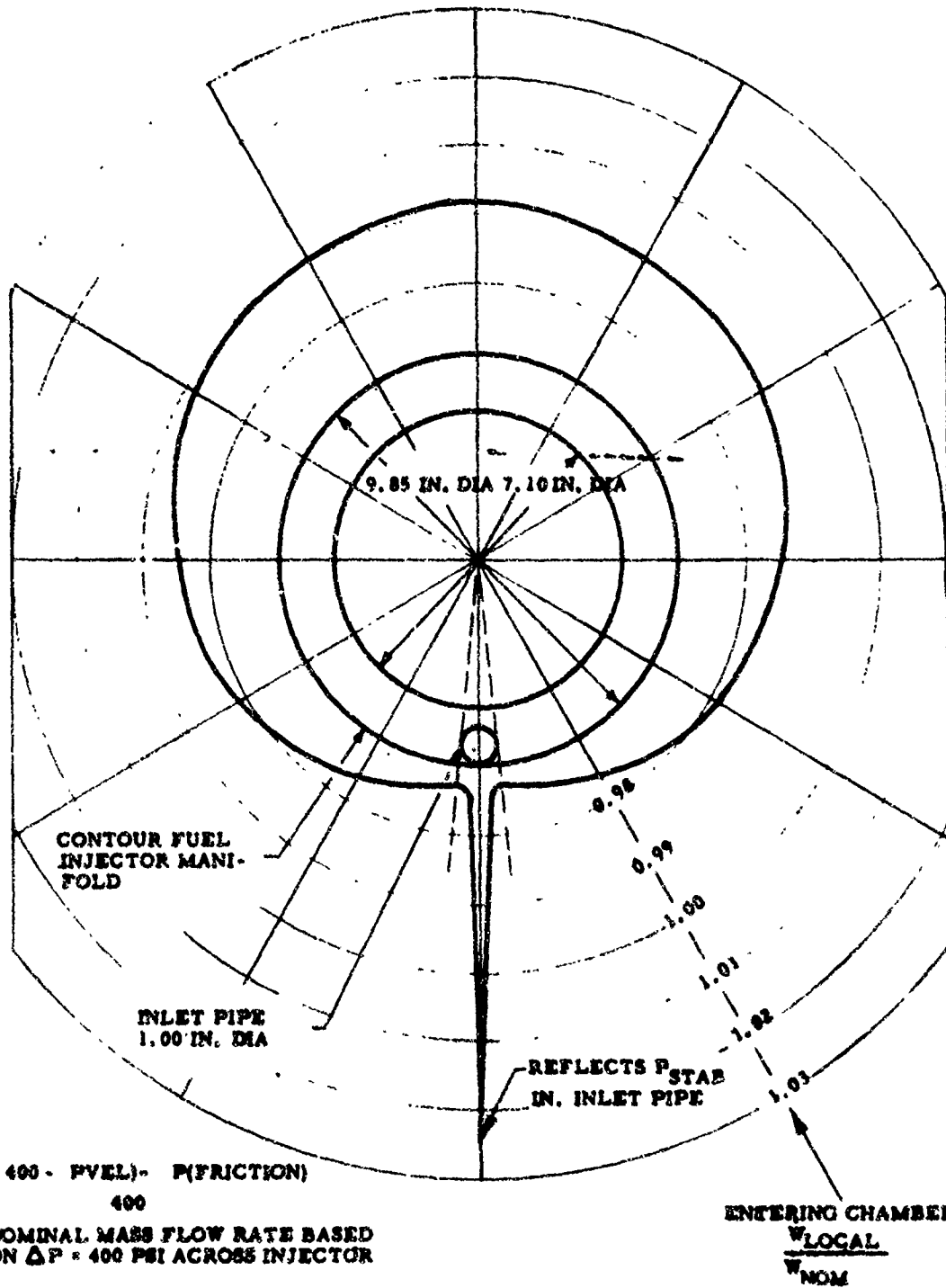
Advanced TPA B-Design Stator Boundary Conditions

Figure XVIII-15

UNCLASSIFIED

UNCLASSIFIED

Report 10830-Q-4



Mass Flow Distribution Around Primary Fuel Injector

Figure XVIII-16

UNCLASSIFIED

UNCLASSIFIED

Report 10830-Q-4

XIX.

RELIABILITY

A. MODES-OF-FAILURE ANALYSIS (MOFA)

(u) An evaluation of methods for interlocking the two fuel-control valves was completed. The conclusions were:

1. No interlocks are needed in a minimum-cost test program using only residual hardware. A simple valve-malfunction shutdown system is, however, warranted.

2. To minimize the risk of losing new hardware, an interlock device should be considered. A mechanical interlock would be desirable and would offer a small advantage over a comparable electrical system.

(u) Work was continued to evaluate module failures that could occur during the startup and shutdown transients. The principal modes have been listed.

B. DESIGN REVIEW

(u) An investigation was conducted to determine the compatibility of DuPont PR-143 AB fluid with space radiation environments if used for ARES purge seals. Based on information currently available, this fluid will withstand radiation encountered during extended space missions without the formation of insoluble solids or sludge. Some reduction in viscosity (less than 8%) can be expected, and some volatile products may be formed.

(u) A representative of the ARES Reliability Group has assumed the function of secretary of the Design Review Committee. A review was held on design modifications for the 2D nozzle with the representative from Reliability acting in this capacity.

C. TEST-PLAN REVIEW

(u) Test plans for the primary combustor and combustion seal have been reviewed. The review consisted of comparing expected test data with test objectives and investigating the test safety measures devised for preserving the test hardware.

D. TEST-DATA REVIEW

(u) A test program was conducted to evaluate explosive welding as a method of joining the up-flow cooling tubes to the thrust chamber flange. The test results indicated that this joining process will yield reliable, leak-proof joints. A report was issued describing in detail the development of the process for this particular application.

UNCLASSIFIED

Report 10830-Q-4

XIX, Reliability (cont.)

E. MAINTAINABILITY ANALYSIS

(u) A preliminary report on ARES maintainability is in preparation. The report will be distributed to all affected design groups for comments.

F. RELIABILITY PREDICTION

(u) Malfunction data from TITAN and Integrated Components programs were accumulated to establish probabilities of occurrence for similar malfunctions in ARES components.

(u) Work has also started to determine the performance reliability of the ARES module. This performance reliability quantitatively measures the probability of meeting the performance goals called-out in the Work Statement. The initial objective of this analytical work is to determine whether module performance requirements can be satisfied allowing for performance variability of major module components, using fuel-control valve balancing only. Preliminary work consisted of reviewing quantitative effects (dimensional and nondimensional) of a number of independent design variables on key performance parameters. Review of these influence coefficients revealed those independent design parameters whose variations most significantly influence performance variability.

Unclassified
Security Classification

Report 10830-Q-4

DOCUMENT CONTROL DATA - R&D		
<small>(Security classification of title, body of abstract and indexing annotation must be entered when the overall report is classified)</small>		
1. ORIGINATING ACTIVITY (Corporate author)		2c. REPORT SECURITY CLASSIFICATION
Aerojet-General Corporation P.O. Box 1947, Sacramento, California		Confidential
		2d. GROUP
		Four
3. REPORT TITLE		
ADVANCED ROCKET ENGINE--STORABLE(u)		
4. DESCRIPTIVE NOTES (Type of report and inclusive dates)		
Quarterly Technical Report (April through June 1966)		
5. AUTHOR(S) (Last name, first name, initial)		
Aerojet-General Corporation Advanced Storable Rocket Engine Division		
6. REPORT DATE	7a. TOTAL NO. OF PAGES	7b. NO. OF REFS
July 1966	268	11
8a. CONTRACT OR GRANT NO.	8c. ORIGINATOR'S REPORT NUMBER(S)	
AF 04(611)-10830	Aerojet-General Report 10830-Q-4	
a. PROJECT NO.	8d. OTHER REPORT NO(S) (Any other numbers that may be assigned to the report)	
	AFRPL-TR-66-153	
10. AVAILABILITY/LIMITATION NOTICES		
11. SUPPLEMENTARY NOTES		12. SPONSORING MILITARY ACTIVITY
		AFRPL, Research and Technology Division, Edwards AFB, Calif.
13. ABSTRACT		
<p>(u) The objective of the ARSE (Advanced Rocket Engine, Storable) program is to demonstrate the engineering practicality and the performance characteristics of an advanced storable propellant modular engine embodying high chamber pressure and the staged-combustion cycle.</p> <p>(u) This fourth quarterly report describes the technical accomplishments of the reporting period. Generally, the period was characterized as one in which many analyses and designs were completed, fabrication of many components was completed, and testing was accelerated. The most noteworthy accomplishment was the successful hot firing of two different modular injectors using the intensifier test system.</p>		

DD FORM 1 JAN 66 1473

Unclassified
Security Classification

14	KEY WORDS	LINK A		LINK B		LINK C	
		ROLE	WT	ROLE	WT	ROLE	WT

INSTRUCTIONS

1. ORIGINATING ACTIVITY: Enter the name and address of the contractor, subcontractor, grantee, Department of Defense activity or other organization (corporate author) issuing the report.

2a. REPORT SECURITY CLASSIFICATION: Enter the overall security classification of the report. Indicate whether "Restricted Data" is included. Marking is to be in accordance with appropriate security regulations.

2b. GROUP: Automatic downgrading is specified in DoD Directive 5200.10 and Armed Forces Industrial Manual. Enter the group number. Also, when applicable, show that optional markings have been used for Group 3 and Group 4 as authorized.

3. REPORT TITLE: Enter the complete report title in all capital letters. Titles in all cases should be unclassified. If a meaningful title cannot be selected without classification, show title classification in all capitals in parenthesis immediately following the title.

4. DESCRIPTIVE NOTES: If appropriate, enter the type of report, e.g., interim, progress, summary, annual, or final. Give the inclusive dates when a specific reporting period is covered.

5. AUTHOR(S): Enter the name(s) of author(s) as shown on or in the report. Enter last name, first name, middle initial. If military, show rank and branch of service. The name of the principal author is an absolute minimum requirement.

6. REPORT DATE: Enter the date of the report as day, month, year; or month, year. If more than one date appears on the report, use date of publication.

7a. TOTAL NUMBER OF PAGES: The total page count should follow normal pagination procedures, i.e., enter the number of pages containing information.

7b. NUMBER OF REFERENCES: Enter the total number of references cited in the report.

8a. CONTRACT OR GRANT NUMBER: If appropriate, enter the applicable number of the contract or grant under which the report was written.

8b, 8c, & 8d. PROJECT NUMBER: Enter the appropriate military department identification, such as project number, subject number, system numbers, task number, etc.

9a. ORIGINATOR'S REPORT NUMBER(S): Enter the official report number by which the document will be identified and controlled by the originating activity. This number must be unique to this report.

9b. OTHER REPORT NUMBER(S): If the report has been assigned any other report numbers (either by the originator or by the sponsor), also enter this number(s).

10. AVAILABILITY/LIMITATION NOTICES: Enter any limitations on further dissemination of the report, other than those

imposed by security classification, using standard statements such as:

- (1) "Qualified requesters may obtain copies of this report from DDC."
- (2) "Foreign announcement and dissemination of this report by DDC is not authorized."
- (3) "U. S. Government agencies may obtain copies of this report directly from DDC. Other qualified DDC users shall request through _____."
- (4) "U. S. military agencies may obtain copies of this report directly from DDC. Other qualified users shall request through _____."
- (5) "All distribution of this report is controlled. Qualified DDC users shall request through _____."

If the report has been furnished to the Office of Technical Services, Department of Commerce, for sale to the public, indicate this fact and enter the price, if known.

11. SUPPLEMENTARY NOTES: Use for additional explanatory notes.

12. SPONSORING MILITARY ACTIVITY: Enter the name of the departmental project office or laboratory sponsoring (paying for) the research and development. Include address.

13. ABSTRACT: Enter an abstract giving a brief and factual summary of the document indicative of the report, even though it may also appear elsewhere in the body of the technical report. If additional space is required, a continuation sheet shall be attached.

It is highly desirable that the abstract of classified reports be unclassified. Each paragraph of the abstract shall end with an indication of the military security classification of the information in the paragraph, represented as (TS), (S), (C), or (U).

There is no limitation on the length of the abstract. However, the suggested length is from 150 to 225 words.

14. KEY WORDS: Key words are technically meaningful terms or short phrases that characterize a report and may be used as index entries for cataloging the report. Key words must be selected so that no security classification is required. Identifiers, such as equipment model designation, trade name, military project code name, geographic location, may be used as key words but will be followed by an indication of technical context. The assignment of links, rules, and weights is optional.